LBNL-41275
UC-1600

Ernest Orlando Lawrence Berkeley National Laboratory

Radiant Cooling in U.S. Office Buildings: Towards Eliminating the Perception of Climate-Imposed Barriers

Corina Stetiu

Environmental Energy Technologies Division

January 1998

Ph.D. Thesis

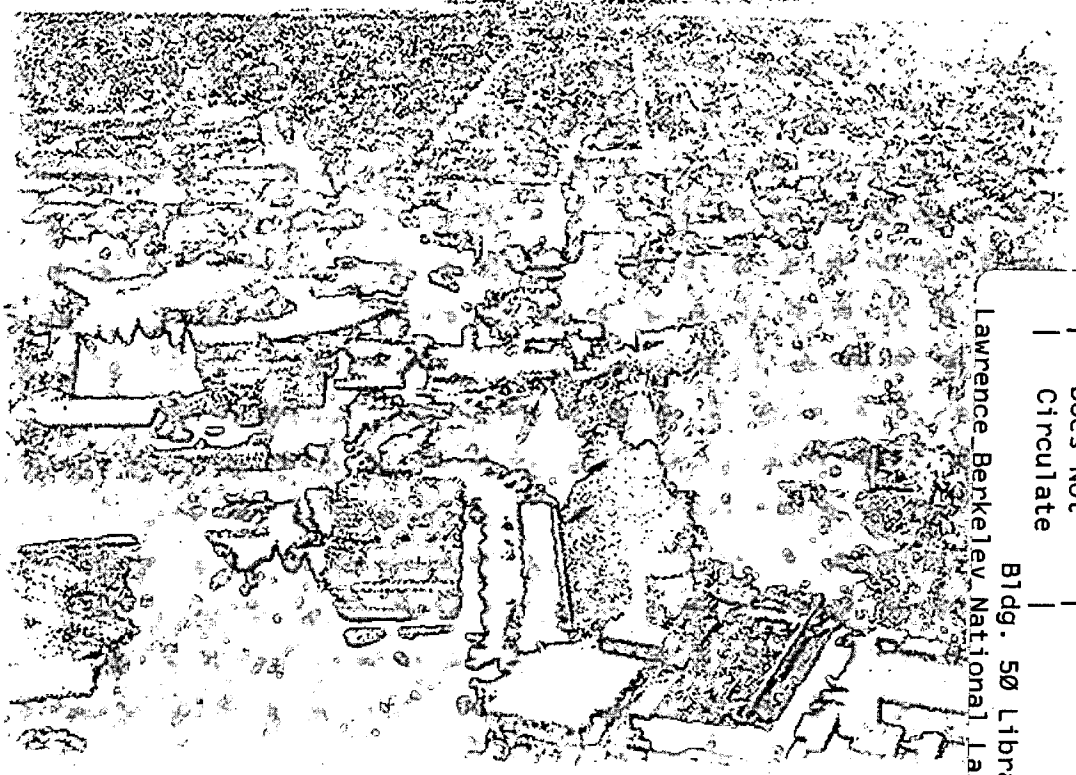

REFERENCE COPY
Does Not
Circulate

Bldg. 50 Library - Ref.
Lawrence Berkeley National Laboratory

LBNL-41275
Copy 1

DISCLAIMER

This document was prepared as an account of work sponsored by the United States Government. While this document is believed to contain correct information, neither the United States Government nor any agency thereof, nor the Regents of the University of California, nor any of their employees, makes any warranty, express or implied, or assumes any legal responsibility for the accuracy, completeness, or usefulness of any information, apparatus, product, or process disclosed, or represents that its use would not infringe privately owned rights. Reference herein to any specific commercial product, process, or service by its trade name, trademark, manufacturer, or otherwise, does not necessarily constitute or imply its endorsement, recommendation, or favoring by the United States Government or any agency thereof, or the Regents of the University of California. The views and opinions of authors expressed herein do not necessarily state or reflect those of the United States Government or any agency thereof or the Regents of the University of California.

LBNL-41275
UC-1600

Radiant Cooling in US Office Buildings:

Towards Eliminating the Perception of Climate-Imposed Barriers

Corina Stetiu

Ph.D. Thesis

Energy and Resources Group

University of California, Berkeley

and

Environmental Energy Technologies Division

Lawrence Berkeley National Laboratory

University of California

Berkeley, CA 94720

January 1998

This work was supported by the Assistant Secretary for Energy Efficiency and Renewable Energy, Office of Building Technology of the U.S. Department of Energy under Contract No. DE-AC03-76SF00098. This work was also partly funded by the California Institute for Energy Efficiency (CIEE), a research unit of the University of California. Publication of research results does not imply CIEE endorsement of, or agreement with, these findings, nor that of any CIEE sponsor.

Abstract

Radiant Cooling in US Office Buildings:

Towards Eliminating the Perception of Climate-Imposed Barriers

by

Corina Stetiu

Doctor of Philosophy in Energy and Resources

University of California at Berkeley

Professor Gene I. Rochlin, Chair

The intensive use of compressor-driven cooling in the developed countries has both direct and indirect negative effects on the environment that are realized on local and global scales. Predicted increases in the use of air-conditioning in the developing countries will magnify the range and scope of these effects. Much attention is therefore being given to improving the efficiency of air-conditioning systems through the promotion of more efficient cooling technologies.

One such alternative, radiant cooling, is the subject of this thesis. Performance information from Western European buildings equipped with radiant cooling systems indicates that these systems not only reduce the building energy consumption but also provide additional economic and comfort-related benefits. Their potential in other markets such as the US has been largely overlooked due to lack of practical demonstration, and to the absence of simulation tools capable of predicting system performance in different climates.

This thesis describes the development of RADCOOL, a simulation tool that models thermal and moisture-related effects in spaces equipped with radiant cooling systems. The thesis then conducts the first in-depth investigation of the climate-related aspects of the performance of radiant cooling systems in office buildings. The results of the investigation show that a building equipped with a radiant cooling system can be operated in any US climate with small risk of condensation. For the office space examined in the thesis, employing a radiant cooling system instead of a traditional all-air system can save on average 30% of the energy consumption and 27% of the peak power demand due to space conditioning. The savings potential is climate-dependent, and is larger in retrofitted buildings than in new construction.

This thesis demonstrates the high performance potential of radiant cooling systems across a broad range of US climates. It further discusses the economics governing the US air-conditioning market and identifies the type of policy interventions and other measures that could encourage the adoption of radiant cooling in this market.

For Carole

TABLE OF CONTENTS

ABSTRACT i

TABLE OF CONTENTS iii

LIST OF FIGURES x

LIST OF TABLES xiv

ACKNOWLEDGMENTS xvii

1. INTRODUCTION 1

1.1 Background 1

1.1.1 Motivation for this research 3

1.1.2 Thesis objectives 4

1.2 Thesis Outline 5

1.3 References 6

2. PRESENT STATE OF KNOWLEDGE ABOUT RADIANT COOLING SYSTEMS 8

2.1 All-Air Systems vs. Radiant Cooling Systems 8

2.2 Short History of Radiant Cooling Systems 9

2.3 Thermal Comfort Considerations 13

2.4 The Cooling Power of Radiant Cooling Systems 15

2.5 Numerical Modeling of Radiant Cooling Systems 18

2.6 Cooling Performance of Radiant Cooling Systems: Case Studies 18

2.7 Cooling Performance of Radiant Cooling Systems: Back-of-the-Envelope Calculation 20

2.8 Economics of Radiant Cooling Systems 22

2.9 Types of Radiant Cooling Systems 23

2.10 Radiant Cooling System Controls 28

2.11 Summary 29

2.12 References 29

3. RADCOOL - A TOOL FOR MODELING BUILDINGS EQUIPPED WITH RADIANT COOLING SYSTEMS 33

3.1 Modeling Approach 33

3.1.1 Model capabilities 34

3.1.2 Model limitations 34

3.2 Model Evaluation 35

3.2.1 Intermodel comparison with DOE-2 35

3.2.2 Comparison with measured data 41

3.3 Conclusions 49

3.4 Future work 49

3.5 References 51

4. RADIANT COOLING IN US OFFICE BUILDINGS: DESIGN OF THE MODELING PROJECT 53

4.1 Introduction 53

4.2 The Issue 53

4.3 The Parametric Study 54

4.4 Working with the RADCOOL-Imposed Constraints 56

4.4.1 The base-case building 56

4.4.2 The base-case space 60

4.4.3 The locations for the parametric study 67
4.4.4 The location-specific simulation periods 71
4.5 Comparing the Results of the RADCOOL and DOE-2 Simulations 79
4.5.1 Using the results of RADCOOL and DOE-2 to compare the energy consumption and peak power demand of the radiant cooling system and the all-air system 80
4.6 Capabilities and Limits of the Parametric Study 81
4.7 References 83

5. RADIANT COOLING IN US OFFICE BUILDINGS: RESULTS OF THE MODELING PROJECT 85
5.1 Chapter Outline 85
5.2 Indoor Conditions 86
5.3 The Energy Consumption and Peak Power Demand of the Radiant Cooling System 94
5.3.1 Energy consumption of the radiant cooling system 95
5.3.2 Peak power demand of the radiant cooling system 96
5.4 The Energy Consumption and Peak Power Demand of the All-Air System 97
5.4.1 Energy consumption of the all-air system 97
5.4.2 Peak power demand of the all-air system 99
5.5 Comparison of the Performance of the Radiant Cooling System and of the All-Air System 99
5.5.1 Energy consumption 99
5.5.2 Peak power demand 102
5.5.3 Climate-induced trends into the energy and peak power savings of the radiant cooling system 103
5.6 Additional Modeling 111

5.6.1 Description of the additional simulations 111
5.6.2 Results of the additional simulations 112
5.7 Conclusions 115
5.8 References 116

6. RADIANT COOLING AND THE US MARKET 117
6.1 Introduction 117
6.2 The Economic Theory of Increasing Returns 117
6.3 The Regulatory Response 120
6.3.1 Theory 120
6.3.2 Application to cooling technologies 121
6.3.3 Other measures 123
6.4 Conclusion 127
6.5 References 127

7. FUTURE RESEARCH DIRECTIONS 129

Appendix A
THE THERMAL BUILDING SIMULATION MODEL RADCOOL 132
A.1 SPARK as the Environment for RADCOOL 132
A.2 The Structure of RADCOOL 133
A.2.1 Preliminary data processing 134
A.2.2 Create the SPARK files describing the problem, run SPARK 134
A.2.3 Output data processing 134
A.3 The SPARK Building Component Library 134
A.4 The Passive Building Components 137

A.4.1 One-dimensional heat transfer 137

A.4.1.1 The one-dimensional heat conduction/storage equation 137

A.4.1.2 The RC approach to solve the heat conduction/storage equations for one solid layer in SPARK 139

A.4.2 The structure of the passive wall in SPARK 140

A.4.2.1 The equations for the temperature nodes in SPARK 141

A.4.2.2 Test to determine the accuracy of the RC model for one-dimensional heat transfer 142

A.4.3 Exterior surface radiant heat balance for a wall with thermal mass 144

A.4.3.1 The convective heat flux on the surface of a wall 145

A.4.3.2 The long wave (IR) heat flux exchange between a wall and its exterior surroundings 146

A.4.3.3 The solar radiation incident on the surface of a wall 148

A.4.4 Interior surface radiant heat balance for a wall with thermal mass 149

A.4.4.1 The convective heat flux on the interior surface of a wall 150

A.4.4.2 The long wave radiative exchange between a wall and the other room surfaces 151

A.4.4.3 Solar and internal radiation incident on the interior surface of a wall 153

A.4.5 The four-layer passive floor with thermal mass 154

A.4.5.1 Comparison between the floor and the wall with thermal mass 154

A.4.5.2 The exterior surface radiant heat balance for a passive floor with thermal mass 155

A.4.6 The two-pane window with thermal mass 156

A.4.6.1 Comparison between a two-pane window and a multi-layer wall 156
A.4.6.2 Heat conduction/storage for a two-pane window 156
A.4.6.3 The heat balance for the exterior pane of a two-pane window 158
A.4.6.4 The heat balance for the interior pane of a two-pane window 158
A.5 The Active Building Components 159
A.5.1 Two-dimensional heat transfer analysis 159
A.5.1.1 The two-dimensional heat conduction/storage equations 160
A.5.1.2 The RC solution to the two-dimensional heat conduction/storage equations 160
A.5.1.3 The two-dimensional model of the ceiling in SPARK 161
A.5.1.4 Test to determine the accuracy of the RC model for two-dimensional heat transfer 165
A.5.2 The two-dimensional SPARK model of the core-cooling ceiling 166
A.5.2.1 Heat transfer between the pipe and the water when the water is flowing 167
A.5.2.2 Heat transfer between the pipe and the water when the water is recirculated 168
A.5.2.3 Heat transfer between the pipe and the water when the water is stagnant 170
A.5.2.4 The two-dimensional model of a cooled ceiling 171
A.5.3 The cooling panel 173
A.5.3.1 The model of the cooling panel 173
A.6 Types of Radiant Cooling System Controls 176
A.6.1 The thermostat-based control 176

A.6.2 The timer-based control 176
A.6.3 The hybrid control 178
A.7 The Indoor Air 179
A.7.1 The air temperature 179
A.7.2 Discretization of the room air domain in RADCOOL 180
A.7.3 Room air heat balance 181
A.7.4 Plenum air heat balance 187
A.7.5 Room air moisture balance 189
A.8 Linking Objects 197
A.9 Tasks Performed in the "Preliminary Data Processing" Section 197
A.9.1 Data collection 197
A.9.2 Weather-related data 198
A.9.2.1 Algorithms to calculate the direct and diffuse solar radiation on a surface 199
A.9.3 Surface-to-surface shape factors 202
A.10 References 205

Appendix B
ENERGY CONSUMPTION AND PEAK POWER DEMAND OF THE RADIANT COOLING AND ALL-AIR SYSTEMS: RESULTS OF THE PARAMETRIC STUDY 208

LIST OF FIGURES

Chapter 2

2.1. Air flow and heat exchange in a room with cooled ceiling. 12

2.2. Construction of a cooling panel. 24

2.3. Heat transfer for the panel system (cooling mode). 25

2.4. Construction of a cooling grid. 26

2.5. Heat transfer for ceiling with cooling grid. 26

2.6. Heat transfer for concrete core cooling system. 27

Chapter 3

3.1 Single-zone structure simulated for the intermodel comparison. 36

3.2 The three wall assemblies simulated for the intermodel comparison. 38

3.3 Outside and indoor air temperature: wall assembly 1 (concrete). 40

3.4 Outside and indoor air temperature: wall assembly 2 (typical construction). 40

3.5 Outside and indoor air temperature: wall assembly 3 (wood). 41

3.6 The DOW Chemicals test room orientation and layout. 42

3.7 Composition of the vertical walls in the DOW Chemicals test room. 43

3.8 Composition of the roof and floor in the DOW Chemicals test room. 43

3.9 Air temperature inside the DOW Chemicals test room. 48

Chapter 4

4.1 Base-case building orientation and layout. 58

4.2 Base-case building construction for the parametric study. 59

4.3 Space contributions to the building energy consumption. Statistic performed for 11 building locations. 63

4.4 Estimate of building energy consumption from space energy consumption. 64
4.5 Ventilation strategies: schedules for weekday hours. 66
4.6 Climate classification based on the dehumidification energy and total energy necessary to condition the ventilation air. 69
4.7 US commercial buildings - classification by principal activity. 72

Chapter 5

5.1 Indoor air temperature comparison at the New Orleans location during the week of system peak. Space ventilated continuously, half rate at night. 87
5.2 Indoor air temperature comparison at the New Orleans location during the day of system peak. Space ventilated continuously, half rate at night. 87
5.2 Indoor air relative humidity comparison at the New Orleans location during the week of system peak. Space ventilated continuously, half rate at night. 88
5.4 Comparison of cooling panel surface temperature and dew-point temperature. New Orleans, space ventilated continuously, half rate at night 88
5.5 Indoor air temperature comparison at the New Orleans location during the week of system peak. Space ventilation interrupted at night. 89
5.6 Indoor air temperature comparison at the New Orleans location during the day of system peak. Space ventilation interrupted at night. 89
5.7 Indoor air relative humidity comparison at the New Orleans location during the week of system peak. Space ventilation interrupted at night. 90
5.8 Comparison of cooling panel surface temperature and dew-point temperature. New Orleans, space ventilation interrupted at night. 90

5.9 Distribution of the energy and peak power savings of the radiant cooling system with the number of locations. Space ventilation interrupted at night. 104
5.10 Energy savings over the cooling season: trend across climates. 106
5.11 Fractional energy savings over the cooling season: trend across climates. 107
5.12 Peak power savings: trend across climates. 108
5.13 Fractional peak power savings: trend across climates. 109
5.14 Distribution of the energy and peak power savings of the radiant cooling system with the number of locations. 110
5.15 Energy savings over the cooling season: data for New Orleans and Phoenix. 113
5.16 Peak power savings: data for New Orleans and Phoenix. 114

Appendix A

A.1 RADCOOL program flow. 133
A.2 Volume element for conduction heat flow. 137
A.3 A wall layer with three sub-layers. 140
A.4 A wall layer with four sub-layers. 141
A.5 The RC model of the 4-layer wall. 141
A.6 Temperature at the midpoint of a homogeneous wall: comparison between the one-dimensional SPARK model and the analytical solution. 144
A.7 The heat flux balance at the exterior surface node. 145
A.8 The long wave radiation exchange at the exterior surface of a wall. 146
A.9 The heat flux balance at the interior surface temperature node. 149
A.10 Different gradients for air and room temperatures. 150
A.11 The RC circuit of a two-pane window. 156
A.12 A 3x5 grid. RC equivalent circuit for heat transfer calculations. 162

A.13 A 5x5 grid. RC equivalent circuit for heat transfer calculations. 163
A.14 Temperature at the midpoint of a homogeneous ceiling: comparison between the 3x5 grid SPARK model and the analytical solution. 165
A.15 Temperature at the midpoint of a homogeneous ceiling: comparison between the 5x5 grid SPARK model and the analytical solution. 166
A.16 Structure of a cooled ceiling with imbedded pipes. 166
A.17 Equivalent RC circuit for heat transfer calculation in the case of a cooled ceiling. 172
A.18 Layout of a cooling panel system. 174
A.19 The heat balance in the case of the cooling panel. 175
A.20 Thermostat-based control strategy. 177
A.21 Timer-based control strategy. 177
A.22 Hybrid control. 178
A.23 Air temperature nodes in a room modeled by RADCOOL. 180
A.24 Heat balance for the room air. 182
A.25 Heat balance for the plenum air. 188
A.26 Relative positions of two rectangular surfaces that give exact solutions for the shape factors. 203
A.27 Radiation exchange between finite areas with one area subdivided. 205

LIST OF TABLES

Chapter 2

2.1 Data about the radiant cooling systems installed in Germany in 1994. 13

2.2 Assumptions used for the comparison of peak power requirements for an all-air system and a RC system conditioning the same office space. 21

2.3 Estimated electrical power demand for the removal of internal loads from a two-person office with a floor area of 25 m^2. 22

2.4 Estimated annual energy consumption [kWh/m^2] for a European office building with a floor area of 5000 m^2. 23

2.5 Estimated space requirements for air-conditioning systems in a European office building with a floor area of 5000 m^2. 23

Chapter 3

3.1 Material properties used in the intermodel comparison. 37

3.2 Summary of assumptions for the intermodel comparison. 39

3.3 Material properties used in the comparison with measured data. 44

3.4 Summary of assumptions for the comparison with measured data. 47

Chapter 4

4.1 Material properties simulated in the parametric study. 57

4.2 Energy consumption for cooling and dehumidification of ventilation air. Climate classification and locations selected for the study. 70

4.3 Office buildings in the largest metropolitan areas and their distribution with respect of the climate classification. 71

4.4 Summary of assumptions for the parametric study. 77

Appendix A

A.1 Material-specific coefficients occurring in equation (A.136). 193

A.2 Material-specific coefficients occurring in equation (A.145). 195

A.3 Permeability, diffusion coefficient, and effective penetration depth of different materials. 196

A.4 Coefficients for equation (A.150). 200

A.5 Coefficients for equation (A.160). 202

Appendix B

B.1 Energy consumption and peak power demand in New Orleans. SW orientation, new building construction. 209

B.2 Energy consumption and peak power demand in Cape Hatteras. SW orientation, new building construction. 210

B.3 Energy consumption and peak power demand in New York City. SW orientation, new building construction. 211

B.4 Energy consumption and peak power demand in Fort Worth. SW orientation, new building construction. 212

B.5 Energy consumption and peak power demand in Chicago. SW orientation, new building construction. 213

B.6 Energy consumption and peak power demand in Boston. SW orientation, new building construction. 214

B.7 Energy consumption and peak power demand in San Jose, CA. SW orientation, new building construction. 215

B.8 Energy consumption and peak power demand in Phoenix. SW orientation, new building construction. 216

B.9 Energy consumption and peak power demand in Scottsbluff. SW orientation, new building construction. 217

B.10 Energy consumption and peak power demand in Salt Lake City.
SW orientation, new building construction. 218
B.11 Energy consumption and peak power demand in Seattle.
SW orientation, new building construction. 219
B.12 Energy consumption and peak power demand in New Orleans.
NE orientation, new building construction. 220
B.13 Energy consumption and peak power demand in Phoenix.
NE orientation, new building construction. 221
B.14 Energy consumption and peak power demand in New Orleans.
SW orientation, old building construction. 222
B.15 Energy consumption and peak power demand in Phoenix.
SW orientation, old building construction. 223

ACKNOWLEDGMENTS

First and foremost, I must thank my advisers Gene Rochlin and Helmut Feustel, without whose help this thesis would have never come into existence.

However busy, Gene always found time to meet with me, listen to my concerns, and help me get un-stuck. A true ERGie himself, Gene encouraged me time and again to look at everything in context, and taught me to be self-conscious while doing research. Some of my best memories of graduate school are those of sharing laughter and brownies with Gene while discussing my work. Thank you.

Helmut dedicated many hours and lots of energy to help me formulate a thesis topic that was interesting and challenging for both of us. By constantly questioning the direction of my research and the validity of my results, Helmut taught me to defend my point of view, and helped me remain focused. He also ensured my financial support all the way through graduate school, so I can avoid going in debt before graduation. Thank you.

I must also thank Bill Nazaroff and Cris Benton. They were always available to discuss my progress, and offered invaluable suggestions at various stages of my work. I thank them for their time, help and encouragements. Without their advice my struggles would have been significantly more painful, and this dissertation much harder to "digest".

I am grateful to *Meierhans & Partner, AG* for their financial support during my first year as a graduate student, and for sharing their field measurements with me. I thank the California Institute for Energy Efficiency for funding the development of RADCOOL through an "exploratory project". I thank Richard H. Karney for the financial support that I received through the years from the US Department of Energy, and for his constant interest in my work.

Carrying out the computer work that constitutes the core of this thesis would have been impossible without the help of the Simulation Research Group at the LBNL. Fred Winkelmann, Fred Buhl, Ender Erdem and Kathy Ellington showed me the tricks behind the magic of building simulations, and provided guidance in my early work with SPARK. Thank you.

Two other colleagues at LBNL have constantly helped me through the years. Brian Smith made sure that my computer was always ready for data-crunching, and designed many of the figures in the thesis. Rick Diamond good-naturedly answered all my questions, offered useful inputs and comments, and cheered me up when times were rough. Thank you both.

The friendships with which I have been blessed at Berkeley have helped me overcome the initial (and later) difficulties associated with studying in the US. Many thanks go to my dear friends Libby Schnieders, Katy Janda, Alison Kwok, JoAnn Ten Brinke, Karin Hansen, Elana Swartzman and Scott Benson, and to my roommates Marc Melcher, Jack Dennerlein, Chris Pawlowski, Shirley Yang and Hana Filip.

For their unconditional love, I am eternally grateful to my family. Without the encouragement and support that they have constantly offered me, I would have never launched into this great adventure of becoming... a doctor!

Finally, I thank my best friend and husband, David Jump, for having always been there for me. David has stood by me at times of disappointment, and has shared my joy for every success, however minor. He has supported my decisions, and has shown me how to have fun throughout it all. Through his personal and professional achievements, he has been a constant source of inspiration. Thank you with all my heart.

Chapter 1
INTRODUCTION

1.1 Background

Keeping cool in hot climates has long been a human preoccupation. For thousands of years, people have used a variety of architectural techniques (thermal mass, shading, strategically-placed vents, atria, etc.) to adapt dwelling design and cultural practice to local climate conditions. After the industrial revolution, many of these techniques were adapted to the new requirements of large buildings. The tradition of massive, daylit buildings, with courtyards and airshafts, is still visible today in older European and North American office buildings, especially in the south.

In 1902, while searching for a method to control humidity in a printing plant, Carrier invented the refrigerative chiller. Within a few years, the world had access to a device that could cool any boxy, sealed building, regardless of how much heat it gained and trapped [1]. However, the mechanical cooling of buildings did not become widespread in the United States until after World War II. As the electrification of the American South progressed, air-conditioning was first introduced in movie theaters, then made its way into factories, homes, offices, department stores, even automobiles. By the 1950s, the reliability of air-conditioning, the adoption of fluorescent lights and of solar control glazing, and the steadily falling price of electricity, allowed architects throughout the country to abandon the ancient techniques of climate-responsive design, and to focus on the artistic side of design instead. Today, even portions of outdoor facilities (football stadiums, zoos, amusement parks, etc.) are air-conditioned. Air-conditioning is ubiquitous; its presence has become the expected norm.

In the 1950s air-conditioning played a significant role as stimulus to commercial and residential growth in the American Southwest. Since then, it has evolved from a region-specific solution to a perceived necessity virtually nationwide. One of the consequences of today's intensive use of air-conditioning is that building professionals have lost much of their ability to design climate-responsive buildings. The compartmentalization of the building profession [2], and the divergent interests of the different parties involved in the building process, make modern buildings costlier to build, and considerably costlier to cool and ventilate than need be. In addition, worker surveys reveal that commercial building occupants are increasingly dissatisfied with the thermal conditions of their workplace [3], and that occupant exposure to air-conditioned indoor environments sometimes leads to adverse health conditions [4]. When trying to address these problems, innovative designers have begun to recognize the importance of restoring some natural variability into buildings, thereby making interior spaces healthier, more pleasant, and often more energy efficient. However, due to the same divergence of interests among the parties involved in the building process, this attempt to return to a climate-responsive design is slow and inefficient.

Another consequence of the widespread use of air-conditioning in the United States is that, although air-conditioning is responsible for only 12% of the total building energy consumption [5], its electrical power demand is considered to be "the load from hell" [6]. Because the electricity demand due to space cooling is high and seasonal, it forces utilities to make investments in power generation equipment that is only used on the hottest days of the year. The cost of this inefficient capacity is then passed on to all utility ratepayers, whether they own an air-conditioning system or not. In addition, the costs of increased emissions from electricity production, and the environmental costs of chlorofluorocarbon (CFC) use in air-conditioners, are borne globally [7].

A last consequence is that increased use of air-conditioning in the developing countries will multiply local and global environmental problems. In Southeast Asia, for example, the need for mechanical cooling is often secondary to the desire to demonstrate social status or international stature through the acquisition of modern technology. But the adoption of the "good american life" imposes the comfort standards developed in temperate regions on individuals that were previously adapted to hot and humid climates. This reduces their tolerance for heat and humidity, forces their acclimatization to artificially-created conditions, and ultimately results in a waste of energy and resources [8]. The use of air-conditioning in the developing countries can only exacerbate the local energy and global environmental effects.

One step towards resolving this complex set of interlocking problems would be to reformulate the "expected norm" in a way that would encourage climate-responsive design all around the world. However, while current energy and environmental problems are at a scale that would benefit from swift and effective action, the adoption of climate-responsive design would likely take a long time. Furthermore, this solution would not address the problems associated with the operation of the numerous energy-intensive buildings that are already in use. As an alternative solution, much attention is dedicated today to incorporating energy efficient technologies in building design. Although this course of action does not influence the "expected norm" directly, it addresses the energy and environmental problems to some extent, and it is beneficial for new construction and retrofit projects alike.

Anticipating the problems that may be caused in the future by current building design, the US Office of Technology Assessment (OTA) indicated that the use of cost-effective, commercially available technologies in the United States could reduce total building energy use by about one-third by 2015, relative to a business-as-usual baseline [9]. One of the actions recommended by the OTA to achieve this goal is the reduction of the efficiency gap between the average new cooling equipment and the most efficient cooling equipment available: substituting the average new cooling equipment with energy efficient cooling equipment can save up to 28% of the US energy consumption due to space conditioning [5]. The OTA recommendations were corroborated by Feustel and collaborators [7], who showed that alternative cooling technologies can reduce the energy consumption and peak power demand due to space conditioning while striving to provide

indoor conditions very similar to those provided by the compressor-driven technology.

Severe urban air pollution, high energy prices, and concerns about energy security have prompted Western European countries to encourage the reduction of building energy consumption and peak power demand through the adoption of new building standards. These standards call for better building design in general, and for the replacement of the traditional all-air systems with alternative, more efficient building conditioning systems in particular. At the recommendation of the OTA, similar efforts are currently in progress in the United States, carried out under government and/or utility sponsorship. However, while alternative cooling technologies and sources[1] are intensively used in new construction and retrofit projects in Western Europe, the relatively low energy prices in the US, together with the decentralization and fragmentation of the building industry, have so far been a barrier to the large-scale implementation of alternative cooling technologies in the United States.

1.1.1 Motivation for this research

While examining the literature that addresses the issue of alternative cooling technologies in Western Europe and the US, Feustel and Stetiu [10] noted the conspicuous absence from the US market of radiant cooling, an alternative cooling technology that is currently implemented in Western European commercial buildings. A complete explanation for the absence of radiant cooling systems from the US market would very likely require the description of a complex interaction of technical, economic, social, and cultural factors. Instead of addressing this ambitious task, this thesis investigates whether, and how well, radiant cooling systems could perform in commercial buildings in the US, discusses the economics governing the US air-conditioning market, and identifies the type of policy interventions and other measures that could encourage the adoption of radiant cooling in this market.

The available information regarding the performance of radiant cooling systems indicates that these systems not only reduce the energy consumption and peak power demand due to space conditioning, but that they also provide draft-free and noise-free cooling, reduce building space requirements, and might even have lower first-cost if maximum specific cooling loads are above 50 - 55 W/m^2. By using back-of-the-envelope calculations, Feustel and Stetiu estimated that the use of radiant cooling systems in commercial buildings in the US could reduce the building energy consumption due to space conditioning by 40% and the peak power demand by 28%.

Radiant cooling systems provide thermal comfort inside a building by means of radia-

1. Alternative cooling systems available on the Western European market are evaporative cooling, desiccant cooling, absorption cooling and radiant cooling. Commonly used cooling sources (or heat sinks) are natural cooling and ventilation, cooling towers, and ground coupling.

tive heat exchange with a cold surface, and maintain acceptable indoor air quality by supplying the necessary amount of fresh air with an air distribution system. By separating the tasks of thermal conditioning and ventilation, radiant cooling systems eliminate air recirculation, thus reducing the energy consumption due to space conditioning. However, the presence of a cold surface in a space increases the risk of condensation, a phenomenon unacceptable from the point of view of occupant comfort, as well as because it can damage the building structure, building finishes, and the radiant system itself. To prevent the formation of condensation on the cooling surface, radiant cooling systems commonly control the moisture content of the indoor air by dehumidifying the ventilation air. In hot humid climates, the dehumidification of the ventilation air can be extremely energy intensive.

No known research has addressed the climate-compatibility of radiant cooling systems so far, partly because a software tool that can model the thermal behavior of radiant cooling systems in buildings has not been available. There is no doubt that a radiant cooling system can be designed to cool a building located in any climate. However, it is unclear whether the radiant cooling system can prevent the formation of condensation in any climate, and still require less energy and peak power to operate than a traditional all-air system. Because the available data regarding the performance of commercial buildings equipped with radiant cooling systems refer to a few buildings in Germany and Switzerland, it is possible that the European buildings studied so far are located in climates in which radiant cooling systems are inherently more efficient than all-air systems. Therefore, it is currently difficult to argue that installing a radiant cooling system instead of an all-air system in a commercial building located in *any* climate would reduce that building's energy consumption and peak power demand due to space conditioning. The research presented in this thesis is the first in-depth investigation into the climate-related aspects of the performance of commercial buildings equipped with radiant cooling systems. Its results provide information regarding the potential of radiant cooling systems to reduce energy consumption and peak power demand in the typical climates found in the US.

1.1.2 Thesis objectives

The first objective of this thesis is to describe the development of RADCOOL, a simulation tool that can model the dynamic thermal and moisture-related effects associated with the functioning of radiant cooling in buildings. RADCOOL is an original computer model, designed by the author of this thesis to provide information about loads, heat extraction rates, air temperature, and surface temperature distributions in a building. RADCOOL can evaluate system sizing and system configuration, and can assist in HVAC system design. RADCOOL can also be used in the evaluation of issues such as controls, and the dynamic response of the building systems to load changes, and can be extended to study indoor thermal comfort and building energy use. The ultimate goal for

RADCOOL is to operate as a DOE-2[1] module. This would allow building practitioners to access the capabilities of this program through the familiar DOE-2 interface.

The second objective of the thesis is to use RADCOOL in an investigation of the climate-related aspects of the performance of buildings equipped with radiant cooling systems. To accomplish this, the thesis conducts a parametric study consisting of simulating a building with pre-established construction, orientation, occupancy rates, etc., under different weather-imposed boundary conditions. The study is designed to provide two types of results. First, an indication of whether buildings equipped with radiant cooling systems can be operated to avoid side effects such as condensation at any location in the US. Second, an accounting of the energy consumption and peak power demand of the radiant cooling system. The comparison of RADCOOL simulation results with similar simulation results obtained for the same building equipped with a traditional all-air system provides estimates of (1) the energy savings potential of the radiant system, and (2) the dependence of these energy savings on the climate in which the building is located.

The third objective of the thesis is to assess the prospects of radiant cooling capturing a share of the US air-conditioning market. To do so, the thesis discusses the economics of this market, and identifies the measures that would encourage the incorporation of radiant cooling in building design in the United States.

1.2 Thesis Outline

The core of the thesis begins in Chapter 2 with a summary of the present state of knowledge about radiant cooling systems. It contains a short history of radiant cooling, information about the performance of existing buildings equipped with radiant cooling systems, and a discussion of the advantages and disadvantages of radiant cooling systems as compared to traditional air-conditioning systems.

Chapter 3 describes the design, evaluation, and limits of RADCOOL, the computer model developed specifically for the simulation of buildings equipped with radiant cooling systems. Because the simulation of such buildings requires the evaluation of surface temperature distributions, RADCOOL is based on a complete energy-balance calculation. The environment for RADCOOL is the Simulation Problem Analysis and Research Kernel (SPARK) [12], a code that provides a methodology for describing and solving the dynamic, non-linear equations corresponding to complex physical problems. The physical equations that constitute the basis of RADCOOL are presented in Appendix A.

Chapter 4 describes the modeling project designed to evaluate the compatibility between buildings equipped with radiant cooling systems and typical climates found in the US.

1. DOE-2 is a widely-used building simulation program [11]. In its present stage of development, DOE-2 cannot model buildings equipped with radiant cooling systems.

The evaluation consists of RADCOOL simulations for an office space equipped with a radiant cooling system, and DOE-2 simulations for the same space equipped with a traditional all-air system, carried out in parallel for a number of US climates. This chapter contains (1) a discussion of the selection of building design, locations, and simulation periods, necessary because of the computational constraints of RADCOOL, (2) the strategy adopted for comparing the RADCOOL results and the DOE-2 results, and (3) an evaluation of the uncertainties introduced by these operations.

The results of the modeling project and its findings are presented in Chapter 5 and Appendix B. The modeling project was designed to allow the differences between the RADCOOL results and the DOE-2 results to be attributed to the differences between the heat transfer mechanisms employed by the radiant cooling system and the traditional all-air system. This feature provides estimates of the energy and peak power savings potential of the radiant cooling system at each of the locations selected for the study. Based on these results, the energy consumption and peak power demand of the radiant cooling system at a certain location and the energy consumption and peak power demand of the all-air system at the same location can be correlated. As this quantitative relationship is location-dependent, its existence allows the prediction of the savings achievable by installing a radiant cooling system instead of an all-air system at any location (in the US or elsewhere).

To put these results in context, Chapter 6 discusses the economics governing the US air-conditioning market, and exposes the types of policies and other measures that would encourage the adoption of alternative cooling technologies in general, and of radiant cooling in particular, on this market. Drawing from the results of the thesis and the discussion in Chapter 6, Chapter 7 identifies directions for future research.

1.3 References

1. M. Shepard, J. Gregerson, D. Houghton, L. Fryer, J. Elleson, B. Pattinson, W. Hawthorne, L. Webster, J. Stein, D. Davia and S. Parsons, *Commercial space cooling and air handling technology atlas*. E-Source Inc., Boulder, CO, June 1995.

2. Amory Lovins, *Energy efficient buildings: institutional barriers and opportunities*. E-Source Strategic Issues Paper, Boulder, CO, 1992.

3. Volker Hartkopf, Personal communication. Center for Building Performance and Diagnostics, Carnegie Mellon University, Pittsburgh, PA, January 1995.

4. M. Mendell and A. H. Smith, *Consistent pattern of elevated symptoms in air-conditioned buildings: a reanalysis of epidemiologic studies*. Am. J. Public Health, (80) (10) 1990.

5. U.S. Congress, Office of Technology Assessment, *Building energy efficiency.* OTA-E-518 (Washington, DC: U.S. Government Printing Office, May 1992).

6. Max Sherman, Personal Communication. California Institute for Energy Efficiency, Berkeley, CA, 1991.

7. Helmut Feustel, A. de Almeida and C. Blumstein, *Alternatives to compressor cooling in residences.* Energy and Buildings, (18) (3-4) 1992.

8. John Busch, *A tale of two populations: thermal comfort in air-conditioned and naturally ventilated offices in Thailand.* Energy and Buildings, (18) (3-4) 1992.

9. U.S. Congress, Office of Technology Assessment, *Changing by degrees: steps to reduce greenhouse gases.* OTA-O-482 (Washington, DC: U.S. Government Printing Office, February 1991).

10. Helmut E. Feustel and C. Stetiu, *Hydronic radiant cooling - preliminary assessment.* Energy and Buildings, (22) (3) 1995.

11. Simulation Research Group (Lawrence Berkeley Laboratory) and Group Q-11 (Los Alamos National Laboratory), *DOE-2 Engineering manual.* Rep. LBNL-11353, 1982.

12. Edward F. Sowell, W. F. Buhl, A. E. Erdem and F. C. Winkelmann, *A prototype object-based system for HVAC simulation.* Proc. Second Int. Conf. on System Simulation in Buildings, Liège, Belgium, December 1986. Rep. LBNL-22106, 1986.

Chapter 2

PRESENT STATE OF KNOWLEDGE ABOUT RADIANT COOLING SYSTEMS

2.1 All-Air Systems vs. Radiant Cooling Systems

An air-conditioning system is designed to control indoor temperature and humidity, and to provide fresh, filtered air to building occupants.[1] The majority of air-conditioning systems currently in operation are all-air systems, meaning that they employ air not only for the ventilation task, but also as a heat and humidity transfer medium.

The overall energy used to cool buildings with all-air systems includes the energy necessary to power the fans that transport cool air through the ducts. Because the fans are usually placed in the air stream, fan movement heats the conditioned air, thus adding to the thermal cooling peak load. Usibelli and collaborators [2] found that, in the typical office building in Los Angeles, air transport accounts for 13% of the building peak cooling demand. By comparison, external loads account for 42%, lighting for 28%, people for 12%, and office equipment for 5% of the building peak cooling demand.

Computer modeling for different California climates using the California Energy Commission (CEC) base case office building show that, at the time of the peak cooling load, only 10% to 20% of the supply air is fresh air [3]. Only this small fraction of the supply air is necessary to ventilate buildings to maintain acceptable indoor air quality. The difference in volume between supply air and fresh outside air is made up by recirculated air. The recirculated air is necessary in all-air systems to remove excess heat from a building and maintain a comfortable indoor environment. This additional amount of supply air often causes draft,[2] and may contribute to indoor air quality problems due to the dispersal of pollutants throughout the building. Due to inefficiencies in the duct systems, recirculation also exacerbates duct air leakage and heat transfer through duct walls [4].

A radiant cooling (RC) system consists of a cooled surface and an air distribution system. The RC system employs long-wave (infrared) radiation to the cooled surface to remove unwanted heat from a space, and maintains acceptable indoor air quality and controls indoor air humidity by supplying fresh, filtered, dehumidified air through its air distribution system. In its operation as an air-conditioning systems, a RC system thus

1. Commercial buildings typically feature DOP-tested [1] 30%-efficient filters at the fresh air intake. The use of higher-efficiency filters would lead to improved indoor air quality, but also to a higher pressure drop across the supply fan, and thus to higher energy use by the air-conditioning system. A compromise value for filter efficiency in commercial applications is 60%, although few buildings employ such filters.

2. Draft is an undesired local cooling of the human body caused by air movement.

separates the task of sensible cooling from those of humidity control and ventilation. Because it relies on radiation from a cooled surface to provide sensible cooling, a RC system can provide comfort at a higher indoor air temperature than an all-air system.

Most RC systems use water as a transport medium to connect the interior radiant surface with an exterior heat sink. The thermal properties of water allow RC systems to (1) remove a given amount of heat from a building and use less than 25% of the transport energy necessary for an all-air system to remove the same amount of heat, (2) shift the peak cooling demand to later in the day, and (3) more easily interface with thermal energy storage systems. Because RC systems can use large surfaces for heat exchange (usually the radiant surface occupies most of the ceiling or of a vertical wall in a space), the temperature of the cooling water must be only a few degrees lower than the room air temperature. This small temperature difference allows the use of either heat pumps with very high coefficient of performance (COP) values, or of alternative cooling sources (for example, indirect evaporative cooling), to further reduce the electric power demand of the building.

By transporting only the air necessary for ventilation purposes, RC systems significantly reduce both the volume and the velocity of air transported through buildings, thus practically eliminating draft. At the same time, because the air does not play a major sensible cooling role, it does not have to be cooled far below the indoor air temperature. This reduces the problems caused by duct leakage and heat loss from ducts. The relatively low air volume supplied by RC systems also allows the reduction of the space necessary for the ventilation system and its duct work. RC systems only require about 25% of the building volume occupied by a traditional air-conditioning system. Floor-to-floor building height can thus be reduced by reducing plenum height from the typical 1 to 3 m to a quarter of this size. Alternatively, building occupants can enjoy spaces with higher ceilings.

2.2 Short History of Radiant Cooling Systems

Mechanical heating and cooling of indoor spaces has been practiced for a long time. The thermal structures at Bath, England, and Rome, Italy, represent the first known type of large-surface radiant heating system. Built more than 2000 years ago, the Roman hypocaust system consisted of raised floors made of concrete and covered in mosaic tiles. Hot gases from a furnace travelled through the hollow spaces under the raised floors until they were released in the atmosphere through a flue in a wall [5]. Anecdotal information suggests that, around the same time, the Turks were cooling their dwellings by tapping cold river water and circulating it through interstices in walls or floors [6].

Radiant heating as practiced by the Romans was not adopted throughout the world. One possible explanation resides in the cost of the installations in the Roman thermal buildings, as well as in the complexity of their design. Instead, for centuries fireplaces served as a main source of heat. Around the middle of the 18th century cast-iron stoves

became the preferred heating source [7]. Next, the hot water boiler was introduced, together with its system of large pipes through which the hot water was carried. The first known such design is attributed to Sir John Stone, who installed a heating system of pipes in the Bank of England in 1790. From here the design of radiators evolved gradually, the use of water giving way to that of steam, then again to water, this time pumped through thinner pipes. The compact radiators used today were introduced at the beginning of this century.

The modern development of radiant heating started in 1907, when Arthur H. Barker, a British professor, discovered that small hot water pipes embedded in plaster or concrete formed a very efficient heating system [5]. Subsequently, "panel heating" was used in Europe in conventional buildings, on the open terraces of many sanatoriums, and in an open-air roofed pavilion at a British World Fair [7]. In the US, Frank Lloyd Wright installed radiant panel heating in the Johnson Wax Building in 1937. By 1940, "Architectural Record" reported the existence of eight such installations in different types of buildings in the US: four residences, a church, a high school, an office building, and an airplane hangar [7]. In the beginning radiant systems were considered suitable for moderate climates only. Over time, however, projects showed that radiant heating can be designed to operate efficiently and comfortably in any climate.

Radiant heating installations are easily converted into radiant cooling installations by running cold water through the radiant panels. Most of the early cooling ceiling systems developed in the 1930s failed, however, because condensation often occurred in cooling mode. Subsequent studies showed that this problem could be avoided if the radiant system was used in conjunction with a small ventilation system designed to lower the dew-point of the indoor air. This combination proved successful in a department store built in 1936-1937 in Zürich, Switzerland [8], and in a multi-story building built in the early 1950s in Canada [7].

In the San Francisco Bay Area, the Kaiser Building in Oakland, dating from the early 1950s, is equipped with a radiant cooling system. A study conducted in 1994 [9] showed that this system does not perform to the satisfaction of the occupants: it fails to provide acceptable thermal comfort. The study demonstrated that the failure of the system is due to the design of the building (single-pane windows with aluminum frames, a large facade facing west), to a gradual increase of personal computers and office equipment over time, and to the relatively low cooling power of the radiant panels employed.

Given the benefits of radiant systems - improved comfort due to the radiant exchange, less building volume requirement, less energy consumption - it is not clear why all-air systems prevailed starting in the 1950s. One explanation might reside in the historical development of mechanical cooling in the US: the implementation of air-conditioning started in the US South, where the weather is typically hot and humid. The high amount of dehumidification required to provide acceptable comfort indoors must have been considered incompatible with the small amount of air employed by radiant cooling

systems. Regardless of the cause, however, radiant cooling systems were essentially forgotten from the 1950s until the mid-1980s.

During the past decade, building occupants have developed a critical attitude towards all-air systems. Terms such as "complaint buildings" and "sick buildings" were born. Several studies on the subject of occupant satisfaction in air-conditioned and naturally-ventilated buildings came to the conclusion that the number of unsatisfied occupants in air-conditioned buildings is significantly higher than in naturally ventilated buildings [10] - [13]. Esdorn and collaborators [14] state that "the existence of air-conditioning systems is actually only noticed when they are not functioning properly."

All-air systems can employ one of two strategies to remove heat from a building: (1) supply the required amount of ventilation air at a very low temperature (cold air distribution systems), and (2) supply moderately cool air at a rate exceeding the required amount of ventilation air (recirculating air systems). The first strategy leads to the uneven distribution of fresh air in the occupied zone. The second strategy achieves better mixing, but often leads to draft, as the air flow is normally turbulent in the occupied zone. Depending on the air temperature and turbulence level, even low air velocities (less than 0.2 m/s) have been shown to elicit complaints from 10 to 20% of the building occupants [15].

Due to comfort problems and the excessive use of transport energy by all-air systems, new ventilation strategies appeared in the late 1980s [16]. Among these, displacement ventilation was specifically developed to overcome the problems of mixing ventilation systems. Displacement ventilation consists of air flows of low turbulent intensity that supply clean air to the breathing zone and displace contaminants [17]. The natural driving forces of the vertical air transport are the heat sources in the space, as they create convective air currents (plumes). The ventilation efficiency of the resulting air flow pattern is greatly improved.[1]

Upward displacement ventilation shows a characteristic temperature profile caused by the convective currents driven by the heat sources. As supply air enters the room at floor level, the temperature gradient forms a barrier that prevents low energy currents from reaching the top of the room. Upward displacement ventilation also achieves some cooling. However, the cooling capacity of displacement ventilation systems is small because (1) the temperature gradient between feet and head cannot exceed 3 °C due to comfort requirements, therefore the inlet air cannot be too cold [17], and (2) displacement ventilation systems supply only the small amount of air needed for ventilation [19] - [20].

The most efficient use of displacement ventilation is in association with a cooling source that does not require air transport inside the room. The logical choice is the coupling of displacement ventilation systems with radiant cooling surfaces, a strategy that also allows

1. Ventilation efficiency is a measure of how quickly a ventilation system removes a contaminant from a room [18].

the separation of the tasks of ventilating and cooling in the building [17]. The theoretical air flow pattern and the heat exchange mechanisms in a room with a cooled ceiling and a displacement ventilation system are shown in Figure 2.1.

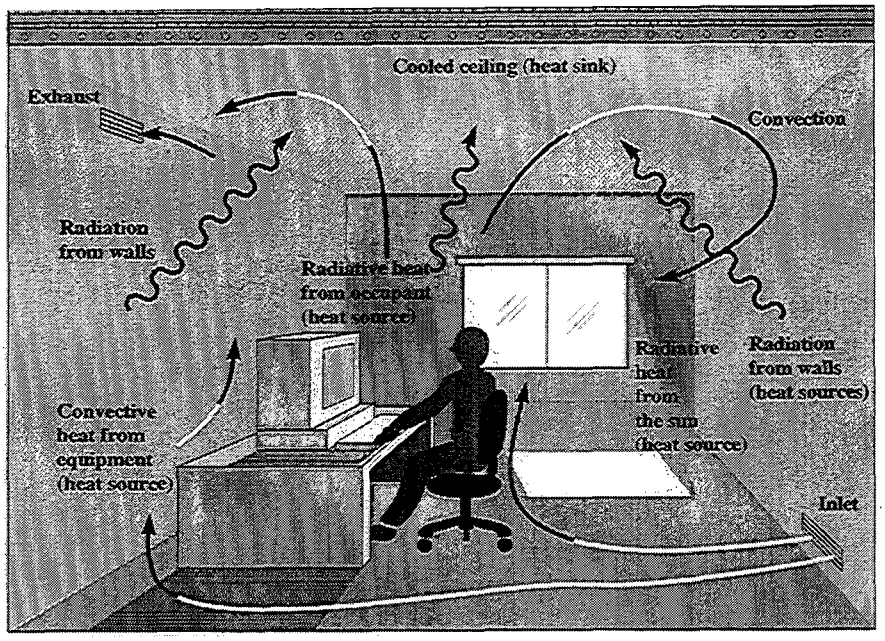

Figure 2.1. Air flow and heat exchange in a room with cooled ceiling.

It is worth noting that, if the radiant cooling surface is too cold, its presence in a space might cause vertical mixing, and thus lower the efficiency of the displacement ventilation. In practice however, the temperature of the radiant cooling surface is only a few degrees lower than that of the ambient air, and radiantly cooled spaces present characteristic, relatively stable, vertical air stratification.

Recent information about building practices in Europe [6] shows renewed interest in radiant cooling. A relatively large number of commercial buildings in Germany (see Table 2.1) and Switzerland are currently equipped with radiant cooling systems. In the US, radiant cooling systems have been installed in only two contemporary projects, both new construction: a commercial facility in Utah and a residence in Arizona. The author has been unable to find information about other projects that might involve radiant cooling in the near future.

Table 2.1 Data about radiant cooling systems installed in Germany in 1994 [6].

	Surfaces installed [1000 m^2]		Unfulfilled orders [1000 m^2]	
	New buildings	Retrofits	New buildings	Retrofits
Jan. 1 - Mar. 31	215	99	295	95
Jan. 1 - Dec. 31	496	314	435	300

2.3 Thermal Comfort Considerations

The human body continuously generates heat, with an output varying between 100 W for a sedentary person and 1000 W for a person exercising strenuously. To perform normal functions the body has to maintain a balance between heat generation and heat loss. Thermal comfort is usually defined as thermal neutrality,[1] and represents the condition in which a person would prefer neither warmer nor cooler surroundings.

Heat can be lost by the body in different ways: radiation to surrounding surfaces, convection to the ambient air, conduction, evaporation, respiration and excretion. Radiation has the highest heat transfer coefficient, and is followed in order by convection and conduction. The possibilities of increasing heat loss through respiration and excretion are very limited.

To explain the impact of radiation, Baker [21] gives the following example: "A person sitting out of doors under a clear sky on a summer evening may be chilly although the air temperature is in the high 70s (°F). Were he indoors at this same temperature, he probably would feel uncomfortably warm. The appreciable heat loss by radiation to the clear sky explains the different sensations of comfort between outdoors and indoors."

Heat loss by radiation is caused by the difference between the body surface temperature and the mean radiant temperature, which is a function of the temperatures of the surrounding surfaces. Fanger [22] defines mean radiant temperature as follows: "The mean radiant temperature in relation to a person in a given body posture and clothing placed at a given point in a room, is defined as that uniform temperature of black surroundings which will give the same radiant heat loss from the person as the actual case under study."

The mean radiant temperature is easy to define but quite complicated to calculate or measure in practice because of the nature of the variables required in the characterization

1. A person exposed to radiation asymmetry might experience thermal neutrality, but is frequently uncomfortable.

of the radiant exchange. For example, due to the non-uniform distances and angles of a person in relation to the walls, floor and ceiling of an enclosure, each part of the enclosure must be treated separately in the mean radiant temperature calculation. If a given surface is not isothermal, it must be divided into a collection of smaller isothermal surfaces. Each surface can be assumed to have high emissivity [23]. The radiation emitted and reflected from any surface is considered distributed as diffuse radiation, which is a good approximation for all normal non-metallic surfaces [22]. The enclosure surfaces often found in a typical room have rectangular shape, therefore the angle factors in the mean radiant temperature calculation are defined between a person and a number of vertical or horizontal planes. The body posture of a person is also important. The mean radiant temperature in relation to a standing person is not necessarily the same as in relation to a seated one [22]. Likewise, the location and orientation of the person inside the room must be known, because the mean radiant temperature often varies from point to point. The first experiments of thermal and comfort sensations to radiation experienced by seated persons were conducted by Schlegel and McNall [24], and McNall and Biddison [25].

If a person could not lose heat by radiation, and if convection were the only available heat loss mechanism, the rate of heat loss from the body would correspond to the air velocities close to the human skin. An increase in air velocities leads to an increase in heat loss. However, increasing air velocities beyond a certain limit would lead the air flow close to the skin into turbulent regime. Depending on the air temperature and turbulence intensity, further increase of air velocity in this regime may cause draft, and therefore a different type of discomfort.

Air movement plays a special role among the factors influencing comfort. According to Esdorn and collaborators [14], air movement is the single largest cause of complaints from building occupants. Beside the average air velocity, the fluctuation of the air velocity has an important influence on convective heat transfer at the human body surface. Mayer [26] relates comfort directly to the convective heat transfer coefficient, rather than to the average air velocity. According to Mayer [27], draft is felt at an air temperature of 22 °C if the convective heat transfer coefficient is above 12 W/m^2-K. This translates to average air velocities for laminar flows of 1.35 m/s, for transition flows of 0.15 m/s, and for turbulent flows of 0.10 m/s.[1] Lower air temperatures significantly reduce the acceptable air velocities.

The combined effects of radiation and convection inside an enclosure are often evaluated by using a parameter called the "operative temperature". Operative temperature is defined as the average of the ambient temperature and the mean radiant temperature inside the enclosure, weighed by their respective heat transfer coefficients. Another

1. Although this estimate may seem counterintuitive, it is consistent with the work of Fanger and collaborators [15]. They show that supplying air at 22 °C with a velocity of 0.10 m/s and 30% turbulence intensity would elicit complaints of draft from 10% of building occupants.

environmental index is the "effective temperature" ET*. Effective temperature combines ambient temperature, radiant temperature and humidity into a single index. Operative temperature and effective temperature as comfort parameters do not indicate the presence of radiation asymmetry inside an enclosure. Asymmetric or non-uniform thermal radiation may be caused in winter by cold windows, uninsulated walls or heated ceilings, and in summer by mechanically cooled ceilings. In cases where radiation asymmetry is important, the use of operative temperature or effective temperature in evaluating thermal comfort ought to be done cautiously, because it may lead to erroneous results.

Fanger [22] shows that the overall thermal sensation can be predicted by "the comfort equation", an equation that connects six variables that have a large influence on comfort. Fanger's comfort variables are: activity level (heat production in the body), thermal resistance of the clothing (clo-value), air temperature, mean radiant temperature, relative air velocity, and water vapor pressure in the ambient air. In his work, Fanger showed that although individuals of different gender, age, or race prefer the same thermal environment (i.e. indicate the same environmental conditions when in thermal neutrality), not all individuals react identically when exposed to heat or cold, low or high air velocities, etc. Fanger's work constitutes the basis for most of the contemporary comfort studies and comfort standards. For example, the "comfort zones" specified in ASHRAE Standard 55-92 [28] and ISO Standard 7730 [29] are based on Fanger's results. The "comfort zone" sets limits for the variation of each of the comfort variables, so that the resulting indoor environment be acceptable to 90% of building occupants (ASHRAE Handbook of Fundamentals [30], Chapter 8). In theory, air-conditioning systems are designed to maintain indoor conditions within the "comfort zone". In practice however, most air-conditioning systems maintain only the indoor air temperature and moisture within the limits specified by the "comfort zone".

2.4 The Cooling Power of Radiant Cooling Systems

Beside ensuring the cooling of a building, the operation of a radiant cooling system has to prevent or minimize two side-effects associated with the presence of the cold surface in the building. Prevention of these adverse side-effects limits the cooling power of the RC system.

The first side-effect is a decline in comfort due to the asymmetrical character of the radiant exchange in a room with a cooled surface. Based on Fanger's limit of 5% uncomfortable as a rule for determining the acceptability of a system, a radiant temperature asymmetry of 10 °C is acceptable in the presence of a cool wall, and of 14 °C is acceptable in the presence of a cooled ceiling [31]. Kollmar [32] shows that in an office environment the lower limit for cooled ceiling temperatures is 15 °C.

The second side-effect is condensation. In theory, the surface temperature of the radiant surface must not be lower than the dew-point temperature of the air in the cooled zone.

There are three strategies to minimize the risk of condensation inside a building equipped with a radiant cooling system: (1) control indoor and outdoor humidity sources (for example, by placing cooking zones near the return registers, venting showers directly to the outside, sealing windows shut, venting the building entrance, etc.), (2) for a given radiant surface temperature, reduce the dew-point temperature by dehumidifying the supply air, and (3) for a given range of the dew-point temperature of the ambient air, set a limit for the minimum radiant surface temperature. In practice, a combination of the three strategies is used: (1) radiant cooling systems are installed mainly in office buildings, where the internal sources of moisture are relatively easy to control; (2) the ventilation air is supplied at a certain temperature, and therefore is simultaneously dehumidified to a certain level; (3) the lower limit of the radiant surface temperature is generally set 2 °C higher than the average dew-point temperature of the ambient air.

The cooling power of a RC system is a function of the heat transfer between the room and the cooled ceiling. This heat transfer has two components: radiation and convection. The radiation heat transfer can be calculated based on the room geometry and room surface characteristics. The convective heat transfer is a function of the air velocity at the ceiling level, which in turn depends on the room geometry, the location and power of the heat sources, and the location of the air inlet and exhaust.

Trogisch [33] compares experimentally-derived heat transfer coefficients for cooled ceilings with the description of convective heat transfer (downward) from a cold flat surface, as published in textbooks. He finds that investigations concerning cooled ceilings report overall heat transfer coefficients of 9 to 12 W/m^2-K. Given a heat transfer coefficient for radiation of about 5.5 W/m^2-K for a difference of 10 °C between the mean radiant temperature and the cooled surface temperature, the resulting convective heat transfer coefficient would be in the order of 3.5 to 6.5 W/m^2-K. However, this range for the convective heat transfer coefficient is characteristic for forced convection, while in reality the air movement near the ceiling is driven by the temperature difference between the room air and the cool surface. Trogisch concludes that measurements and textbook formulas for heat transfer coefficients do not agree, therefore textbook formulas for the convection near the radiant surface should not be used in the evaluation of the overall heat transfer coefficient.

Radiant cooling elements extract heat from a room by cooling the air directly, through convection, and indirectly, by cooling the other surfaces of the room envelope. If the difference between the average room envelope temperature and the air temperature is small, the two effects can be estimated jointly [34]. Under this assumption, the specific cooling power of a cooled ceiling can be expressed by the following empirical equation:

$$q = 8.92\,(t_{air} - t_{cold\ surface})^{1.1} \qquad (2.1)$$

where

q is the sum of the convective and radiant heat transfer [W/m^2].

The 9 to 12 W/m^2-K overall heat transfer coefficient, together with the maximum temperature difference of 10 °C between the cooled surface temperature and the mean radiant temperature reported by Trogisch [33], suggest that the cooling power of radiant cooling ceilings is generally limited to around 120 W/m^2. A survey of cooled ceilings [35] reports cooling outputs ranging from 40 to 125 W/m^2. However, the survey is based on information from manufacturers, and does not specify the boundary conditions under which the reported cooling outputs were measured. This brings up the necessity of establishing standards for both measurement conditions, and measurement techniques for the cooling output of radiant panels. As discussed below, significant efforts have already been made in this direction.

• A test facility and a method of testing have been developed at the Department of Veterans Affairs. Their final report [36] proposes a procedure for the measurement of the thermal performance of radiant panels in the test facility and indicates the accuracy of the instrumentation necessary.

• ASHRAE's technical committee *TC 6.5 Radiant Space Heating and Cooling* currently sponsors committee SPC 138 P. The purpose of SPC 138 P is to establish a method of testing that enables the rating of the thermal performance of radiant panels used for heating and/or cooling of indoor spaces [37].

• In Germany two competing test procedures have been published. The Fachinstitut Gebaeude-Klima (FGK) presented its testing procedure in December 1992 [38]. The FGK industrial standard is based on the measurement of the cooling power of radiant panels in a rectangular enclosure (2.4 m x 1.2 m x 1.5 m) with an internal operative temperature of 26 °C. The panel water supply temperatures are 12, 14, and 16 °C. The DIN-standard was presented in April 1993 [39]. It measures the performance of radiant panels in the presence of natural convection. The test is based on measurements performed in a closed test chamber (4 m x 4 m x 3 m) with a conditioned metal envelope. The cooling load is simulated by 12 perforated tubes containing three 60 W bulbs each. The measurements are performed under steady-state conditions, for a range of temperatures and water mass flows.

While testing procedures and future standards can rate the performance of a radiant cooling system with panels under given boundary conditions, the efficiency of the same system in a specific, but different, application is difficult to determine. The difficulty arises from the fact that the rated performance greatly depends on the testing procedure. For example, a procedure for measuring the efficiency of a cooled ceiling could use the temperatures of the ceiling and of the exhaust air in a test room as a measure for the convective heat transfer between the ceiling and the room air. In a hypothetical situation, a shortcut between the supply and the exhaust of the ventilation system in the test room could cause high air velocities near the ceiling surface. In this situation a large fraction of the exhaust air would be air that has been cooled by the ceiling but that has not interacted with the rest of the room. The small difference between the temperatures of the ceiling

surface and the exhaust air would suggest in this case a convective heat transfer higher than in reality. The measurements would therefore appear as having been performed under low air flows, and the ceiling would appear to have high cooling power. The functioning of the same ceiling in a normal situation (without the short-circuit causing forced convection) is likely to give different results. Noting the importance of information collected from such measurements, these considerations show the current difficulties encountered by a building designer faced with a specific application. Before deciding to use a type of radiant cooling system, a designer should consider the details of the testing/rating procedure performed for the given type, and compare the rating with that for other types of radiant cooling systems available on the market.

2.5 Numerical Modeling of Radiant Cooling Systems

The theoretical performance of radiant cooling systems can be evaluated by numerical modeling of the thermal behavior of buildings equipped with radiant cooling systems. The few computer models currently available were developed as design tools for radiant cooling systems. In general, these codes cannot be used to determine the behavior of radiant systems in any conditions other than the design conditions.

Emulating building engineering practice, the code developed by Kilkis and collaborators [40] proposes a design procedure for radiant cooling systems that assumes steady-state conditions. Koschenz and Dorer [41] acknowledge the fact that the design of radiant cooling systems should be done based on dynamic calculations. However, their design procedure does not employ a truly dynamic method, as they use a step-by-step approach that ignores feedback effects in the thermal balance of their test room. Niu and van der Kooi [42] propose a similar step-by-step approach.

The simulation codes developed so far are either stand-alone programs [40], [42], or use sections of existing building energy analysis programs (for example, instead of developing a simulation code for an entire numerical room, Koschenz and Dorer [41] create a numerical room by connecting their code for a cooled ceiling with TRNSYS modules for the other room surfaces). Consequently, none of the large building energy analysis programs available publicly (DOE-2, TRNSYS, BLAST) has the capability to simulate buildings cooled by radiant cooling systems. There have been attempts to adapt DOE-2 so that it can approximate radiant cooling performance [43] -[44]. However, this approach involves laborious artifices, and is not accessible to the average DOE-2 user. A separate module simulating the specifics of radiant cooling systems should therefore be designed and integrated into one of the existing building analysis programs.

2.6 Cooling Performance of Radiant Cooling Systems: Case Studies

In the absence of a computer program to evaluate the dynamic effects associated with the

operation of a RC system, back-of-the-envelope calculations, pilot projects, and case studies based on existing buildings are the only sources of quantitative information about radiant cooling system performance. This section describes two experimental investigations of the performance of radiant cooling. The next section contains a back-of-the-envelope calculation of the peak power savings potential of a radiant cooling system as compared to an all-air system.

Kuelpmann [45] reports on an experimental investigation in a temperature-controlled test cell. In his experiments the air was supplied at floor level and exhausted approximately 0.2 m below the ceiling level. Internal loads were simulated by fluorescent lights and by electrically heated mannequins seated next to computer displays. External loads were introduced by heating either one of the side walls, or the floor. For displacement ventilation and no cooling with supply air, the room air temperatures measured at different heights did not differ very much.

The extraction of 100 W/m^2 internal load by the radiant cooling system caused temperature differences of approximately 2 °C between the air supply and exhaust registers. Upon increasing the temperature difference between the room air and the supply air, the vertical profile of the room temperature became more pronounced. In this case, in the lower part of the room, the vertical temperature profile became close to, or exceeded the comfort limits.

In all cases examined by Kuelpmann the differences between the room air temperature and the surface temperatures of the "internal walls" were relatively small (0.4 °C). Due to the radiation exchange with the cooled ceiling, the floor surface temperature was usually below the wall surface temperatures.

Kuelpmann measured air flow velocities at 1 m distance from the supply air grille, at 0.1m height above ground. At an air exchange rate of 3.2 air changes per hour (ACH) and a supply air temperature of 19 °C, the measured mean air velocity and turbulence intensity were low (0.12 m/s and 20%).

Measurements of radiant temperature asymmetry at 100 W/m^2 cooling power in Kuelpmann's showed an 8 °C difference at 1.1 m above the floor level, in the middle of the room. This corresponds to less than 2% of occupants dissatisfied [28].

The performance of radiant cooling was also tested in two parliamentarian offices in Bonn, Germany [46]. The outside air, supply air and room air temperature and relative humidity were measured. Temperature measurements were also made in the supply and return water registers of the radiant system, and at three points on the ceiling surface. For an outside air temperature of 30 °C the air velocities measured in the occupied zone were less than 0.10 m/s. Below the ceiling, near-surface air velocities between 0.10 and 0.15 m/s were detected. These low velocities indicate that less than 40% of the heat transfer to the cooled ceiling occurs by convection.

2.7 Cooling Performance of Radiant Cooling Systems: Back-of-the-Envelope Calculation

The following exercise uses simple calculations to compare the electrical peak power demand of an all-air system and a RC system that provides the same indoor air temperature and relative humidity to a given space.

Consider an office space with a floor area of 25 m^2, two-person occupancy, and total heat gain (solar heat gain and internal gains from occupants, equipment and lights) of 2000 W. The specific cooling load amounts to 80 W/m^2 of floor area, which is in the range manageable by a radiant cooling system. The room temperature setpoint is 26 °C. Additional assumptions and design considerations are shown in Table 2.2.

The all-air system supplies cooling to the room as follows: a cooling coil dehumidifies the outside air according to the target room conditions. ASHRAE Standard 62-1989 [47] specifies a minimum air volume flow of 36 m^3/h person, which means that for this example the minimum outside air volume flow must be 72 m^3/h. To remove internal heat gains, a recirculating volume flow of 678 m^3/h is necessary. For an outside air temperature of 32 °C and a return air temperature of 26 °C, the mixing temperature is 26.5 °C. Similarly, the humidity ratio of the mix of outside and return air is 10.75 g water/kg dry air.

The 26.5 °C mix of outside and return air is directed through a cooling coil. To adjust for the temperature increase due to the fan work, the air must be cooled further than the 18 °C specified as supply air temperature. The temperature adjustment depends on the pressure drop, fan efficiency and volume flow. In this example, the air handling temperature rise is considered equal to 1.0 °C, therefore the supply air is cooled to 17 °C.

To remove the internal latent load generated by the two occupants of the office space, the mix of supply and return air must be dehumidified below the design humidity ratio of the office space (10.6 g water/kg dry air). Consequently, the 18 °C air is supplied to the office with a humidity ratio of 10.47 g water/kg dry air.

To compare the two systems, the boundary conditions must be the same. This includes the efficiencies of fans and motors, the pressure drops on the supply and exhaust fans, and the coefficient of performance (COP) of the chiller. Considering the air volume flow and the pressure drop across the fans (see Table 2.2), the supply fan electrical power demand is 222 $W_{electric}$, and the return fan electrical power demand is 111 W_e. The cooling coil requires 721 W_e for air sensible cooling and 216 W for air dehumidification.

While the all-air system removes the cooling load by means of circulating cold air, the RC system removes the load mainly by means of water circulation. The tasks of the ventilation side of the RC system are to supply the room with the fresh air rate specified by ASHRAE Standard 62-1989 (72 m^3/h for a double-occupancy office), and to avoid humidity buildup by controlling the dew-point in the room. To provide a stable displace-

Table 2.2 Assumptions used for the comparison of peak power demand for an all-air system and a RC system conditioning the same office space.

	Both Systems	
Room Conditions:		
Cooling Load [W/m^2]	80	
Room Air Temperature [°C]	26	
Relative Humidity [%]	50	
Humidity Ratio [$g_{water}/kg_{dry\ air}$]	10.6	
Number of People	2	
Outside Air Conditions:		
Air Temperature [°C]	32	
Relative Humidity [%]	40	
Humidity Ratio [$g_{water}/kg_{dry\ air}$]	12.1	
Enthalpy [kJ/kg]	63.0	
	All-air system	RC system
Design Consideration:		
Outside Air Flow [m^3/h]	72	72
Supply Air Flow [m^3/h]	750	72
Supply Fan [W_e]	222	22
Return Fan [W_e]	111	11
Water Pump [W_e]	--	20
Temperature Differences:		
Room Air - Supply Air [°C]	8	3
Room Air - Ceiling [°C]	0	8
Supply Water - Return Water [°C]	--	2
Efficiencies:		
Fan: Hydraulic/Mechanical/Electrical [%]	60/80/98	60/80/98
Water Pump [%]	--	60
Pressure Drop:		
Supply Duct/Return Duct/Water pipe [Pa]	500/250/--	500/250/4000
COP	3	3

ment ventilation, the ventilation air should supplied at only about 3 °C below the room air temperature. The required temperature of the supply air cannot be more than 23 °C. The cooling power of the ventilation air is about 72 W (3 W/m^2). The radiant cooling ceiling must therefore remove the difference to 80 W/m^2.

To remove the internal latent load, the supply air must be dehumidified to 9.2 g water/kg dry air, which indicates that the outside air must be cooled to 13 °C, which is lower than the prescribed 23 °C supply temperature. However, a reheater can be installed which warms the air using waste heat from the compressor. The air could be warmed more efficiently if channeled through building components before arriving to the room inlet. This would save the power to reheat and provide some conditioning at the same time.

The power demand calculation for the RC system shows that the electrical power demand is 22 $W_{electric}$ for the supply fan, 11 W_e for the return fan, and 20 W_e for the water pump. The cooling coil requires 21 W_e for air sensible cooling, 641 W_e for water sensible cooling, and 216 W_e for air dehumidification.

Table 2.3 summarizes the components of the electrical power demand of the all-air system and the RC system. The values in the table show that the electrical power demand of the RC system is only 71.5% of the electrical power demand of the all-air system.

Table 2.3 Estimated electrical power demand for the removal of internal loads from a two-person office with a floor area of 25 m^2.

	All-Air System	RC System
Supply Fan [W]	222	21
Air Sensible Cooling [W]	721	--
Air Dehumidification [W]	216	216
Exhaust Fan [W]	111	11
Water Pump [W]	--	20
Water Sensible Cooling [W]	--	641
Total	1270 W	909 W
	100%	71.5%

2.8 Economics of Radiant Cooling Systems

Although companies that manufacture radiant cooling systems provide general design and cooling power information, they generally do not disclose information regarding the economics of already-installed systems, on the grounds that it is proprietary. However, a few papers were found that address the economics of radiant cooling systems.

Feil [48] compares different ventilation/cooling systems for an office. In a comparison with a variable air volume (VAV) system, Feil shows that a RC system has lower first-cost if the peak specific cooling load is higher than 55 W/m^2. The break-even specific cooling load of 55 W/m^2 corresponds to a first cost of approximately 575 DM/m^2 of floor space (in 1991 DM). Because the first cost structure is different in US and in Germany, translating this first cost into US$/m^2 provides a value of little significance for the US market.

Hoenmann and Nuessle [49] estimate yearly energy consumption for an office building in Europe (see Table 2.4). The building has 5000 m^2 of floor area distributed over four floors. The peak specific cooling load is 50 W/m^2. The relatively low savings potential for the overall energy consumption of the building (less than 8%), is due to the large energy consumption by heating and lighting. Unfortunately, the authors do not provide consumption data for cooling only. Furthermore, the VAV system uses an economizer mode, while the analogous savings potential is not matched in the RC system by a water-side economizer.

Table 2.4 Estimated annual energy consumption [kWh/m^2] for a European office building with a floor area of 5000 m^2 [49].

	VAV System	RC System
Heating	43	43
Domestic Hot Water	4	4
Lighting	34	34
Miscellaneous	10	10
Ventilation	12	8
Fans/Pumps	31	24
Cooling	7	8
Total	141	131

The space requirement for the two systems are shown in Table 2.5 [49]. The largest space savings, 36%, appear in the equipment rooms, followed by 28% for the air shafts.

Table 2.5 Estimated space requirements for air-conditioning systems in a European office building with a floor area of 5000 m^2 [49].

	VAV System	RC System
Shafts [m^2]	25	18
Equipment Rooms [m^2]	165	107
Plenum Height [m]	0.4	0.1

For systems with dropped ceilings the reduction in height per floor is in the order of 0.15 to 0.20 m. Radiant systems that consist of water coils embedded into the ceiling lead to even higher space savings.

For first cost calculations, Hoenmann and Nussle [49] estimate that their aluminum panel system has a lower first cost than an all-air system if peak specific cooling loads exceed 50 W/m^2, and ventilation air is supplied at an air exchange rate of 3 ACH.

2.9 Types of Radiant Cooling Systems

Most radiant cooling systems belong to one of four different system designs. The most often used system is the panel system, built from aluminum panels with metal tubes connected to the side of the panel facing away from the conditioned space (see Figure 2.2).

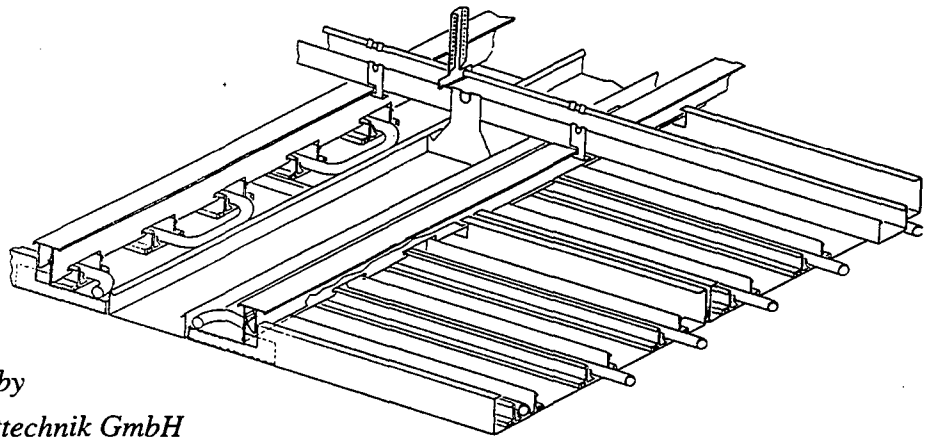

Drawing by
Fläkt Lufttechnik GmbH

Figure 2.2 Construction of a cooling panel [49].

The connection between the panel and the tubes is a critical detail. Poor connections provide only limited heat exchange between the tubes and the panel, resulting in increased temperature differences between the panel surface and the cooling fluid. Panels built in a "sandwich system" include the water flow paths between two aluminum panels (similar to the evaporator in a refrigerator). This arrangement reduces the heat transfer problem and increases the panel surface directly cooled.

In the case of panels suspended below a concrete slab, approximately 93% of the cooling power is available to cool the room. The remaining 7% cools the floor of the room above

(see Figure 2.3).[1]

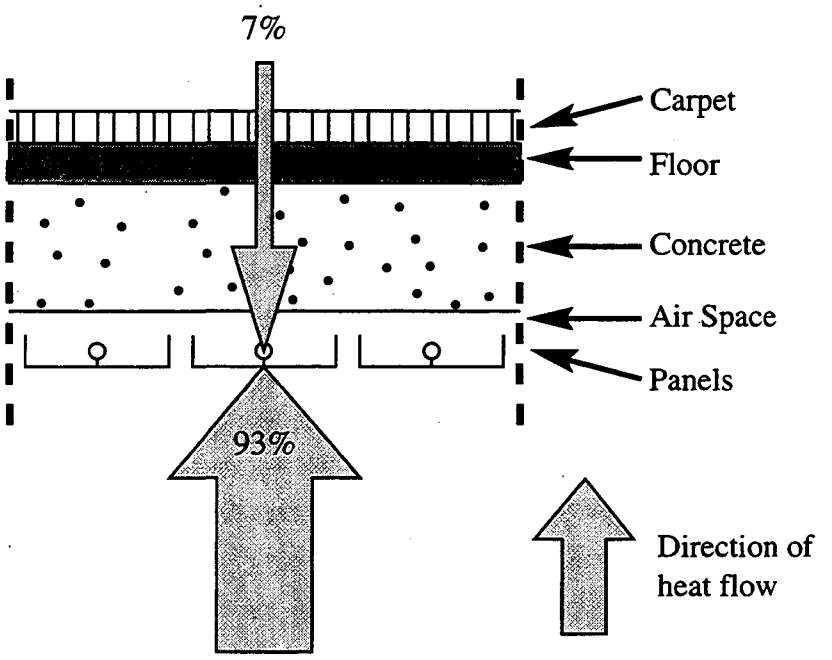

Figure 2.3 Heat transfer for the panel system (cooling mode) [50].

The temperature profiles for the different ceiling panel systems have been published by Graeff [51].

Cooling grids (Figure 2.4) made of small plastic tubes placed close to each other can be embedded in plaster or gypsum board. Cooling grids can also be mounted on ceiling panels such as acoustic ceiling elements. This second system was developed in Germany and has been on the market for several years. Because the plastic tubes are flexible the cooling grid system may be the best choice for retrofit applications.

When the tubes are embedded in plaster the heat transfer from the room above is higher than in the case of cooling panels (Figure 2.5). The heat transfer to the concrete slab couples the cooling grid to the structural thermal storage of the slab. Adding a layer of insulation below the floor reduces the cooling power dedicated to cooling the floor of the room above.

Plastic tubes mounted on suspended cooling panels show thermal performance compara-

1. While cooling the floor of the room above does not constitute a loss of cooling energy, it may cause discomfort due to un unwanted cooling of the occupants at ankle level. Therefore, it is preferable that the fraction of the cooling power dedicated to cooling the room be as high as possible.

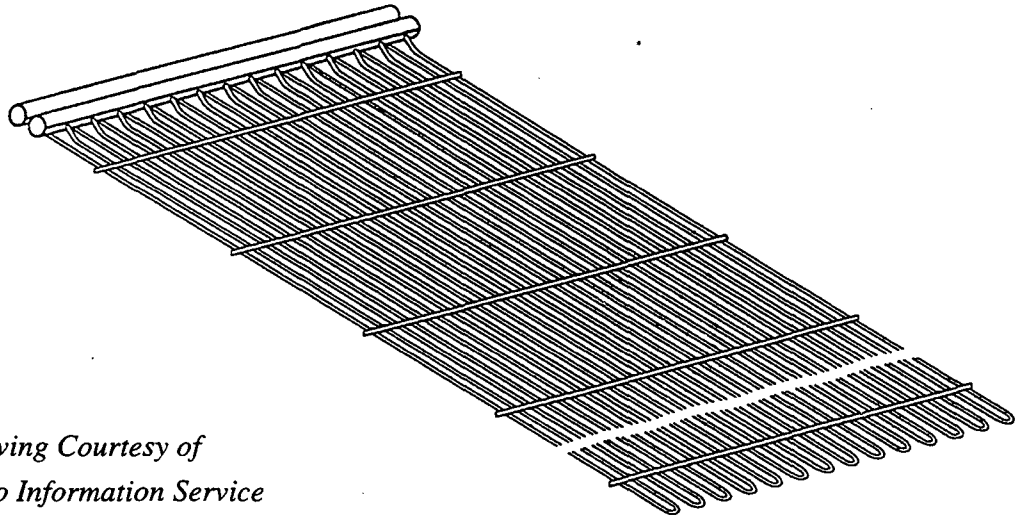

Drawing Courtesy of
KaRo Information Service

Figure 2.4. Construction of a cooling grid [49].

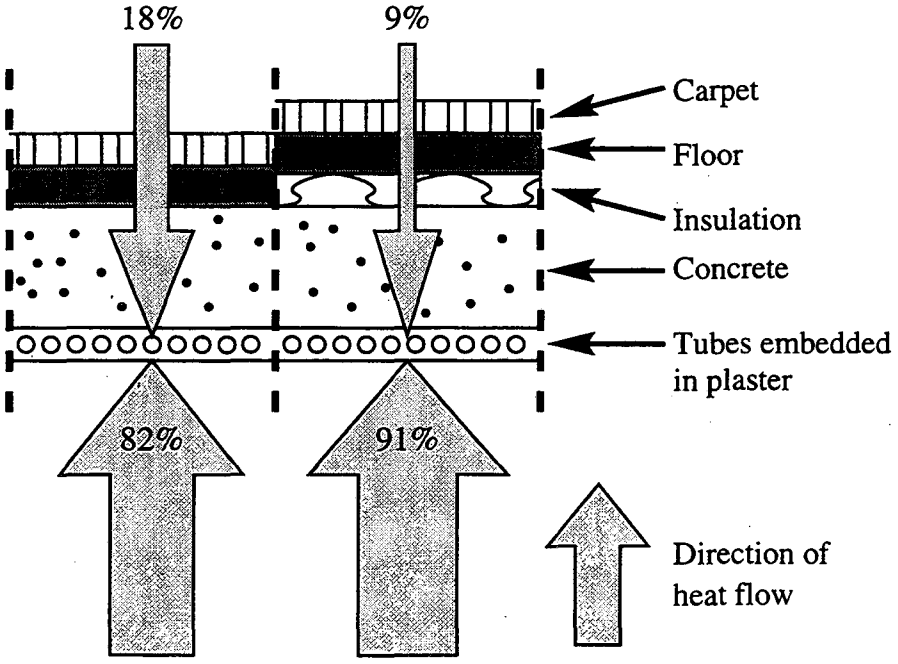

Figure 2.5 Heat transfer for ceiling with cooling grid [50].

ble to that of the panel systems described above. Tubes embedded in gypsum board can

be directly attached to a wooden ceiling structure without a concrete slab. Insulation must be applied in this case to reduce the cooling of the floor above.

A third system is based on the idea of a floor heating system. Plastic tubes are embedded in the core of a concrete ceiling. The thermal storage capacity of the ceiling allows for peak load shifting but limits the ability to control the concrete core system. Relatively high surface temperatures are therefore required for the ceiling, to avoid the uncomfortable conditions that would occur in the case of a sudden drop in loads. This high temperature requirement limits the cooling power of the system [52].

The concrete core cooling system is particularly suited for coupling with alternative cooling sources, especially the heat exchange with cold night air. The faster warming of rooms with a particular high thermal load can be avoided by operating the water pump for short times during the day. A balance between these warm rooms and rooms with a lower thermal load can be achieved this way.

Due to the location of the cooling tubes in the core cooling system, a higher portion of the cooling is applied to the floor of the space above the slab. Approximately 83% of the heat removed by the circulated water is from the room below the slab, while 17% is from the room above (Figure 2.6 [50]).

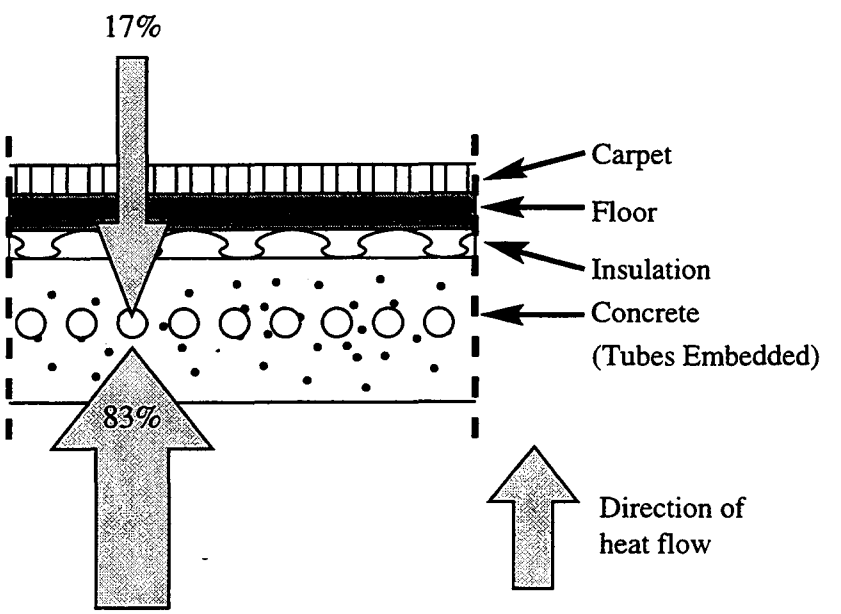

Figure 2.6 Heat transfer for concrete core cooling system [50].

A fourth system has been developed in Germany, but is also commercially available in California. It provides cooling to a raised floor. In this system the ventilation supply plenum is located under the floor. Air is supplied below the windows, reducing the radiative effect of cold window surfaces in winter and hot window surfaces in summer [53].

2.10 Radiant Cooling System Controls

In spaces conditioned by radiant cooling systems, the cooling power of radiant heat exchange is limited by the need avoid the formation of condensation on the radiant surface. As discussed in Section 2.4, the risk of condensation is avoided in practice by simultaneously dehumidifying the ventilation air to a certain level, and maintaining the cooling surface above the dew-point of the ambient air for all operational conditions. If the dew-point is further reduced through dehumidification of the supply air, the temperature of the radiant surface can also be reduced, and higher sensible loads can be removed by radiation. As the cooler temperature of the radiant surface increases radiation asymmetry and decreases operative temperature and effective temperature, precautions must be taken in such a case not to exceed the comfort limits in the space. In particular, the temperature of the cooling surface should not be reduced below the limit of 15 °C [32], and the indoor air temperature should be controlled so that the effective temperature is maintained within the range specified by ASHRAE Standard 55-1992 [28] (23-26 °C for summer conditions and 20-23 °C for winter conditions).

Another strategy of reducing the risk of damage due to condensation is to switch off the supply of cold water as soon as the relative humidity reaches "dangerous" levels. A variation of this control scheme consists of window contacts that switch off the water supply if windows are opened.

The different types of RC systems presented in Section 2.9 have very different response times, and this influences the temperature control strategy that can be employed for each type of system. Panel systems with water supply close to the cooling surface and with little thermal mass have a response time comparable to all-air systems. The cooling grid system and concrete cooling system work with high thermal mass and are relatively slow in response to load changes. However, control strategies can be designed to allow all types of radiant systems to promptly remove the cooling loads associated with indoor temperature swings. For example, Meierhans [50] reports on the control strategy adopted in an office building equipped with a core cooling radiant system. He states that operating the radiant system at night to pre-cool the building structure eliminates the need for mechanical daytime cooling during most of the cooling season (the ventilation system *is* operated during the day). Information regarding the internal sensible loads of the building allows the adaptation of this nighttime pre-cooling operation to virtually any daytime cooling needs of the building. Such an operation of the radiant system not only makes the system compatible with operable windows, but also restores some natural variability into the building.

2.11 Summary

Following a few applications in the late 1930s to the 1950s, radiant cooling was more or less abandoned in Europe as well as in the United States. User complaints about all-air systems have changed some designers' attitude towards these systems, and have led to new system designs incorporating better controls. When combined with efficient ventilation systems, and when the humidity controls and operation strategies are finely-tuned to respond to the specific needs of each situation, RC systems present several advantages when compared to traditional all-air systems.

The reviewed literature shows that RC systems provide draft-free cooling, reduce building space requirements, reduce the energy consumption for thermal distribution and for space conditioning, and might even have lower first-cost, if peak specific cooling loads exceed 50 - 55 W/m^2.

Literature has not been found that describes the dynamic thermal behavior of RC systems in buildings. Dynamics are important because the comfort temperature in a space is not only dependent on the air temperature, but also on the (dynamic) variation of the surface temperatures in the space. Since existing thermal building simulation programs do not provide the data necessary for evaluating the dynamic performance of RC systems, the development of dynamic models is the logical next step in examining their potential.

2.12 References

1. National Air Filtration Association, *NAFA Guide to air filtration, first edition*. NAFA, Washington, DC, 1993.

2. Anthony Usibelli, S. Greenberg, M. Meal, A. Mitchell, A. Johnson, G. Sweitzer, F. Rubinstein, D. Arasteh, *Commercial-sector conservation technologies*. Rep. LBNL-18453, 1985.

3. Helmut E. Feustel, *Economizer rating*. Final Rep. prepared for Southern California Edison Company, 1989.

4. David Jump and M. Modera, *Energy impacts of attic duct retrofits in Sacramento houses*. Proc. ACEEE 1994 Summer Study on Energy Efficiency in Buildings, American Council for an Energy Efficient Economy, Washington, DC.

5. T. Napier Adlam, *Radiant heating*. Second Edition, The Industrial Press, New York, 1949.

6. Helmut E. Feustel, Personal communication, Lawrence Berkeley National Laboratory, June 1995.

7. John K. Manley, Editor, *Radiant heating, radiant cooling*. School of Architecture, Pratt Institute, 1954.

8. F. E. Giesecke, *Hot-water heating and radiant heating and radiant cooling*. Technical Book Company, Austin, 1946.

9. Helmut E. Feustel, C. Stetiu, R. Meierhans, and U. Schulz, *Hydronic radiant cooling - a case study.* Proc. Healthy Buildings '94, Budapest, Hungary, 1994.

10. P. Kroeling, *Gesundheits- und Befindensstoerungen in klimatisierten Gebaeuden.* Zuckschwerdt Verlag, Munich, 1985.

11. P. O. Fanger, *Strategies to avoid indoor climate complaints*. Proc. Third Int. Congr. Building Energy Management, ICBEM '87, Presses Polytechnique Romandes, Lausanne, Switzerland, 1987.

12. M. Mendell and A. H. Smith, *Consistent pattern of elevated symptoms in air-conditioned office buildings: a reanalysis of epidemiologic studies.* Am. J. Public Health, (80) (10) 1990.

13. M. J. Mendell, *Nonspecific symptoms in office workers: a review and summary of the epidemiologic literature*. Indoor Air, (3) (4): 227-236, 1993.

14. H. Esdorn, H. Knabl, and R. Kuelpmann, *Air-conditioning, new horizons - new opportunities*. Proc. Indoor Air '87, Berlin, Germany, 1987.

15. P.O. Fanger, A. Melikov, H. Hanazawa, and J. Ring, *Air turbulence and sensation of draught*. Energy and Buildings (12) (1) 1988.

16. G. M. Keller, *Energieaufwand fuer den Lufttransport mindern*. Clima Commerce Int., (21) (2) 1988.

17. E. Skaret, *Displacement ventilation*. Proc. Roomvent '87, Stockholm, Sweden, 1987.

18. H. Sutcliff, *A guide to air change efficiency.* Tech. Note AIVC TN 28, Air Infiltration and Ventilation Centre, Coventry, 1990.

19. H. M. Mathisen, *Analysis and evaluation of displacement ventilation.* Ph.D. thesis, Rep. No. 1989:31 Division of Heating and Ventilation, NTH, Switzerland, 1989.

20. C. W. Cox, P. J. Ham, J. M. Koppers and L. L. M. Van Schijndel, *Displacement ventilation systems in office rooms - a field study.* Proc. Room Vent '90, Oslo, Norway, 1990.

21. M. Baker, *Improved comfort through radiant heating and cooling*. ASHRAE J., (2) (2) 1960.

22. P. O. Fanger, *Thermal comfort analysis and applications in environmental engineering*. Mc.Graw Hill, New York, 1972.

23. C. O. Pedersen, D. Fisher and P. C. Lindstrom, *Impact surface characteristics on radiant panel output.* Rep. ASHRAE-876 TRP, 1997.

24. J. C. Schlegel and P. E. McNall, *The effect of asymmetric radiation on the thermal and comfort sensations of sedentary subjects.* ASHRAE Trans., (74) 1968.

25. P. E. McNall, and R. E. Biddison, *Thermal and comfort sensations of sedentary persons exposed to asymmetric radiant fields.* ASHRAE Trans., (76) (1970).

26. E. Mayer, *Auch die Turbulenzen sind wichtig.* Clima Commerce Int., (19) (10) 1985.

27. E. Mayer, *Air velocity and thermal comfort.* Proc. Indoor Air '87, Berlin, Germany, 1987.

28. ASHRAE Standard 55-1992, *Thermal environmental conditions for human occupancy.* American Society of Heating, Refrigeration and Air-Conditioning Engineers, Inc., Atlanta, 1992.

29. ISO, *Moderate thermal environments - determination of the PMV and PPD indices and specification of the conditions for thermal comfort.* International Standards Organization, Standard 7730, Geneva, Switzerland, 1984.

30. ASHRAE Handbook, *Fundamentals.* American Society of Heating, Refrigeration and Air-Conditioning Engineers, Inc., Atlanta, 1993.

31. P. O. Fanger, B. M. Ipsen, G. Langkilde, B. W. Olesen, N. K. Christensen, and S. Tanabe, *Comfort limits for asymmetric thermal radiation.* Energy and Buildings, (8) 1985.

32. A. Kollmar, *Die zulaessige Kuehldeckentemperatur aus waermephysiologischer Sicht.* Gesundheits-Ingenieur, (88) (5) (1967).

33. A. Trogisch, *Kuehldecke und Lueftung.* Clima Commerce Int., (24) (4) 1991.

34. B. Glueck, *Leistung von Kuehldecken.* Kuehldecke und Raumluft, Fachinstitut Gebaeude-Klima, Stuttgart, Germany, 1990.

35. Anon., *Marktuebersicht Kuehldecken.* KI Klima-Kaelte-Heizung, (1-2) 1993.

36. Anon., *Radiant metal ceiling panels -a method of testing performance.* Department of Veterans Affairs (date unknown).

37. Anon., *SPC 138P, Method of testing for rating hydronic radiant ceilings.* Handout at the SPC138P Meeting, June 1996, San Antonio, TX.

38. FGK Vorschrift KD 1, *Vorschriften des Fachinstituts Gebaeude-Klima e.V. fuer: Waermetechnische Messungen an Kuehldeckenelementen.* Fachinstitut Gebaeude-Klima e.V., Bissingen-Bietigtheim, Germany, 1992.

39. DIN 4715 Entwurf, *Raumkuehlflaechen; Leistungsmessung bei freier Stroemung; Pruefregeln.* Beuth Verlag GmbH Berlin, Germany, 1993.

40. i. B. Kilkis, S. S. Sager and M. A. Uludag, *A simplified model for radiant heating and cooling panels*. Simulation Practice and Theory, (2) 1994.

41. M. Koschenz and V. Dorer, *Design of air systems with concrete slab cooling*. Proc. 5th Int. Conf. Air Distribution in Rooms, Yokohama, Japan, 1996.

42. J. Niu and J. van der Kooi, *Indoor climate in rooms with cooled ceiling systems*. Building and Environment, (29) (3) 1994.

43. Bruce E. Birdsall, W. F. Buhl, K. L. Ellington, A. E. Erdem, F. C. Winkelmann, J. J. Hirsch, and S. D. Gates, *DOE-2 Basics*. Rep. LBNL-35520, 1994.

44. Gerhard Zweifel, *Simulation of displacement ventilation and radiative cooling with DOE-2*. ASHRAE Trans., (99) (2) 1993.

45. R. Kuelpmann, *Thermal comfort and air quality in rooms with cooled ceilings - results from scientific investigations*. ASHRAE Trans., (99) (2) 1993.

46. H. Esdorn and M. Ittner, *Betriebsverhalten von Deckenkuehlsystemen*. HLH Heizung-Lueftung- Haustechnik, (41) 1990.

47. ASHRAE Standard 62-1989, *Ventilation for acceptable indoor air quality*. American Society of Heating, Refrigeration and Air-Conditioning Engineers, Inc., Atlanta, 1989.

48. K.-H. Feil, *Wirtschaftliche Betrachtungen zu Kuehldecken in Bueroraeumen*. Kuehldecke und Raumlueftung, Fachinstitut Gebaeude-Klima e.V., Bietigheim-Bissingen, Germany, 1991.

49. W. Hoenmann and F. Nuessle, *Kuehldecken verbessern Raumklima*. Kuehldecke und Raumlueftung, Fachinstitut Gebaeude-Klima e.V., Bietigheim-Bissingen, Germany, 1991.

50. Robert Meierhans, Personal communication, Lawrence Berkeley National Laboratory, November 1992.

51. B. Graeff, *Kuehldecke und Raumklima*. Kuehldecke und Raumlueftung, Fachinstitut Gebaeude-Klima e.V., Bietigheim-Bissingen, Germany, 1991.

52. R. Meierhans and M. Zimmermann, *Slab cooling and earth coupling*. Proc. Innovative Cooling Systems, International Energy Agency, Energy Conservation in Buildings and Community Systems, Solihull, UK, 1992.

53. Anon., *Advanced hydronic heating and cooling technology*. Leaflet, eht-Siegmund, Inc., Tustin, CA (date unknown).

Chapter 3

RADCOOL - A TOOL FOR MODELING BUILDINGS EQUIPPED WITH RADIANT COOLING SYSTEMS

3.1 Modeling Approach

The review presented in Chapter 2 indicates that commercial buildings equipped with radiant cooling (RC) systems may require less energy and peak power for thermal conditioning than buildings equipped with traditional all-air systems. Unfortunately, because the information currently available is applicable only to a small number of buildings, it is inadequate in assisting the general design and operation of buildings equipped with radiant cooling systems. Moreover, the transient behavior of radiant cooling systems exposed to variable loads defies evaluation by simple calculation. Under these circumstances, a computer program capable of simulating the dynamic effects associated with the functioning of RC systems constitutes a necessary tool for the study of the thermal performance of buildings equipped with radiant cooling systems.

It is often difficult to simulate new technologies with existing building simulation programs (such as DOE-2, BLAST, TRNSYS). This feature can be generally traced back to the initial stages in the development of these programs. In the case of DOE-2, the choice of algorithms was mainly dictated by the limited capabilities of computers in the early 1980s. Specifically, to simplify calculations and reduce simulation time, DOE-2 calculates the heat transfer through building components (walls, windows) with the response factor method.[1] DOE-2 then estimates the cooling and heating loads for each space by using the weighting factor method.[2] Since these modeling methods bypass the calculation of the surface temperature distributions of building components at least in its present stage of development, DOE-2 cannot model buildings equipped with radiant cooling systems. After employing extensive modeling artifices, the few DOE-2 users who have attempted to model existing buildings equipped with radiant cooling systems have failed to produce results that agreed with measurements from these buildings (see for example [2]).

---

1. The response factor method calculates the heat gain or loss through a building component by reducing the "heat excitation" due to weather conditions, interior loads, etc. to a collection of triangular pulses. The solution of the one-dimensional heat diffusion equation with the triangular pulses as boundary conditions consists of a set of response factors. The response factors provide a quantitative description of the heat transfer through the building component due to the given "heat excitation" [1].

2. The weighting factor method uses z-transfer functions to calculate the cooling and heating loads of a space from instantaneous heat gains or losses (due to heat transfer through building components, interior loads, etc.). The calculation produces a set of parameters that provide a quantitative description of how much of the heat entering the space is stored, where it is stored, and how fast the heat stored is released during later hours [1].

The author designed the program RADCOOL specifically to simulate the dynamic performance of buildings equipped with radiant cooling systems. RADCOOL (described in detail in Appendix A) is a highly modular building simulation tool based on a complete energy-balance calculation.[1] The ultimate goal for RADCOOL is to operate as a DOE-2 module as soon as DOE-2 development will allow the calculation of surface temperature distributions in buildings. Functioning as a DOE-2 module would allow RADCOOL access to the results obtained by other DOE-2 modules such as the module that calculates the direct and diffuse solar radiation incident on a building surface of any orientation, the subroutine that allows access to weather data, etc. This in turn would reduce the preliminary work presently necessary in the RADCOOL simulation process. Incorporating RADCOOL into DOE-2 would also eliminate several limitations currently imposed on RADCOOL simulations (see Section 3.1.2).

3.1.1 Model capabilities

RADCOOL consists of a library of building components, plus a method to assemble these components into numerical building models. Consequently, each building modeled in RADCOOL corresponds to a specific group of assembled components. This allows RADCOOL to simulate buildings with virtually any construction and layout, whether equipped with radiant cooling systems, or with traditional all-air systems. The current capabilities of RADCOOL depend on the components already present in the building component library (see Appendix A). These capabilities can be extended relatively easily by adding new building components to the library.

The results of a RADCOOL calculation provide information about loads, heat extraction rates, air temperature, and surface temperature distributions in a building. RADCOOL can evaluate system sizing and system configuration, and therefore can assist in HVAC system design. RADCOOL can also be used in the evaluation of issues such as controls, and the dynamic response of the building to load changes, and it can be extended to study indoor thermal comfort and building energy use.

3.1.2 Model limitations

Some of the limitations of RADCOOL are associated with current calculation capabilities of computers, while other limitations are associated with the input data required to

1. A complete energy-balance calculation involves (1) setting up the system of equations that describes the thermal behavior of a building structure as a whole, and (2) solving the system with the boundary conditions imposed by the weather, internal loads, and HVAC system operation. A complete-energy balance calculation is more complex and time-consuming than the approach adopted in DOE-2. However, it allows the evaluation of temperature distributions, a feature necessary for modeling buildings equipped with radiant cooling systems.

perform a given simulation.

At the present development stage of computers, the limiting factor for a RADCOOL calculation is the simulation time. The simulation of a structure containing more than one zone, or the simulation of a single-zone space during time periods longer than 10 days, require a few days of elapsed time to complete execution on a SUN workstation using a *SPARC-5* processor. As the use of RADCOOL is presently limited to workstations, the modeling capabilities of RADCOOL are restricted to single-zone structures, and to simulation periods of less than 10 days. Incorporating RADCOOL into DOE-2 as a module should eliminate these limitations.

In principle, RADCOOL can model any type of building structure, assuming that the user provides the thermal properties of the construction materials. RADCOOL can also model the thermal loads associated with any type of building occupancy, lighting, plug loads, and any type of weather-induced boundary conditions for a building, assuming that the user is able to provide all information necessary for the modeling process. In other words, the level of sophistication of the RADCOOL calculations, as well as the degree in which the RADCOOL results approach reality, depend strongly on the inputs supplied by the user.

3.2 Model Evaluation

To evaluate the results obtained from RADCOOL simulations, the ideal test would consist of (1) monitoring a large number of buildings equipped with radiant cooling systems, (2) using RADCOOL to simulate these buildings, and (3) comparing the simulation results with the measurements. Unfortunately, data measured in buildings equipped with radiant cooling systems are not available. Consequently, the evaluation of RADCOOL [3] was limited to: (1) performing an intermodel comparison with DOE-2, and (2) performing a comparison with data measured inside *one* building equipped with a radiant cooling system.

3.2.1 Intermodel comparison with DOE-2

To evaluate the modeling capabilities of RADCOOL, the results obtained by RADCOOL and DOE-2 were compared in a domain where both programs were applicable. Specifically, the intermodel comparison was based on the results obtained from parallel simulations of a single-zone structure that does not incorporate radiant cooling surfaces.

A number of studies have evaluated the modeling capabilities of the DOE-2 building simulation program (see for example [4] and [5]). These studies have found that the results obtained by simulating an existing building in DOE-2 can agree very well with data measured inside the same building.

Description of the inputs to the simulation

The single-zone structure simulated by RADCOOL and DOE-2 is a shed with the dimensions of 4 m x 5 m x 3 m. All vertical walls, and the roof of the structure are exposed to weather conditions. Its floor is in direct contact with the ground. The structure has one window with western exposure. Figure 3.1 shows the spatial geometry and the window location of the single-zone structure.

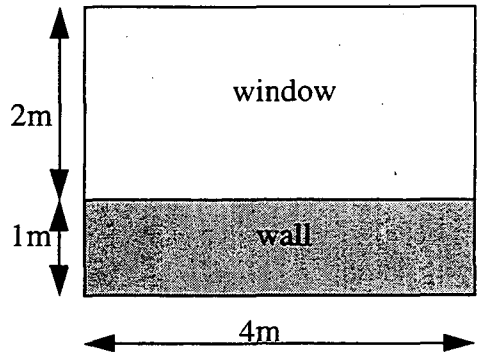

Elevation - the West-facing wall

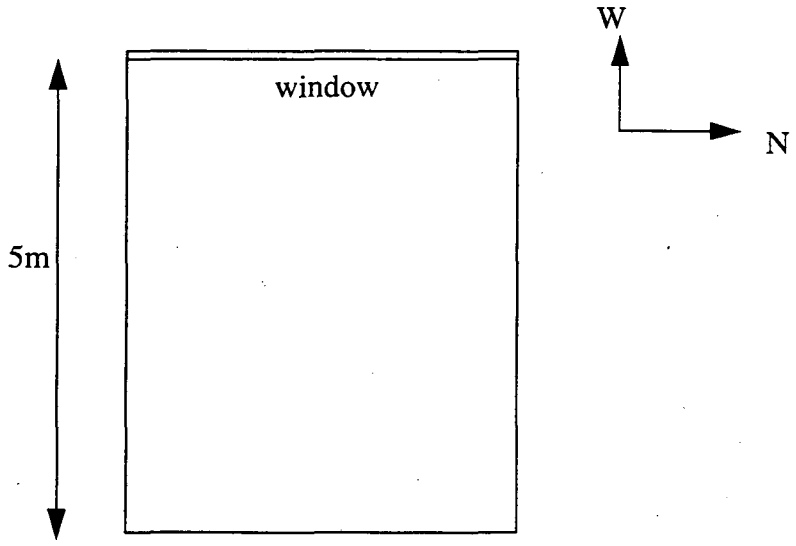

The single-zone structure- plan

Figure 3.1. Single-zone structure simulated for the intermodel comparison.

The Red Bluff Typical Meteorological Year (TMY) weather file was used to obtain the weather-induced boundary conditions for the single-zone structure.[1] Thus, the outside air temperature, outside air humidity ratio, direct and diffuse solar radiation, cloud cover, ground temperature, etc. that constitute input for the simulation correspond to the weather conditions typical for Red Bluff, California.

To provide a realistic basis for intermodel comparison, the "pre-heating" procedure typical for DOE-2 was simulated in both programs. The "pre-heating" procedure ensures consistent and well-defined initial conditions, adjusted to the climate in which the structure is modeled. In DOE-2 the "pre-heating" procedure consists of modeling the structure with weather-induced boundary conditions obtained by repeating several times the weather for the first day to be modeled. As the intermodel comparison is based on the indoor results obtained by simulating the structure with the weather-induced boundary conditions corresponding to June 1 in Red Bluff, the "pre-heating" procedure consists of simulating the single-zone structure with boundary conditions obtained by repeating seven times the weather conditions for June 1, and using the results as initial conditions.

The intermodel comparison aimed to show the similarities, or discrepancies, in the heat transfer calculations performed by RADCOOL and DOE-2. Consequently, no internal loads, mechanical cooling or ventilation, or infiltration were modeled for the test room.

To compare the results of the two programs for different types of building construction, three wall assemblies were modeled (Figure 3.2).

For simplicity, the four vertical walls, roof and floor of the single-zone structure were simulated as having the same material composition. The material properties simulated in the intermodel comparison are listed in Table 3.1. The simulation assumptions are summarized in Table 3.2.

Table 3.1. Material properties used in the intermodel comparison.

	Density [kg/m^3]	Specific heat [kJ/kg-K]	Conductivity [W/m-K]
Concrete	2400	1.04	1.80
Wood	800	2.20	0.20
Gypsum board	1000	0.80	0.40
Fiberglass	90	0.60	0.036
Glass	2700	0.84	0.78

1. A TMY file is created by selecting the most representative calendar months from surface meteorological data and solar radiation data recorded on an hourly basis over a 20- or 30-year period at a given location. A TMY weather file is therefore a weather file representative for the weather at that location.

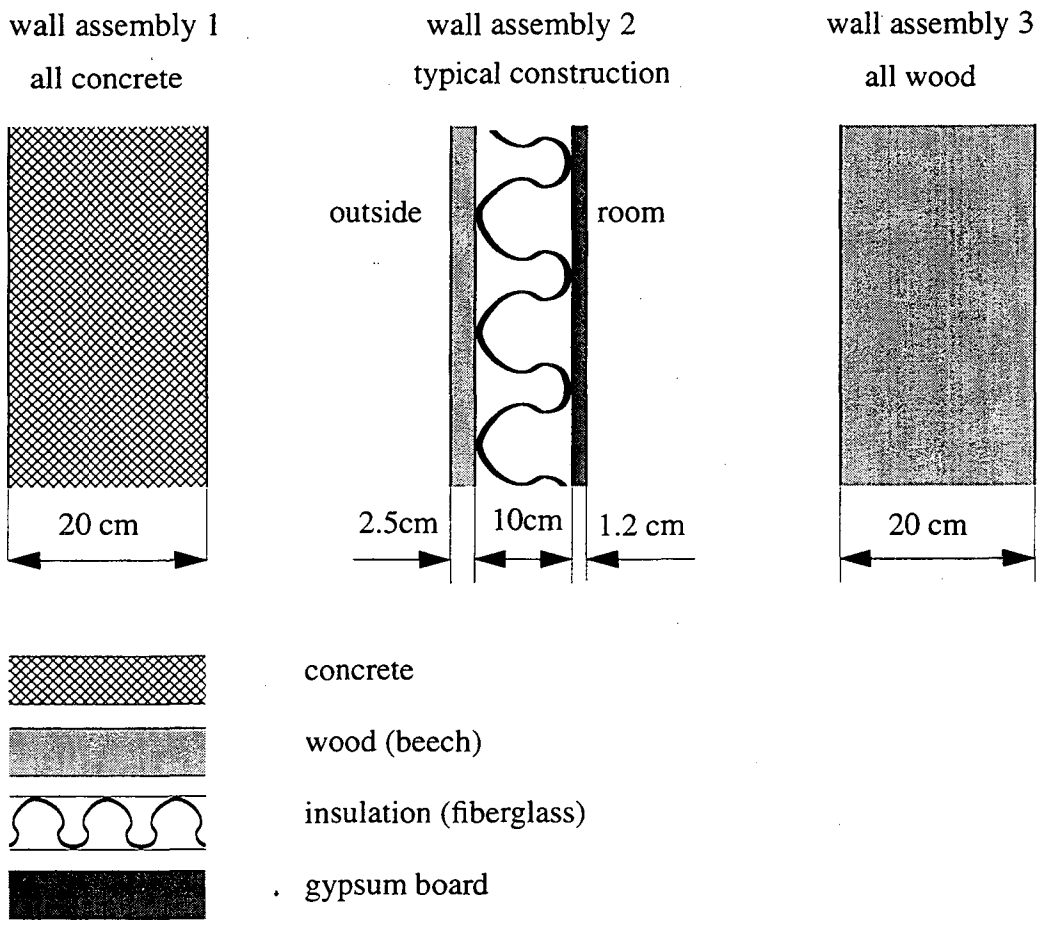

Figure 3.2. The three wall assemblies simulated for the intermodel comparison.

Results

Figures 3.3 - 3.5 show the indoor air temperature of the single-zone structure as simulated by RADCOOL and DOE-2 for the three types of wall assemblies described in Figure 3.2. The RADCOOL indoor air temperatures presented in these figures are the result of several iterations in which certain coefficients were adjusted to match the DOE-2 assumptions as closely as possible. Once adjusted, the same coefficients were used for all three structures.[1] For the purpose of comparison, the Figures 3.3 - 3.5 also contain

1. The RADCOOL input for the three structures contains the same parameters except for the material properties of the wall assemblies.

TABLE 3.2. Summary of assumptions for the intermodel comparison.

Assumptions	RADCOOL and DOE-2
Geographical location	Red Bluff, CA
Structure geometry, dimensions and orientation	Figure 3.1
Window exposure	western
Construction of vertical walls, roof and floor	Figure 3.2 and Table 3.2
Window type	single-pane, clear glass
Internal loads	none
Mechanical cooling	no
Mechanical ventilation	no
Infiltration	no

the outside air temperature.

The concrete walls of the first structure have high conductivity (1.8 W/m-K), and high thermal mass. During daytime, the walls and roof are exposed to direct solar radiation on the exterior side, and to the solar radiation entering through the window on the interior side. This incident heat is conducted into the walls and stored, warming them up. At the same time, solar radiation entering through the window, and convective heat transfer with the warm walls warm up the indoor air (Figure 3.3). Because a large fraction of the solar radiation incident on the structure is stored in the walls, the indoor air reaches its maximum temperature a few hours after the outside air. Heat storage in the walls also reduces the diurnal amplitude of the indoor air temperature as compared to the outside air.

The second wall assembly represents a typical exterior wall. An insulation layer is "sandwiched" between an exterior wood board and an interior gypsumboard layers. The whole structure is designed to minimize the heat conducted through the building envelope. Because the walls are highly insulated, solar radiation entering through the window during the day warms up mainly the gypsumboard layer and the indoor air (Figure 3.4). Then the indoor air (along with the structure) cools down at night mainly due to heat loss through the window. Overall, the diurnal variation of the indoor air temperature the second structure is much higher compared to that of the outside air. The time of maximum of the indoor air temperature is much delayed as a result of storage effects into thegypsumboard layer, and of the insulated character of the structure.

The wood walls of the third structure have lower conductivity (0.2 W/m-K) than the

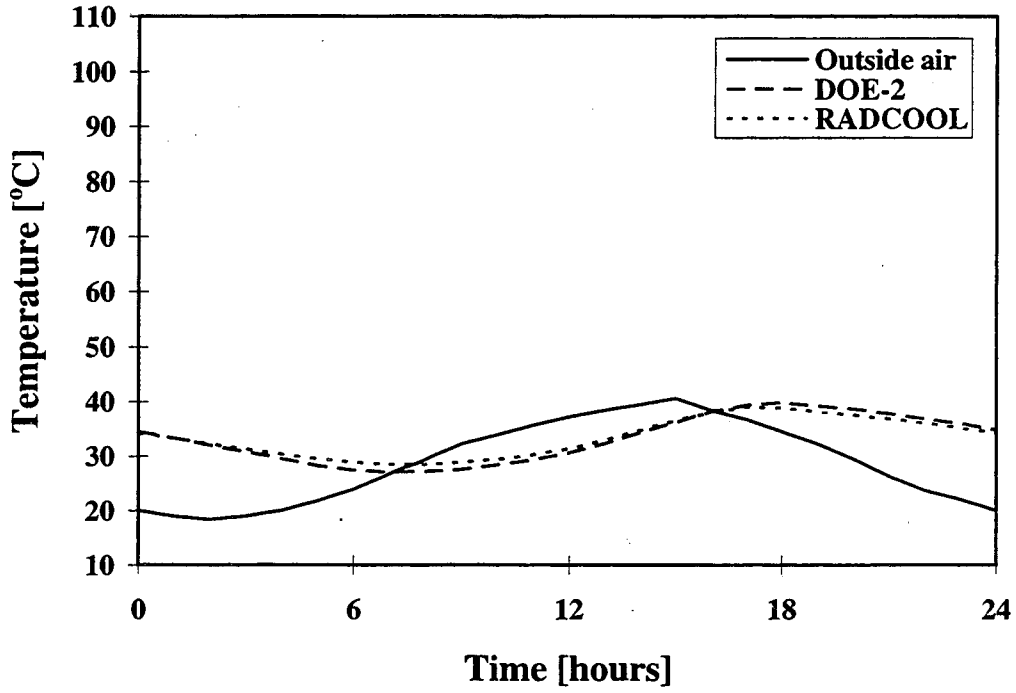

Figure 3.3. Outside and indoor air temperature: wall assembly 1 (concrete).

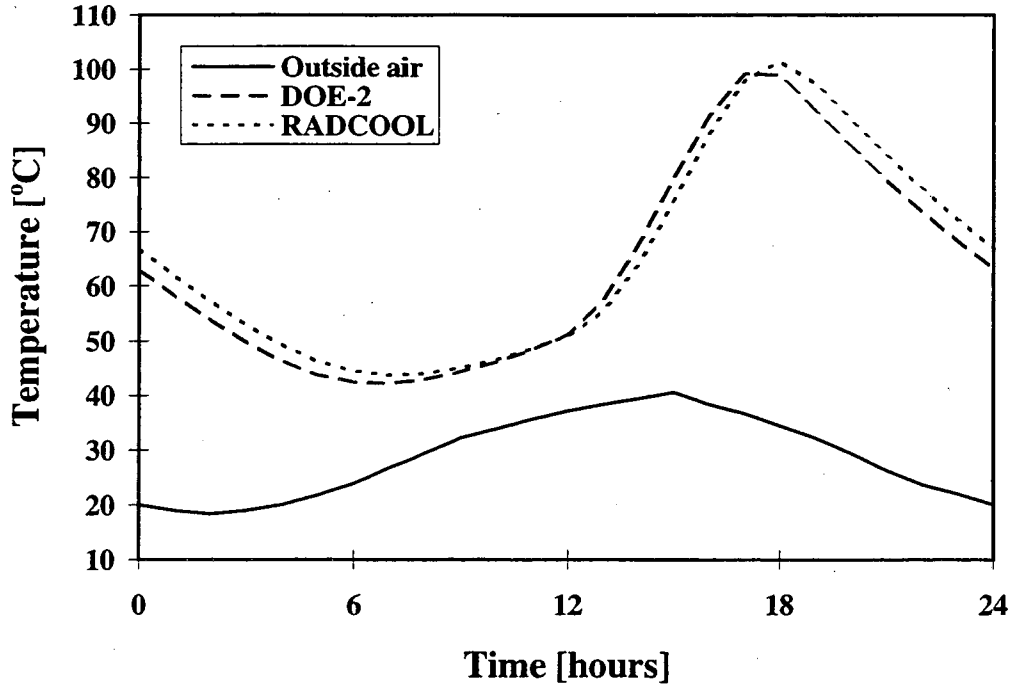

Figure 3.4. Outside and indoor air temperature: wall assembly 2 (typical construction).

concrete walls of the first structure. As a result, less heat is stored in the wall itself, because less heat is conducted from the surfaces of the wall towards the inside of the wall. The indoor air of the structure heats mainly due to the solar radiation entering the window (Figure 3.5). The indoor air temperature of the wood structure is higher, but it has a lower diurnal variation when compared to the indoor air temperature of the concrete structure.

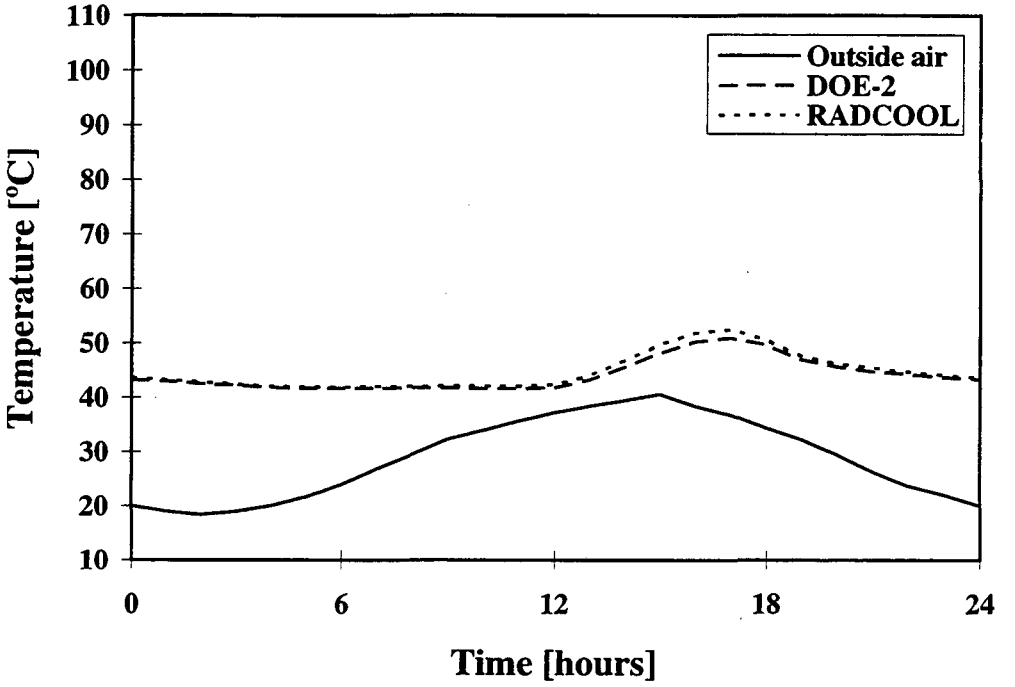

Figure 3.5. Outside and indoor air temperature: wall assembly 3 (wood).

The intermodel comparison shows that the predictions for the indoor air temperature made by RADCOOL and DOE-2 are very similar. The predicted temperatures agree within 2° C.

3.2.2 Comparison with measured data

The performance of RADCOOL was also tested by comparing its results with measurements from a building equipped with a radiant core cooling system.

The DOW-Europe test room

Measurements were performed in the Swiss building housing the European headquarters of DOW Chemicals (geographical location 47 °N and 9 °E). The test room monitored to

determine the performance of the core-cooling radiant system is located on the top floor of the building (height = 12.8 m above the ground). The room has the dimensions of 2.9 m x 4.3 m x 2.85 m, and its facade is oriented 65° East of South (see Figure 3.6).

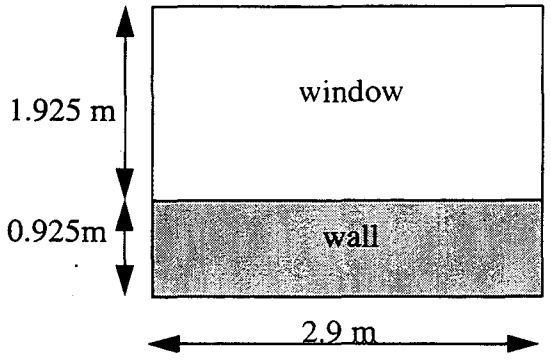

Elevation - the SE-facing wall

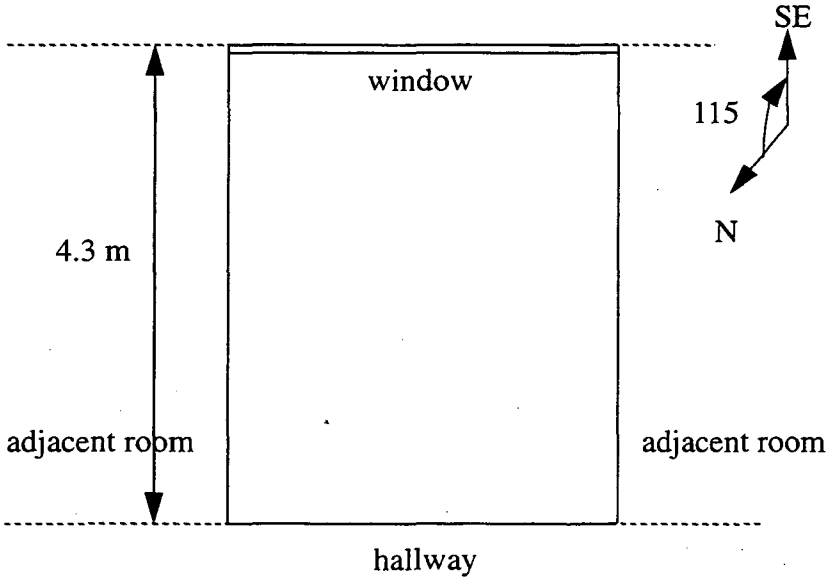

The test room - plan

Figure 3.6. The DOW Chemicals test room orientation and layout.

Wall composition

Figures 3.7 and 3.8 show the composition of the test room walls. The room's exterior

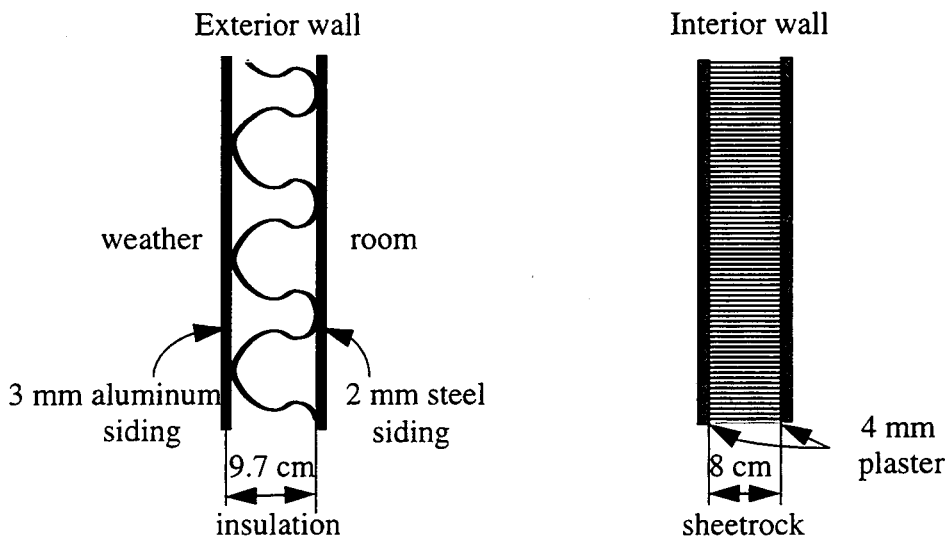

Figure 3.7. Composition of the vertical walls in the DOW Chemicals test room.

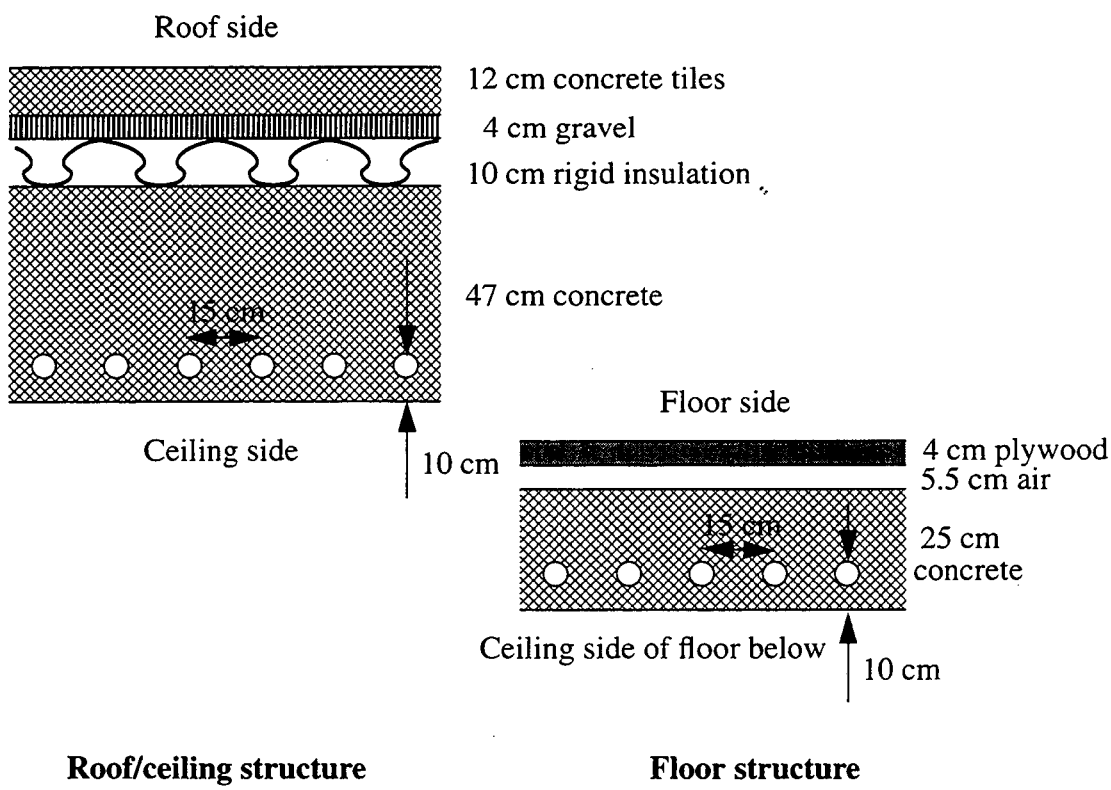

Figure 3.8. Composition of the roof and floor in the DOW Chemicals test room.

facade has the overall dimensions of 2.9 m x 2.85 m. The facade incorporates a double-pane window of 2.9 m x 1.925 m and an overall U-value of 1.75 W/m^2-K [6]. The wall below the window has the dimensions of 2.9 m x 0.925 m and an overall U-value of 0.34 W/m^2-K. Automatic shades are installed over the windows, on the exterior of the facade. The shades are operated by a sensor parallel to the window surface. A control mechanism closes the shades when the total (direct plus diffuse) solar radiation incident on the window becomes higher than the threshold of 120 W/m^2, and opens them when the total solar radiation incident on the window drops below 120 W/m^2.

The interior walls consist of sheetrock and plaster.

The ceiling of the test room (which is also the roof of the building) has the dimensions of 2.9 m x 4.3 m. Its overall U-value is 0.32 W/m^2-K.

The test room has a raised floor over the cooled concrete slab of the room below. The dimensions of the floor are also 2.9 m x 4.3 m, and its overall U-value is 2.5 W/m^2-K.

The material properties used in the comparison between RADCOOL results and measured data are presented in Table 3.3.

TABLE 3.3. Material properties used in the comparison with measured data.

	Density [kg/m^3]	Specific heat [kJ/kg-K]	Conductivity [W/m-K]
Insulation batt	85	830	0.034
Plaster board	1400	900	0.70
Sheetrock	1000	1100	0.40
Concrete	2400	1040	1.80
Rigid insulation	33	1400	0.032
Gravel	1650	900	0.70
Plywood	800	2500	0.15

Loads

At the time when measurements were performed inside the DOW Chemicals test room, internal loads were modeled by controlling the operation of several light bulbs installed in the room. This measure was considered necessary in order to eliminate any unexpected results that might occur due to random occupant behavior. Occupancy was physically simulated as: 436 W (35 W/m^2), from 8 a.m. to 12 p.m. and from 1 p.m. to 5 p.m., Monday through Friday. No occupancy was simulated during the weekend.

The solar radiation intensities necessary for simulation of the test room were obtained

from weather tapes recorded at a weather station located at 20 km distance from the building. There are no tall buildings on the site, and the DOW Chemicals building is not shaded by any horizon obstacles.

Blower-door tests performed in the test room showed that the infiltration rate was 0.2 ACH. A constant infiltration rate of 0.2 ACH was assumed in RADCOOL, even during the periods when the ventilation system supplies air to the building.

System

The cooled ceiling. The radiant system inside the core cooling ceiling is composed of water pipe registers that cover an area of 8.3 m^2 each.[1] The pipes are made of polyethylene, have 16 mm exterior and 12 mm interior diameters, and are placed 15 cm on centers, 10 cm deep inside the concrete. The water flow in each register is constant throughout the day at 100 l/h. Given the size of the test room, 1.5 registers cover the cooled ceiling, so a total of 150 l/h (0.042 kg/s) of water flows through the core cooling ceiling. The temperature of the supply water was recorded and is thus available for the simulation.

Ventilation. Air is supplied to the room at a rate of 1.1 ACH (36 m^3/h) during "occupancy hours" and at the rate of 0.55 ACH during "off-occupancy" hours. The temperature of the supply air was measured and is available for the simulation.

Boundary conditions

The modeling of the test room in RADCOOL requires information regarding the thermal behavior of the room boundaries. Boundary conditions that can be used in the modeling process are: the temperatures of the wall surfaces inside the room, the temperatures of the wall surfaces in the adjacent rooms, or the air temperatures in the adjacent rooms.

No measurements of surface temperatures were made while the test room was monitored. The only air temperature measurements were made in (1) the test room, (2) one adjacent room, and (3) the hallway (see Figure 3.6). Under these circumstances, several assumptions were necessary in the modeling of the test room.

The two rooms adjacent to the test room were modeled as having equal air temperatures. The air temperature available from one adjacent room was thus used as a boundary condition on both "lateral walls" of the test room.

The air temperature in the room located below the test room was assumed to be equal to the air temperature in the test room. Since one of the goals of the RADCOOL simulation

1. Figure 2.4 in Chapter 2 is an example of a cooling grid register. The registers used in core cooling ceilings are similar, but composed of thicker pipes that are spaced at 10-20 cm on centers. When assembling a core cooling ceiling, registers are imbedded in concrete side by side and connected. From the point of view of the water flow, there is "parallel" connection among registers.

was to calculate the indoor air temperature in the test room, the measured air temperature could not be used as input to the simulation. Consequently, RADCOOL assumed that the air temperature in the room below (boundary condition) was equal to the calculated test room temperature.

The test room air temperature was measured by two sensors, one located 10 cm above the floor (ankle level) and the other located at 1.1 m above the floor (head level of a seated person). The sensor located at ankle level reports a lower temperature than the sensor located at head level. The report accompanying the data [6] states that the floor surface temperature was approximately equal to the air temperature measured at ankle level. The RADCOOL simulation assumed that the indoor air of the test room was well mixed. The temperature of the air near the floor was therefore considered to be equal to the average room air temperature.

Measurements of the inlet water temperature in the ceiling registers of the test room were available, but measurements of the inlet water temperature in the ceiling registers of the room below (lower side of the floor) were not available. Since all the ceiling registers of the DOW Chemical building receive the cool supply water from the same chiller, the RADCOOL simulation assumed that the two inlet water temperatures were equal.

Measurements of the outside air temperature were made in the vicinity of the building. The outside air temperature was also available from weather tapes recorded at a weather station located at 20 km distance from the building. To capture microclimate characteristics, the RADCOOL simulation used the air temperature measured near the building as input. Solar measurements from the weather station were used as input for the direct and diffuse solar radiation incident on the exterior wall of the test room.

The operation of the window shades was "measured," but the variation of the air temperature of the test room does not agree with the window shade operation reported. Specifically, the window shades are reported to have been open during the last two days of the simulated period (weekend days), but the air temperature in the test room is not high enough to support this information. Consequently, the RADCOOL simulation used a window shade schedule calculated on the basis of the 120 W/m^2 threshold during working days, and modeled the window shades as being shut during the weekend.

The RADCOOL simulation assumed that the absorption and transmission coefficients of the window panes were constant over time. Absorption coefficients of 0.05 and transmission coefficients of 0.6 were used for both direct and diffuse radiation. In reality these coefficients are not equal for direct and diffuse radiation; in addition, they vary over time and are functions of the position of the sun relative to the window surface.

Other modeling assumptions

As stated in Appendix A, to avoid lengthy calculations regarding the distribution of the solar load inside the space, RADCOOL adopted the DOE-2 procedure in which each

wall receives a certain percentage of the solar radiation entering the space. In the case of the DOW-Europe test room, the following percentages were modeled: the floor received 57% of the solar radiation entering the space, the vertical walls and the ceiling received area-weighed shares of 38% of the solar radiation entering the space, and the remaining 5% of the solar radiation entering the space was reflected back out through the window.

To simulate the loads generated inside the space in RADCOOL, some assumptions related to the character of these loads were necessary. As stated above, a total load of 456 W was physically modeled by operating electrical lamps inside the space. The RADCOOL simulation assumed that 35% of the total load (150 W) represented convective loads and 65% (286 W) represented radiant loads. The simulation assumptions are summarized in Table 3.4.

TABLE 3.4. Summary of assumptions for the comparison with measured data.

Assumptions	RADCOOL
Geographical location	47 °N, 9 °E
Structure geometry, dimensions and orientation	Figure 3.6
Window exposure	65 ° east of south
Construction of vertical walls, roof and floor	Figures 3.7 and 3.8, and Table 3.2
Window type	double-pane, tinted glass U-value = 1.75 W/m^2-K
Window shading	external shades controlled by radiation sensor parallel to window surface
Internal loads	35 W/m^2, 35% convective and 65% radiative
Internal load schedule	8 a.m. to 12 p.m. and 1 p.m. to 5 p.m., Monday through Friday; no internal load on weekends
Mechanical cooling	core-cooling ceiling
Water volume flow and inlet temperature	180 l/h, 24 h/day measured, variable temperature
Ventilation air volume flow and inlet temperature	36 m^3/h from 8 a.m. to 5 p.m., and 18 m^3/h from 5 p.m. to 8 a.m. Monday through Friday, and 18 m^3/h on weekends; measured, variable temperature
Infiltration	0.2 ACH, constant rate

Results

To evaluate RADCOOL's performance, simulated indoor air temperatures were compared with the measurements of the air temperature at 1.1 m above the floor. Figure 3.9 shows this comparison. The RADCOOL air temperature represents the result of the first attempt to model the test room. Fine-tuning of the RADCOOL input is possible, but requires access to detailed building information.

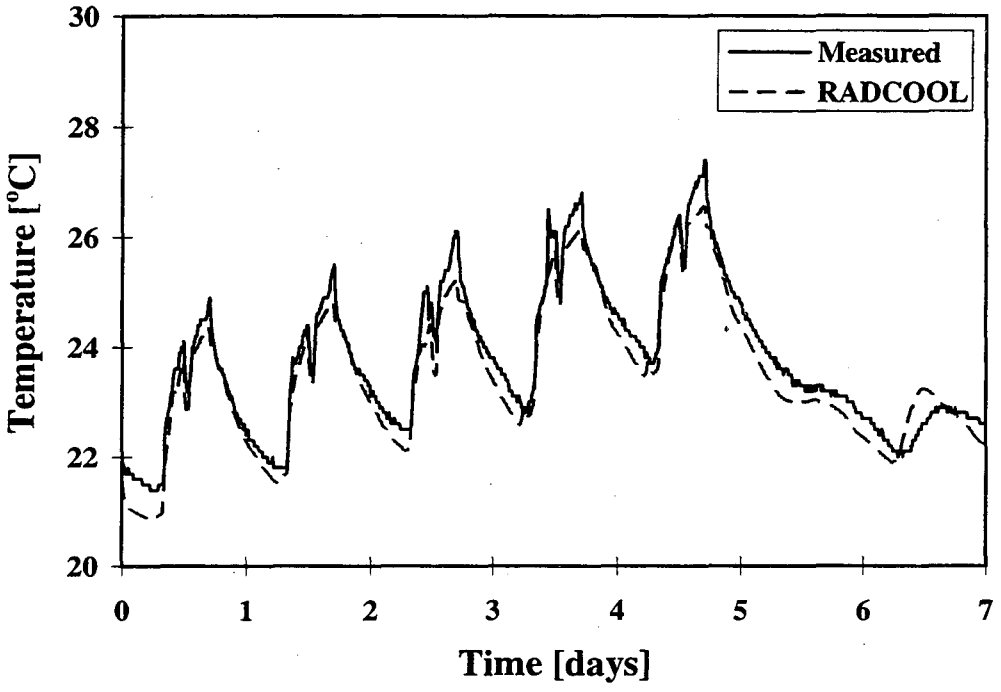

Figure 3.9. Air temperature inside the DOW Chemicals test room.

The RADCOOL simulation results for the room air temperature show good agreement with the air temperature measured at 1.1 m above the floor. There are two minor differences between the two curves. The first difference is a small discrepancy between the times at which the air temperature curves reach the daily minima. The RADCOOL results predict that the building cools faster than indicated by the measurements. The second difference consists of a discrepancy between the predicted and the measured maximum air temperature. On the first 6 days the RADCOOL simulation prediction for the daily maximum is lower than the value measured, while on day 7 the RADCOOL prediction is higher. For the last day of the simulation, RADCOOL also predicts that the peak temperature would occur about four hours earlier than the time of the measured peak. Both differences might be due to a discrepancy between the simulated operation

and the real operation of the window shades. If the building orientation used to calculate the schedule of the window shades is off by a few degrees, the real solar heat gain into the test room is different than that simulated, and it elicits a different thermal response from the building envelope. Consequently, the indoor air temperature predicted by RADCOOL is slightly different from the indoor air temperature measured in the test room because the orientation of the building modeled by RADCOOL may be slightly different when compared to the orientation of the real DOW Chemicals building.

3.3 Conclusions

Section 3.2 shows that there is good agreement between the results of the RADCOOL simulations and the results of DOE-2 simulations, and between the results of the RADCOOL simulations and measured data. There is a good chance that, if future RADCOOL modeling is performed similarly, the RADCOOL predictions regarding the operation and functioning of "passive" structures, or of single-zone structures equipped with radiant cooling systems, will be as reliable as those reported in this Chapter.

3.4 Future Work

The present capabilities of RADCOOL (see Section 3.1 and Appendix A) limit the use of the program to a specific class of problems. There are certain modules which, if added to the current library, would allow the RADCOOL user to study a much larger variety of problems. The following paragraphs will describe those modules.

Room air stratification

The air stratification occurring in buildings equipped with radiant cooling systems is significantly different from the air stratification occurring in buildings conditioned by conventional HVAC systems. A radiant cooling ceiling produces a relatively uniform vertical temperature, except in the vicinity of the ceiling.

Because the ceiling of a building equipped with radiant cooling system is cold, the air next to it is cooled by convection. This leads to the appearance of a steep temperature gradient near the ceiling, as the air close to the ceiling becomes colder than the air in the rest of the space. This gradient plays an important role in the functioning of radiant cooling system, because generally the temperature of the contents of the space is close to the air temperature. A high air temperature gradient near the ceiling allows the system to remove large cooling loads. However, if the air in the vicinity of the ceiling becomes too cold (as may happen in the case when the ceiling much colder than necessary for internal load removal), it will move downward and a cold air draft will result [7]. A cold air down-draft has two major consequences. First, depending on the air velocity, a cold air draft might reduce indoor comfort. Second, assuming that the radiant cooling system is

combined with a displacement ventilation system, a significant cold air down-draft would interfere with the efficient functioning of the displacement ventilation system: it would cause the contaminated air near the ceiling to mix with the room air, thus reducing air quality inside the space.

While none of the investigations into the performance of radiant cooling systems has reported the existence of cold air down-draft, there is some risk that it may occur in the future. These considerations show the importance of modeling the air movement inside spaces cooled by radiant cooling systems. Computational fluid dynamics (CFD) programs are available that can model air movement inside virtually any space. Given the present computation capabilities of computers (excluding CRAYs), it is still unrealistic to attempt an integration of RADCOOL with a CFD program. However, results from CFD research could be used to derive a "simplified CFD model" describing the air movement inside a space cooled by a radiant cooling system. This simplified model could then be implemented as a separate module in the RADCOOL library. The RADCOOL user would thus be able to make some estimates of (1) the air stratification problem, and (2) the air velocities inside the modeled space, without causing a significant increase of the computation time.

There are several reasons why a "simplified CFD model" has not already been added to the RADCOOL library. First, measurements inside buildings newly-equipped with radiant cooling systems indicate that the indoor conditions are comfortable. Furthermore, there are virtually no documented building occupant complaints regarding the performance of the radiant systems currently available on the market.[1] The development of the "simplified CFD model" was therefore considered secondary to the development of the other components of RADCOOL. Second, deriving the "simplified CFD model" implies access to a CFD program, and expertise to use this program. Neither of these conditions was fulfilled within the time-frame of the present thesis. Third, such a project would need financial support. Assuming that expertise, access, and financial support are available in the future, the addition of a "simplified CFD model" to RADCOOL would provide additional information regarding the performance of buildings equipped with radiant cooling systems.

Thermal comfort and radiant temperature at the occupant location

As stated in Appendix A, RADCOOL calculates only the long-wave radiation exchange between the surfaces (walls, windows, ceiling, floor) of the modeled space. A module

1. The Kaiser Building in Oakland, California, built in the 1950s, was equipped with one of the first radiant systems. A study conducted there in 1994 [8] showed this early system fails to provide acceptable thermal comfort. The study also showed that replacing the old radiant panels with the improved panels available on the market today would simultaneously restore comfort to the building *and* save 50% of the current energy consumption due to air-conditioning. The proposed project was never completed, as the building owner considered that replacing the existing chiller with a more powerful model was preferable.

that calculates the long-wave radiation exchange between the occupants of a space and the envelope of the space would be a useful addition to the RADCOOL library. The addition of this module to the RADCOOL library together with the room air movement module would provide the user with access to a complete set of thermal comfort variables.

Cooling sources

The RADCOOL user is currently limited to modeling a cooled and ventilated single-zone space. RADCOOL does not model the mechanisms by which the cooling agents (water and/or air) are conditioned. Thus, a RADCOOL simulation assumes that water at a given temperature, and air at a given temperature and humidity ratio, are always available as required to meet the cooling loads.

A number of modules that simulate the behavior of cooling sources are already available for implementation in the RADCOOL library. For example, Ranval [9] proposes a module that simulates the behavior of a cooling tower. Testing the performance of a cooling source, however, requires the simultaneous implementation of several cooling modules in the RADCOOL library, and access to benchmark data describing the performance of that cooling source (design specifications, or access to measured data).

3.5 References

1. Simulation Research Group (Lawrence Berkeley National Laboratory) and Group Q-11 (Los Alamos National Laboratory), *DOE-2 Engineering manual.* Rep. LBNL-11353, 1982.

2. Gerhard Zweifel, *Simulation of displacement ventilation and radiative cooling with DOE-2.* ASHRAE Trans., (99) (2) 1993.

3. Corina Stetiu, H. E. Feustel and F. C. Winkelmann, *Development of a model to simulate the performance of radiant cooling ceilings.* ASHRAE Trans., (101) (2) 1995.

4. *DOE-2 Verification project,* Phase 1, Final Report. Los Alamos National Laboratory, Rep. LA-10649-MS, 1986.

5. K. J. Lomas, H. Eppel, C. Martin and D. Bloomfield, *Empirical validation of thermal building simulation programs using test room data*, Volume 1: Final report. International Energy Agency, 1994.

6. Robert Meierhans, *Raumklimatisierung durch naechtliche Abkuehlung der Betondecke.* 8 Schweizerisches Bauseminar, Energieforschung im Hochbau, EMPA-KWH, CH-8600 Duebendorf, Switzerland, 1994.

7. Helmut E. Feustel and C. Stetiu, *Hydronic radiant cooling - preliminary assessment.* Energy and Buildings, (22) (3) 1995.

8. Helmut E. Feustel, C. Stetiu, R. Meierhans, and U. Schulz, *Hydronic radiant cooling - a case study.* Proc. Healthy Buildings '94, Budapest, Hungary, 1994.

9. William Ranval, F. X. Rongere, and F. C. Winkelmann, *Cooling tower modeling.* Electricité de France, Rep. HE-12-W3393, 1992.

Chapter 4

RADIANT COOLING IN US OFFICE BUILDINGS: DESIGN OF THE MODELING PROJECT

4.1 Introduction

Chapter 2 discussed the energy and peak power savings potential of buildings equipped with radiant cooling systems. Such buildings are currently built in Europe, either as new construction or as retrofits. Despite general efforts to promote energy efficient technologies on the US market, traditional all-air systems are still installed in new and retrofitted commercial buildings in the US. There is no evidence that the US air-conditioning market will adopt and promote radiant cooling systems in the near future.

Attempting to explain the absence of radiant cooling systems from the US market is beyond the scope of this thesis. A complete explanation would very likely require the description of a complex interaction of technical, economic, social, and cultural factors. Instead of undertaking this ambitious task, this thesis limits itself to investigating one technical aspect of the operation and functioning of buildings equipped with radiant cooling systems: the compatibility of radiant cooling systems with the range of climates characteristic for the United States. There is no doubt that radiant cooling systems can *cool* buildings located in any climate, if the peak specific cooling load is below 140 W/m^2. The notion of "compatibility" is used here to indicate that it is currently unclear whether (1) a radiant cooling system can be operated to provide *comfortable conditions* inside a building located in any climate, and (2) the control strategies used to ensure comfort in "problem-climates" still allow the radiant cooling system to save energy and peak power when compared with a traditional all-air system.

4.2 The Issue

Although recent information regarding Western European building practices indicates that implementation of radiant cooling systems is currently in progress in commercial buildings [1], the available information regarding the performance of buildings equipped with radiant cooling systems is limited to data gathered from a few buildings in Germany and Switzerland. According to these data, buildings recently equipped with radiant cooling systems consume less energy and require less peak power for conditioning, than similar buildings equipped with traditional all-air systems. Furthermore, there are virtually no occupant complaints regarding indoor comfort in these buildings. However, because the available data are scarce, it is possible that all the buildings that have been studied are located in climates in which radiant cooling systems are inherently more efficient than all-air systems (for instance, warm, dry climates). Therefore, it is difficult to argue that the choice of a radiant cooling system instead of an all-air system

would make *any* commercial building more energy efficient and more comfortable.

This thesis addresses the topic of compatibility between radiant cooling systems and the climates in which the buildings are located mainly through the issue of moisture control in the operation of radiant cooling systems. Chapter 2 has stated that, if the dew-point of the indoor air drops below the surface temperature of the radiant cooling system, condensation will appear on the radiant surface. Condensation is unacceptable from the point of view of occupant comfort, as well as because it can cause damage to the building structure, building finishes, and the radiant system itself. Chapter 2 has also stated that indoor moisture levels can be controlled, and the risk of condensation can be reduced, by dehumidifying the supply air. However, in humid climates, this dehumidification process could be so energy intensive that it may exceed the savings achieved by the choice of the radiant system instead of an all-air system.

There is no known research that has addressed the climate-compatibility of radiant cooling systems in detail. Common sense suggests that the climates where buildings equipped with radiant cooling systems would function with a small risk of condensation, and achieve substantial energy and peak power savings, are the warm and hot dry climates. If the reverse of this statement were true, namely that buildings equipped with radiant cooling systems could not function optimally and/or would achieve minimal savings in other climates, radiant cooling systems may prove inadequate or unattractive for most of the US territory. Such a conclusion could provide a partial explanation for the absence of radiant cooling systems from the US market.

4.3 The Parametric Study

The lack of information regarding the performance of radiant cooling systems in different climates is partly due to the absence of a building simulation program that can model heat transfer phenomena in buildings equipped with radiant cooling systems. The program RADCOOL, described in Chapter 3 and Appendix A, was specifically designed to fill this gap. RADCOOL can calculate loads, heat extraction rates, air temperature and surface temperature distributions in a building equipped with a radiant cooling system. As it can evaluate system sizing and system configuration, RADCOOL results can also assist in establishing design parameters for radiant cooling systems (for example, mass flow for the cooling water, pipe spacing, etc.).

Access to RADCOOL offers the possibility of conducting parametric studies. In particular, a parametric study can be designed to investigate the topic of climate-compatibility of buildings equipped with radiant cooling systems. This thesis conducted a parametric study consisting of modeling a single-zone space, in an office building with pre-established construction, orientation, occupancy rates, etc., under different weather-imposed boundary conditions.

The parametric study was designed to provide two types of results. First, the study would show whether buildings equipped with radiant cooling systems might have condensation problems in any of the climates characteristic for the US. Second, the study would allow the calculation of the energy consumption and peak power demand of the radiant cooling system. By comparing these results with similar results obtained for the same building equipped with a traditional all-air system, some estimates can be made regarding (1) the energy and peak power savings potential of the radiant cooling system, and (2) the dependence of these savings on the climate in which the building is located.

To achieve the objectives described above, the modeling project conducted by this thesis consisted of parallel RADCOOL [2] and DOE-2 [3] simulations modeling the indoor conditions of the selected office space. The RADCOOL program modeled the space as conditioned by a radiant cooling system. To study the influence of night ventilation on the indoor environment of the space, the study investigated two different night ventilation strategies.

The DOE-2 program was used to model the same office space as conditioned by a variable air volume (VAV) system during occupancy hours, and by a constant volume system (CV) during the time when no building occupants are present. The design parameters of the all-air system are finely-tuned so that the indoor air temperature and humidity ratio during occupancy hours, and the outside air ventilation flow during the whole day, are virtually the same as those obtained inside the space equipped with the radiant cooling system.

To investigate the influence of geographical location on the performance of the two systems, RADCOOL and DOE-2 simulations were carried out, and the indoor conditions obtained, for the test space subjected to different climate-imposed boundary conditions. For each climate, the results were examined to determine the presence or absence of condensation, as well as whether the indoor air temperature and relative humidity met standard comfort requirements. Then, in each climate, estimates were made for the energy consumption and the peak power demand of the radiant cooling system and the all-air system.

The author notes that an ideal evaluation of the savings potential of radiant cooling systems in commercial buildings would involve a comparison between radiant cooling system performance and the performance of a traditional all-air system that provides the same *indoor comfort* to a given space. Such a comparison could be achieved by designing the two systems to match a comfort index for the overall sensation of indoor thermal comfort. For example, the "predicted mean vote" (PMV) index predicts the mean response of a large group of people according to a thermal sensation scale [4]. Two spaces characterized by the same PMV are considered to offer the same level of thermal comfort. When estimating radiant cooling performance, a PMV-based comparison would be beneficial because the presence of a relatively large cooling surface in the space reduces the mean radiant temperature inside the space. Consequently, the radiant

cooling system can provide a given level of comfort at an indoor air temperature higher than that necessary to the all-air system to provide the same level of comfort. However, the calculation of the PMV requires access to information regarding all four physical comfort parameters (air temperature, partial pressure of water vapor, mean radiant temperature and air velocity). As stated in Chapter 3, DOE-2 does not provide information regarding indoor surface temperatures. In addition, in their present stage of development, neither DOE-2 nor RADCOOL provide the information necessary in an estimate of the average indoor air velocity. Consequently, the parametric study conducted in this thesis is based on matching only two indoor comfort parameters: the indoor air temperature and humidity. Due to the lack of information regarding the other two physical comfort parameters, the author cannot estimate how the performance results reported in this thesis might related to performance results obtained by conducting a parametric study matching the indoor comfort in the space under study.

4.4 Working with the RADCOOL-Imposed Constraints

Chapter 3 states that RADCOOL is currently able to simulate (1) a single-zone space, and (2) a week-long modeling period. Due to these constraints, the parametric study described in the preceding section could not be carried out in an ideally general and detailed way. This section reviews the assumptions made in order to conduct the study, and discusses the uncertainties introduced by making these assumptions.

Regardless of its assumptions and uncertainties, the parametric study has certain merits. First, it establishes a methodology for conducting climate-compatibility investigations. Second, it is reproducible, therefore it can be extended as soon as the calculation capacities of computers evolve. Third, to the author's knowledge, it represents the first effort to study the performance of buildings equipped with radiant cooling systems under different climate conditions. Finally, its results suggest climate-dependent trends in the energy consumption and the peak power demand of a radiant cooling system.

4.4.1 The base-case building

This study assumes a commercial building context because the available information regarding the performance of radiant cooling systems in Western European buildings suggests that the commercial sector represents the main market for these systems [1]. This can be explained based on the need for strict moisture control in buildings equipped with radiant cooling systems, and on the fact that in commercial buildings the indoor moisture sources are limited (occupants, coffee makers, plants), and they can be controlled relatively easily. Among the existing types of commercial buildings, the study focused on office buildings because human activity in office buildings is quasi-predictable.

The study is conducted on an imaginary building designed by the International Energy

Agency to serve as base-case for building energy and indoor air quality studies [5]. The design corresponds to a medium-size office building with single- and multi-occupancy offices located on the building facades, and with a core space dedicated to utility activities (see Figure 4.1). The building is rectangular and its longer facade is oriented 45° east of north. Figure 4.1 shows only one floor of the building. In what follows, the author will refer to this floor as "the whole building".

To ensure compatibility between this base-case building and US building standards, the study focuses on a building structure complying with the California Title 24 building standard [6]. It features a curtain-wall construction (see Figure 4.2) with a U-value of 0.45 W/m^2-K for the opaque part. The vision glazing of the curtain-wall construction consists of double-pane windows with a center-of-glass U-value of 1.31 W/m^2-K. No drapes or mechanical shading are simulated for the windows. The interior walls of the building consist of a 6-cm air layer sandwiched between two layers of plasterboard, each 1-cm thick (Figure 4.2). The U-value of the interior walls is 1.95 W/m^2-K.

The ceiling and floor are made out of 32-cm thick reinforced concrete. When the building is equipped with a radiant cooling system, the spaces have an additional dropped panel system made out of 20-cm wide aluminum panels with water pipes attached on the plenum side of the panels. The panel system covers the entire dropped ceiling. The plenum delimited by the panel system and the reinforced concrete ceiling is 10 cm deep.

The material properties simulated in the parametric study are presented in Table 4.1.

TABLE 4.1. Material properties simulated in the parametric study.

	Density [kg/m^3]	Specific heat [kJ/kg-K]	Conductivity [W/m-K]
Concrete	2400	1100	1.80
Glazing	2460	750	0.80
Insulation	48	840	0.06
Gypsum board	800	1090	0.16
Plaster board	900	800	0.21
Aluminum	2770	875	177.0

It is difficult to evaluate the uncertainty introduced in the results by this particular choice of a base-case building. In an ideal situation, the parametric study would be repeated for a large number of building types, and the results would be compared to those obtained by the present study. However, given the current capabilities of RADCOOL, as well as the time frame of a dissertation, this task is unrealistic. Still, as Chapter 5 will show, the

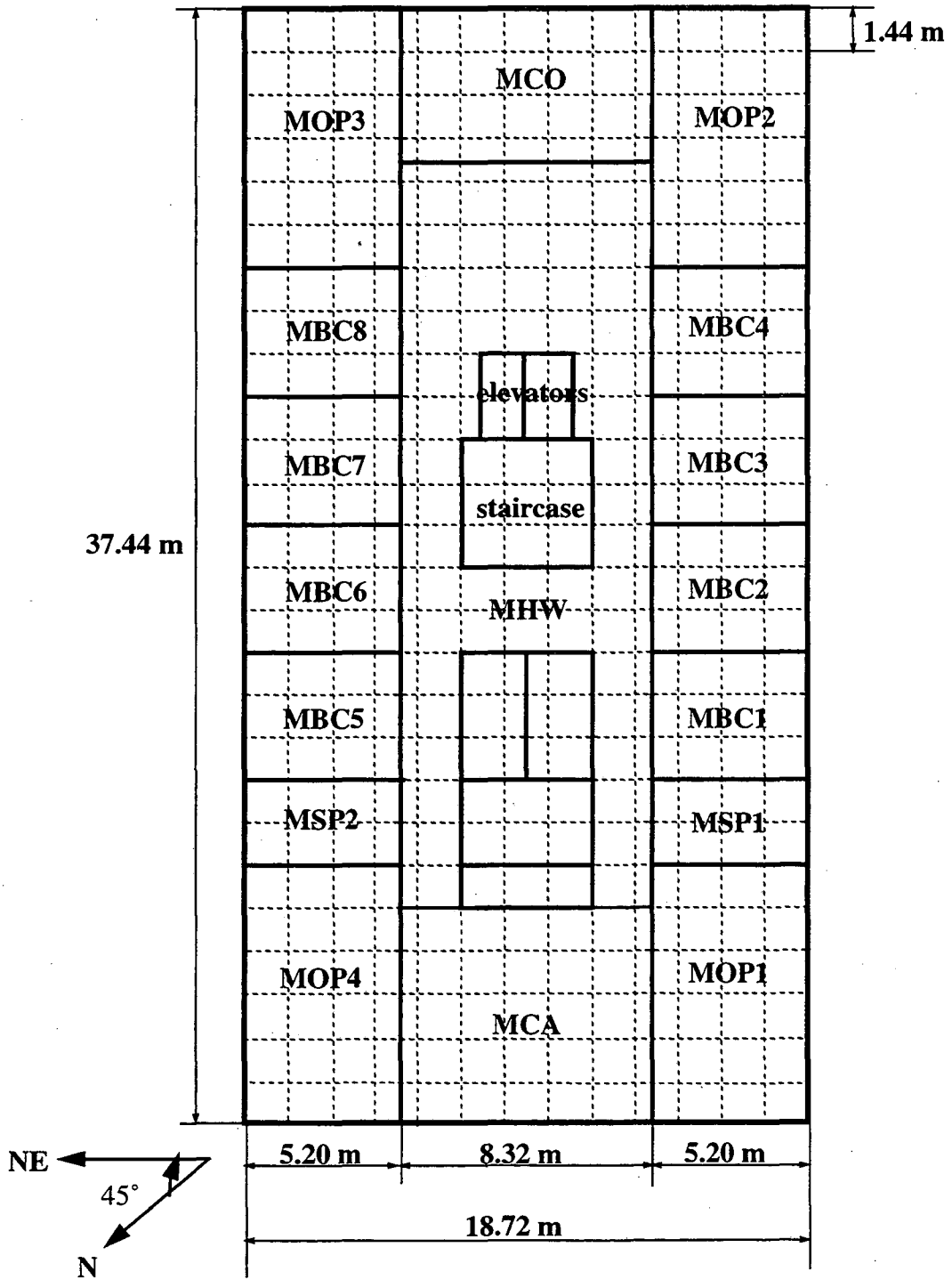

Figure 4.1. Base-case building orientation and layout.

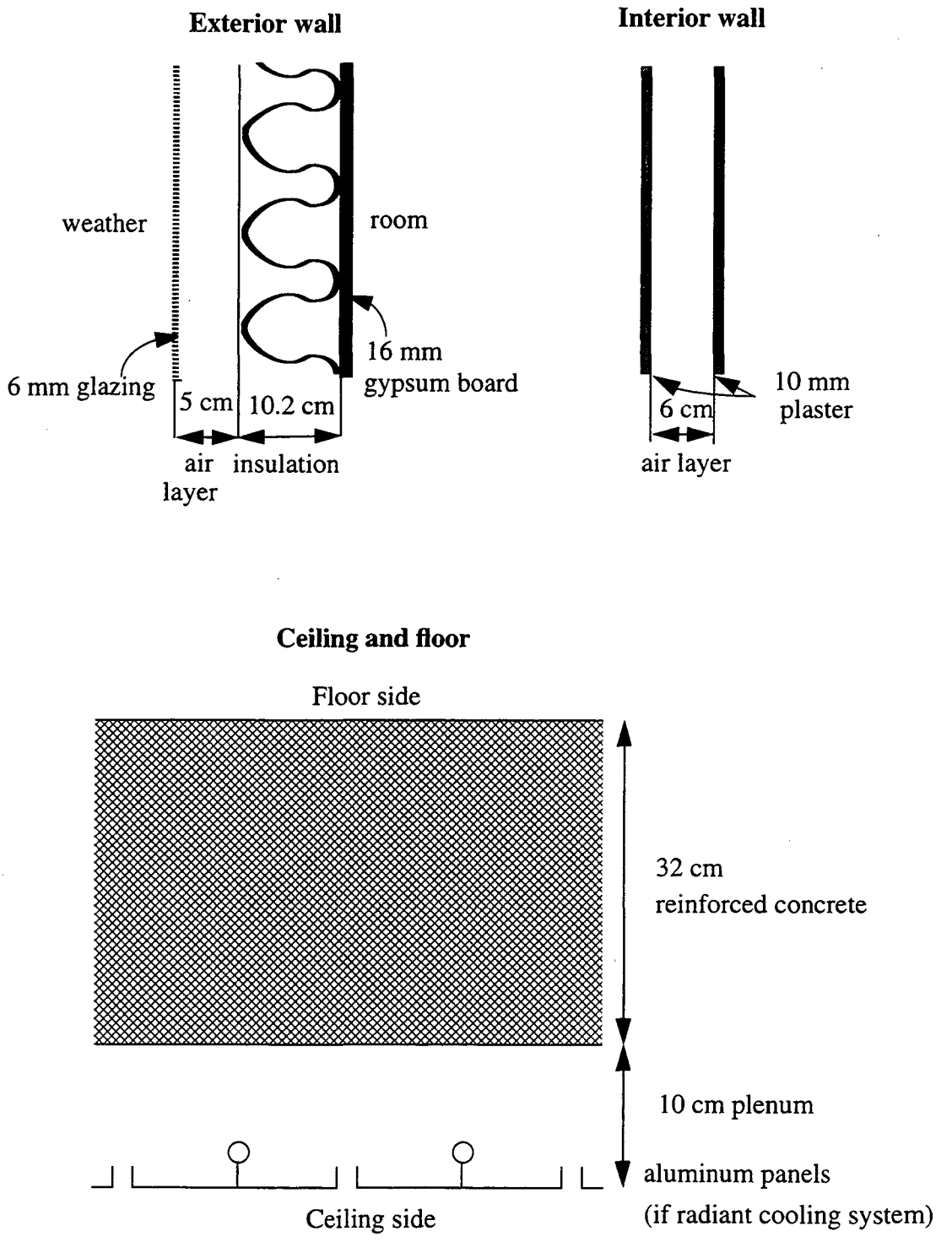

Figure 4.2. Base-case building construction for the parametric study.

parametric study was extended by performing a few additional simulations. The additional simulations show that the conclusions of the study would remain qualitatively the same, even though the results of the study would be quantitatively different for a lighter building structure.

4.4.2 The base-case space

The choice of a space

Because the modeling capabilities of RADCOOL are limited to a single-zone space, conducting the parametric study involved the choice of one room of the base-case building. The character of the RADCOOL requirements, as well as the layout of the base-case building, influenced the choice of the space as follows.

As discussed in Chapter 3, a space can be simulated in RADCOOL only if its internal loads and boundary conditions are known. Because the base-case building selected for this study does not exist in reality, information describing its indoor conditions can only be obtained by modeling the building with a different program (for instance, with DOE-2). However, the boundary conditions obtained from a different program would allow the assumptions embedded in that program to influence the results of the RADCOOL simulation. It would therefore be preferable to obtain the boundary conditions in a different manner.

An examination of the building layout in Figure 4.1 leads to the conclusion that different spaces require different amounts of data for simulation. For example, the boundaries of the corner offices (MOP1-4), the conference room (MCO), the cafeteria (MCA), or the hallway (MHW) are more complex. By contrast, the simulation of some of the middle-of-facade spaces presents less difficulty.

Since the spaces MBC1-4 and MBC5-8, respectively, have the same exposure and internal loads, it is possible that they may have virtually identical indoor conditions. Preliminary DOE-2 simulations verify that the air temperatures of the spaces MBC1-4 and MBC5-8, respectively, differ by no more than 0.1 °C at all times. Consequently, heat transfer through the side walls of spaces MBC2-3 and MBC6-7 can be neglected. A similar argument can be developed regarding the boundary conditions on the ceiling and floor of the spaces MBC2-3 and MBC6-7. If the space to be modeled is located on a middle floor (not a basement, and not a top floor), it is very likely that the indoor conditions in the spaces immediately above and below are the close to those in the given space.

The only boundary condition remaining to be established is that on the "back walls" of spaces MBC2-3 and MBC6-7. Figure 4.1 shows that the "back walls" separate the individual spaces from the central hallway (MHW). Since the hallway is not subject to solar loads, it is possible that the conditions inside the hallway do not vary very much over

time. Preliminary DOE-2 simulations verify that, if the hallway is mechanically conditioned, its indoor air temperature remains virtually constant. Once established, this constant temperature can serve as a boundary condition in the RADCOOL simulation.

Because the spaces MBC2 and MBC3 are virtually identical, MBC2 can be considered representative for the thermal behavior of MBC3. Similarly, MBC6 can be considered representative for the thermal behavior of MBC7.

To choose between the spaces MBC2 and MBC6, the author noted that these two spaces differ only through their orientation. The space MBC2 has a south-western exposure, while MBC6 has a north-eastern exposure. The choice of MBC2 would therefore favor the study of a space with large solar loads. In particular, the total load of the space may exceed 100 W/m^2 in some climates. In such a case, the cooling capacity of the radiant cooling system might be exceeded, and the system would fail to adequately condition the space. The choice of MBC6 instead of MBC2 would focus the study on a space with small solar loads, and would therefore eliminate the chance of revealing instances in which the space overheats. To investigate the scenario representing a more difficult situation for the radiant system, the space MBC2 is a better choice for the parametric study than the space MBC6.

Once again, it is difficult to assess the uncertainty introduced by selecting the space MBC2 instead of MBC6, or any other space. To partially address this problem, additional modeling was performed to calculate the energy and peak power savings associated with conditioning the MBC6 space. As in the case of a lighter building structure, the additional modeling shows that the conclusions of the study would remain qualitatively the same, but the results of the study would be quantitatively different, if the study were based on a similar space with a different orientation.

Because the study is limited to the simulation of a single-zone space, it would be interesting to know whether the results obtained by studying the energy consumption and peak power demand due to conditioning the MBC2 space could be used as an estimate for the energy consumption and peak power demand due to conditioning the whole building in Figure 4.1. One possible strategy to estimate the uncertainty associated with extrapolating the results from any particular space to the whole building consists of (1) modeling the whole building, (2) determining the results for a selected space, and (3) calculating the extrapolation factor from the space to the building. In particular, since the purpose of this study revolves around estimating the energy consumption due to air-conditioning the space, the extrapolation factor can be calculated as the building air-conditioning energy consumption divided by the space air-conditioning energy consumption.

It is important to note, however, that for a building with a fixed orientation, structure, internal loads, and design conditions, the extrapolation factor thus calculated depends on the building location (climate at the building site). Repeating the building simulation for a number of locations would generate climate-dependent results for the space air-conditioning energy consumption and building air-conditioning energy consumption. The

extrapolation factor corresponding to each climate can then be obtained, and statistical calculations can be used to determine the average climate-induced extrapolation factor, as well as its standard deviation. The relationship between the air-conditioning energy consumption of the space and that of the building could thus be summarized by two statistical terms. These two terms could then be used to predict the building air-conditioning energy consumption from the space air-conditioning energy consumption calculated in any new climate.

There are two major caveats to this method of assessing uncertainty. First, such an extrapolation factor is valuable only if it does not depend on the building location, or if its dependence on building location is weak. Only in this case can the prediction of the air-conditioning energy consumption of the building from the air-conditioning energy consumption of the selected space be relatively accurate. If the extrapolation factor is strongly correlated to the building location, the standard deviation of this factor will be large, therefore it will be difficult to predict the energy consumption of the building from the energy consumption of the space with good accuracy.

The second caveat to this method of assessing uncertainty is that the average extrapolation factor and its standard deviation have so far been considered independent of the building simulation program used to determine them, of the type of air-conditioning system modeled, and of the design conditions specified for the operation of the air-conditioning system. In reality, the two statistical quantities are probably functions of all these factors. However, given the goals of the parametric study, the climate-dependence of the extrapolation factor associated with a given space are most critical.

As an illustration of the above, Figures 4.3 and 4.4 contain the results of a series of DOE-2 simulations for the building in Figure 4.1 equipped with the all-air system. The simulations were performed for 11 US climates.

Figure 4.3 contains the results of the statistical calculations performed on the air-conditioning energy consumption of each individual space in Figure 4.1. The bars in Figure 4.3 represent climate-averaged fractions, calculated as the ratios of the energy consumption of each space to the building energy consumption. The "error bars" represent the climate-induced variabilities of each of these average fractions, calculated as standard deviations.

The results in Figure 4.3 show that the corner spaces MOP1-4, the cafeteria, MCA, and the conference room, MCO, account for relatively large fractions of the building energy consumption. The standard deviations associated with these fractions are large, indicating a strong climate-induced variability. As expected, spaces MBC1-4 and MBC5-8, respectively, account for virtually equal fractions of the building energy consumption. The variability associated with the spaces MBC1-4, is larger than that associated with the spaces MBC5-8. Because all space parameters are the same for MBC1-4 and MBC5-8, this difference in variability can be explained on the basis of the different exposures of these spaces (south-western for MBC1-4, as compared to north-eastern for MBC5-8).

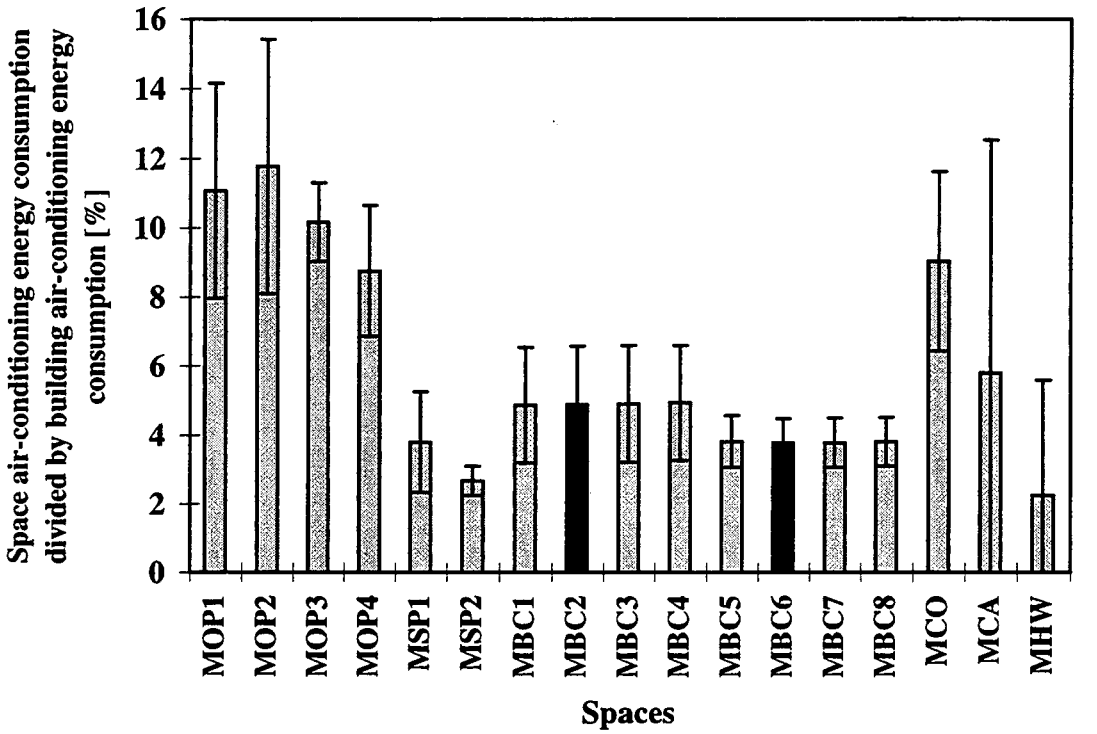

Figure 4.3. Space contributions to the building air-conditioning energy consumption. Statistic performed for 11 building locations.

To use the extrapolation factors in Figure 4.3 in an estimate for the air-conditioning energy consumption of the whole building at a new location, the numerical value of the space air-conditioning energy consumption should be divided by the extrapolation factor of the space (the height of the bar in Figure 4.3 that corresponds to the given space). Because each fraction in Figure 4.3 has an "error bar" associated with it, the extrapolation of the energy consumption of a space to the building energy consumption will result in an energy interval, instead of an energy value. A large energy interval implies that estimating the building air-conditioning energy consumption based on the air-conditioning energy consumption of a given space has a large associated error.

As an example, consider a hypothetical climate in which the building in Figure 4.1 would consume 100 kWh/m^2 annually for air-conditioning. Assume that the air-conditioning energy consumption of each space is also known. The results of predicting the air-conditioning energy consumption of the building from the air-conditioning energy consumption and the extrapolation factor of each space are presented in Figure 4.4.

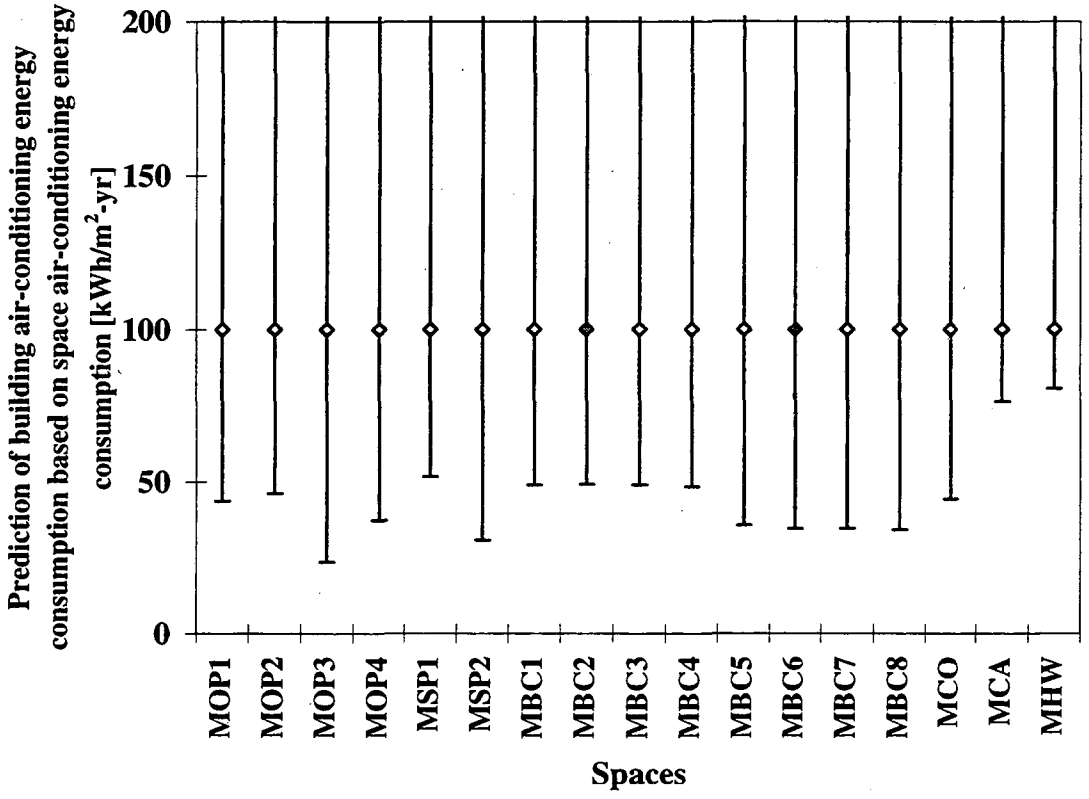

Figure 4.4. Estimate of building energy consumption from space energy consumption. Error bars indicate 90% confidence intervals (n=11).

As the figure shows, using the average value of the extrapolation factor for each space to predict the average air-conditioning energy consumption of the whole building results in the same value of 100 kWh/m^2-yr. However, as each extrapolation factor has its own standard deviation, "90% confidence intervals" can be determined for the prediction corresponding to each space. As the "error bars" in Figure 4.4 indicate, the errors introduced by the extrapolation are very large for all spaces. In conclusion, the extrapolation factor method presented should not be used to estimate the building air-conditioning energy consumption based on the air-conditioning energy consumption of any individual space.

The space characteristics

Space description. The MBC2 office is rectangular with an area of 22.5 m^2 (see Figure 4.1). The facade window area (vision glazing of the curtain-wall construction) is equal to 20% of the floor area of the space.

Internal loads. The model for the MBC2 office space was written to include a variable

weekday occupancy pattern in the range of 1 to 2 persons with a weekday schedule from 8 a.m. to 5 p.m.[1] The model describes zero occupancy during the weekend. When "present", each person generates 115 W of heat, of which 75 W are sensible and 40 W are latent. No other sources of latent heat are simulated. The office equipment modeled in the space (computers, printers, lights) has a constant load output of 275 W between 8 a.m. - 5 p.m. on weekdays. No equipment load is simulated during the weekend.

Infiltration. The model for the MBC2 office space describes an infiltration rate of 0.2 ACH (13.5 m^3/h) during the time when the building is not pressurized (the ventilation system is off). An infiltration rate of zero is modeled when the ventilation system is on.

Radiant cooling (RC) system. Cooling water is supplied to the radiant cooling panels at the rate of 180 kg/h and with a constant inlet temperature. The inlet water temperature is selected at each location to adapt the cooling power of the radiant system to the climate-induced cooling load and to maintain the indoor air temperature close to a prescribed design point (24 °C). For the purpose of the study, the RC system is modeled as having a timer-based control. On time coincides with occupancy time (8 a.m. to 5 p.m.).

A constant volume (CV) system provides ventilation. The system supplies outside air only, at the minimum rate specified by ASHRAE Standard 62-1989 [7] (72 m^3/h for a double-occupancy office space). The inlet air temperature is constant and equal to 20 °C. The inlet air humidity ratio is constant and equal to 9.5 g water/kg dry air (65% relative humidity). For the purpose of the study, two ventilation strategies were simulated in order to investigate the influence of overnight moisture buildup due to infiltration on the indoor conditions (see Figure 4.5).

The first ventilation strategy reduces the ventilation air flow during off-occupancy hours (weekend days included). This strategy is mainly beneficial in hot humid climates, as the pressurization of the building by the ventilation system does not allow overnight humidity buildup; this in turn reduces the next day's power demand for the dehumidification of the supply air (to remove the additional latent load).

The second ventilation strategy supplies air at half rate for two hours before occupancy time, and for one hour after occupancy time, and interrupts the ventilation during the remaining 12 hours. During weekend days, the space is ventilated during 12 hours, from 6 a.m. to 6 p.m., albeit at half rate. This strategy is beneficial in any climate, as it ventilates the building before the occupants arrive and after they leave. By switching off the ventilation system for most of the night hours, this strategy reduces the energy consumption and power demand of the air distribution system.

1. As the activity in each office building reflects the type of activity taking place inside, it is difficult to establish a "typical" office building occupancy pattern. The hypothetical 8 a.m. to 5 p.m. schedule used in this study was selected to simplify the interpretation of simulation results.

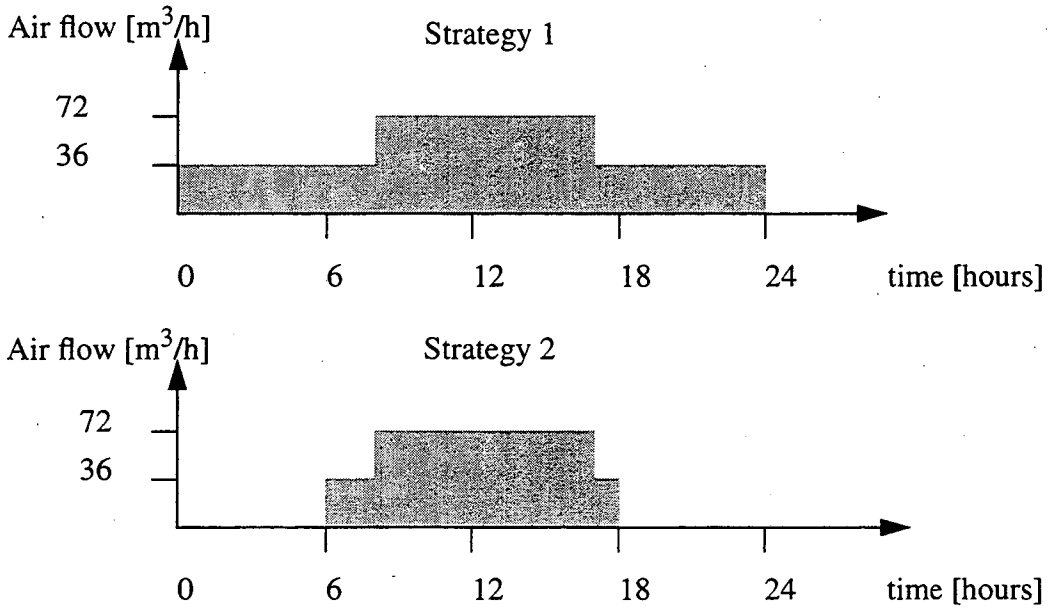

Figure 4.5. Ventilation strategies: schedules for weekday hours.

All-air system. A variable air volume (VAV) system was modeled in DOE-2 during occupancy hours. At each location, the system was designed to match (1) the outside air supply rate of the radiant cooling system, and (2) the indoor air temperature and humidity ratio provided by the radiant cooling system during occupancy hours. To achieve this match, the size of the system, the design cooling coil temperature, the minimum air flow, etc. were established at each location separately.

After occupancy hours, a constant volume (CV) system replaces the VAV system to supply outside air only, at the constant rate of 36 m^3/h. To match the conditions imposed on the radiant cooling system, the CV system functions according the same night ventilation strategies. To provide similar indoor conditions as a basis for comparison, the CV system dehumidifies the outside air to 9.5 g water/kg dry air whenever the outside air humidity ratio is higher than this value.

It is difficult to estimate the uncertainties introduced in the simulation results by the selection of these particular parameters for occupancy schedules, activity levels, equipment power and schedules, the design point, schedules and operation strategies of the two air-conditioning systems, etc., without performing parametric studies for each parameter. The author notes however, that matching the design of the two systems based on the indoor air temperature and humidity introduces a bias in favor of the all-air sys-

tem. As stated in Section 4.3, using a matching index incorporating the mean radiant temperature would have been to the advantage of the radiant cooling system because the presence of the cooling surface in the space lowers the mean radiant temperature. To match the PMV of the space conditioned by the all-air system, the radiant system would have been able to reduce the cooling power of the radiant surface, which would have translated into lower sensible energy consumption and power demand. However, because DOE-2 and RADCOOL do not provide all the parameters necessary in the calculation of the PMV, it is difficult to estimate the magnitude of the bias introduced in the results by matching the two systems *only* on the basis of the indoor air temperature and humidity.

4.4.3 The locations selected for the parametric study

As RADCOOL simulations take a significant amount of time (about 4 hours of computer time elapse for each simulation on a workstation for 10 days of weather data), the parametric study consists of simulations of the base-case space at only a small number of US locations. To capture the characteristics of a wide range of US climates, the locations were chosen on the basis of a climate classification. The classification criteria reflect the character and purpose of the study.

Climate classification

One of the goals of the parametric study is to compare the energy consumption and peak power demand of a radiant cooling system with those of an all-air system that provides similar indoor air temperature and humidity during occupancy hours. To avoid biasing the results of the study in favor of either system, the climate classification should be based on criteria that have the same influence on the energy consumption of both systems. In general, an air-conditioning system responds to the following weather-induced loads: (1) heat gain by conduction through the building structure; (2) solar heat gain through the windows; (3) infiltration of moist air during periods of non-positive pressure; and (4) conditioning (cooling and/or dehumidification) of the outside air necessary for ventilation.

The heat gain by conduction through the building structure and the solar heat gain through the windows affect the operation of a building conditioning system in similar ways. Consequently, these two components can be examined together when evaluating the response they elicit from the building conditioning system.

The heat gained by conduction and transmission of solar radiation through the building facade is removed from the space by each of the two systems in a characteristic way. The radiant system adjusts water flow and/or water temperature to control the temperature of the radiant surface. The all-air system adjusts the quantity and/or temperature of the recirculation air supplied to the space. Because the two systems use different heat

transfer mechanisms to remove the heat from the building, the heat gain through the facade influences the two systems differently. A climate classification based on this factor alone may therefore bias the results of the parametric study in favor of one system or the other.

The moisture buildup due to infiltration during periods of non-positive pressure (for example, when the ventilation is switched off at night) also affects the two systems differently. While both systems use air circulation to remove the accumulated moisture, the air volume supplied to the space by the all-air system once the air supply has been switched on, is much larger than that supplied to the space by the radiant cooling system (the all-air system dehumidifies the *mix* of outside air and recirculation air). Using the moisture buildup parameter as a basis for climate classification would once again bias the results of the parametric study in favor of one system or the other.

Both the radiant cooling system and the all-air system supply the same amount of outside air to the building: the minimum ventilation rate specified by ASHRAE Standard 62-1989 [7] during occupancy hours (72 m^3/h), and half that amount, or zero during off-occupancy hours, depending on the ventilation strategy. As discussed in Chapter 2, for a radiant cooling system the cooling power of the ventilation air is small when compared to the cooling power of the radiant surface. Because the outside air represents a small fraction of the air volume supplied to the space by the all-air system, space cooling is accomplished mainly by the recirculation air. In this study both systems (1) condition the same space located in the same climate, (2) supply the same amount of outside air to the building, (3) dehumidify the supply air to the same level, and (4) provide the same indoor conditions to the building. A climate classification based on the energy associated with conditioning (cooling and/or dehumidification) of the ventilation air ought to introduce the least possible bias in the results.

These considerations led to the following strategy for the climate classification. First, the energy to condition the outside air during an arbitrarily-selected cooling season (May 1 through October 31) was calculated at all US locations for which weather tapes were available.[1] For simplicity, the calculation used the same design conditions for the outside air supply at all locations: the ventilation flow rate corresponding to the first ventilation strategy used in the study (see Figure 4.5), a temperature of 20 °C, and a humidity ratio of 65% (9.5 g water/kg dry air).

Next, the locations were classified in nine groups according to (1) the relative importance of dehumidification in the total energy necessary to condition the ventilation air at each location, and (2) the absolute value of the total energy necessary to condition the ventilation air at each location. This classification allows the groups to contain approximately the same number of locations. Figure 4.6 shows each group as a collection of points located inside contour lines. Finally, at least one location from each group was

1. Weather tapes provide information about the characteristic weather at a given location.

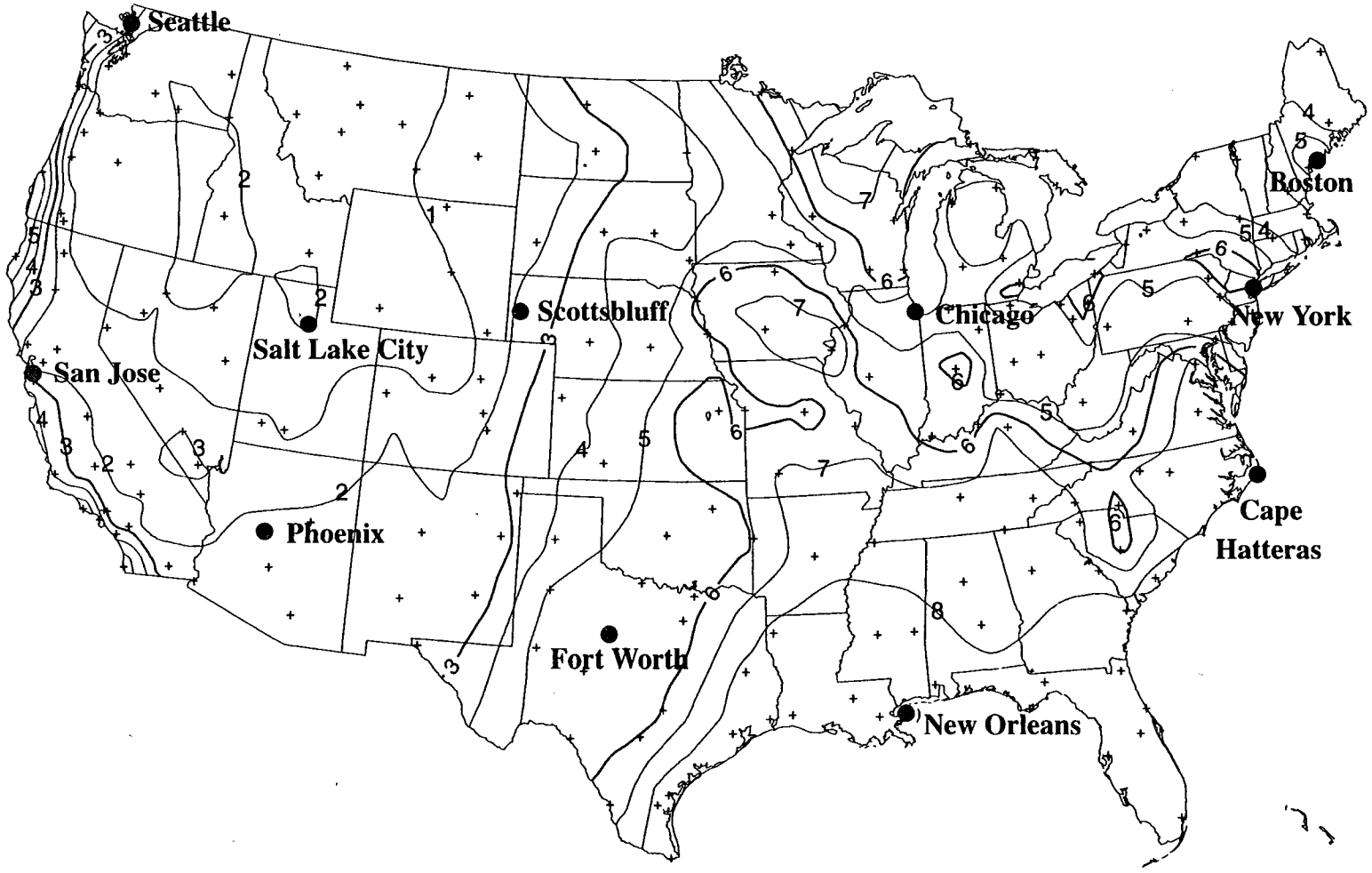

Figure 4.6. Climate classification based on the dehumidification energy and total energy necessary to condition the ventilation air.

selected for the study. Table 4.2 presents the selected locations.

TABLE 4.2. Energy consumption for the cooling and dehumidification of ventilation air. Climate classification and locations selected for the study.

Dehumidification fraction of the total cooling energy for ventilation	Total cooling energy for ventilation [MJ-h/kg]	Group number	Location selected
Dry 0-50%	0 - 5.7	1	Seattle, WA
	5.7 - 12.4	2	Salt Lake City, UT
	12.4 - 54.4	3	Phoenix, AZ Scottsbluff, NE
Moist 50-67%	0 - 18.0	4	Boston, MA San Jose, CA
	18.0 - 28.2	5	Chicago, IL
	28.2 - 88.9	6	Fort Worth, TX
Humid 67-100%	0 - 22.0	7	New York, NY
	22.0 - 59.7	8	Cape Hatteras, NC
	59.7 - 114.7	9	New Orleans, LA

To understand the role of the climate classification in interpreting the results of the study, information was obtained regarding the commercial building stock covered by each of the 9 climate groups. The results are presented in Table 4.3. According to these data, the climate groups 1-3 (dry climates) include only 10% of the commercial building stock in the large metropolitan areas. Climate groups 4-6 (moist climates) and 7-9 (humid climates) each include over 40% of the commercial building stock. Assuming that radiant cooling systems are adequate to handle the different sensible and latent loads occurring in different office buildings, compatibility between the radiant cooling system and the dry climates only (climate groups 1-3), would indicate that the market for radiant cooling in the US is restricted to only a small fraction of the existing commercial building stock. Compatibility between the radiant cooling system and more climate groups would indicate a larger potential market for radiant cooling in the US.

As indicated earlier, condensation problems may arise when a radiant cooling system is installed in a building in which the indoor activity is associated with significant moisture production. Residences, hotels and restaurants are examples of such buildings. In addition, buildings with high specific cooling loads might be poor candidates for radiant cool-

TABLE 4.3. Office buildings in the largest metropolitan areas and their distribution with respect of the climate classification.

Climate	Occupied commercial area [$10^6 m^2$ (Msqft)]	Percentage of total	
group 1	11.1 (119.7)	5.05	Dry climates 10.66%
group 2	5.1 (54.4)	2.42	
group 3	7.1 (76.7)	3.19	
group 4	17.2 (185.2)	8.31	Moist climates 41.56%
group 5	49.5 (532.9)	22.52	
group 6	24.5 (263.6)	10.73	
group 7	49.1 (528.9)	24.69	Humid climates 47.78%
group 8	41.8 (449.4)	15.01	
group 9	19.3 (208.0)	8.08	
Total	224.7 (2418.8)	100.00	

Source: Statistical Abstract of the United States 1995, Table 1229, "Commercial Office Space - Inventory and Vacancy Rates for the Largest Metropolitan Areas: 1994"

ing because the cooling power of radiant cooling systems is limited to 140 W/m^2.

Buildings that have poorly insulated envelopes fall into this category. Consequently, compatibility between the building equipped with the radiant cooling system and a certain climate group does not imply that the market for radiant cooling in the US covers the *entire* commercial building stock covered by that group.

Figure 4.7 presents a classification of the existing US commercial building stock by the main type of activity taking place in each building. The lighter area on Figure 4.7 represents buildings that are generally associated with large indoor moisture production (lodging, food sales, etc.), or buildings that might not need mechanical cooling (parking lots, some warehouses). The data in Figure 4.7 imply that, if buildings equipped with radiant cooling systems could function without the risk of condensation and were adequate to handle sensible loads in all US climate groups, the US market for radiant cooling would cover approximately 65% of the existing US commercial building stock.

4.4.4 The location-specific simulation periods

An estimate of the energy consumption and peak power demand of the radiant cooling

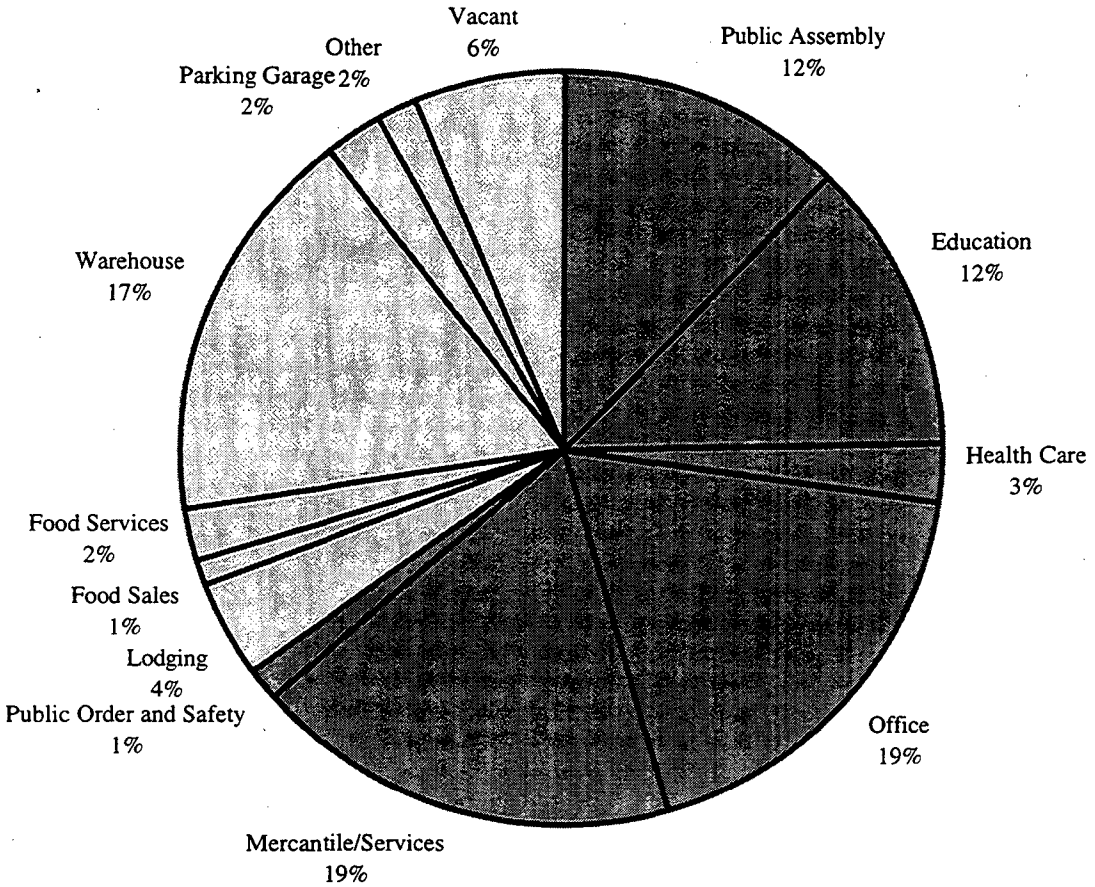

Figure 4.7. US commercial buildings - classification by principal activity.

Source: Statistical Abstract of the United States 1995, Table 1241, "Commercial Buildings - Selected Characteristics, by Square Footage of Floor Space: 1992"

system and the all-air system over the entire cooling season would provide the ideal data in the comparison of the performance of the two systems. However, RADCOOL simulations are limited to one week of weather data. If this modeling period is chosen at random, the extrapolation of the energy consumption and peak power demand from the selected week to the whole year has very little meaning. A selection process is therefore necessary to determine the location-specific week-long modeling period that best represents the climate characteristics of the entire cooling season.

Because the parametric study compares the energy consumption *and* peak power demand of a radiant cooling system with those of an all-air system that provides similar indoor conditions during occupancy hours, the selection process was conducted to choose *two* one-week periods at each location. The location-specific "typical week"

reflects the average energy consumption of the all-air system over the cooling season. The location-specific "week of system peak" is a week centered around the day when the all-air system power demand is at its highest for the cooling season.

The typical week

The typical week is the location-specific week that reflects the average energy consumption of the air-conditioning system over the cooling season. The estimate for the system energy consumption during this week can therefore be considered generally representative of the system energy consumption over the cooling season.

Previous work. The challenge of establishing what is a "typical period of time" associated with estimating the energy consumption of a building first arose in the late 1970s. Several building energy simulation models had been generated by this time, but the computational capacity of computers limited the length of the simulation and/or the size of the building to be simulated. Progress in the computational power and capacity of computers has generally eliminated this issue in the last 10 years, except of course, for computational fluid dynamics (CFD) and programs such as RADCOOL. Continued efforts in the area of "typical weather" focus on establishing the characteristic weather at a given site by examining a large number of yearly data, describing weather trends, and creating "typical weather files" for building simulation programs. The weather files employed in the present study are the results of such efforts.

Recognizing the importance of the weather patterns on the energy consumption of a building, most of the early work on the topic of "typical weather" focused on performing some sort of "compression" of the available weather data. To this end, programs were designed that processed a full year of weather data and created a short version of each month. The simulation of a building using the resulting "typical weather" provided some information about the energy consumption of the building during the whole year.

A selection criterion is obviously needed to decide which days to select out of a year of weather data to generate the "compressed" months. The examination of two papers on the subject shows that different authors had different perspectives concerning the selection criterion.

Arens and Nall [8] focused on producing an algorithm that would be biased as little as possible towards any particular type of building or climate. Their technique estimated the impact of a number of weather parameters on the energy consumption of a building. After performing a large number of simulations, the authors were able to attach numerical weights to four weather parameters: dry-bulb temperature, humidity ratio, wind speed, and cloud cover. This allowed them to rank all the 4-day successions in a month, and then designate the 4-day period that best represents the month from the point of view of the building energy consumption. By comparing the energy consumption calculated using the compressed weather data with that calculated using the whole weather

file, they showed that the error introduced in the prediction of energy consumption of a building by using the compressed data was approximately 3.5%.

Degelman [9] focused on matching his "compressed weather" data with a given set of buildings, both commercial and residential. By performing a large number of building simulations, he established the five weather parameters that most influence the energy consumption of a building: dry-bulb temperature, dew-point temperature, horizontal solar radiation, wind speed, and atmospheric pressure. He then identified the succession of 7 days in each month that introduces the least amount of error in predicting the number of degree days of heating and cooling at a given location. Finally, he tested his algorithm by performing a large number of simulations for different buildings and climates. His conclusion is that, for a given balance point temperature, the results obtained using the compressed weather file do not introduce more than 3% error in the estimate of energy use, regardless of the building type and climate used for simulations.

Both these papers show encouraging results of the use of compressed weather files. To obtain the compressed weather interval best suited for building energy consumption calculations, both procedures perform multiple simulations. In addition, both procedures rely heavily on the building energy use to determine the best selection criterion.

Procedure for determining the typical week of the cooling season. Due to the nature of RADCOOL, performing multiple simulations to establish the typical week at each location is out of the question. However, there are no such restrictions for performing multiple DOE-2 simulations for the building equipped with the all-air system.

As the energy consumption pattern of the radiant cooling system is probably different than the energy consumption pattern of the all-air system, the use of the energy consumption of the all-air system to designate the typical week may introduce errors in the results. However, the parametric study evaluates the energy consumption of the radiant cooling system and compares it with the energy consumption of the all-air system. Because the all-air system constitutes the basis of this comparison, it is not unreasonable to choose the typical week based on the energy consumption of the all-air system.

Since the typical week is location-specific, the following selection procedure was repeated for each of the 11 locations selected for the parametric study:

1. The base-case space equipped with the all-air system was simulated in DOE-2. The energy consumption of the all-air system was calculated for a pre-established cooling season (May 1 - October 31). The average seasonal energy consumption of the system as calculated was derived.

2. The average system energy consumption was determined for all the sliding weeks occurring in the cooling season. Sliding weeks are 7-day successions that start on each successive date; examples of sliding weeks are: May 1-7, May 2-8,..., October 25-31.

3. The difference between the weekly energy average and the seasonal energy average

was calculated for each sliding week.

4. The weeks were ranked according to the difference in the week-specific and seasonal energy averages.

5. The week with the lowest difference between the average weekly energy consumption and the average seasonal energy consumption was selected as the typical week. The estimate of the system energy consumption during this week provides the best approximation for the system energy consumption over the cooling season.

The typical weeks occur at the end of May through the beginning of June at 7 of the 11 selected locations, and at the end of August through the beginning of September at 4 of the 11 selected locations. This result is intuitively correct because, in contrast to the internal loads which remain approximately constant over the cooling season, the weather-induced cooling loads vary a fair amount. The mean behavior can be captured only by the weeks belonging to the "transition" (Spring or Fall) months.

The week of system peak

The week of system peak at each location is the week during which the power demand of the all-air system is the highest of the entire cooling season. The rationale for selecting the week of system peak based on the power demand of the all-air system is similar to that used to select the typical week. The time of the all-air system peak power demand can be easily established by performing a DOE-2 simulation for the entire cooling season. The time of the peak power demand of the radiant cooling system is difficult to determine because it is not practical to perform a RADCOOL simulation for the entire cooling season.

Performing the comparison between the peak power demand of the radiant cooling system and that of the all-air system during the week of system peak of the all-air system may introduce errors in the results of the study because the radiant cooling system may not reach its peak demand during the same week. In such a case the results of the comparison would indicate that the radiant cooling system has a larger potential to reduce the peak demand than it actually has. However, since the interior loads of the base-case space do not change during the simulated year, the time of the peak power demand should be driven by weather-induced loads (the conduction and solar heat gain through the facade). If this were true, the peak power demand of the radiant cooling system during the week of system peak of the all-air system may in fact coincide with the peak power demand of the radiant cooling system over the entire cooling season.

To determine the week of system peak the following procedure was repeated for each of the 11 locations selected for the parametric study:

1. The base-case space equipped with the all-air system was simulated in DOE-2 and the hourly power demand of the all-air system was calculated for the same pre-established cooling season (May 1 - October 31).

2. The time of the peak power demand of the all-air system was established at each location.

3. The week of system peak at each location was selected as the week centered on the day containing the peak power demand.

The base-case space equipped with the radiant cooling system was modeled in RADCOOL with the weather conditions imposed by the week of system peak. The hourly power demand was calculated and the time of the peak power demand was determined. In general, the peak power demand of the radiant cooling system occurs later than the peak power demand of the all-air system. The maximum time difference between the peaks is three hours.

The week of system peak is less location-specific than the typical week. The week of system peak occurs at the end of July through the beginning of August at all the selected locations. At all locations, the weather during the week of system peak is hot, and the humidity is at its highest. This indicates that weather-induced loads have significant influence on the time of the system peak demand.

Plausibility check

To verify that the procedure to select the typical week provides reasonable results, two tests were conducted. First, the difference between the average energy consumption during the week of system peak and the average energy consumption during the cooling season was calculated. At all 11 locations the differences between the two averages were large. Thus, the selection criterion for the typical week designates the week of system peak as "far from season average".

Second, the energy consumption of the all-air system during the designated typical week was compared to the energy consumption of the system during the cooling season. At all 11 locations the energy consumption during the "typical" week represents 3.8% of the energy consumption over the established cooling season. The number of hours in a week (168) divided by the number of hours during the cooling season (4416) is also equal to 3.8%. The extrapolation of the energy consumption during the typical week to the energy consumption of the cooling season should therefore introduce little error, at least for the all-air system. In contrast, the week of system peak accounts for an average of 6.7% (the range over all locations is 4.5-9.6%) of the energy consumption over the cooling season. Extrapolating the energy consumption of the week of system peak to obtain the energy consumption of the cooling season would therefore lead to an over-estimate of the latter.

Discussion

Building simulations can determine the relationship between the energy consumption during the typical week and the energy consumption during the cooling season only for the all-air system. Due to the selection procedure, the relationship obtained is independent of the building location: the same factor of 3.8% links the air-conditioning energy

consumption during the "typical" week to the air-conditioning energy consumption during the pre-established cooling season. However, the use of the 3.8% factor to predict the energy consumption of the radiant cooling system over the same cooling season implies that the energy consumption pattern of the radiant cooling system is similar to that of the all-air system. This assumption may be true, but has not been confirmed. This observation imposes the following restrictions on the interpretation of the results:

(1) It is reasonable to compare the radiant cooling system with the all-air system during the typical week of the all-air system. The result of this comparison provides an estimate for the difference in energy consumption of the two systems during this typical week. If this estimate is used to calculate the difference in the energy consumption of the two systems over the entire cooling season, the final result should be reported together with all the assumptions that were made to obtain it (Table 4.4).

TABLE 4.4. Summary of assumptions for the parametric study.

Assumptions	RADCOOL	DOE-2
Geographical locations	Figure 4.6 and Table 3.2	
Simulation periods	two week-long periods at each location (Section 4.4.4)	
Structure geometry, dimensions and orientation	base-case building: Figure 4.1 base-case space: MBC2 in Figure 4.1	
Window exposure	south-western	
Construction of vertical walls, roof and floor	Figure 4.3 and Table 3.1	
Window type	double-pane, U-value = 1.75 W/m^2-K	
Window shading	none	
Internal loads	22.5 W/m^2, 57% convective and 43% radiative	
Internal load schedule	8 a.m. to 5 p.m., Monday through Friday; no internal load on weekends	
Infiltration	0.2 ACH when space not ventilated	
Mechanical cooling	radiant panel system	VAV system

TABLE 4.4. (continued) Summary of assumptions for the parametric study.

Assumptions	RADCOOL	DOE-2
Cooling schedule	8 a.m. to 5 p.m., Monday through Friday no cooling on weekends	
Cooling system design strategy and setpoint	match indoor air temperature (24 °C 1 °C) and relative humidity (30 to 60%) during occupancy time	
Cooling air or water volume flow and inlet temperature	180 l/h 17.5 °C in Phoenix and Salt Lake City 20 °C at other 9 locations	variable volume variable temperature (not below 15 °C)
Ventilation air volume flow	Daytime: Monday through Friday: 36 m^3/h from 6 a.m. to 8 a.m. 72 m^3/h from 8 a.m. to 5 p.m., and 36 m^3/h from 5 p.m. to 6 p.m. weekends: 36 m^3/h from 6 a.m. to 6 p.m. Nighttime: 36 m^3/h from 6 p.m. to 6 a.m. or none, depending on ventilation strategy (Figure 4.5)	
Ventilation air inlet temperature	17.5 °C in Phoenix and Salt Lake City 20 °C at other 9 locations	variable temperature (not below 15 °C)

(2) The conclusions that can be drawn from the comparison of the two systems over the week of system peak and the typical week provide an initial indication of the potential of radiant cooling systems to reduce the energy consumption and peak power demand due to air-conditioning while providing similar indoor conditions as an all-air system. The generalization of these results requires further research.

4.5 Comparing the Results of the RADCOOL and DOE-2 Simulations

The parametric study compares the energy consumption and peak power demand of a radiant cooling system and an all-air system providing similar indoor air temperature and humidity to a commercial building. The study relies on RADCOOL simulations to obtain information regarding the performance of the radiant cooling system, and on DOE-2 simulations to describe the performance of the all-air system. In general, the use of two distinct programs to simulate two different systems may introduce uncertainties in the results. The parallel use of RADCOOL and DOE-2 in this study could not be avoided because at its present development stage DOE-2 is not able to simulate the performance of radiant cooling systems, and RADCOOL is not able to simulate the operation of a VAV system. However, the comparison of the results of RADCOOL and DOE-2 should not introduce significant uncertainties in the results because:

(1) both programs simulate the same base-case space with the same orientation and the same boundary conditions; Chapter 2 has described the intermodel comparison between RADCOOL and DOE-2 for a passive structure, and has shown that the two programs provide essentially the same results for the indoor conditions of this structure;

(2) the all-air system modeled in DOE-2 is designed to match the indoor air temperature and humidity obtained by the radiant cooling system simulation during occupancy time;[1]

(3) the same calculation strategy is used in the evaluation of the energy consumption and peak power demand of the two systems (see below).

1. To match the indoor conditions provided by the radiant cooling system, the design of the all-air system has to be finely-tuned (adjustments of the cooling coil temperature, supply temperature, recirculation air flow, etc. are needed). Common sense suggests that the fine-tuning process may change the energy consumption pattern of the all-air system and the time at the peak power demand occurs for this system. However, preliminary DOE-2 simulations show that the typical week and the week of system peak that would be selected after the fine-tuning has been achieved are the same as the typical week and the week of system peak that were selected before the fine-tuning has been achieved. The fine-tuning process does not appear to influence at all the results of the study.

4.5.1 Using the results of RADCOOL and DOE-2 to compare the energy consumption and peak power demand of the radiant cooling system and all-air system

The study uses the system parameters from the RADCOOL and DOE-2 simulations (air volume flow, supply air temperature, supply air humidity ratio, fan power, water volume flow, supply water temperature, and pump power), as well as weather parameters (air temperature, humidity ratio, solar radiation) to calculate the energy consumption and peak power demand of the radiant cooling system and all-air system, respectively. The assumptions of the study - a single-zone space conditioned by an air-conditioning system terminal - confine the energy and peak power accounting to space boundaries.[1] Thus the energy and peak power calculations carried by the study correspond to the readings of hypothetical space meters monitoring the sensible, latent, and distribution loads on the air-conditioning terminal due to its removing of sensible and latent heat from the base-case space.

Energy consumption and peak power calculation. The sensible load imposed on the air-conditioning terminal includes the power necessary to remove excess space heat, and to cool the outside air fraction necessary for ventilation. This translates into cooling the heat transfer medium used by each system (air for the all-air system, and air and water for the radiant cooling system) by a cooling coil. The thermal calculation consists of evaluating the power necessary to the cooling coil to cool a given volume flow of conditioning agent by the number of degrees equal to the difference between return temperature (specific to each calculation step) and supply temperature (dictated by the design supply setpoint). The volume flow of the conditioning agent is known at each time step.[2]

The latent load consists of the power necessary to remove excess latent heat from the space. The removal of excess latent heat is accomplished by controlling the moisture content of the air supplied to the space. The all-air system calculation evaluates the power necessary to the cooling coil to lower the moisture content of a given volume flow of supply air between mixing conditions (of outside and recirculation air) and design supply conditions. The radiant cooling system calculation evaluates the power necessary to lower the moisture content of the outside air volume flow between outside conditions and design supply conditions.

The distribution load of the all-air system consists of the fan power necessary to supply the cool air to the space. The fan power is calculated by DOE-2 for each hour when the system is active and is a function of the hourly air volume flow. The distribution load of the radiant cooling system consists of the pump power necessary to supply the cool

1. The "terminal" of the all-air system consists of the air supply register. The "terminal" of the radiant cooling system consists of the radiant surface and the ventilation air supply register.

2. The air volume flow supplied by the all-air system during work hours is variable (VAV system) and adjusted to the sensible loads of the space, and is constant or zero during off-occupancy hours. The air volume flow and water volume flow supplied by the radiant cooling system are constant or zero by design.

water to the radiant cooling panels, and the fan power necessary to supply the ventilation air to the space. The pump and fan power of the radiant cooling system are constant when operated.

To provide a basis for the comparison of the energy consumption and peak power demand of the all-air system and radiant cooling system, all three components of the load on the air-conditioning terminal (sensible, latent, and distribution) should be expressed in the same units. As the results of the calculation correspond to the readings of energy and power meters, the units of choice are those of electrical energy (kWh_e) and electrical power (W_e).

The distribution load is already expressed in terms of electrical power demand. However, the sensible and latent loads are expressed in terms of thermal power demand. Converting these units in terms of electrical power demand requires an assumption about the coefficient of performance (COP) of the cooling coil-chiller combination serving each system. For simplicity, the study used a constant COP for the both the cooling coil-chiller combination serving the radiant cooling system and for that serving the all-air system. In reality, the COP varies as a function of the load. The numerical value of the COP of commercially-available chillers varies between 2.5 (for rooftop units) and 5 to 6 (for centrifugal chillers) at design point [10]. The parametric study uses a COP of 3 in its thermal-to-electric conversion calculations.

Comparing the energy consumption and peak power demand of the two systems. The comparison of the peak power demand of the all-air system and the radiant cooling system consists of (1) calculating the electrical sensible, latent, and distribution loads for each hour of the week of system peak, (2) determining the hour when the peak electrical load occurs for each system separately, and (3) evaluating the difference between the peak load of the all-air system and that of the radiant cooling system.

The comparison of the energy consumption of the all-air system and radiant cooling system consists of (1) calculating the electrical sensible, latent and distribution loads for each hour of the typical week, (2) summing these values and multiplying by the time step to evaluate the electrical energy consumption during the typical week for each system, and (3) evaluating the difference between the energy consumption of the all-air system and that of the radiant cooling system.

The results of the energy and peak power calculation are presented in Appendix B and will be discussed in Chapter 5.

4.6 Capabilities and Limits of the Parametric Study

The goals of the parametric study described in this Chapter are (1) to establish whether buildings equipped with radiant cooling systems can function in US climates without the risk of condensation, and (2) to compare the energy consumption and peak power demand

of a radiant cooling system and an all-air system that provide similar indoor conditions to a commercial building space during occupancy time. Due to the design of the parametric study, the comparison of the results obtained for the building equipped with the radiant cooling system and the building equipped with the all-air system will mainly reflect the difference between the performance of the two systems. It is worthwhile to note, however, that the results are influenced by the type of building in which the two systems operate, as well as by the building location, internal loads, etc. The study captures the climate-variability of its results by repeating the simulations and performing the comparison of the results at a number of "typical" locations. Assumptions and limitations notwithstanding, this parametric study is the first in-depth investigation into the climate-related aspects of the performance of buildings equipped with radiant cooling systems. Further research is necessary to generalize the results to any building type, as well as into other "dimensions". The capabilities and limits of the study are summarized below.

Capabilities: the study

(1) proposes a methodology for the comparison of the simulated energy consumption and peak power demand of two different building conditioning systems;

(2) conducts parallel simulations of a radiant cooling system and an all-air system for several US climates; investigates the potential of the radiant cooling system to use less energy and require less peak power to condition a base-case space;

(3) investigates the capability of radiant cooling systems to operate in US climates with a small risk of condensation; establishes climate-dependent trends in the energy consumption and the peak power demand of a radiant cooling system;

(4) reflects the indoor conditions of a selected space in a new office building structure;

(5) adds to the present state of knowledge about how buildings equipped with radiant cooling systems might function;

(6) can be extended to include other building types, locations, simulation periods, etc., when the calculation capacity of computer improves;

(7) can be adapted to specific projects and can be used in building design decisions as soon as RADCOOL and DOE-2 are integrated.

Limits: the study

(1) uses RADCOOL to simulate the performance of the radiant cooling system; this limits the study to:

- one building having pre-established structure and layout;

- one space having a "rationally" pre-established orientation, occupancy rate, interior loads, boundary conditions, and cooling system design;

- two study periods limited to one week of weather data each;

- a small number of locations;

(2) uses DOE-2 to simulate the performance of the all-air system; this restricts the use of comfort parameters as matching parameters for the indoor conditions simulated by the two programs to the indoor air temperature and humidity;

(3) does not cover all possible US building locations;

(4) does not cover all possible system designs and chiller performance coefficients (COP);

(5) does not provide information regarding the response of the radiant cooling system to sudden internal load changes (such as a case in which several people walk into a conference room for a meeting);

(6) does not provide information regarding the performance of the radiant cooling system in buildings with high internal loads, in buildings with poorly insulated structures, or in buildings with significant indoor or outdoor sources of moisture;

(7) introduces uncertainty into the extrapolation of its results to the whole base-case building, and/or to the entire cooling season at each location; this uncertainty has many components (e.g. relationship between space air-conditioning energy consumption and building air-conditioning energy consumption, relationship between the energy consumption of radiant cooling system during the designated typical week and during the entire cooling season, time of peak power demand of the radiant cooling system), and each component is difficult to estimate.

4.7 References

1. Helmut E. Feustel, Personal communication. Lawrence Berkeley National Laboratory, June 1995.

2. Corina Stetiu, H. E. Feustel, and F. C. Winkelmann, *Development of a simulation tool to evaluate the performance of radiant cooling ceilings*. Rep. LBNL-37300, 1995.

3. Simulation Research Group (Lawrence Berkeley Laboratory) and Group Q-11 (Los Alamos National Laboratory), *DOE-2 Engineering manual*. Rep. LBNL-11353, 1982.

4. ASHRAE Handbook, *Fundamentals*. Atlanta: American Society of Heating Refrigerating and Air-Conditioning Engineers, Inc., 1993.

5. International Energy Agency, Annex 28 - Low Energy Cooling, *Low energy cooling subtask 2: detailed design tools, reference building description*. IEA, Zürich, Switzerland, 1996.

6. California Energy Commission, *Energy efficiency standards for residential and non-residential buildings*. CEC P400-95-001, 1995.

7. ASHRAE Standard 62-1989, *Ventilation for acceptable indoor air quality.* Atlanta: American Society of Heating Refrigerating and Air-Conditioning Engineers, Inc., 1989.

8. Edward A. Arens and D. H. Nall, *Climate data abbreviation for the computerized calculation of heating and cooling requirements in buildings*. Rep. NBSIR 78-1525, 1978.

9. Larry O. Degelman, *Energy calculation sensitivity to simulated weather data compression.* ASHRAE Trans., (87) (1) 1981.

10. M. Shepard, J. Gregerson, D. Houghton, L. Fryer, J. Elleson, B. Pattinson, W. Hawthorne, L. Webster, J. Stein, D. Davia and S. Parsons, *Commercial Space Cooling and Air Handling Technology Atlas*, E-Source Inc., Boulder, Colorado, June 1995.

Chapter 5

RADIANT COOLING IN US OFFICE BUILDINGS: RESULTS OF THE MODELING PROJECT

Chapter 4 described the parametric study designed for examining the topic of compatibility between office buildings equipped with radiant cooling systems and climates representative for the US. Because the study is based on RADCOOL simulations, and because RADCOOL has certain limitations, several assumptions were necessary regarding the base-case space to be modeled in the study (Table 4.4). To capture most of the characteristics of a wide range of US climates, a selection process allowed the choice of a small number of representative US locations. A different selection process was then employed to choose two location-specific week-long time periods for which the space simulation was carried. This chapter presents the results of the parametric study.

5.1 Chapter Outline

The indoor air temperature and humidity ratio of the space as simulated by RADCOOL and DOE-2 are presented in Section 5.2. The section focuses on the indoor conditions at the New Orleans, LA location. Common sense indicates that operating the radiant cooling system in this hot-humid Louisiana climate should be difficult: reducing the risk of condensation on the cooling surface represents a significant challenge. The section compares the indoor air temperature and relative humidity provided by the simulated radiant cooling and all-air systems, discusses the heat transfer phenomena specific to the two systems, and examines the effectiveness with which the night ventilation strategies studied reduce the risk of condensation on the cooling surface. Because the results obtained in the other 10 climates selected for the study are qualitatively similar, discussing the simulated space indoor conditions in all climates would be redundant.

Appendix B contains the results of the energy consumption and peak power demand calculations for the radiant cooling system and the all-air system conditioning the space located in the 11 climates of the study. Section 5.3 discusses the results for the radiant cooling system, while Section 5.4 discusses the results for the all-air system. In Section 5.5 the energy consumption and peak power demand of the radiant cooling system and all-air system are compared. Based on this comparison, the savings potential of the radiant cooling system is calculated and a quantitative relationship is derived linking the savings potential of the radiant cooling system with the "opportunity for savings" offered by the all-air system. To verify the applicability of this quantitative relationship for other building structures and other space orientations, Section 5.6 describes a few additional simulations. Section 5.7 summarizes the conclusions of the parametric study.

5.2 Indoor Conditions

The simulations conducted in the parametric study involve modeling of a base-case space with two ventilation strategies, at 11 representative US locations, during two week-long periods for each location. The base-case space simulated by the study is MBC2 in Figure 4.1. The facade of the space is exposed to climate-induced loads; its window has a south-western orientation. The lateral walls, ceiling and floor of the space are considered to be exposed to the same conditions on both of their surfaces. The "back wall" separates the space from a hallway with a constant air temperature. Table 4.4 summarizes the modeling assumptions of the parametric study.

The base-case space serves as a two-person office between 8 a.m. and 5 p.m., Monday through Friday, and contains some equipment generating heat during occupancy hours. To remove the sensible and latent loads due to indoor activity and solar gains, the space is conditioned by an air-conditioning terminal (the air supply register of an all-air system, or the radiant surface and air supply register of a radiant cooling system). The air-conditioning terminal maintains the indoor air temperature within one degree of the 24 °C setpoint, and the indoor air relative humidity below 60% during occupancy hours. Space cooling terminates at the end of the work day. The night ventilation strategy employed (see Figure 4.5 and Table 4.4) dictates whether or not dehumidified air is supplied to the space during off-occupancy hours. If space ventilation occurs through the night, the fresh air supplied is not only dehumidified but also cooled. The cooling power of this low volume flow of air is relatively small.

Figure 5.1 shows the simulated indoor air temperature of the base-case space during the week of system peak at the New Orleans, LA location, for the first ventilation strategy (space continuously ventilated, albeit half rate at night). As the peak demand occurs on Monday, July 25 at the New Orleans location, the week of system peak centered on this day is Friday, July 22, through Thursday, July 28 (i.e. the day of the all-air system peak demand is the fourth day in the figures). To illustrate the influence of mechanical cooling and ventilation on the indoor air temperature, Figure 5.2 shows the hourly variation of this temperature during the day of system peak. Figure 5.3 presents the simulated indoor air relative humidity during the week of system peak in New Orleans, for the space ventilated continuously. To facilitate a discussion of humidity control strategies for the radiant cooling system, Figure 5.4 compares the radiant surface temperature and dew-point temperature of the base-case space ventilated continuously. Figures 5.5 through 5.8 present results similar to those in Figures 5.1 through 5.4, but corresponding to the second ventilation strategy (space ventilation interrupted at night).

Results similar to those presented in Figures 5.1 through 5.8 were obtained for the week of system peak *and* the typical week at all 11 locations selected for the study.

Due to the design of the parametric study, the indoor air temperature and the indoor relative humidity during occupancy hours (8 a.m. to 5 p.m. on workdays) are similar for the

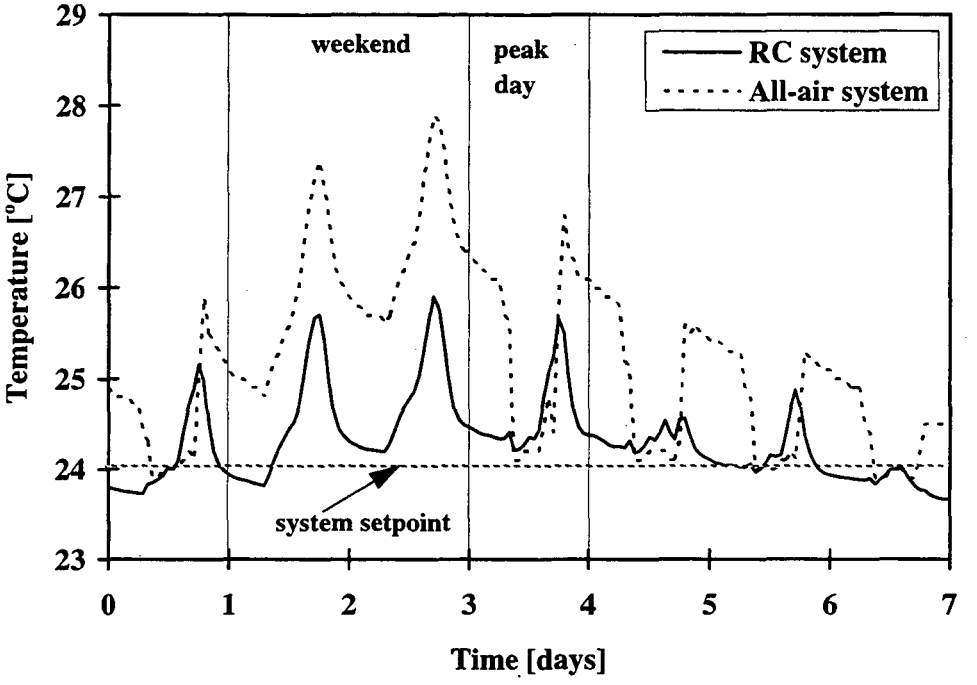

Figure 5.1. Indoor air temperature comparison at the New Orleans location during the week of system peak. Space ventilated continuously, half rate at night.

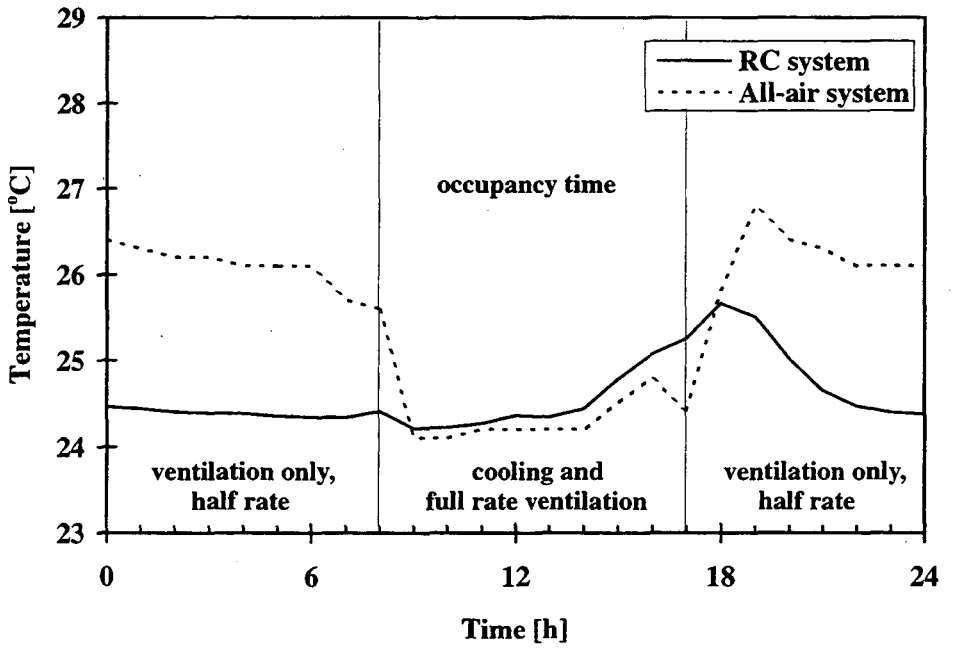

Figure 5.2. Indoor air temperature comparison at the New Orleans location during the day of system peak. Space ventilated continuously, half rate at night.

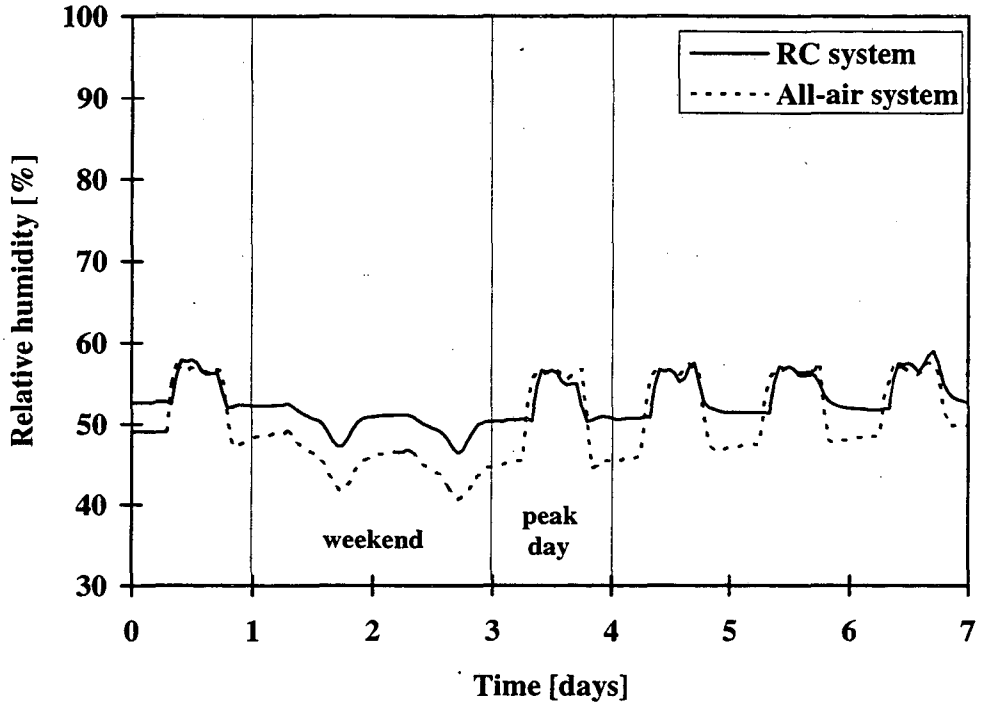

Figure 5.3. Indoor air relative humidity comparison at the New Orleans location during the week of system peak. Space ventilated continuously, half rate at night.

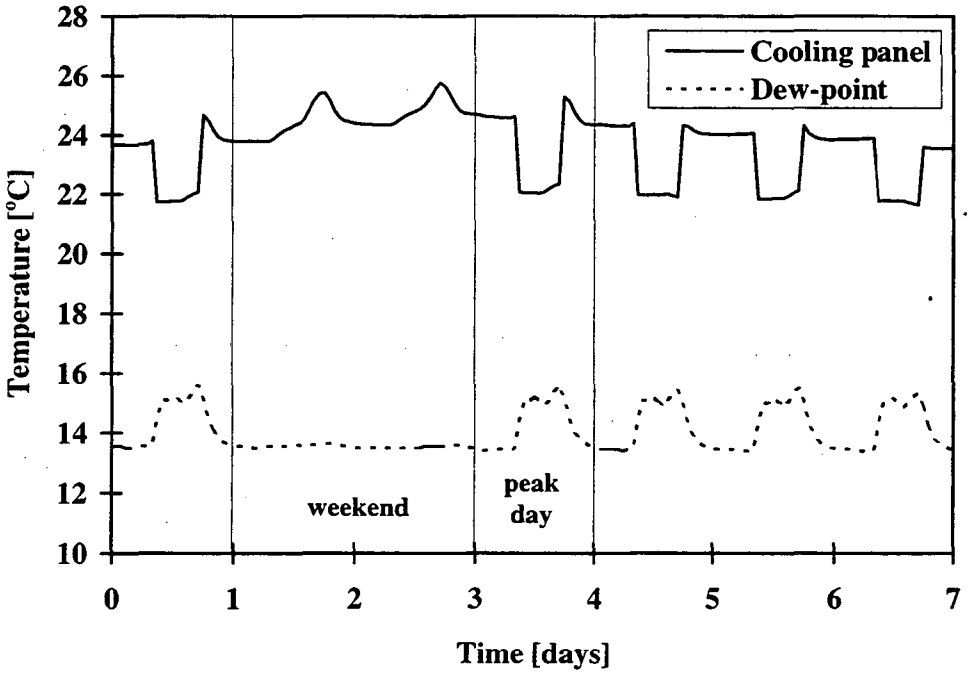

Figure 5.4. Comparison of cooling panel surface temperature and space dew-point temperature. New Orleans, space ventilated continuously, half rate at night.

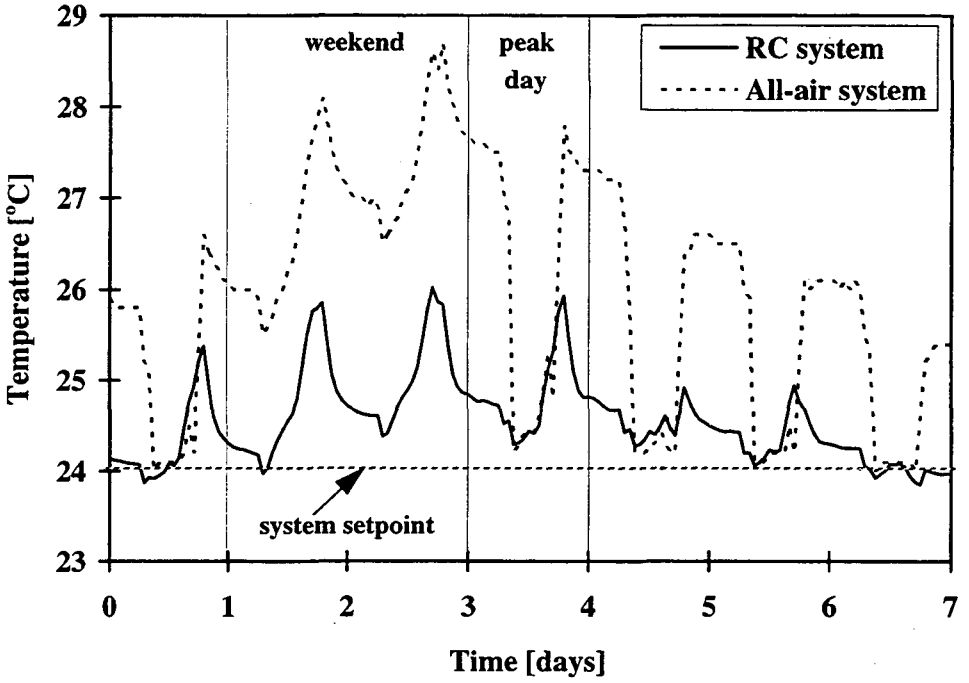

Figure 5.5. Indoor air temperature comparison at the New Orleans location during the week of system peak. Space ventilation interrupted at night.

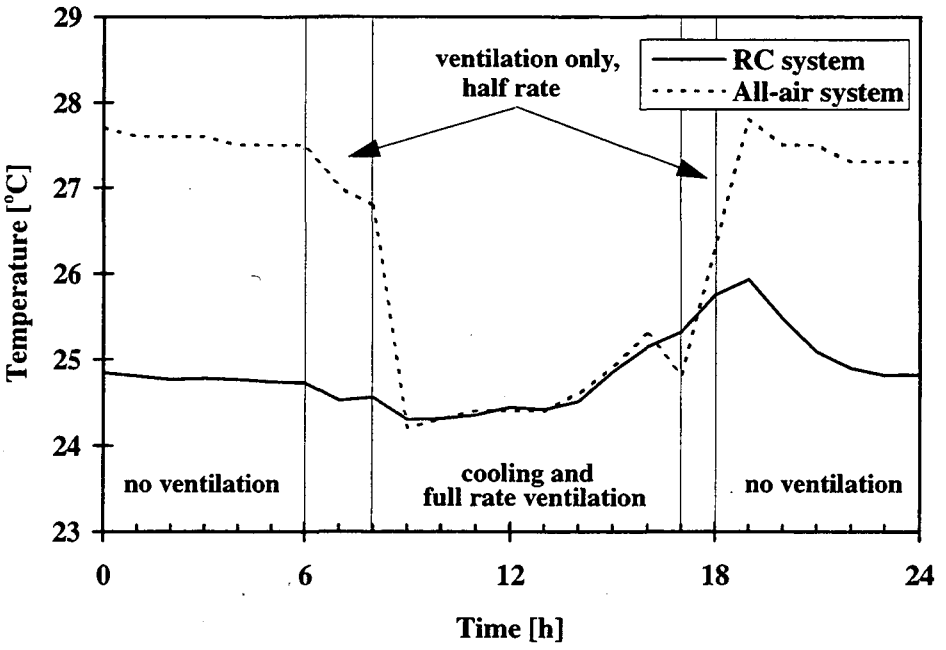

Figure 5.6. Indoor air comparison at the New Orleans location during the day of system peak. Space ventilation interrupted at night.

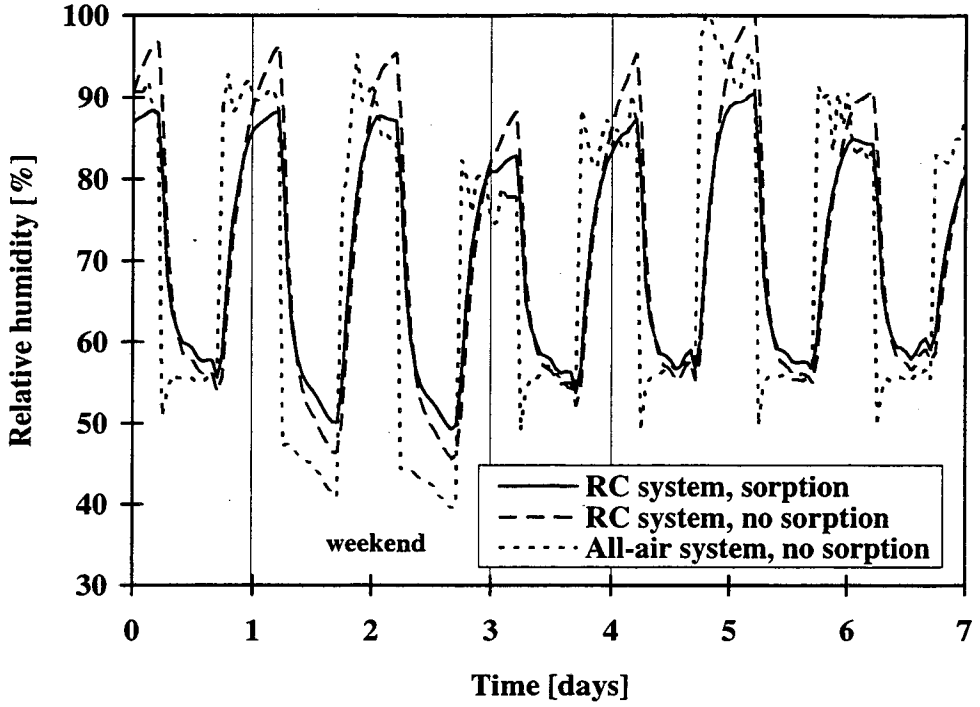

Figure 5.7. Indoor air relative humidity comparison at the New Orleans location during the week of system peak. Space ventilation interrupted at night.

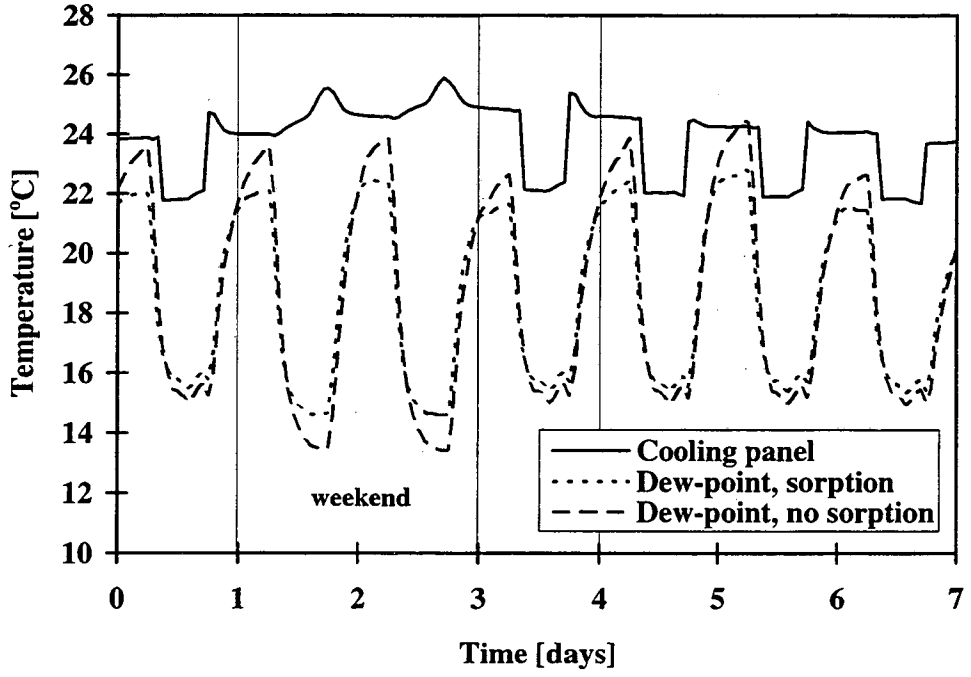

Figure 5.8. Comparison of cooling panel surface temperature and space dew-point temperature. New Orleans, space ventilation interrupted at night.

space equipped with the radiant cooling system and the space equipped with the all-air system. The indoor air temperature presents a variation of a few tenths of a degree around the 24 °C setpoint (Figures 5.2 and 5.6), and the indoor relative humidity presents a variation of a few percent around the value of 60% (Figures 5.3 and 5.7). The indoor air temperature and relative humidity in the space conditioned by the radiant cooling system and the all-air system are not exactly the same because the two systems employ different mechanisms to provide space conditioning.

The indoor air temperature presents a higher variation during off-occupancy hours (Figures 5.2 and 5.6) and the two weekend days (Figures 5.1 and 5.5). This occurs because the main source of cooling for the space (the ceiling panels for the radiant cooling system, and the recirculated fraction of the supply air for the all-air system) is switched off during this time. Even if the space is ventilated during the night, the cooling power of this low volume flow is relatively small.

Figures 5.2 and 5.6 demonstrate that, for a 24-hour period, the indoor air temperature of the space conditioned by the radiant cooling system is more stable than that in the space conditioned by the all-air system. The mechanisms used by the two systems to cool the space explain this result. The heat removal mechanism employed by the all-air system provides cooling to the indoor air directly, and to the occupants indirectly, through convective exchange with the cool air. Because convective heat exchange does not cool the surfaces of the space very efficiently, they store heat during the day.[1] When the mechanical cooling stops at the end of occupancy hours, the space surfaces release the stored heat, causing a sharp increase of the indoor air temperature. The amplitude of this increase is 2.5 to 3 °C, higher if space ventilation also stops. Then the space cools slightly overnight. When the space ventilation starts before the next occupancy period, the indoor air temperature presents a slow decrease. A rapid 1 - 2 °C decrease follows after the mechanical cooling is switched on.

By comparison, the radiative heat exchange mechanism employed by the radiant cooling system provides cooling to the occupants directly through radiation, and to the indoor air indirectly through convective heat exchange with the cooled ceiling. Because the vertical walls and the floor also exchange heat with the cooled ceiling, they are actively cooled during the day, therefore they can store less heat than their counterparts in the space conditioned by the all-air system. It is important to note that although they are actively cooled during the day, the vertical walls and the floor are still warmer than the indoor air. When the cooling stops, these building components release the heat stored during the day. Consequently, the indoor air temperature increases sharply, but only by

1. The assumption used to model the lateral walls, ceiling and floor is that these surfaces have the same boundaries on both surfaces (temperature and heat flux). While this translates into zero heat transfer through the midpoint of such a building component, it does not prevent each half of the building component from storing and releasing heat into the space to which it belongs.

1.5 - 2 °C. The indoor air temperature of the space conditioned by the radiant cooling system is thus more stable over a 24-hour period than the indoor air temperature of the space conditioned by the all-air system.

The first ventilation strategy supplies dehumidified air continuously to the base-case space to pressurize the space and avoid humidity buildup by infiltration. Figure 5.3 demonstrates that this strategy maintains the relative humidity of the space inside the comfort range at all times.[1] To save dehumidification and fan energy during off-occupancy hours, the second ventilation strategy interrupts the ventilation of the base-case space for 12 hours overnight. The moisture mass balance performed in this case shows that, due to infiltration-driven humidity buildup, the relative humidity of the indoor air increases substantially during the 12 hours when the space is not pressurized (see Figure 5.7).

Figures 5.4 and 5.8 demonstrate that dehumidifying the supply air to maintain the indoor air relative humidity just below the upper limit of the comfort range (60%) during occupancy hours lowers the dew-point temperature inside the space to about 15.5 °C. If cooling water at 20 °C is supplied to the ceiling panels during this time, the mean temperature of the radiant surface becomes about 22 °C. A temperature difference of 6.5 °C between the average radiant surface temperature and the dew-point temperature (4.5 °C between the coldest end of the ceiling panes and the dew-point temperature) is adequate to ensure that no condensation forms on the surface of the ceiling panels.

After the supply of cooling water has been discontinued, radiation from the vertical walls and floor causes the panel surface temperature to increase to around 24 °C. Assuming that infiltration with moist outside air can be avoided by supplying ventilation air at half rate (Figure 5.4), dehumidifying the ventilation air to 9.5 g water/kg dry air maintains the dew-point temperature of the space around 13.5 °C during off-occupancy hours. The 8.5 °C temperature difference between the panel surface and the dew-point indicates that condensation does not form on the surface of the ceiling panels during off-occupancy hours. Dehumidifying the outside air to about 15.5 g water/kg of dry air would have been sufficient to maintain this temperature difference at 3 °C.

If ventilation with dehumidified air is discontinued during off-occupancy hours, or if infiltration with moist outside air cannot be avoided, condensation may appear on the surface of the ceiling panels. The data presented in Figure 5.7 and 5.8 show that it is important to account for the mechanism of moisture sorption on the space surfaces (see Appendix A) when examining the effects of infiltration on the moisture balance of the indoor air.

Specifically, if the moisture balance does not account for sorption (as in the case of DOE-2, for instance), the simulated indoor air relative humidity becomes equal to the

1. According to ASHRAE Standard 55-1992 [1] the comfort range for the relative humidity in an office space setting (light sedentary activity, and occupants wearing clothing adequate to the season) is 30 to 60%.

outside air relative humidity shortly after space ventilation is interrupted. Because none of the moisture migrating into the space is stored in the surfaces, the simulation results for the week of system peak in New Orleans indicate that the indoor air reaches saturation in the early morning hours of the fifth day (dotted line for DOE-2 results and dashed line for RADCOOL results in Figure 5.7). As the ceiling panels are colder than the indoor air, air saturation indicates the presence of condensation on the surface of the panels. Figure 5.8 confirms that during the early morning hours of the fifth day the dew-point temperature of the space becomes higher than the surface temperature of the ceiling panels.

If sorption is accounted for in the moisture mass balance,[1] the simulation results show that the relative humidity of the indoor air increases during the off-occupancy hours, but the air does not become saturated (solid line for RADCOOL results in Figure 5.7). Figure 5.8 confirms that in this case, the dew-point temperature inside the space remains at least one degree lower than the temperature of the radiant surface.

As Figures 5.1 and 5.5 show, supplying cold water at 20 °C to the ceiling panels at the New Orleans location provides the radiant surface with sufficient cooling power to remove the cooling loads from the base-case space. If the cooling water were supplied at a temperature lower than 20 °C (to increase the cooling power of the radiant surface, for example), the ceiling panels would not warm up past the dew-point temperature of the space during the off-occupancy hours, and condensation would form on the panel surface. Consequently, if the supply water temperature at the New Orleans location were lower than 20 °C, space ventilation with dehumidified air would be strongly recommended to avoid condensation on the panel surface. Similar results were obtained for the Cape Hatteras, New York, Fort Worth, and Chicago locations. At the other 6 locations, infiltration with outside air does not increase the dew-point temperature of the space past 18 °C, therefore lowering the water supply temperature by a few degrees does not increase the risk of condensation.

If the space could not be pressurized and/or infiltration could not be avoided, supplying dehumidified air during off-occupancy hours would reduce the relative humidity inside the space and would reduce the risk of condensation. The optimum level of dehumidification of the supply air in such a case is subject for future research.

It is important to note that moisture sorption on the walls has a significant influence on the moisture mass balance of the indoor air only when the relative humidity of the air presents a large variation (for example, when moisture is produced or transported inside the space).[2] In such a case, some of the moisture is stored in the walls by sorption, and

1. The RADCOOL calculation assumes that the space walls are covered in an oil-based paint and the floor is covered in linoleum. Since the radiant surface modeled consists of aluminum panels, no sorption is modeled for the ceiling panels.

2. Here the term "wall" refers to any space surface that is not covered with cooling panels.

the indoor air relative humidity increases at a slower rate. Later, when the source of moisture has disappeared, the walls dry out, thus releasing the moisture back into the air. Conversely, when the indoor air relative humidity varies very little over time, as in the case when the space is continuously ventilated (Figure 5.3), there is no significant moisture sorption in the walls. Consequently, when the space is pressurized to avoid infiltration, sorption can be safely ignored when performing the moisture mass balance for the indoor air.

It is also important to note that the radiant cooling system can maintain the indoor air temperature around the setpoint of 24 °C because (1) the structure of the space is well insulated, and (2) the internal loads are relatively low. Because the radiant cooling systems currently available on the market have a maximum cooling power of 140 W/m^2, these systems might not be able to supply sufficient cooling to a poorly-insulated space with high internal loads. Common sense indicates that the boundary between the domains in which radiant cooling systems might and might not supply sufficient cooling is also a function of climate. Identifying this boundary is subject to further research.

5.3 The Energy Consumption and Peak Power Demand of the Radiant Cooling System

The parameters used in the RADCOOL simulations of the space conditioned by the radiant cooling system, and in the DOE-2 simulations of the space conditioned by the all-air system, allow the calculation of the sensible, latent and distribution loads for each system terminal. This section discusses the results of the calculation performed for the radiant cooling system while the next section discusses the results for the all-air system.

According to the results of the parametric study, at 9 of the 11 locations examined, supplying cooling water at 20 °C to the ceiling panels allows the radiant cooling system to maintain the indoor air temperature within one degree of the 24 °C design setpoint during occupancy hours. If the moisture mass balance accounts for sorption on the walls and floor of the space, the simulation results indicate that condensation does not form on the surface of the ceiling panels at any of the locations studied. This statement holds for the typical week and the week of system peak, and for both ventilation strategies.

The locations where the ceiling panels do not have sufficient cooling power if the cooling water is supplied at 20 °C are Phoenix, AZ and Salt Lake City, UT. In these two climates the daily maximum radiant load exceeds 40 W/m^2, the outside air temperature exceeds 35 °C, and the outside relative humidity is 10% on average (during both the typical week and the week of system peak). At these locations the radiant cooling system cannot maintain the ambient temperature near the 24 °C setpoint unless the cooling water and ventilation air are supplied at 17.5 °C. Because Phoenix and Salt Lake City are dry locations, lowering the supply water temperature does not increase the risk of con-

densation on the ceiling panels, and lowering the temperature of the supply air does not increase the latent load of the system.

5.3.1 Energy consumption of the radiant cooling system

When the space is ventilated continuously, night ventilation contributes to the total energy consumption of the radiant cooling system terminal. Night ventilation accounts for a larger fraction of the total energy consumption of the system terminal in hot, humid climates where air dehumidification is energy-intensive. In cooler and drier climates, night ventilation contributes only marginally to the total all-air system energy consumption. Night ventilation accounts for a fraction between 2% (Seattle) and 19% (New Orleans) of the total energy consumption of the radiant cooling system terminal during the typical week, and between 4% (Seattle) and 26% (New Orleans) during the week of system peak.

At all locations studied, the energy consumption due to cooling and dehumidifying the ventilation air is *lower* when the space ventilation is interrupted at night (second ventilation strategy) than when the space is ventilated continuously (first ventilation strategy). The decrease in energy consumption due to interrupting the space ventilation at night is greater in moist climates, where the outside air often becomes saturated at night. Interrupting the space ventilation at night avoids the dehumidification energy consumption associated with conditioning this very moist air.

In the parametric study, the main source of space cooling is switched off at the end of the occupancy hours. In the case of the radiant cooling system terminal, this translates into interrupting the supply of cooling water to the ceiling panels. This reduces the radiative cooling of the other surfaces significantly, but not entirely, as the ceiling panels are still colder than the other surfaces. Interrupting the space ventilation an hour later (second ventilation strategy) eliminates the forced convective cooling of the space as well. Consequently, when the vertical walls and floor release the heat accumulated during the day, the cooler ceiling absorbs a higher quantity of heat than it would absorb if the space were still ventilated. When the cooling water supply to the ceiling panels is switched on again the next day, the water must cool the warmer ceiling surface before the ceiling itself can cool the space. Therefore, the cooling coil energy consumption due to water cooling *increases* when the space ventilation is interrupted at night. This increase happens at all locations, and is highest in hot dry climates.

When space ventilation is interrupted at night, the avoided sensible and latent cooling coil energy consumption prevails over the increase in the sensible cooling coil energy consumption for water cooling. Consequently, the total energy consumption of the radiant cooling system *decreases* when the ventilation is interrupted at night. The reduction in total energy consumption is in the range from 2% (New York) to 18% (New Orleans) during the typical week, and from 4% (Seattle) to 26% (New Orleans) during the week

of system peak. The reduction is higher during the week of system peak because the energy benefits associated with interrupting the space ventilation at night are larger in the hot season. The reduction is highest in hot humid climates.

At the level of the cooling coil serving the radiant cooling system, the energy consumption due to water sensible cooling is higher than the energy consumption for air sensible cooling at all locations studied. This is consistent with the fact that, by design, the radiant cooling system cools the space mainly by radiation, and water is the cooling agent connecting the radiant surface to the cooling coil. When the space is continuously ventilated, water cooling accounts for a fraction between 70% (New Orleans) and 98% (Seattle) of the cooling coil sensible energy consumption during the typical week, and for a fraction between 59% (Phoenix) and 87% (Seattle) during the week of system peak. When space ventilation is interrupted at night, the energy consumption due to air sensible cooling decreases and the energy consumption due to water cooling increases. Water cooling accounts for a fraction between 75% (New Orleans) and 98% (Seattle) of the cooling coil sensible energy consumption during the typical week, and for a fraction between 70% (New Orleans) and 89% (Seattle) during the week of system peak.

The energy consumption due to air dehumidification varies widely across the climates. When the space is continuously ventilated, the latent fraction of the total energy consumption of the cooling coil is in the range from 0% (Salt Lake City) to 41% (New Orleans) during the typical week, and from 0% (Salt Lake City) to 53% (New Orleans) during the week of system peak. When the space ventilation is interrupted at night, the energy consumption due to dehumidification decreases. The latent fraction of the total energy consumption of the cooling coil is in the range from 0% (Salt Lake City) to 32% (New Orleans) during the typical week, and from 0% (Salt Lake City) to 43% (Cape Hatteras) during the week of system peak.

Because the radiant cooling system supplies the same (constant) air and water volumes to the system terminal at all locations studied, the energy consumption due to water distribution (pump) and air distribution (fan) are the same at all locations, during the typical week and the week of system peak.

5.3.2 Peak power demand of the radiant cooling system

The peak power demand due to conditioning the space does not vary much across the climates.[1] When the space is continuously ventilated, the peak electrical power demand of the radiant cooling system is in the range from 20.5 W_e/m^2 (Seattle) to 30.3 W_e/m^2 (Cape Hatteras). When the ventilation is interrupted at night, the space is not mechani-

1. The total (hourly) load due to space conditioning is calculated as the sum between the sensible and latent loads on the cooling coil (due to air cooling and dehumidification and water cooling), and the fan and pump loads (due to air and water distribution). The peak power demand is the highest hourly load.

cally cooled, and the peak electrical power demand increases. In this case, the electrical peak power demand of the radiant cooling system varies in the range from 20.9 W_e/m^2 (Seattle) to 30.7 W_e/m^2 (Cape Hatteras).

As discussed in Section 4.5.1, the load calculations assumed that the cooling coil-chiller combination serving the radiant cooling system terminal has a constant coefficient of performance, COP = 3. Because the fan and pump load contributions to the total peak power demand are small, the ratio of the peak thermal load to the peak electrical load is almost 3:1. The results reported in this section imply that the radiant cooling system can successfully remove a thermal load of about 60 W/m^2 (Seattle) - 90 W/m^2 (Cape Hatteras) from the base-case space. This range is consistent with the cooling power of radiant cooling systems currently available on the market [2].

In what follows, the calculations for the energy consumption and peak power demand of the all-air system also assume a constant COP = 3 for its cooling coil-chiller combination. It is important to note, however, that both the chiller serving the radiant cooling system and the chiller serving the all-air system function in part-load during most of their on-time. The COP of a chiller in part-load is lower than the COP at design point.

5.4 The Energy Consumption and Peak Power Demand of the All-Air System

5.4.1 Energy consumption of the all-air system

The all-air system employs a variable air volume system during occupancy hours (8 a.m. to 5 p.m.) and a constant volume system, or no system at all, during off-occupancy hours. When the space is ventilated continuously, night ventilation contributes to the total energy consumption of the all-air system terminal. Night ventilation accounts for a fraction of 2% (Seattle) to 19% (Fort Worth) of the total energy consumption during the typical week, and for a fraction of 3% (Seattle) to 23% (New Orleans) during the week of system peak.

Depending on the outside air conditions, interrupting the space ventilation at night sometimes leads to a decrease, other times to an increase in the cooling coil *sensible* energy consumption (due to cooling the supply air). Two factors contribute to this result. First, if the space is continuously ventilated, some of the energy stored in the walls during the day is removed at night. Interrupting the space ventilation at night reduces heat removal and leads to an increase of the cooling coil sensible load during the next day. Second, the cooling coil on-time is longer when space is ventilated continuously than when the space ventilation is interrupted at night.

Depending which of the two factors prevails, the cooling coil sensible energy consumption will increase or decrease when the space ventilation is interrupted. The following rule of thumb holds for the climates selected for the parametric study: if the daily mini-

mum of the outside air temperature is higher than 18 °C, the continuous ventilation of the space is associated with a high cooling coil energy consumption. Consequently, the energy saved by reducing the on-time of the cooling coil offsets the extra energy that must be removed from the space the next day due to heat not released from the building structure. Overall, at locations where the daily minimum outside air temperature is higher than 18 °C, the cooling coil sensible energy consumption *decreases* when the space ventilation is interrupted at night. These locations are New Orleans, Fort Worth, and Phoenix during the typical week, and New Orleans, Cape Hatteras, New York, Fort Worth, Chicago, Boston, Phoenix, and Salt Lake City during the week of system peak.

If the daily minimum is below 18 °C, the energy required to cool the night ventilation air is minimal. Consequently, when the space ventilation is interrupted at night, the extra energy that must be removed from the space the next day offsets the savings achieved by reducing the cooling coil on-time. Thus the cooling coil sensible energy consumption *increases* if space ventilation is interrupted at night at the locations where the daily minimum of the outside air temperature is below 18 °C. This happens in New York, Chicago, Boston, San Jose, Scottsbluff, Salt Lake City, and Seattle during the typical week, and in San Jose, Scottsbluff, and Seattle during the week of system peak.

Similarly to the cooling coil serving the radiant cooling system terminal, the energy necessary for air dehumidification by the cooling coil serving the all-air system terminal varies widely across the climates. When the space is continuously ventilated, the latent fraction of the cooling coil total energy consumption is in the range from 0% (Salt Lake City) to 30% (New Orleans) during the typical week, and from 0% (Salt Lake City) to 40% (New Orleans) during the week of system peak. When space ventilation is interrupted at night, the energy consumption due to latent heat removal decreases at all locations where dehumidification is required. The reduction in dehumidification energy is higher in the hot climates. The latent fraction of the total cooling coil energy consumption varies in the range from 0% (Salt Lake City) to 22% (New Orleans) during the typical week, and from 0% (Salt Lake City) to 28% (New Orleans) during the week of system peak.

At all locations, the all-air system must remove a larger quantity of energy from the space when the space ventilation is interrupted at night than when the space is continuously ventilated. This additional energy has a sensible component, mostly due to higher heat release from the walls into the space in the absence of ventilation, and a latent component, mostly due to humidity buildup through infiltration in the absence of ventilation. The all-air system removes the additional energy the next day. This leads to an increase in cooling coil energy consumption, but also to an increase in fan energy consumption (the larger air volume supplied to meet the higher load requires a larger fan). The increase in fan energy consumption due to the interruption of space ventilation at night is larger in the moist climates, where moisture buildup is large. The range of the increase in fan energy consumption due to interrupting the space ventilation at night is from 9% (Salt Lake City) to 48% (New York) during the typical week, and from 8% (Salt Lake

City) to 39% (New York) during the week of system peak.

5.4.2 Peak power demand of the all-air system

As in the case of the radiant cooling system terminal, the total peak power demand of the all-air system terminal does not vary much across building locations. When the space is continuously ventilated, the electrical peak power demand of the system is in the range from 29.8 W_e/m^2 (Seattle) to 45.9 W_e/m^2 (Phoenix). The peak power demand of the system is higher for the all-air system than for the radiant cooling system mainly due to the larger fan power demand of the all-air system. When the space ventilation is interrupted at night, the electrical peak power demand of the all-air system increases, and is in the range from 30.3 W_e/m^2 (Seattle) to 48.5 W_e/m^2 (Phoenix).

5.5 Comparison of the Performance of the Radiant Cooling System and of the All-Air System

5.5.1 Energy consumption

At all the locations studied the energy consumption of the radiant cooling system terminal was lower than the energy consumption of the all-air system terminal. This statement holds for the typical week as well as for the week of system peak, and for both ventilation strategies. The purpose of this Section is to quantify the energy savings.

The results of the parametric study show that the numerical value of the energy savings achieved by replacing the all-air system terminal with the radiant cooling system terminal varies as a function of the building location. Savings in moist climates are lower than savings in dry climates. This result follows from one of the assumptions of the parametric study, namely that both systems condition (cool and dehumidify) the same quantity of outside air.[1] Because the radiant cooling system and the all-air system maintain a similar relative humidity inside the space, the energy required for dehumidification is similar for the two systems, and the dehumidification process does not provide any "opportunity for savings". The "opportunity for savings" resides in the fact that removing heat from the space by circulating relatively large volumes of air is more energy-intensive than removing heat from the space by circulating water and ventilation air. In other words, the sensible air cooling and fan energy consumption of the all-air system are higher than the sensible air cooling, sensible water cooling, fan and pump energy consumption of the radiant cooling system. The sensible and fan energy provide less "opportunity for savings" in moist climates than in dry climates because in moist cli-

1. In an ideal situation, the operation of the radiant cooling system and that of the all-air system would be matched based on the indoor effective temperature of the base-case space. It is unclear whether the results reported in this section are applicable to such a case.

mates dehumidification accounts for a large fraction of the total energy consumption.

At all locations, the energy savings achieved when the space ventilation is interrupted at night are larger than the energy savings achieved when the space is ventilated continuously. This happens primarily because the all-air system provides an "opportunity for savings" mainly during occupancy hours.[1] Interrupting the space ventilation at night is associated for both systems with the need for more sensible cooling energy, and for the all-air system with the need of more fan energy during the next day. This increases the "opportunity for energy savings" when the ventilation is interrupted at night, as compared to the case when the space is continuously ventilated.

The results of the parametric study show that energy savings achievable during the typical week are different from the energy savings achievable during the week of system peak. The energy savings achieved during the week of system peak are higher than the savings achieved during the typical week at 7 of the 11 building locations, and lower than the savings achieved during the typical week at 4 of the 11 building locations.

The design and operation of the VAV system explain this result. In order to meet the cooling load at a given time, the VAV system adjusts the flow rate (and the temperature, if necessary) of the supply air. The supply air flow rate and temperature at each time step are thus a function of the temperature and moisture of the outside air, the temperature of the return air, and system design requirements such as the setpoints for the minimum supply air temperature and the indoor relative humidity. If the outside air is hot and moist, the cooling coil serving the VAV system must cool and dehumidify a relatively warm and moist air mix (between the required quantity of fresh air and recirculation air). In this situation the energy consumption of the cooling coil is high. If the outside air temperature is low, the cooling coil must cool and dehumidify a relatively cold and dry air mix. In this situation the energy consumption of the cooling coil serving the VAV system is low.

In the context of the parametric study, when the outside air temperature is lower during the typical week than during the week of system peak, the energy consumption of the all-air system during the typical week is lower than during the week of system peak. If the space is ventilated continuously, the energy consumption of the all-air system is further reduced during the typical week because the outside air is cold, therefore the cooling coil energy consumption is minimal.[2] By comparison, the radiant cooling system

1. When the cooling has stopped at the end of occupancy hours, the radiant cooling system terminal and the all-air system terminal employ identical constant volume systems for ventilation. If the first ventilation strategy is employed, the relatively low cooling power of the ventilation air offers little "opportunity for savings". If the second ventilation strategy is employed, no ventilation air is supplied to the space, therefore there is no "opportunity for savings".

2. The ventilation system can supply air to the space at a minimum temperature dictated by a pre-set minimum surface temperature of the cooling coil (usually 15 °C for the all-air system in this study).

always supplies the same quantity of outside air at 20 °C (17.5 °C in Phoenix and Salt Lake City) and 9.5 g water/kg dry air, to minimize the risk of condensation on the cooling surface.[1] The energy consumption of the radiant cooling system also becomes lower during the typical week as compared to the week of system peak. However, the reduction in the energy consumption of the radiant cooling system is lower than that of the all-air system because (1) the space is mainly cooled by radiation during the day, and (2) at night the ventilation air is still supplied at 20 °C (or 17.5 °C) and 9.5 g water/kg dry air. Consequently, if the outside air temperature is lower during the typical week than during the week of system peak, the energy savings during the typical week are lower than the energy savings during the week of system peak. This happens in New York, Fort Worth, Boston, San Jose, Scottsbluff, Salt Lake City, and Seattle.

If the outside air temperature is high during the typical week (New Orleans, Cape Hatteras, Phoenix), or if the outside air moisture content is high during the typical week (Chicago), the all-air system functions at a point of relatively high energy consumption. The energy consumption is relatively high because (1) the cooling coil serving the all-air system must cool and dehumidify a mix of warm and/or moist outside and recirculation air, and (2) the air volume supplied to the space is relatively large, and so is the fan that circulates this air volume. By comparison, the energy consumption of the radiant cooling system is relatively low during the typical week because (1) this system removes most of the cooling loads by radiation; the connection between the radiant surface and the cooling coil is accomplished by water circulation, and (2) the quantity of outside air that the system must cool and dehumidify is much smaller than the quantity of mixed air that the all-air system must cool and dehumidify. Consequently, if the outside air temperature and/or the outside air humidity is high during the typical week, the energy savings during the typical week are higher than the energy savings during the week of system peak.

To summarize, the all-air system is favored in the climates where the weather during the typical week is cool and dry. Conversely, the radiant cooling system is favored in the climates where the weather during the typical week is warm and/or moist. However, at all locations, the energy consumption of the radiant cooling system is lower than the energy consumption of the all-air system. The potential energy savings during the typical week are in the range from 6% (Seattle) to 36% (Phoenix) when the space is ventilated continuously, and in the range from 23% (Seattle) to 42% (Phoenix) when the space ventilation is interrupted at night.[2] The average and standard deviation of the energy savings

1. This does not imply that the radiant cooling system must mechanically *heat* the outside air at night. If the outside air temperature is less than 20 °C, it can be warmed up by using waste heat from the compressor operating the cooling coil, or by channeling it through building components (however, this strategy requires special design for the air inlet).

2. The energy savings are calculated as the difference between the total energy consumption of the all-air system and the total energy consumption of the radiant cooling system, divided by the total energy consumption of the all-air system.

during the typical week are 25.4% and 9.6% when the space is continuously ventilated, and 34.8% and 6.7% when the space ventilation is interrupted at night.

It important to note that, when the space is continuously ventilated, supplying fresh air at a temperature lower than 20 °C or (17.5 °C) in dry climates would *not* lead to condensation on the radiant surface. Consequently, if the radiant cooling system had been designed to take advantage of this opportunity to reduce the load on the cooling coil at night, the calculated energy savings would have been higher than those reported in this section.

5.5.2 Peak power demand

Due to the difference in heat removal mechanisms of the radiant cooling system and all-air system, the two systems reach their peak power demand at different times during the peak day. The time of peak of the all-air system usually happens shortly after noon. The time of peak of the radiant cooling system usually happens one or two hours later.

In all the climates studied the peak power demand of the radiant cooling system is lower than that of the all-air system. This statement is true for the typical week as well as for the week of system peak, and for both ventilation strategies. It can be explained based on (1) the heat removal mechanisms of the two systems (radiant vs. convective), and (2) the size of the fan employed by each of the two systems at the time of the peak demand (the radiant cooling system employs a much smaller fan than the all-air system).

The peak power savings do not vary much with the building location.[1] As in the case of the energy savings, the peak power savings are larger when the space ventilation is interrupted at night than when the space is continuously ventilated. This happens primarily because, when space ventilation is interrupted at night, the energy that must be removed during the next day increases, so the peak cooling demand increases for both systems. Because the all-air system cools the space mainly by convection, and because it employs a larger fan than the radiant cooling system, the increase in the peak power demand of the all-air system is larger than the increase in the peak power demand of the radiant cooling system.

At 9 of the 11 locations selected for the study the peak power savings during the typical week are *higher* than the peak power savings during the week of system peak. The locations where the peak power savings during the typical week are *lower* than the peak power savings during the week of system peak are New York and Boston. This result can be explained based on the weather conditions at the time of the peak load: during the

1. The peak power savings are calculated as the difference between the peak power demand of the all-air system and the peak power demand of the radiant cooling system, divided by the peak power demand of the all-air system.

week of system peak the weather is sunny, while during the typical week it is overcast, and/or raining. Consequently, the solar heat gain is high during the week of system peak and low during the typical week. Since the internal loads are assumed to not change during the year, the time and amplitude of the peak load are driven by the weather-induced loads. During the week of system peak in New York and Boston, the dominant component of the peak load is the sensible load due to space solar heat gain. During the typical week, the dominant component of the peak load is the latent load due to air dehumidification. As the cooling coils serving the radiant cooling system and the all-air system handle the same latent loads, the "opportunity for power savings" of the radiant cooling system is larger when the load is mainly sensible, and smaller when the load is mainly latent. Consequently, the peak power savings in New York and Boston are larger during the week of system peak than during the typical week.

The peak power savings during the week of system peak vary between 22% (New York) - 35% (Phoenix) when the space is continuously ventilated, and between 23% (New York) - 37% (Phoenix) when the space ventilation is interrupted at night. The average and standard deviation of the peak power savings over all the climates considered are 27.2% and 4.0% when the space is continuously ventilated, and 28.4% and 4.3% when the space ventilation is interrupted at night.

5.5.3 Climate-induced trends into the energy consumption and peak power savings of the radiant cooling system

The results reported in the preceding sections associate numerical values to the ability of the simulated radiant cooling system to save energy and peak power at a given location. These results can be presented in the form of a distribution of the energy and peak power savings with the number of locations at which given savings are achieved. Figure 5.9 shows the distribution corresponding to the second ventilation strategy. The results in Figure 5.9 show that, when the space ventilation is interrupted at night, the simulated radiant cooling system requires on average 35% less energy, and 28% less peak power than the simulated all-air system to provide similar indoor temperature and relative humidity to the base-case space during occupancy hours.

The distribution in Figure 5.9 does not provide the capability to predict the savings that could be achieved by replacing the all-air system with a radiant cooling system at a given location. At present, much information is available regarding the design and functioning of all-air systems, but little information is available regarding the design and functioning of radiant cooling systems. Consequently, a quantitative link between the energy and peak power savings of the simulated radiant cooling system and the energy consumption and peak power demand of the simulated all-air system would constitute a useful addition to the existing knowledge about radiant cooling systems. Such a link would also provide the means to estimate the savings that could be achieved if the radiant cooling system replaced the all-air system at any given location.

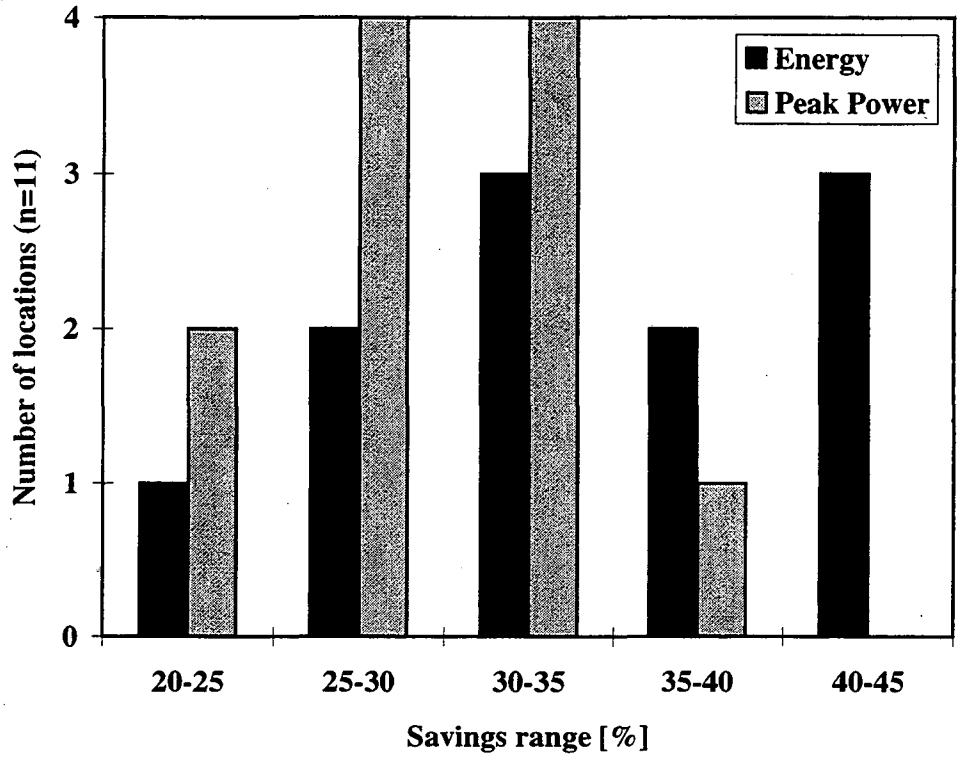

Figure 5.9. Distribution of the energy and peak power savings of the radiant cooling system with the number of locations. Space ventilation interrupted at night. Energy average = 34.8%, standard deviation = 6.7%. Peak power average = 28.4%, standard deviation = 4.3%.

The following observations were useful when establishing this quantitative link:

(1) The results of the parametric study show that the indoor conditions of the base-case space do not comply with the new version ASHRAE Standard 62 (currently under revision) for all cases studied. According to ASHRAE Standard 62R [3], the indoor air relative humidity should be maintained below 70% at all times. The results of the parametric study indicate that at the humid locations (New Orleans, Cape Hatteras, New York, Fort Worth, and Chicago), the indoor air relative humidity exceeds 70% if the space ventilation is interrupted at night. However, the indoor air relative humidity is always maintained below 70% at these locations if the space is ventilated continuously. To comply with ASHRAE Standard 62R, the base-case space located at the humid locations should therefore be continuously ventilated (should employ the first ventilation strategy).

(2) Interrupting the space ventilation at night at the drier locations (Phoenix, Scottsbluff, Salt Lake City, Seattle, Boston, and San Jose) does not interfere with the requirements of ASHRAE Standard 62R. Furthermore, this ventilation strategy reduces the energy consumption and peak power demand due to air-conditioning the space, as compared to the

ventilation strategy requiring continuous space ventilation. Consequently, to allow for the optimal design of the two systems from the point of view of their energy consumption, the ventilation of the base-case space should be interrupted at night (the second ventilation strategy should be employed) at the drier locations.

(3) Due to the design of the parametric study, the simulated radiant cooling system and the all-air system cool and dehumidify the same amount of outside air, and provide a similar air relative humidity inside the base-case space. Because the two systems consume the same amount of dehumidification energy, the dehumidification process does not provide any "opportunity for savings" (nor any energy penalties) to the radiant cooling system. Conversely, the sensible load on the cooling coil, and the fan load due to air distribution of the all-air system offer "opportunity for savings" The savings achieved by the radiant cooling system should therefore correlate with the sensible cooling and fan energy consumption (or peak power demand) of the all-air system.

Figure 5.10 presents the energy savings of the radiant cooling system as a function of the sum between the sensible cooling and the fan energy consumption of the all-air system.[1] The data points and the solid-and-dotted line in the figure correspond to the results reported in Section 5.5.1 and 5.5.2, which assume a COP of 3 for the cooling coil-chiller combinations serving the two systems. The dashed lines in Figure 5.10 correspond to similar calculations of the all-air system and radiant cooling system energy consumption, performed with the assumption that the cooling coil-chiller combinations serving both systems have COP values of 2.5 and 6, respectively.

The linear regression between the two quantities indicates that the radiant cooling system can achieve high energy savings at the locations where the sum between the sensible cooling coil and fan energy consumption of the all-air system is high. An examination of the locations associated with the data points in Figure 5.10 shows that the absolute energy savings are highest in the hot climates and lowest in the cold climates, regardless of the dehumidification energy consumption.

The regression line for COP = 3 also shows that, at locations where the sum between the seasonal sensible cooling and fan energy consumption of the all-air system is lower than 10 kWh_e/m^2, replacing the all-air system with a radiant cooling system will not save any energy. The 10 kWh_e/m^2 value can be interpreted as the sensible cooling and fan energy consumption associated with supplying only the ventilation air to the space. Among the locations examined, Seattle presents the lowest sum between the seasonal sensible cooling and fan energy consumption of the all-air system: 18.1 kWh_e/m^2.

1. The energy savings of the radiant cooling system were calculated as the absolute difference between, the total (sensible, latent and distribution) energy consumption of the all-air system and the total energy consumption of the radiant cooling system. To obtain the seasonal energy savings, the seasonal sum between the cooling and fan energy consumption of the all-air system, the calculations were done for the typical week, then extrapolated to the cooling season (see Section 4.4.4).

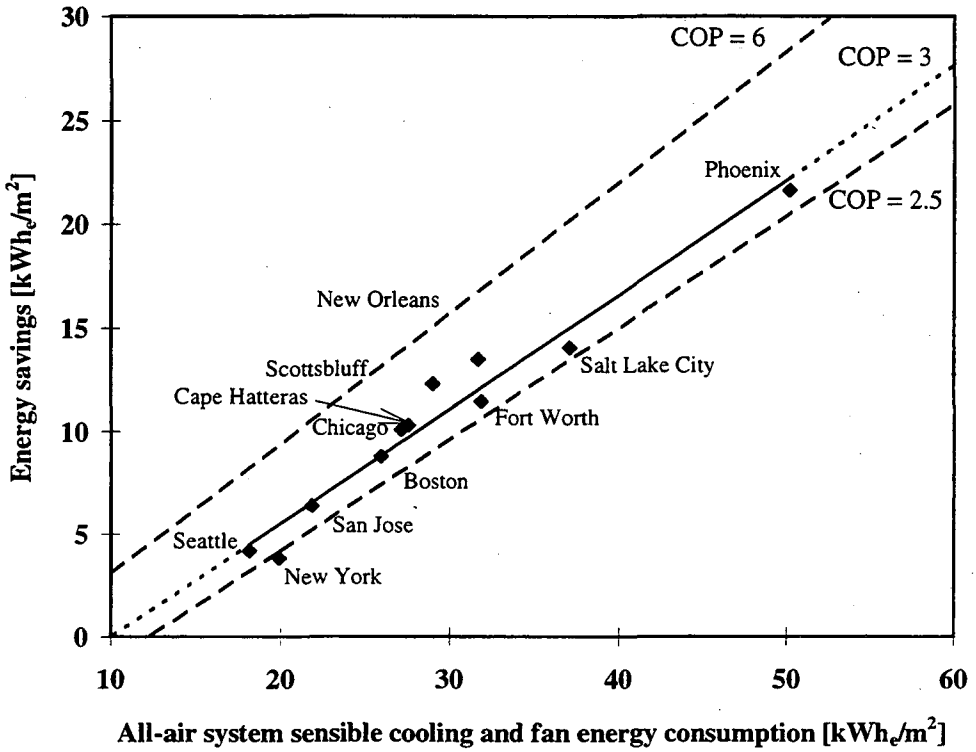

Figure 5.10. Energy savings over the cooling season: trend across climates.

The regression line corresponding to COP = 2.5 has a slightly lower slope than the slope of the regression line for COP = 3, while the regression line corresponding to COP = 6 has a slightly higher slope. Consequently, if the chiller consumes less electrical energy to achieve the same thermal cooling at the coil, the fraction of the sensible cooling and fan energy that can be saved by replacing the simulated all-air system with the simulated radiant cooling system increases. It is important to note that the "closeness" of the regression lines corresponding to different COP values is due to the assumptions embedded in the parametric study. Although it is difficult to estimate the applicability of these results in other situations, the existence of a linear relationship between the savings achieved by the radiant cooling system and the "opportunity for savings" offered by the all-air system is an important result.

Section 5.4.1 presents the energy savings of the radiant cooling system as fractional savings.[1] The solid-and-dotted regression line corresponds to a cooling coil-chiller combi-

1. The fractional energy savings were calculated as the difference between the total (sensible, latent and distribution) energy consumption of the all-air system and the total energy consumption of the radiant cooling system, divided by the total energy consumption of the all-air system.

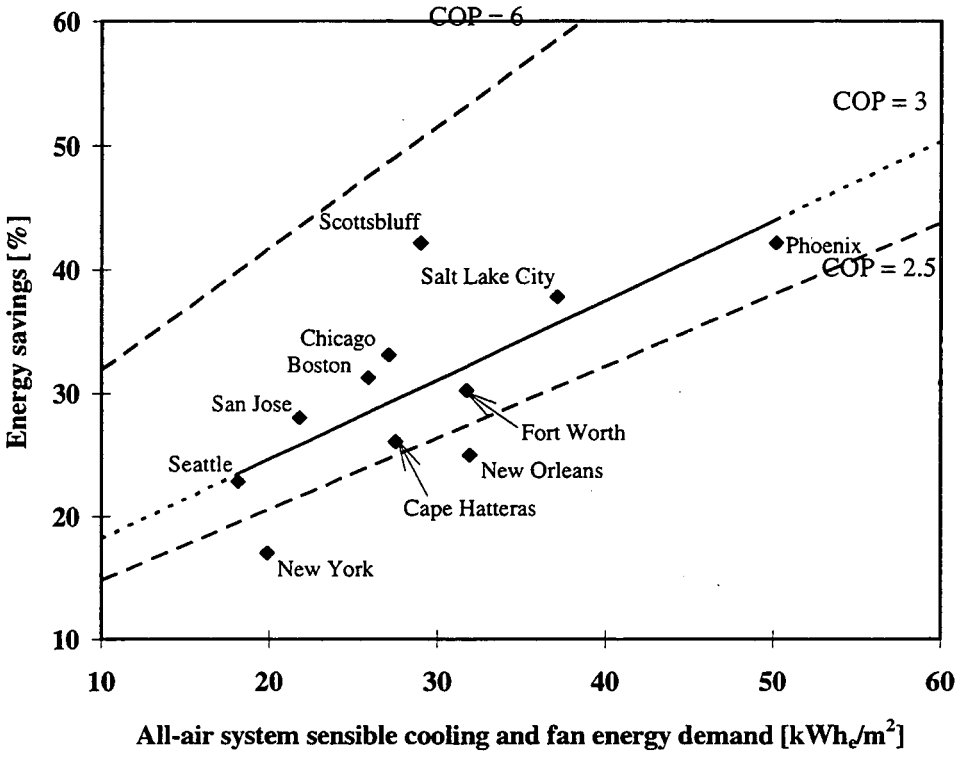

Figure 5.11. Fractional energy savings over the cooling season: trend across climates.

nation with a COP of 3, and the dashed regression lines to cooling coil-chiller combinations with COP values of 2.5 and 6, respectively. Figure 5.11 shows that the correlation between the fractional savings of the radiant cooling system and the sensible cooling and fan energy consumption of the all-air system is not very strong (the data points have a wider spread around the regression line). This result is intuitively correct, because the fractional savings also depend on the latent energy consumption of the cooling coil serving the all-air system terminal.

Figure 5.11 also shows that the fraction of the sensible cooling and fan all-air system energy consumption that can be saved by replacing this system with the radiant cooling system is highest in hot dry climates and lowest in cold moist climates. This result confirms the earlier observations regarding the "opportunity for energy savings" of the radiant cooling system.

The correlations in Figures 5.10 and 5.11 suggest that there is no upper limit for the energy savings that can be achieved by replacing the all-air system with the radiant cooling system. According to Feustel and Stetiu [2], the achievable fractional energy savings

may be as high as 45% for a cooling coil-chiller combination with a COP of 3. On the regression line, this corresponds to a seasonal sum between the sensible cooling and fan energy consumption of the all-air system of roughly 51.5 kW_e/m^2. By comparison, the seasonal sum between the sensible and fan energy consumption of the all-air system is 50.2 kW_e/m^2 at the Phoenix location. Although the Phoenix climate is representative of the hottest US climates, higher values for the energy consumption can be obtained in lighter, less insulated building structures.

Figure 5.12 presents the peak power savings of the simulated radiant cooling system as a function of the sum between the sensible cooling and fan power demand of the simulated all-air system at the time when it reaches its peak demand. The two quantities correlate linearly, indicating that the radiant cooling system can achieve high peak power savings at the locations where the sum between the sensible cooling and fan power demand at the time of the all-air system peak is high. The peak power savings increase with an increase of chiller COP.

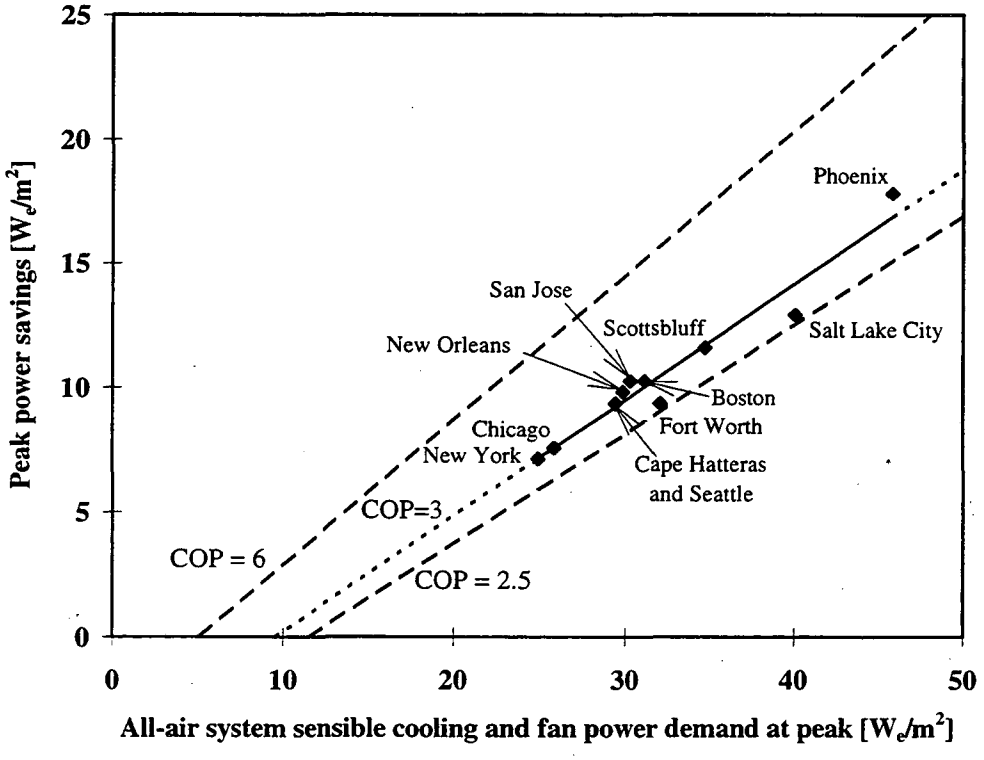

Figure 5.12. Peak power savings: trend across climates.

The data in Figure 5.12 show that the absolute peak power savings are highest in the hot, dry climates, and the lowest in the cold humid climates. Furthermore, the absolute peak

power savings are relatively high in all dry climates and relatively low in all moist climates. This is intuitively correct, because the "opportunity for savings" at the time of the all-air system peak power demand is high in hot climates, and is low in moist climates.

The regression line for COP = 3 suggests that, if the sum between the cooling and fan power demand of the all-air system at the time of peak is less than 8 W_e/m^2, replacing the all-air system with the radiant cooling system will not save any peak power demand. This value designates the peak sensible cooling and fan load associated with supplying only the fresh air volume to the space.

Figure 5.13 presents the fractional power savings of the radiant cooling system as a function of the sum between the cooling and fan power demand of the all-air system at the time of peak.[1]

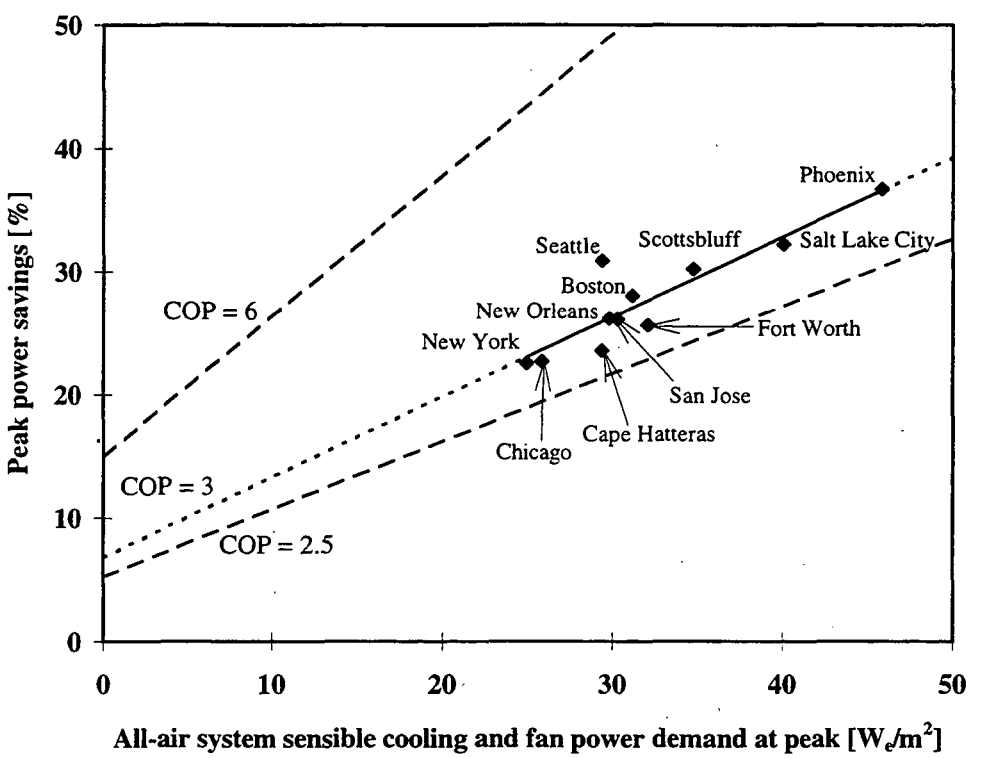

Figure 5.13. Fractional peak power savings: trend across climates.

1. The fractional power savings were calculated as the difference between the *total* (sensible, latent and fan) peak power demand of the all-air system and the *total* peak power demand of the radiant cooling system, divided by the *total* peak power demand of the all-air system.

As in the case of the fractional energy savings, the correlation for COP = 3 is not as strong as that in Figure 5.12, because the fractional power savings are also a function of the dehumidification load at the time of the system peak. However, Figure 5.13 is consistent with Figure 5.12 in showing that the highest peak power savings are achieved in the hot, dry climates.

The foregoing results can be summarized in the form of a distribution of the energy and peak power savings by number of locations where these savings are achieved (see Figure 5.14). The data used in Figure 5.14 correspond to the ventilation strategy necessary at each location to maintain indoor air relative humidity below the 70% upper limit required by ASHRAE Standard 62R [3]. According to the results in Figure 5.14, replacing the all-air system with the radiant cooling system in the base-case space saves an average of 30% of the energy consumption and 27% of peak power demand of the all-air system conditioning this space.

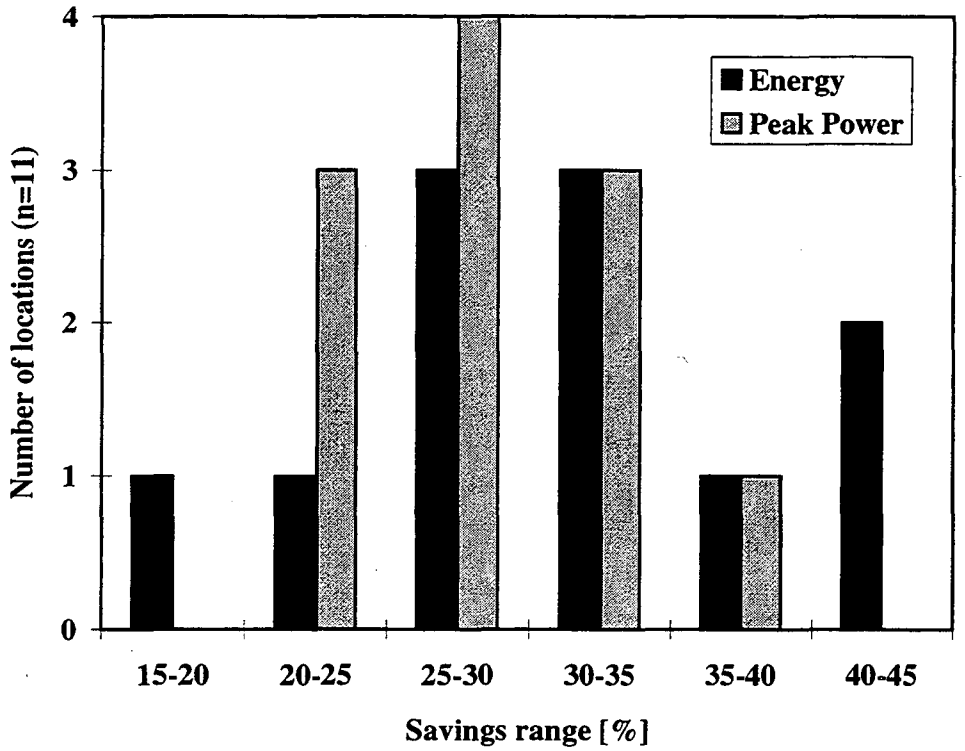

Figure 5.14. Distribution of the energy and peak power savings of the radiant cooling system with the number of locations. Energy average = 30.5% standard deviation = 7.9%. Peak power average = 27.7%, standard deviation = 4.4%.

5.6 Additional Modeling

The results reported in Section 5.5 provide a first estimate for the savings achievable by installing the simulated radiant cooling system instead of the simulated all-air system in a new office space. However, before this information is used to calculate how much energy and peak power *any* radiant cooling system can save if installed in a building, the following limitations have to be considered. First, the results presented in Section 5.5 were obtained by comparing the performance of a simulated radiant cooling system with that of a simulated all-air system that conditions the same specific single-zone office space. It is not certain that the results obtained for the base-case space selected for the study can be used to calculate the savings potential of a radiant cooling system with a different design, conditioning a different space, or a whole building. It is worthwhile mentioning, however, that the integration of RADCOOL into DOE-2 would allow building practitioners to perform simulations for a the building structure of their choice, and to evaluate the savings potential of a radiant cooling system of specified design, as compared to an all-air system of specified design.

Second, the results presented in Section 5.5 were obtained for a new office space with a state-of-the-art envelope complying to current California standards. But the number of new office buildings that will be built in the future is relatively small compared to the number of older office buildings that will be retrofitted. If radiant cooling achieves significant market penetration in the US, radiant cooling systems are more likely to be installed during a retrofit than during the construction of a new structure. It would be interesting to know whether the results obtained for the base-case space in the state-of-the-art structure can be used to draw conclusions about the savings potential of a radiant cooling system in a different building structure.

To extend the building domain where the results obtained in this thesis are applicable, additional modeling is necessary. The following sections will present the results of a few additional simulations. This work explores the extent to which the correlations obtained for the base-case space may change when the energy and peak power savings of the simulated radiant cooling system are calculated for a different space in the building, and for a different building structure.

5.6.1 Description of the additional simulations

To partially address the applicability of the results reported in Section 5.5.3 as an estimate for the energy savings potential of the radiant cooling system in a different space, modeling was performed to simulate the energy consumption and peak power demand associated with conditioning a space with a different orientation. The space MBC6 was chosen for this purpose (see Figure 4.1). The MBC6 space differs from the base-case space MBC2 only through its orientation (north-eastern, as compared to south-western for MBC2). The space MBC6 was simulated in the same conditions as the space MBC2,

but at two locations only: New Orleans and Phoenix. These two locations represent two extreme climates: the New Orleans climate is hot and moist (group 9 in the climate classification described in Section 4.4.3), so the savings potential of the radiant cooling system should be relatively small. By contrast the Phoenix climate is hot and dry (group 3), and the radiant cooling system should achieve high savings. For consistency with the previous work, night ventilation with dehumidified air was simulated in the MBC6 space at the New Orleans location, and no mechanical night ventilation was simulated at the Phoenix location.

To partially address the applicability of the results reported in Section 5.5.3 to calculate the energy savings potential of the radiant cooling system in a different building structure, additional modeling was performed to calculate the energy consumption and peak power demand associated with conditioning the base-case space MBC2 in a building of older vintage. The structure chosen for this purpose has a facade corresponding to the building stock dating from the 1950s: the opaque part consists of metal panels, insulation, and sheetrock, and has a U-value of 1.74 W/m^2-K. The facade has single-pane windows with a center-of-glass U-value of 5.58 W/m^2-K. For simplicity, the interior walls and the ceiling and floor have the same structure as that of the state-of-the-art building. The base-case space was simulated at the same two locations: New Orleans and Phoenix. For consistency with the previous work, night ventilation with dehumidified air was simulated in the MBC6 space at the New Orleans location, and no mechanical night ventilation was simulated at the Phoenix location.

It is important to note that, for consistency with the previous work, the simulation of the space with the "older" building structure was made assuming (1) the same (relatively low) internal loads as those in the parametric study, and (2) the possibility of avoiding infiltration at the New Orleans location by pressurizing the space. Depending on the building to be retrofitted, one or both of these assumptions may not hold. High internal loads at hot dry locations might indicate that radiant cooling systems do not have enough cooling power to condition certain retrofitted buildings. High infiltration rates *and* high internal loads at hot humid locations might indicate a relatively high risk of condensation in certain buildings, even if continuous ventilation is employed. In such extreme conditions, the decision to install a radiant cooling system must be based on simulations performed for each retrofitted building separately. The building practitioner must then make a decision based on (1) the lowest acceptable energy savings of the radiant cooling system as compared to an all-air system, and (2) the highest acceptable risk of condensation.

5.6.2 Results of the additional simulations

Figures 5.15 and 5.16 show graphs similar to those in Figures 5.10 and 5.12. The data points represent the energy savings calculated for (1) the space with south-western orientation, in the "new" building structure (diamonds), (2) the space with north-eastern orientation, in the "new" building structure (triangles), and (3) the space with south-

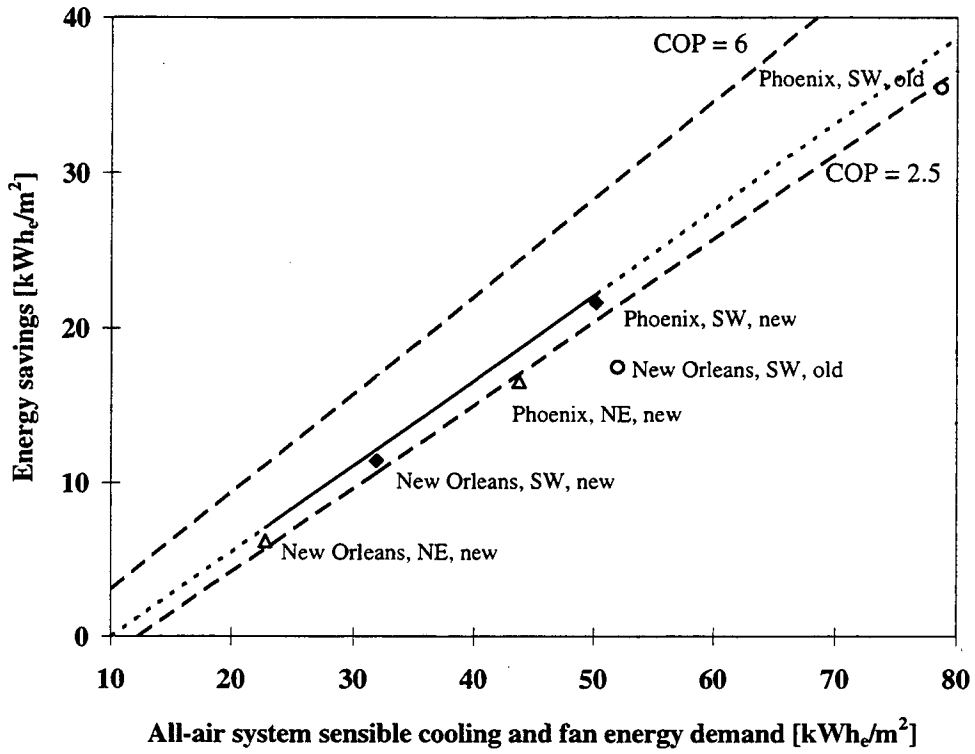

Figure 5.15. Energy savings over the cooling season: data for New Orleans and Phoenix.

western orientation, in the "old" building structure (circles). The data points correspond to a COP of 3 for the cooling coil-chiller combinations serving both systems. The regression lines in Figures 5.15 and 5.16 are the same as those in Figures 5.10 and 5.12.

To understand the position of the new points relative to the regression line, it is important to remember that the radiant system has more "opportunity for savings" when (1) the sensible cooling load is large, and (2) the all-air system requires a large fan for cooling the space.

The space with north-eastern exposure is exposed to sunshine mainly in the morning hours. Therefore, at the time of the maximum solar heat gain (around 9 a.m.), the building structure has not had a chance to warm up. The relatively cold building surfaces store some of the heat, so the sensible cooling and fan loads imposed on the system are somewhat diminished.

By comparison, the maximum solar heat gain occurs around 3 p.m. in the space with south-western orientation. At this time the building structure is already warm, and the building surfaces can store very little additional heat. Consequently, the system that

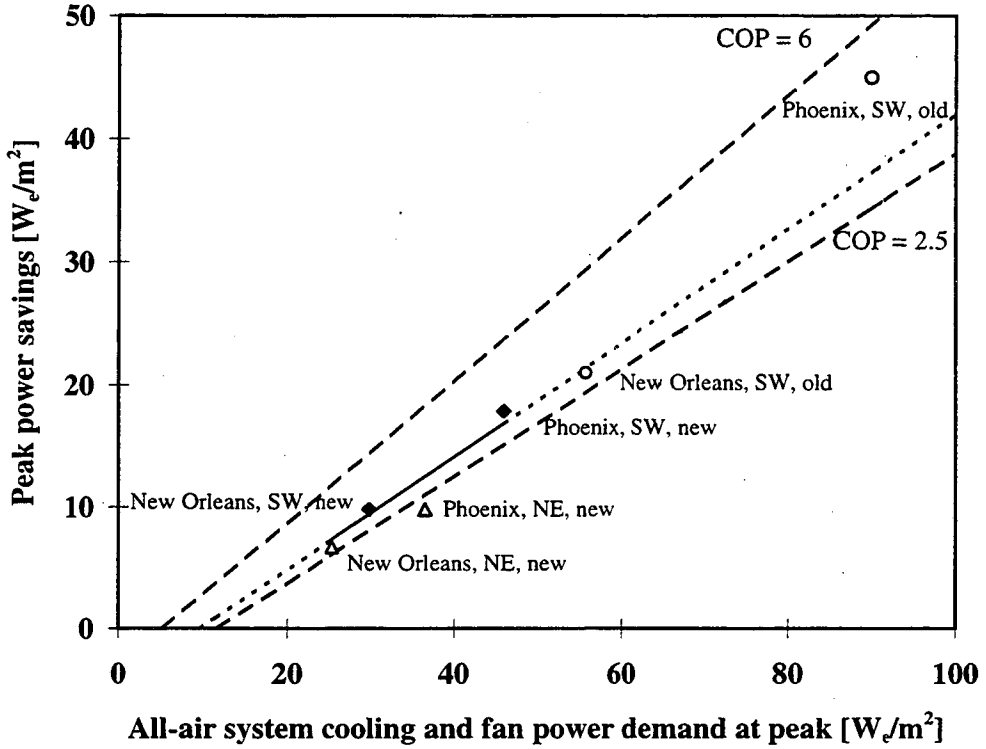

Figure 5.16. Peak power savings: data for New Orleans and Phoenix.

cools the MBC6 space must remove a smaller weather-induced heat load than the system that cools the MBC2 space. The "opportunity for savings" is lower for the MBC6 space than for the MBC2 space, therefore the potential energy and peak power savings are lower. Figures 5.15 and 5.16 confirm this statement.

The solar gain through a poorly insulated structure is larger than the solar gain through a well insulated structure. The results of modeling the "old" structure confirms this observation (Figures 5.15 and 5.16). Because the rate of outside air supplied to the "old" building structure is the same as that supplied to the "new" building structure, the higher savings achieved by the radiant system in the "old" building structure are solely due to the low insulation level of the "old" building. This result indicates that, if the internal loads are not too high and the radiant cooling system can condition buildings of older vintage with a relatively low risk of condensation, the energy and peak power savings achieved by installing radiant cooling systems in retrofit projects be might be larger than those estimated in Section 5.5.

It is important to note that, although the results reported in Sections 5.5 and 5.6 reflect the specific assumptions embedded in the parametric study (occupant and equipment sched-

ules, design and operation of the all-air and radiant systems, the method of matching the indoor conditions of the space, etc.), they confirm that substantial energy and power savings can be achieved by substituting radiation for convection as a heat transfer mechanism, and water for air as a heat transfer medium. Once RADCOOL integration into DOE-2 is achieved, building practitioners will be able to perform similar studies using any specific assumptions.

5.7 Conclusions

(1) Different ventilation strategies are necessary at different locations to ensure that office building conditions comply with the upcoming building regulation (at least with the revised version of ASHRAE Standard 62-1989 [3]). The design of the ventilation strategy for a building, and the design parameters of the building conditioning system, should therefore reflect local climate characteristics. Specifically, the indoor relative humidity of office buildings located in moist climates should be controlled through continuous ventilation with dehumidified air. Because humidity buildup does not constitute a problem in dry climates, moisture control through night ventilation is not necessary in these climates.

(2) An adequately designed and operated radiant cooling system can function in a state-of-the art office building at any US location with a small risk of condensation. In humid climates, the risk of condensation on the radiant surface is greatly reduced if the building is continuously ventilated with dehumidified outside air. Continuous ventilation may fail to lower the risk of condensation to acceptable levels in leaky buildings of older vintage.

(3) Over a 24-hour period, the simulated indoor air temperature in the base-case space conditioned by the radiant cooling system is more stable than the simulated indoor air temperature in the base-case space conditioned with the all-air system.

(4) The simulated radiant cooling system requires less energy and peak power to condition the base-case space than the simulated all-air system. At the locations studied, and in a state-of-the-art office space conditioned to meet the requirements of ASHRAE Standard 62R, the average savings potential of the simulated radiant cooling system is 30% for the energy consumption, and 27% for the peak power demand. If radiant cooling systems can remove the higher cooling loads characteristic for buildings of older vintage, higher savings are achievable in these lighter structures.

(5) The potential savings of the simulated radiant cooling system are lower in cold, moist climates and higher in hot, dry climates. At the locations studied, the achievable energy savings of the system conditioning the base-case space vary between 17% and 42%. The achievable peak power savings vary between 22% and 37%.

(6) The estimated energy and peak power savings increase when the COP of the cooling coil-chiller combination serving the air-conditioning terminal increases.

(7) If the sum between the seasonal sensible cooling and fan energy consumption of the all-air system drops below the level at which ventilation air is sufficient for cooling and dehumidification, the "opportunity for energy savings" disappears. Replacing the all-air system with a radiant cooling system will not reduce energy consumption. A similar statement can be made for the peak power demand.

(8) Additional modeling is necessary to clarify to what extent the results presented in this thesis are applicable to other building structures and to other orientations. In particular, since retrofit projects will probably account for a large share of the construction projects in the near future, the savings potential of radiant cooling systems in retrofit projects should be studied in detail. Installing a radiant cooling system in retrofit projects should be preceded by simulations reflecting the conditions for each retrofit situation. RADCOOL integration into DOE-2 would provide building practitioners with a simulation tool capable of evaluating the performance of radiant cooling systems in any specific building and for any specific climate.

(9) Because many other alternative cooling technologies are viable in hot, dry climates (e.g. cooling towers, evaporative cooling, night ventilation), it is recommended that pilot-projects demonstrating the performance of radiant cooling systems be implemented in the warm and hot humid climates first. This thesis has shown that installing a radiant cooling system instead of an all-air system in new building construction in these climates can reduce the energy consumption and peak power demand due to air-conditioning by an estimated 25%. Of the existing commercial building stock, about 23% is located in warm and hot humid climates (see Table 4.2).

5.8 References

1. ASHRAE Standard 55-1992, *Thermal environmental conditions for human occupancy.* Atlanta: American Society of Heating Refrigerating and Air-Conditioning Engineers, Inc., 1992.

2. Helmut E. Feustel and C. Stetiu, *Hydronic radiant cooling - preliminary assessment.* Energy and Buildings, (22) (3) 1995.

3. ASHRAE Standard 62-Revised (to be published), *Ventilation for acceptable indoor air quality.* Atlanta: American Society of Heating Refrigerating and Air-Conditioning Engineers, Inc.

Chapter 6

RADIANT COOLING AND THE US MARKET

6.1 Introduction

The commitment of Western European countries to reduce their energy consumption translates into regulation that promotes energy efficient technologies. In particular, since cooling of non-residential buildings contributes significantly to electricity consumption and peak power demand, countries like Switzerland and Germany have adopted building standards that call for better building design, and for the replacement of traditional all-air systems with alternative, more efficient building conditioning systems. Information regarding the performance of radiant cooling systems indicates that they not only reduce the energy consumption for thermal distribution and for space conditioning, but also provide draft-free and noise-free cooling, reduce building space requirements, and might even have lower first-cost if the peak specific cooling loads are above 50 - 55 W/m^2. It is therefore not surprising that implementation of radiant cooling systems in Western European commercial buildings is currently under way.

The results of the parametric study conducted in this thesis suggest that installing radiant cooling systems instead of the traditional all-air systems in office buildings in the US can diminish the energy consumption and peak power demand due to space conditioning. Yet despite sustained efforts to promote energy efficiency in buildings, traditional all-air systems are still standard issue for new and retrofitted commercial buildings across the US. Furthermore, there is no evidence that the US air-conditioning market will adopt radiant cooling systems in the near future.

The absence of radiant cooling systems from the US market cannot be explained without examining the complex interaction of several technical, economic, social, and cultural factors. Instead of undertaking this ambitious task, this chapter limits itself to describing the realities of the US air-conditioning market, identifying some of the barriers that any "new" cooling technology must overcome before it can capture a share of this market, and reviewing some regulatory measures that would help alternative cooling technologies in general, and radiant cooling in particular, to overcome these barriers.

6.2 The Economic Theory of Increasing Returns

Conventional economic theory is built on the assumption of diminishing returns: economic actions generate negative feedbacks that lead to a predictable equilibrium for prices and market shares. Such feedbacks tend to stabilize the economy because any major changes will be offset by the very reactions they generate. The economy will therefore have a unique equilibrium point at any given time, a point that marks the "best

outcome" possible for a given structure of the economy, the most efficient use and allocation of resources.

Arthur [1] shows that in reality only the parts of the economy that are resource-based (agriculture, bulk-goods production, mining, etc.) are still subject to diminishing returns. The parts of the economy that are knowledge-based are mostly subject to increasing returns. Products such as computers, pharmaceuticals, automobiles, aircraft, etc., are complicated to design and manufacture, and require large initial investments in research, development, and tooling. Once sales begin, however, incremental production is relatively cheap. Increased production brings additional benefits: producing more units means gaining more experience in the manufacturing process, and achieving greater understanding of how to manufacture additional units even cheaper. Moreover, experience gained with one product or technology can make it easier to produce new products incorporating similar or related technologies.

As opposed to diminishing returns, increasing returns magnify the effects of small economic shifts at the microeconomic level, and allow for many possible equilibrium points at the macroeconomic level. When one economic outcome is realized from the many possible alternatives, there is no guarantee that *that* particular outcome is also "the best". Furthermore, once random economic events select a particular path, the choice may become locked-in regardless of the advantages of the alternatives. If one product in the marketplace gets ahead "by chance", positive feedback often helps it stay ahead and increase its lead. Predictably, shared markets are no longer guaranteed in the parts of the economy governed by increasing returns. Instead of being offered a chance to capture a share of the market, a firm or technology trying to penetrate a locked-in market will be driven to failure, or will be taken over by an already-established firm.

Although the US air-conditioning industry is not knowledge-based, it presents certain similarities to the automobile industry: both are capital-intensive, both market goods that are relatively complicated to design and manufacture, and both require large initial investments in research, development, and tooling. The difficulties generally encountered by "new" space cooling technologies attempting to capture a share of the US air-conditioning market may signal that the economy of the air-conditioning market is subject to increasing returns, and that traditional HVAC systems relying on compressor-driven chillers have locked-in, or almost locked-in the market.

Feustel and collaborators [2] state that compressor-driven chillers are currently "the easy way to supply cooling". To support this statement, they bring the following arguments:

(1) under the current building standards, matching a cooling unit to a building can be done rapidly by using rule-of-thumb calculations;

(2) the first cost of compressor-driven chillers is relatively low;

(3) equipment, parts, and service are readily available;

(4) compressor-driven air-conditioning systems are mechanically reliable (they require little maintenance);

(5) they are available in a variety of sizes, satisfy any cooling requirements, and function even in extreme climatic conditions;

(6) air-conditioning systems relying on compressor-driven chillers are easy to control, and their reaction is relatively rapid.

By comparison, Feustel and collaborators find the following for existing "alternative" cooling technologies:[1]

(1) they require slightly more complicated calculations to design;

(2) their first cost is higher than that of the compressor-driven technology;

(3) equipment and parts are scarce, and expertise for installing and maintaining the systems is lacking;

(4) some "alternative" cooling technologies are unreliable in certain weather conditions, while others are incompatible with certain climates;

(5) most "alternative" cooling technologies have limited output and therefore cannot be employed in buildings with high cooling loads;

(6) most "alternative" cooling technologies require complex controls.

Radiant cooling systems have certain advantages when compared to the other alternative technologies;[2] however, they are still at a disadvantage when compared to all-air systems relying on compressor-driven chillers because:

(1) they require relatively complicated design calculations;

(2) although their first cost is comparable to that of all-air systems relying on compressor-driven chillers in Western Europe, there is very little data available about the cost of radiant cooling systems in the US - North American manufacturers do not disclose first cost information on the grounds that it is proprietary;

(3) although there are a few North American manufacturers who offer equipment and

1. Evaporative cooling, desiccant cooling and absorption cooling are some of the "alternative" cooling technologies currently available on the market. These technologies were developed to replace compressor-driven chillers in its role of cooling source for all-air HVAC systems.

2. Radiant cooling systems are "alternatives" to traditional all-air systems in that they substitute radiation for convection as main heat transfer mechanism, and water for air as heat transfer medium. The radiant cooling systems that have so far been installed in buildings still use chillers, albeit smaller ones, as main cooling source.

parts, expertise for installing and maintaining the systems is lacking;[1]

(4) assuming appropriate design and controls, they are reliable in any US climate, but there is an upper limit to the cooling loads that they can remove from a building.

The air-conditioning industry relying on compressor-driven chillers currently dominates the market largely due to its infrastructure. In 1993 about 70% of the US households had some type of compressor-driven air conditioner, and the Statistical Abstract of the US [3] indicates that the annual revenue from shipments of compressor-driven technology continues to increase.[2] By comparison, the infrastructure needed to support the alternative technologies, including radiant cooling, is not yet fully developed. Information regarding the number and type of buildings conditioned by systems relying on alternative technologies is scarce. The Statistical Abstract of the US does not even list data concerning the sales of "alternative" cooling technologies, or of radiant cooling systems.

6.3 The Regulatory Response

6.3.1 Theory

A sector of the economy governed by diminishing returns can be regulated fairly well by discouraging monopolies and maintaining open markets, but this type of regulation is not appropriate in a sector of the economy governed by increasing returns. Maintaining open markets is crucial for the achievement of technological advances in knowledge-based industries. However, because open markets allow dominant *technologies*, not *firms*, to gain monopoly-like status, policies that discourage monopolies cannot offer the regulation necessary in a sector governed by increasing returns. While addressing this problem, Arthur [1] identifies two types of regulation that are appropriate for a sector of the economy that is governed by increasing returns: policies supporting government subsidization, and policies encouraging joint ventures among small firms.

According to Arthur, government subsidization should be primarily directed towards the

1. The Radiant Panel Association provides the following list of companies that market (heating and cooling) ceiling panels. According to The Radiant Panel Association, no "cooling only" panels are currently manufactured in North America.

Aero Tech Manufacturing, Inc., Salt Lake City, Utah

Engineered Air, Calgary, Alberta

Frenger Canada Inc., Edmonton, Alberta

Shelley Radiant Ceiling Co., Northfield, IL

SUN•El Corporation, Latrobe, Pennsylvania

2. The revenue from shipments of compressor-driven equipment increased from $6.6 billion in 1991 to $7.9 billion in 1993.

protection of new industries, to allow them to capture foreign markets. However, as governments have a hard time justifying expenditures on industries that do not produce immediate profit, the adoption of such policies would probably encounter resistance. Moreover, if one country pursues such policies, others will retaliate in kind, and nobody can achieve any profits.

When stating the above, Arthur obviously forgets that he is proposing regulation directed at encouraging *technology development*. Even if "nobody achieves profits", fierce international competition can lead to significant technological advances for an industry, thus opening public access to improved products. Profits will be achieved during a subsequent stage, through the marketing or use of the improved products. The same can be stated at the national scale: if the government subsidizes a new technology, the large firms that control the market respond by allocating large funds to their own research and development programs. Overall, more research is focused on that technology than before subsidization started, which can lead to significant technological improvements. And, the more information large firms have about a promising "new" technology, the larger the chances that the technology in question will be adopted and promoted.

Although Arthur dismisses the idea of spending public money to support research related to new technologies on the grounds that it would produce minimum profit, he admits that significant technological advances cannot be made without research. Consequently, Arthur supports the adoption of policies that encourage individual firms to invest in research and development, and to promote aggressive searches for product and process improvements. In particular, such policies should favor joint ventures that pool together the resources of many firms, thus allowing them to share up-front costs, marketing networks, technical knowledge and standards. At the international level, such policies should promote strategic alliances that enable companies in several countries to penetrate complex industries together, action that no company could sustain by itself. But even if adequate policies can favor the development of a technology, Arthur warns, its success or failure is dictated by one factor: timing. To have a fair chance to succeed, a firm or technology should enter a market only if it is not locked-in.

6.3.2 Application to cooling technologies

In the specific case of cooling technologies, Feustel and collaborators [2] call for significant policy interventions to allow alternative technologies to gain a share of the air-conditioning market. They state that such policy interventions are justified by the fact that not all the cost of compressor-driven air-conditioning is borne by the consumers. The costs imposed on utilities to support the capacity necessary to meet air-conditioning demand ("the load from hell" [4]) are borne by all utility ratepayers, while the costs of increased emissions from electricity production and of chlorofluorocarbon (CFC) use for air-conditioning are borne globally. Feustel and collaborators show that to be successful,

policies supporting alternative technologies must be based on information regarding the environmental aspects of cooling, as well as end-user behavior.[1] It is worthwhile mentioning, however, that deep understanding of the environmental and behavioral issues associated with space cooling may not necessarily produce arguments for the promotion of alternative cooling technologies. Considering the large, reliable infrastructure that supports the compressor-driven technology, small improvements that remedy the environmental- and end-user problems currently attributed to this technology may prove to be more attractive than the adoption of alternative technologies.

Environmental issues

The externalities arising from the use of compressor-driven air-conditioning have been thoroughly studied and documented. The same cannot be stated about alternative technologies: there is practically no information showing whether the use of alternative technologies is associated with any negative impacts. Theoretically, the net environmental impacts should be positive because alternative technologies reduce energy consumption and limit CFC use. However, to provide real support to policy formulation, any negative impacts must be identified, studied, and documented. Then the social costs of all externalities associated with all technologies should be catalogued and quantified where possible. This would help identify the most effective improvements in each existing technology, and would allow the formulation of policies that support the most beneficial technology.

Behavioral issues

Consumer behavior. Consumer preference for one technology over another should represent the central concern of those involved in formulating policies. At present, consumers perceive the compressor-driven technology as convenient, reliable, and relatively inexpensive. Furthermore, their expectations regarding the performance of a cooling system are based on their experience with the compressor-driven technology. Understanding the extent to which people are willing to part with the familiar compressor-driven technology in exchange for the lower operating costs and environmental benefits of alternative technologies is crucial for determining whether these technologies would be accepted, and which technology would be accepted more easily. In addition, studies focused on identifying those segments of the population where individual motives such as commitment to energy efficiency, or the desire to prevent further pollution of the environment, are prevalent could reveal market niches where alternative cooling technologies would be readily accepted. Studies focused on identifying those segments of the population where individual motives such as reluctance to become a ground-breaking individual, or resistance to invest in an unfamiliar technology are prevalent could

1. Arthur [1] overlooked this aspect of policy adoption: successful policies must be based on reliable information. It is debatable whether this type of subsidization produces any immediate profits.

reveal the sectors of the market where the adoption of alternative technologies should be encouraged through financial incentives.

Moreover, policy formulation should be supported by examples of implementation. Experience shows that public awareness and acceptance of a new technology is usually contingent upon the existence of a few "success stories" to which individuals (and institutions) can relate. In the specific case of radiant cooling, the achievement of pilot projects that include radiant cooling systems in the design of a few high-profile buildings would provide the necessary proof-of-concept, as well as a benchmark for the performance of these systems. Setting the pilot projects in hot- or warm-humid climates would demonstrate the ability of radiant cooling systems to condition even buildings located in extreme climates. Joint US Department of Energy, industry, and utility sponsorship of such pilot projects would help direct public attention towards the different benefits of adopting radiant cooling systems.

Behavior in the building profession. Because they are in a position to decide what technologies to incorporate into their design, architects and engineers constitute a crucial connection between innovation and implementation. However, these building practitioners are not *required* to promote "new" technologies; in fact, they are unlikely to promote a new technology if they perceive that some of its attributes detract them from their goals [5]. In addition, traditional construction methods are deeply embedded, and generally hard to overcome. Consequently, policies promoting a given technology should take into consideration the mechanisms that underlie the decision-making processes in the design activity, and the extent to which the interaction between the different types of professionals in the building community may help or hinder the adoption of the technology in question. In the case of radiant cooling, system particularities call for close cooperation among the building practitioners during the design process. The existence of an upper limit for the cooling load that a radiant cooling system can remove from a building requires the architect and the HVAC engineer to join forces in the design of the building and its cooling system. Considering the extent and the nature of the current interactions between these two types of building practitioners [6], such teamwork may be difficult if not altogether impossible to instill in the absence of special incentives.

6.3.3 Other measures

Because alternative cooling technologies in general, and radiant cooling in particular, must overcome the lack of familiarity and experience, a variety of other measures may be necessary to encourage their market adoption. The measures that Feustel and collaborators [2] propose are incentives, standards, and education programs. This section will discuss the nature of these measures, and the ways in which their adoption would influence the promotion of radiant cooling by the air-conditioning industry. It is worthwhile mentioning that education, incentives and standards are measures that support each other, therefore they should be implemented simultaneously.

Education. Education in the spirit of energy conservation should be directed both towards the public, which generates the demand for a product or technology, and towards the building profession, which is instrumental in adopting an energy efficient technology. In the specific case of alternative cooling technologies, information about functioning principles and energy-related benefits must be added to the general education promoting energy efficiency. Experience shows that, when promoting radiant cooling, the most frequently asked questions by individuals from the public and the building profession alike are:

(1) what is radiant cooling?

(2) how fast do the water pipes start to leak, and what are the consequences of a leaky system?

(3) how do you dispose of the condensation that forms on the cold surface?

These questions demonstrate that, for the most part, North Americans are oblivious to the *existence* of radiant cooling systems. As radiant cooling systems differ from traditional all-air systems more than other alternative technologies, their functioning principle must be explained in detail before any information about their benefits can be understood by the public. Moreover, after an explanation has been offered regarding the principles of radiant cooling, further effort is necessary to overcome the public's preconceptions. Experience with leaky water pipes leads the public to expect that all water pipes will leak sooner or later. Everyday exposure to window condensation naturally brings the assumption that condensation will form on any cold surface. To effectively raise public awareness about radiant cooling systems, these issues must be addressed. It is obvious that the existence of a few pilot projects incorporating the technology would be instrumental in the education process. Buildings equipped with radiant cooling systems would allow individuals to *feel* the cooling effect produced by these systems, and would demonstrate that, when in operation, they neither leak nor "sweat".

The information passed on to the building professionals should clearly be more specific and detailed. To elicit the interest of architects and engineers, these building professionals must be informed in detail about the functioning principle of radiant cooling systems, the energy-related advantages associated with installing such systems in buildings, and the changes that building practices must undergo to support proper installation and operation of radiant cooling systems. Since no building simulation program has thus far been able to model the performance of buildings equipped with radiant cooling systems, the few architects and engineers who may have been aware of the potential benefits of employing radiant cooling systems have not had access to any tool able to verify the soundness of a design incorporating such a system, or its potential to save energy. Its limitations and shortcomings notwithstanding, RADCOOL creation represents a necessary step towards a better understanding of the radiant cooling concept within the building profession. The proposed incorporation of RADCOOL into DOE-2 would facilitate

program improvement, while simultaneously allowing the members of the building community to access this calculation tool through the familiar DOE-2 environment.

Incentives. Informing the public and the building profession about the benefits of a "new" technology does little to encourage the adoption of the technology without the support of financial incentives. Recognizing that the main obstacle in the accomplishment of energy conservation projects is the up front cost required from the end-user to install energy efficient measures, most utilities sponsor demand-side management (DSM) programs. These programs diminish, or even eliminate the up front cost associated with the energy efficiency project, and often offer free installation of measures. The education that the end-user inherently receives when agreeing to participate in such a project is probably more valuable than the information that the market provides regarding a given energy efficient technology or measure. Behavioral changes may also be initiated while carrying out such projects, although it is unclear whether the effects of education through personal contact persist, and for how long.

If offered appropriate financial incentives, architects and engineers could also become interested in including alternative cooling technologies in their design. At present, engineering fees are based on a percentage of the capital cost of the project, subcontract, or equipment installed, not on the energy savings achieved by a particular system design. Since many of the alternative cooling technologies employ smaller-size equipment (ducts, fans, chillers, etc.) when compared to the traditional all-air systems relying on compressor-based chillers, including such systems in building design would reduce the building practitioners' fees. Acknowledging this difficult position, energy saving performance contracts (ESPCs) and performance-based architect and engineer (A/E) compensation programs offer financial means for shifting the designers' incentives towards energy efficiency.

Currently, energy saving performance contracts are almost exclusively used in retrofit situations. At the request of a building owner, an energy service company analyzes the building and identifies different sets of energy efficient measures that could reduce building energy consumption. After a set of measures has been selected, a third party finances the proposed energy conservation measures and their implementation, under the agreement that a share of the savings achieved will be dedicated to repaying the cost of the project. Since compensation to the energy service company provider is based on shared savings defined over some period of time, it is in this company's interest to identify the most beneficial energy efficiency measures, and to provide quality work for their installation.

The performance-based A/E compensation programs use the performance of a new building as built to encourage energy efficient design by granting monetary rewards, and to discourage substandard energy performance by exacting penalties. The "feebate" program currently in progress in Oakland, California [7] is set to reward the building designers for efforts that bring value in the form of energy savings to the owner, while

compensating the owner for having to pay higher energy bills in the case of a poorly performing building. In the "feebate" program, compensation to the A/E firm is conceived as a one-time payment depending on the achieved savings, and is delivered a few years after project completion.

There are two main caveats to the energy conservation projects described above. First, even when the incentives offered to building designers (compensation based on savings) to produce energy efficient design, specific performance standards do not exist to ensure that, once built, the building performs as promised. Second, because traditional design and construction methods are deeply embedded in the building profession, participation in a performance-based A/E compensation program does not necessarily encourage building professionals to implement energy efficiency measures in future designs. This shows the importance of adopting building standards that institutionalize energy efficient building practices.

Standards. Recognizing the importance of energy conservation for building a sustainable economy, the Swiss government called for new building standards in the late 1980s. The canton of Zürich subsequently implemented a new energy law (Vollzugsordner Energie 1989 [8]) that imposes a set of design measures requiring the architect-engineer team to minimize both weather-induced and internal loads in building design. Some of these measures are: a prescribed minimum insulation level, the use of architectural shading and of glazing with a low heat transmission coefficient, the use of efficient hot water systems, a prescribed minimum value for the efficiency of heat recovery systems. After the building design has been completed and compliance with the standard has been verified, the building design team must model the indoor conditions that would be obtained inside the building in the absence of mechanical cooling. If load calculations show that indoor conditions would be uncomfortable, and that indoor comfort cannot be achieved through the implementation of additional architectural measures, the building owner is eligible to apply for a permit to install mechanical cooling in the building. Even if such a permit is granted, the local government often limits the use of compressor cooling to night time hours. Under these circumstances, the capability of core cooling radiant systems to create comfortable indoor conditions during occupancy hours by pre-cooling a building during night time hours, combined with their relatively low electricity demand, have led to their current large-scale implementation in new construction in Switzerland.

The provisions of the energy laws recently implemented throughout Switzerland offer a partial explanation for the current interest in the implementation of energy efficient measures and technologies in building construction in that country. It is obvious that a similar result cannot be obtained in the US without a serious re-examination of current building standards. To this end, issues such as the relevance of the comfort zone (described by ASHRAE Standard 55-1989 [9]), the ideal of maintaining a constant temperature indoors, and the practice of using electricity-driven chillers to provide cooling, should come under close scrutiny.

It is worthwhile mentioning, however, that this type of action may or may not be beneficial from the point of view of alternative cooling systems in general, and of radiant cooling systems in particular. Reformulating the "expected norms" may loosen the requirements imposed on the operation of HVAC systems, thus reducing the "opportunity for savings" for alternative cooling systems. Imposing the generalized use of alternative cooling sources (cooling towers, ground coupling, thermal storage) may lead to traditional all-air systems that are more energy efficient than alternative cooling systems. A tightening of the building standards may call for building design that eliminates the need for air-conditioning altogether. In addition, the lack of an infrastructure, and the need to train building practitioners in the design and installation of radiant cooling systems, may render the promotion of these systems (even when combined with other energy efficient measures) economically unattractive.

6.4 Conclusion

This thesis has shown that radiant cooling systems create comfortable indoor conditions, have high potential to reduce building energy consumption and peak power demand, are economically competitive, and are not restricted to specific geographic areas in the United States. So far, market control by the compressor-driven technology, preconceptions of the public, and the difficulty of overcoming traditional building practices have been serious barriers to the adoption of radiant cooling in the United States. These barriers cannot be overcome without serious commitment to reducing the externalities that arise from the use of the compressor-driven technology. Commitment at government or public level translates into policy formulation, building standards, building practices, and, in time, into individual behavior and expectations. The Swiss example demonstrates the opportunities opened to alternative cooling technologies by government commitment to energy efficiency. In the United States, efforts to promote energy efficiency have so far been visible only at the level of the environmental community. The future will show whether government or public commitment to energy efficiency can be achieved in the United States, and whether market access will thus be opened to alternative cooling technologies in general, and to radiant cooling in particular.

6.5 References

1. W. Brian Arthur, *Increasing returns and path dependence in the economy*, Ann Arbor: University of Michigan Press, 1994.

2. Helmut Feustel, A. de Almeida, and C. Blumstein, *Alternatives to compressor cooling in California climates*. Rep. LBNL-30041, 1991.

3. U.S. Department of Commerce, *Statistical abstract of the United States 1995.* (115th edition.) Washington, DC, 1995.

4. Max Sherman, Personal communication, California Institute for Energy Efficiency, Berkeley, CA, 1991.

5. Kathryn B. Janda, *Designing from experience: the effects of research on practice.* Proc. ACEEE 1996 Summer Study on Energy Efficiency in Buildings, American Council for an Energy Efficient Economy, Washington, DC.

6. Kathryn B. Janda, *Bounded decision-making and analytical biases in demand-side management.* Proc. ACEEE 1994 Summer Study on Energy Efficiency in Buildings, American Council for an Energy Efficient Economy, Washington, DC.

7. John Busch and R. Diamond, *Does the "feebate" approach to A/E compensation lead to an energy-efficient building?*, Proc. 4th National Energy-Efficient New Construction Conference, Vancouver, BC, 1996.

8. Robert A. Meierhans, *Slab cooling and earth coupling*, ASHRAE Trans., (99) 1993.

9. ASHRAE Standard 55-1989, *Thermal environmental conditions for human occupancy.* Atlanta: American Society of Heating Refrigerating and Air-Conditioning Engineers, Inc., 1992.

Chapter 7

FUTURE RESEARCH DIRECTIONS

The results presented in Chapter 5 and the issues discussed in Chapter 6 suggest a number of topics for future work. An investigation of the compatibility of radiant cooling systems with buildings with significant indoor moisture production is a natural follow-up for the technical research described in this thesis. The current general consensus is that, to avoid the negative effects of surface condensation in such buildings, radiant cooling systems would function properly only when combined with very strict zoning of the indoor environment.[1] However, there is currently no definition for the notion of "strict zoning", and no in-depth research has been conducted to determine the consequences of operating a radiant cooling system in a building with significant indoor moisture production in the absence of zoning. The results of such research would be valuable for the definition of the market share that radiant cooling systems could capture in the United States.

A study of the different technologies that can provide the cooling necessary for the operation of building conditioning systems opens an area of combined technical and economic research. Even though there is general consensus that the electricity demand due to space conditioning would decrease if building conditioning systems were combined with alternative cooling sources (cooling towers, ground coupling, thermal storage), in practice most cooling systems work in combination with an electrical chiller. A study of the energy- and cost-related advantages and disadvantages of alternative cooling sources can lead to a partial explanation for the current market preference for electrical chillers. An additional investigation of the performance of all-air systems and radiant cooling systems in combination with alternative cooling sources would evaluate the energy savings potential of radiant cooling systems in the situation in which the use of alternative cooling sources became widespread.

Another technical-economic research area consists of comparing the performance of radiant cooling systems and that of the "alternative" cooling technologies (evaporative cooling, desiccant cooling, absorption cooling) that are already available on the US air-conditioning market. Like radiant cooling systems, alternative cooling technologies theoretically require less energy and peak power to operate, while striving to provide indoor conditions similar to those provided by compressor-driven chillers. In addition, alternative cooling technologies have the advantage of being able to function together with the familiar all-air systems, while the functioning principle of radiant cooling is for the most part, unfamiliar to the public and the building professionals. Defining the sectors of the air-conditioning market where each technology can function optimally, and examining

1. The purpose of zoning is to isolate the spaces with significant moisture production from the rest of the building, thereby reducing the risk of condensation on the cooling surface of the radiant system.

the energy- and cost-related advantages and disadvantages of radiant cooling as compared to the alternative technologies would add to the information necessary to evaluate the chance of radiant cooling systems to be adopted and promoted in the US.

Investigations of user-related advantages and disadvantages of the indoor environment created by radiant cooling systems would contribute to the information about these systems. The data collected so far from buildings equipped with radiant cooling systems indicate that no comfort-related complaints have been documented. The limited character of the available user-related information notwithstanding, it reflects only thermal- and/or health-related comfort criteria, and does not address other subjective issues. For instance, a retail space equipped with a radiant cooling system was found to be virtually dust-free. The explanation of this result rests on the much smaller air supply rates required by this retail store, as compared to similar retail stores conditioned by traditional all-air systems. In addition to the benefits of a cleaner environment, the dust-free system eliminates the time that the employees of the retail store must spend dusting the shelves, allowing them to perform other duties instead. This example shows the importance of interviews and informal discussions with building occupants. Such work would provide some valuable insight into the reality of spending several hours every day in a building conditioned by a radiant cooling system.

Similar investigations of the user-related advantages and disadvantages of innovative all-air systems would help identify directions for the improvement of existing all-air systems. In particular, individually-controlled task conditioning systems deserve more research. Task conditioning system allow the building occupant to adjust the speed, direction, and sometimes temperature of the incoming supply air. They have the potential to improve thermal comfort, ventilation efficiency and air quality. Depending on their design, the use of task conditioning systems instead of traditional air-conditioning systems can lead to energy savings. Defining the sectors of the air-conditioning market where innovative all-air systems in general, and task conditioning systems in particular, can function optimally would add to the information necessary to evaluate the chance of alternative cooling technologies to capture a significant share of the US air-conditioning market.

Finally, the social aspects of space conditioning constitute a research area of increasing interest. It is generally accepted that individual preferences for thermal and other environmental conditions vary from hour to hour, day to day, and person to person, according to a wide range of influences: physiological and psychological factors, cultural factors, clothing, acclimatization, etc. Yet current building standards are largely based on comfort equations developed in the 1970s, originating from experiments conducted in steady-state conditions. As a result, when HVAC engineers design their systems to comply with building standards, they create indoor environments that are uncomfortable for many individuals. This discrepancy between the perceived need for comfort and the techniques used to provide comfort calls for research focusing on individual variation, as well as on past and current norms and expectations. Such research would deepen the

understanding of historical and present methods of climate control, and could unveil new techniques that can simultaneously save energy and improve occupant comfort. Ultimately, such research could constitute the basis for a new collective attitude towards the issue of energy conservation in buildings.

Appendix A

THE THERMAL BUILDING SIMULATION MODEL RADCOOL

A.1 SPARK as the Environment for RADCOOL

The Simulation Problem Analysis and Research Kernel (SPARK) is a modular simulation environment that allows the efficient creation of customized models for detailed analysis of building components, systems and subsystems [1-2]. The use of SPARK as the environment for thermal building simulation programs provides three advantages from the point of view of programming.

First, the structural element of SPARK is an object representing a single equation, either algebraic or differential. Larger SPARK elements (macros) can be created based on single equation objects. This provides flexibility, as the user can define new macro objects whenever the need arises. The use of the single equation as a structural object also provides the benefit of code reuse, as the same object can be used in many macro objects without modification.

Second, the structural objects and macro objects are defined in SPARK as mathematical models only, rather than as algorithms. This means that component models do not have a predetermined specification of input or output variables, so variables can be interconnected arbitrarily. In contrast, most of the widely used modular simulators employ algorithmic component models with prescribed input/output relationships. Such models are inherently less flexible, limiting the class of problems that can be defined without modification of the component models.

Third, in SPARK, components are interconnected merely by identifying object interface variables with problem variables (i.e. variable "x" represents a given quantity in one or more equations). Once all equations (objects) are thus interconnected, some variables are specified by the user as the problem inputs, thereby defining a specific problem. The only requirement is that the problem so defined have a solution that is uniquely determined from the specified inputs. Inverting a problem, i.e. changing which variables are inputs and which are outputs, can be done without revising component models or interconnections.

The use of SPARK as the environment for thermal building simulation programs has one main disadvantage: the difficulty of using logical statements. The use of SPARK is appropriate only if there are many interconnections between variables (i.e. the problem to be solved can be described as a large network of simultaneous equations). Logical statements are by nature bound to a sequential approach to solve a given problem. The

use of logical statements in SPARK is cumbersome, will lead to long computation times, and will require large amounts of disk space.

A.2 The Structure of RADCOOL

RADCOOL was created in the SPARK environment in the form of a SPARK building component library, plus a set of user activities. After taking into consideration the benefits and disadvantages of SPARK, RADCOOL was given the following structure:

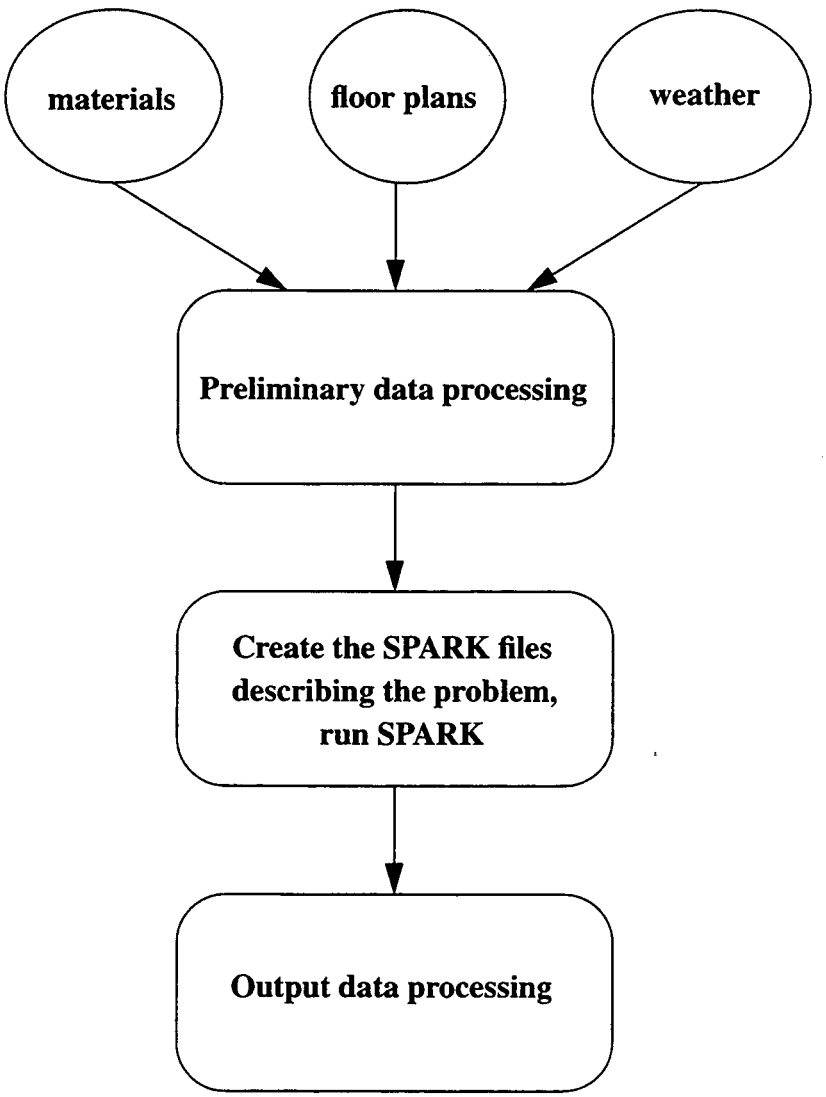

Figure A.1. RADCOOL program flow.

A.2.1 Preliminary data processing

In the "preliminary data processing" section the user gathers data so that a complete description of the simulation problem can be created. This involves obtaining information about building materials, floor plans, internal load schedules, weather data, simulation period, etc. and deciding the length of time steps. In the "preliminary data processing" section the user also performs the calculations necessary to determine shape factors, convection film coefficients, and weather-related variables, because these calculations are not cyclic, so they should not be performed in the SPARK environment.

A.2.2 Create the SPARK files describing the problem, run SPARK

The information acquired in the "preliminary data processing" section provides a unique description of the building to be modeled. Based on this data and using the Network Specification Language, the user creates the files needed for running the building model in SPARK. First, the problem specification (`.ps`) file is created by "assembling" building components from the SPARK component library. Then, based on the user-specified inputs, the constant and dynamic input files are created. The constant input file contains data that does not change with time, such as the thicknesses and thermal properties of building components, building dimensions, shape factors, etc. The dynamic input file contains data that change over time, such as the outdoor air temperature, solar radiation incident on a wall, convection film coefficients, building occupancy, and activity rates.

When all the necessary files have been created, the user runs SPARK. SPARK processes the trio *problem specification file - constant input file - dynamic input file* by creating a C program, compiling it, and executing it. At the end of the simulation the results for each time step are listed in an output file.

A.2.3 Output data processing

In the "output data processing" section the user employs a set of pre-existing programs to display the results of the SPARK simulation in the form of graphs and/or tables. These programs extract and/or plot time-dependent output variables (e.g. air temperature, surface temperatures, water flow rate, water temperature, etc.).

A.3 The SPARK Building Component Library

As described in section A.2, the problem of modeling the thermal behavior of a building in RADCOOL consists of (1) gathering information about the building to be modeled and (2) selecting and "assembling" building components from the SPARK library.

The SPARK building component library contains classes of components. A class of components is defined by its specific properties (e.g. passive or active wall), by the internal links between its sub-classes, and by the links to the other classes of components. The input required for a class reflects the character of the class, and can differ from class to class.

In its present version, RADCOOL has seven classes of components in its SPARK library. The classes are listed below, each class having its corresponding sub-classes attached. The sub-classes are linked together as each class is created.

1. One-dimensional passive four-layer wall with thermal mass.

   a. heat conduction/storage for each of the four layers of the wall.

   b. for exterior walls: radiant heat balance on the exterior surface, including incident solar radiation and long wave radiation exchange with the surroundings.

   c. interior surface radiant heat balance, including infrared and short wave radiation calculations.

2. One-dimensional passive four-layer ground level floor with thermal mass.

   a. heat conduction/storage for each of the four layers of the floor.

   b. exterior heat balance (ground contact).

   c. interior surface radiant heat balance, including infrared and short wave radiation calculations.

3. One-dimensional two-pane window with thermal mass.

   a. heat conduction/storage for each of the two panes.

   b. exterior surface radiant heat balance (for first pane), including calculations of the incident and transmitted solar radiation, and infrared radiation exchange with the surroundings.

   c. interior surface radiant heat balance (for second pane), including infrared and short wave radiation calculations.

4. Two-dimensional active core-cooling ceiling with 5x5 grid structure.

   a. heat conduction/storage for each of the grid cells, and into the water pipes.

   b. heat conduction/storage in the two water regimes (flowing/stagnant).

   c. control strategies for the cooling mode.

   d. for roofs: exterior surface radiant heat balance.

   e. interior surface radiant heat balance.

5. One-dimensional active cooling panel (isothermal panel suspended under a ceiling with thermal mass).

a. heat balance on the top and bottom surfaces of the panel, and heat transfer to the water pipes.

b. heat conduction/storage in the two water regimes (flowing/stagnant).

c. control strategies for the cooling mode.

d. heat conduction/storage and surface balance for the ceiling with thermal mass located above the plenum.

6. Heat and moisture balance for room air (and plenum air, if applicable).

a. room air heat balance.

b. plenum air heat balance.

c. air moisture balance.

7. Linking objects between classes of components.

a. connection between the room air module and the room surfaces (for the modeling of convection heat transfer)

b. connection between the plenum air module and the plenum surfaces, where applicable.

c. interior short wave radiation calculations.

d. interior long wave radiation calculations.

In order to "assemble" a building from components, elements of different classes must be linked together, hence the "linking object" class of components.

Having a single-valued syntax is crucial for this process. In the following, the syntax is the same as that used in the program, which causes a somewhat clumsy appearance of the text and of the equations. However, for better orientation of potential RADCOOL users, readability was given preference over aesthetics.

All variables described in the text have SI units: kilogram [kg], meter [m], second [s] and Kelvin [K], and units derived from these four.

Variable names that start with q or I have units of [W/m^2]. Variable names that start with Q have units of [W]. The names of temperatures start with t, unless in a differential equation involving time, where they start with T.

A.4 The Passive Building Components

A.4.1 One-dimensional heat transfer

A good approximation in the modeling of building components, such as passive walls and windows, is to consider that their surfaces, and all the imaginary internal planes parallel to the surfaces, are isothermal. This approach neglects surface temperature gradients and edge effects. However, the benefits of one-dimensional heat transfer offset the inaccuracies introduced in the results by the isothermal approximation.

A.4.1.1 The one-dimensional heat conduction/storage equation

Consider an infinitely high and wide wall, with homogenous and isotropic material properties, and one-dimensional heat flow perpendicular to the surface of this wall. The temperature at each point over the thickness of the wall can be defined as a space- and time-dependent function, $T = T(x, t)$, where x is the space variable, and t the time variable.

Consider a volume element, ΔV, with heat flux $q(x, t)$ incident on one surface and a heat flux $q(x + \Delta x, t)$ incident on the opposite surface, as shown in Figure A.2.

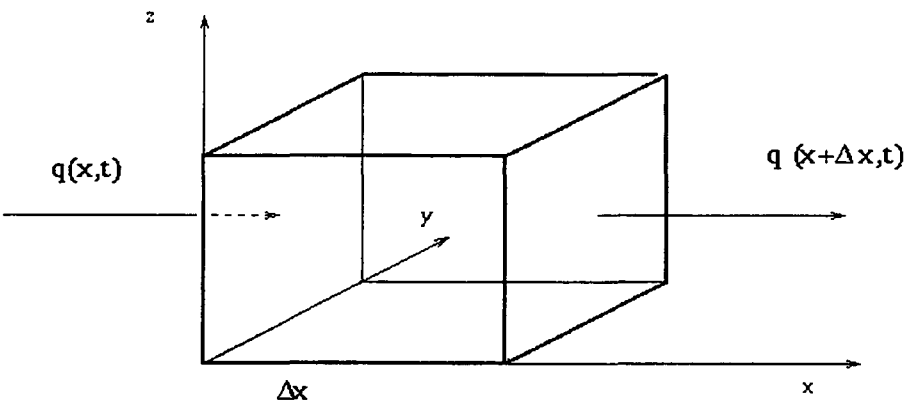

Figure A.2. Volume element for conduction heat flow.

The Fourier equation gives the conduction heat flux as:

$$q(x, t) = -k\frac{\partial}{\partial x}T(x, t) \tag{A.1}$$

where

k is the thermal conductivity of the material [W/m-K].

If $\bar{T}(x, t, \Delta t)$ is defined as:

$$\bar{T}(x, t, \Delta t) = \frac{1}{\Delta t} \int_{t}^{t+\Delta t} T(x, \tau)\, d\tau \tag{A.2}$$

$T_M(x, \Delta x, t)$ as:

$$T_M(x, \Delta x, t) = \frac{1}{\Delta x} \int_{x}^{x+\Delta x} T(\xi, t)\, d\xi \tag{A.3}$$

and $\bar{q}(x, t, \Delta t)$ as:

$$\bar{q}(x, t, \Delta t) = -k \frac{\partial T(x, t, \Delta t)}{\partial t} \tag{A.4}$$

then the heat balance for the volume element over the time period Δt is:

$$\begin{aligned} &S\Delta t\,(\bar{q}(x+\Delta x, t, \Delta t) - \bar{q}(x, t, \Delta t)) \\ &+\Delta V \rho c_t (T_M(x, \Delta x, t+\Delta t) - T_M(x, \Delta x, t)) = 0 \end{aligned} \tag{A.5}$$

where:

S is the surface area of the volume element normal to the direction of heat flow [m^2]

ρ is the density of the material [kg/m^3]

c_t is the specific heat of the material [J/kg-K].

Considering equation (A.4), and the relation between the volume and the thickness of the volume element

$$\Delta V = S\Delta x \tag{A.6}$$

the heat balance equation becomes

$$k\left(\frac{\left(\frac{\partial \bar{T}}{\partial x}\right)_{x+\Delta x} - \left(\frac{\partial \bar{T}}{\partial x}\right)_{x}}{\Delta x}\right) = c_t \rho \frac{T_M(x, t+\Delta t) - T_M(x, t)}{\Delta t} \tag{A.7}$$

In the limit $\Delta x \rightarrow 0$ and $\Delta t \rightarrow 0$, this leads to the heat diffusion equation

$$\frac{\partial T}{\partial t} = \alpha \frac{\partial^2 T}{\partial x^2} \tag{A.8}$$

where α is the thermal diffusivity [m^2/s]:

$$\alpha = \frac{k}{\rho c_t} \tag{A.9}$$

A.4.1.2 The RC approach to solve the heat conduction/storage equation for one solid layer in SPARK

Consider the wall from Section A.4.1.1. Equations (A.1) and (A.8) represent the differential equations for heat conduction through, and heat storage in, the wall. In this section the two equations are simplified and brought into a form that can be easily solved in SPARK. To this end, the space dependence of the temperature must be expressed in finite difference form.

The analogy of the Fourier equation and the heat diffusion equation with Ohm's law and the electrical diffusion equation is obvious. By virtue of this analogy, a "lumped thermal resistance" R_t can be defined as:

$$q = \frac{\Delta T}{R_t} \tag{A.10}$$

and a "lumped thermal capacitance" C_t can be defined as:

$$q = C_t \frac{\partial T}{\partial t}. \tag{A.11}$$

The idea behind the RC approach is to express equations (A.1) and (A.8) by means of (A.10) and (A.11), so that the right-hand side of equation (A.8) can be given a finite difference expression. Comparing (A.10) and a finite difference expression of (A.1), the thermal resistance of a layer of thickness Δx can be defined as

$$R_t = \frac{\Delta x}{k} \tag{A.12}$$

Now comparing (A.8), (A.11) and (A.12), the thermal capacity of a layer of thickness Δx can be defined as

$$C_t = \rho c_t \Delta x \tag{A.13}$$

Using (A.9) in (A.12), (A.13),

$$\alpha = \frac{(\Delta x)^2}{R_t C_t} \tag{A.14}$$

Equations (A.10) - (A.13) give the "lumped RC" model of a homogenous, isotropic wall layer. This model is, however, a crude approximation of the real case, in which each infinitesimal layer dx of the wall can have its own resistance and capacity. To use the RC approach more accurately, a wall must be modeled as composed of a number of layers, each having its own resistance and capacity expressed by equations similar to (A.12) and (A.13), respectively. As the number of layers simulated increases each layer becomes thinner (Δx decreases). In the limit, the RC model approaches the real equations of heat transfer and storage.

A.4.2 The structure of the passive wall in SPARK

Considering that the scope of RADCOOL is to model the thermal performance of buildings, the SPARK module corresponding to the heat conduction/storage sub-component of a wall should be able to handle at least four layers of different materials. To this end, the RC model of each layer was created, then the overall wall component was designed as a system of equations comprising the heat conduction and storage equations for each layer.

Several test programs were written in SPARK to determine the number of sub-layers that must be defined to give good agreement with analytical solutions. The results show that a combination of three resistances and two capacitances (Figure A.3) differs only in the order of a few percent from a combination of four resistances and three capacitances (Figure A.4). However, the computation time increases significantly for the case of four resistances and three capacitances, as compared to the case of three resistances and two capacitances. It was therefore considered appropriate that each layer be modeled as having a maximum of three sub-layers (three resistances and two capacitances).

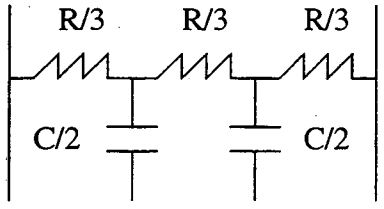

Figure A.3. A wall layer with three sub-layers.

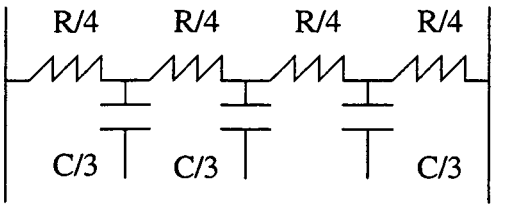

Figure A.4. A wall layer with four sub-layers.

Another important consideration in selecting the final "equivalent circuit" for the wall was that, out of the four wall layers, only the surface layers are exposed to convection, long wave (IR) radiation, and solar radiation (for exterior layer), whereas the two middle layers are not exposed to any sources of radiation. In consequence, in the present version of RADCOOL, each of the two surface layers is modeled as having a structure of three sub-layers, while each of the middle layers is modeled as having a structure of two sub-layers. The equivalent RC circuit is shown in Figure A.5.

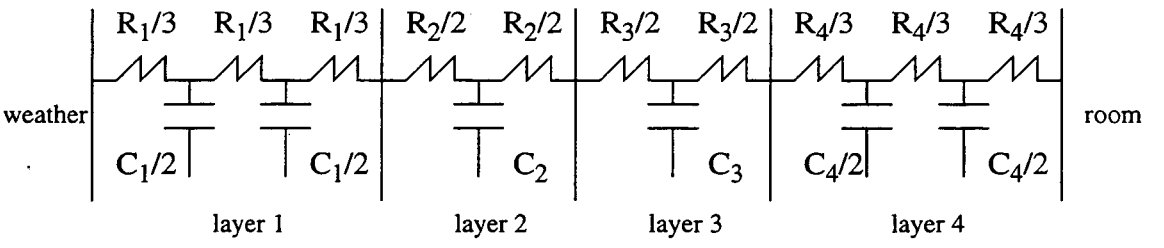

Figure A.5. The RC model of the 4-layer wall.

A.4.2.1 The equations for the temperature nodes in SPARK

The SPARK module that simulates heat conduction/storage in a four-layer passive wall solves the system of equations describing the heat balance at each temperature node. The temperature nodes can be identified from Figure A.5: each surface layer contains two interior temperature nodes, each interior layer contains one interior temperature node, each interface between two layers contains one temperature node, and each wall surface contains one temperature node.

Consider interior node i. Denote by i-1 and i+1 the nodes located immediately adjacent to node i. Denote by R_{i-1} and R_{i+1} the resistances of the sub-layers (i-1, i) and (i, i+1), and by C_i the capacity corresponding to node i. The heat balance equation for node i is:

$$\frac{T_{i-1} - T_i}{R_{i-1}} = C_i \frac{dT_i}{dt} + \frac{T_i - T_{i+1}}{R_{i+1}} \tag{A.15}$$

Consider interface node i. Denote by i-1 and i+1 the nodes located immediately adjacent to node i. Denote by R_{i-1} and R_{i+1} the resistances of the sub-layers (i-1, i) and (i, i+1). The heat flux balance equation for interface node i is:

$$\frac{T_{i-1} - T_i}{R_{i-1}} = \frac{T_i - T_{i+1}}{R_{i+1}} \tag{A.16}$$

Consider wall surface node i. Denote by i+1 the node locate immediately adjacent, inside the wall. Denote by R_{i+1} the resistances of the sub-layer (i, i+1), and by q_i the sum of heat fluxes incident on the wall. The heat flux balance equation for the surface node i is:

$$q_i = \frac{T_i - T_{i+1}}{R_{i+1}} \tag{A.17}$$

The system of equations for a 4-layer wall with the equivalent circuit shown in Figure A.5 is therefore composed of:

- 6 differential equations of type (A.15), corresponding to the interior nodes,
- 3 algebraic equations of type (A.16), corresponding to the interface nodes, and
- 2 algebraic equations of type (A.17), corresponding to the surface nodes.

A.4.2.2 Test to determine the accuracy of the RC model for one-dimensional heat transfer

In order to determine the accuracy of the RC wall model described in section A.4.2.1 the analytical solution of a given problem was compared with the results from the SPARK model of the same problem.

The problem

Consider the problem of one-dimensional heat transfer in a homogenous and isotropic wall of thickness l ($0 < x < l$), with the planes $x = 0$ and $x = l$ kept at temperatures 0 °C and $\sin(\omega t+\varepsilon)$ [°C], respectively [3].

The analytical solution

The temperature of a node at distance x from the plane $x = 0$ is [3]:

$$T(x,t) = A\sin(\omega t + \varepsilon + \phi) + 2\pi\alpha \sum_{n=1}^{\infty} \frac{n(-1)^n(\alpha n^2\pi^2 \sin\varepsilon - \omega l^2 \cos\varepsilon)}{\alpha^2 n^4 \pi^4 + \omega^2 l^4} \sin\frac{n\pi x}{l} e^{-\frac{\alpha n^2 \pi^2 t}{l}} \tag{A.18}$$

where

$$A = \left|\frac{\sinh \mathbf{k}x(1+i)}{\sinh \mathbf{k}l(1+i)}\right| = \left\{\frac{\cosh 2\mathbf{k}x - \cos 2\mathbf{k}x}{\cosh 2\mathbf{k}l - \cos 2\mathbf{k}l}\right\}^{\frac{1}{2}} \tag{A.19}$$

$$\phi = \arg\left\{\frac{\sinh \mathbf{k}x(1+i)}{\sinh \mathbf{k}l(1+i)}\right\} \tag{A.20}$$

and

$$\mathbf{k} = \left(\frac{\omega}{2\alpha}\right)^{\frac{1}{2}} \tag{A.21}$$

The input data

To compare the analytical solution given by equations (A.18) - (A.21) with the results of the SPARK model, a 20 cm concrete wall was modeled and the temperature in the middle of the wall (x = 10 cm) was calculated. The thermal diffusivity was $\alpha = 7.2 \times 10^{-7}$ m^2/s. The sine temperature function at the x = 20 cm surface was chosen to have a period of 24 hours ($\omega = 7.3\ 10^{-5}\ s^{-1}$) and no time lag ($\varepsilon = 0$).

To determine the analytical solution a FORTRAN program was written in which 100,000 terms in (A.18) were summed to calculate the temperature at each time step.

The SPARK program was designed with all four layers having the same thickness (5 cm) and the same thermal properties: density $\rho = 2400$ kg/m^3, specific heat $c_t = 1040$ J/kg-K, and conductivity $k = 1.8$ W/m-K (which gives $\alpha = 7.2\ 10^{-7}$ m^2/s).

Results

Figure A.6 compares the SPARK result with the analytical solution for the temperature in the middle of the wall (x = 10 cm). The SPARK curve is the result of several iterations. The sinusoidal temperature at the x = 20 cm surface of the wall is also shown. There is good agreement between the SPARK result and the analytical solution of the problem.

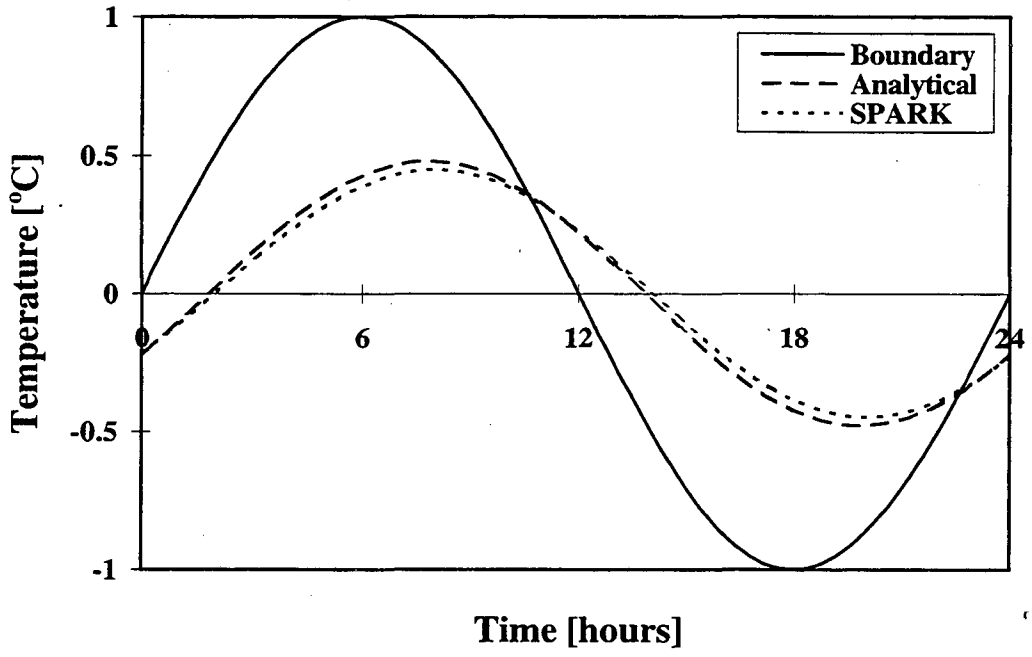

Figure A.6. Temperature at the midpoint of a homogeneous wall: comparison between the one-dimensional SPARK model and the analytical solution.

A.4.3 Exterior surface radiant heat balance for a wall with thermal mass

In this section the radiant heat balance is defined for the exterior (weather-exposed) surface temperature node of a wall (see Figure A.5). The heat fluxes that enter the heat balance equation are shown in Figure A.7.

Heat fluxes into the surface node point are considered positive. All variable names in this object have the suffix *out_obj_i* to emphasize the reference to the exterior surface of the wall number *i*.

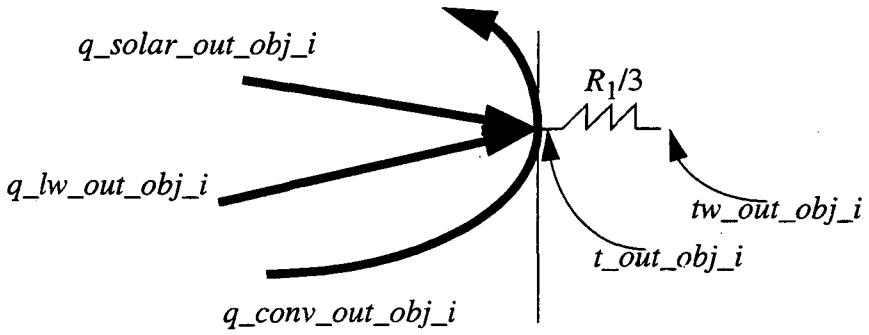

Figure A.7. The heat flux balance at the exterior surface node.

The heat balance is given by:

$$q_{conv-out-obj-i} + q_{lw-out-obj-i} + q_{solar-out-obj-i} = \frac{t_{out-obj-i} - t_{w-out-obj-i}}{\frac{R_1}{3}} \tag{A.22}$$

where

$q_{conv_out_obj_i}$ is the convective heat flux at the exterior surface of wall *i* [W/m^2]

$q_{lw_out_obj_i}$ is the long wave (IR) heat flux from the surroundings of wall *i* [W/m^2]

$q_{solar_out_obj_i}$ is the solar radiation incident on surface of wall *i* [W/m^2].

The right-hand side of equation (A.22) is the conduction flux through the first exterior sub-layer of wall *i* (refer to equation (A.17) and Figure A.5).

A.4.3.1 The convective heat flux on the surface of a wall

The convective heat flux incident on a surface is defined as the product of the convective film coefficient and the temperature difference between the surface and the air near the

surface:

$$q_{conv} = h_{conv}(t_{air} - t_{surface}) \tag{A.23}$$

The air temperature near the wall surface and the convective film coefficient usually depend on the location on the surface.

The convective film coefficient of an exterior wall depends on the outside air temperature and on the wind speed and direction. The convective film coefficient of an interior wall depends on the room air temperature and on the air movement (speed and direction). Consequently, this coefficient is not constant for a surface.

In RADCOOL, the air temperature near the exterior wall in equation (A.23) is considered equal to the outside air temperature. In order to use a realistic convective film coefficient in the calculation, hourly values are obtained from a DOE-2 calculation. The model employed by DOE-2 is based on [4].

A.4.3.2 The long wave (IR) heat flux exchange between a wall and its exterior surroundings

The long wave radiation exchange between the exterior surface of a wall and the building surroundings (the ground, sky and atmosphere) is represented in Figure A.8 [5].

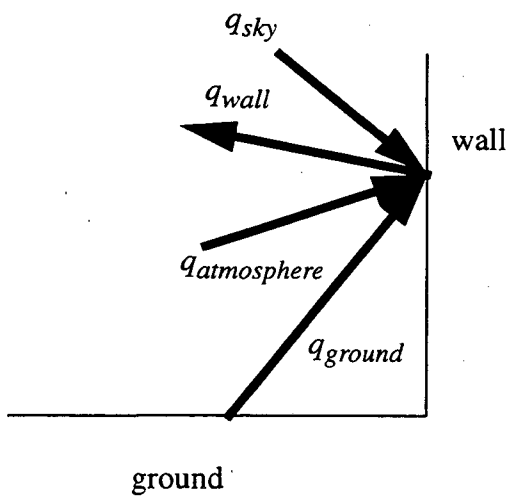

Figure A.8. The long wave radiation exchange at the exterior surface of a wall.

q_{sky} is the long wave radiation from the sky that is absorbed by the wall surface [5]:

$$q_{sky} = \varepsilon_{wall}\sigma\varepsilon_{sky}T_{air}^4 F_{sky}\cos\left(\frac{\Phi_{wall}}{2}\right) \tag{A.24}$$

where

T_{air} is the ambient air drybulb absolute temperature [K]

ε_{wall} is the wall surface emissivity (equal to 0.9 for most building materials)

ε_{sky} is the effective sky emissivity; it depends on the outside air absolute dew-point temperature T_d, and the cloud cover fraction N:

$$\varepsilon_{sky} = \left(0.787 + 0.76 ln\left(\frac{T_d}{273}\right)\right)\left(1 + 0.224N - 0.0035N^2 + 0.00028N^3\right) \tag{A.25}$$

where

σ is the Stefan-Boltzmann constant (5.67×10^{-8} W/m^2-K^4).

F_{sky} is the sky form factor, defined as the fraction of the hemisphere seen by the wall surface that is subtended by the sky; F_{sky} depends on the tilt of the wall, Φ_{wall} (Φ_{wall} = 90° for a vertical wall, Φ_{wall} = 180° for a floor and Φ_{wall} = 0° for a horizontal roof):

$$F_{sky} = \frac{1 + \cos\Phi_{wall}}{2} \tag{A.26}$$

$q_{atmosphere}$ is the long wave radiation from the atmosphere that is absorbed by the wall surface [5]:

$$q_{atmosphere} = \varepsilon_{wall}\sigma T_{air}^4 F_{sky}\left(1 - \cos\left(\frac{\Phi_{wall}}{2}\right)\right) \tag{A.27}$$

q_{ground} is the long wave radiation from the ground absorbed by the wall surface [5]:

$$q_{ground} = \varepsilon_{wall}\sigma\varepsilon_{ground}T_{air}^4 F_{ground} \tag{A.28}$$

ε_{ground} is the ground emissivity (equal to 0.9)

F_{ground} is the fraction of the hemisphere seen by the wall surface as being subtended by the ground; it is also called ground form factor:

$$F_{ground} = \frac{1 - \cos\Phi_{wall}}{2} \tag{A.29}$$

For a building that does not have vegetation (trees, bushes) nearby, $F_{ground} + F_{sky} = 1$.

q_{wall} is the long wave radiation emitted by the wall surface:

$$q_{wall} = \varepsilon_{wall}\sigma T_{wall}^4 \tag{A.30}$$

ε_{wall} is the wall surface emissivity

T_{wall} is the wall surface absolute temperature [K].

The long wave radiation gain on the exterior surface of the wall can be expressed as:

$$q_{lw} = q_{sky} + q_{atmosphere} + q_{ground} - q_{wall} \tag{A.31}$$

A.4.3.3 The solar radiation incident on the surface of a wall

The solar radiation incident on the exterior surface of a wall has a direct and a diffuse component. The wall absorbs a fraction of each, in amounts dictated by the values of the direct and diffuse absorption coefficients of the wall. The total solar radiation absorbed by the wall is therefore the sum of the absorbed direct and absorbed diffuse solar radiation:

$$q_{solar-out-i} = I_{dir-abs-out-i} + I_{diff-abs-out-i} \tag{A.32}$$

where

$$I_{dir-abs-out-i} = abs_{dir-oout-i} I_{dir-out-i} \tag{A.33}$$

$$I_{diff-abs-out-i} = abs_{diff-out-i} I_{diff-out-i} \tag{A.34}$$

where

$I_{dir_abs_out_i}$ is the portion of the direct solar radiation incident on the exterior surface of wall i that is absorbed at the surface [W/m^2]

$abs_{dir_out_i}$ is the direct absorption coefficient of wall i

$I_{dir_out_i}$ is the direct solar radiation incident on the exterior surface of wall i [W/m^2]

$I_{diff_abs_out_i}$ is the portion of the diffuse solar radiation incident on the exterior surface of wall i that is absorbed at the surface [W/m^2]

$abs_{dir_out_}i$ is the diffuse absorption coefficient of wall i

$I_{diff_out_i}$ is the diffuse solar radiation incident on the exterior surface of wall i [W/m^2].

Most building materials have absorptivities of 0.9. The absorptivities of glass surfaces are lower; a typical value for the absorptivity of clear glass is 0.84.

In RADCOOL, the values of the direct and diffuse solar radiation incident on the exterior surface of each wall are requested as inputs. The calculation of these parameters is performed in the "preliminary data processing" section. The calculations will be described in section A.9.2.

A.4.4 Interior surface radiant heat balance for a wall with thermal mass

In this section the radiant heat balance is defined for the interior (room-exposed) surface temperature node of the wall (see Figure A.5). The heat fluxes that enter the heat balance equation are shown in Figure A.9.

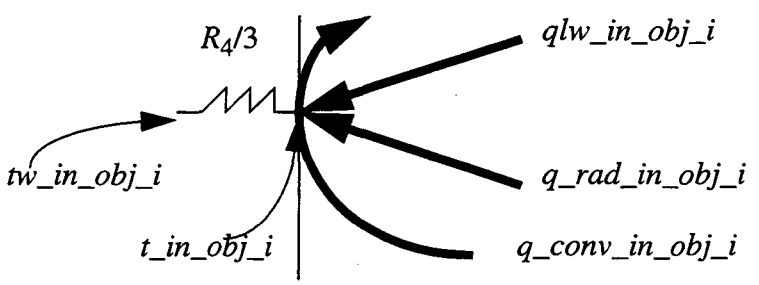

Figure A.9. The heat flux balance at the interior surface temperature node.

Incoming heat fluxes at a node are considered positive. The variable names in this object have the suffix *obj_in_i* to emphasize the reference to the surface of wall *i*. The heat balance is given by:

$$q_{conv-in-obj-i} + q_{lw-in-obj-i} + q_{rad-in-obj-i} = \frac{t_{in-obj-i} - t_{w-in-obj-i}}{\frac{R_4}{3}} \quad \text{(A.35)}$$

where

$q_{conv_in_obj_i}$ is the convective heat flux at the interior surface of wall *i* [W/m^2]

$q_{lw_in_obj_i}$ is the net long wave (IR) radiation flux gain from the radiative exchange between the wall *i* and the other walls in the room [W/m^2]

$q_{rad_in_obj_i}$ is the radiation incident at the interior surface of wall i from the sources inside the room (people, equipment and lights), and from the solar radiation entering the room through transparent surfaces [W/m^2].

The right-hand side of equation (A.35) represents the conduction flux through the first interior sub-layer of wall i (refer to equation (A.17) and Figure A.5).

A.4.4.1 The convective heat flux on the interior surface of a wall

The convective heat flux on the interior surface of the wall is given by equation (A.23).

In most applications the room air temperature and the convective heat coefficient can be averaged over the surface. For example, Figure A.10 shows the surface temperature of a vertical wall and the air temperature near the surface as a function of height. At the "neutral level" both temperatures are the same. The direction of the heat flux is from the wall towards the air at locations under the "neutral level", and from the air to the wall at locations above the "neutral level." In order to simulate each wall surface represented by only one node, an expression for the convection film coefficient at this one node must be found that reflects the variation of this coefficient over the wall surface.

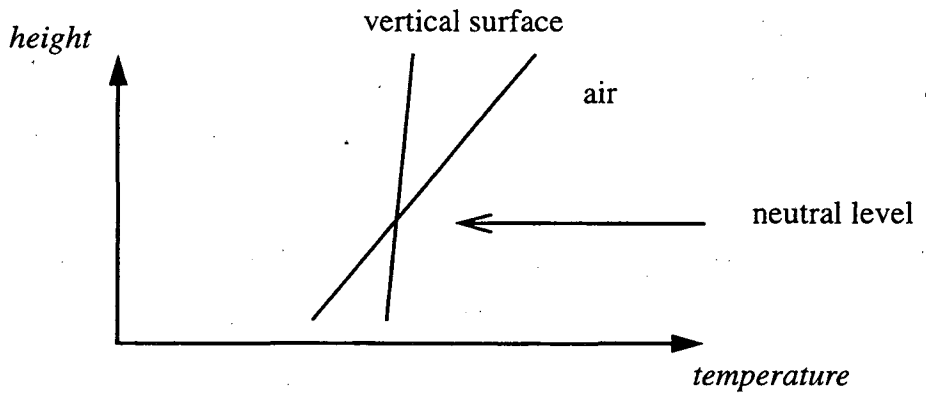

Figure A.10. Different gradients for air and room temperatures.

The interior convective film coefficient, *h_conv_in_i*, depends on the properties of the air, the wall surface roughness, and the air movement near the wall. There are several levels of simplification for calculating this variable.

- constant value: as a first approximation, *h_conv_in_i* may be assumed constant. Building simulation programs employ values in the range from 1 to 3.5 W/m^2-K [6].

- a function of temperature difference between the surface and the air near the surface; there are several such expressions (see [7] for example):

$$h_{conv-in-i} = C_1 (\Delta t)^{C_2} \tag{A.36}$$

where C_1 and C_2 are considered constant, or depend on the properties of the air and of those of the surface.

- a function of the physical properties of the air and the surface; calculating the convective film coefficient based on this method is based on determining air flow patterns near the surface.

Considering the limitations of SPARK, in RADCOOL the interior convective film coefficient is considered constant and equal to the value employed in DOE-2 (3.25 W/m^2-K).

A.4.4.2 The long wave radiative exchange between a wall and the other room surfaces

Consider an enclosure composed of N discrete surfaces, each having a determined temperature T_i. A complex long wave (IR) radiative exchange occurs inside the enclosure as radiation is emitted by a surface, travels to the other surfaces, is partly reflected and re-reflected many times within the enclosure, with partial absorption at each contact with a surface.

There are several approaches for the calculation of the net long wave flux gain by a surface as a result of this radiative exchange inside the enclosure. The two approaches that are adequate for a building simulation program are the *mean radiant temperature* approach and the *net-radiation* approach. RADCOOL uses the net-radiation approach.

The mean radiant temperature approach

This approach approximates that the interaction between a given wall and the rest of the surfaces in the enclosure can be described as the interaction between two surface elements. The equation governing the radiative exchange is the grey body equation for two surface elements, one at the temperature of the wall, and the other at the mean radiant temperature. The mean radiant temperature is defined as the temperature of a half sphere that causes a net heat flux on the wall equal to the heat flux caused by the real enclosure.

Considering that all the walls forming the enclosure have the same emissivity, the net long wave radiation on surface number i can be expressed as

$$q_{long-wave-in-i} = \varepsilon_{in-i}\varepsilon_{sphere-in-i}\alpha_{rad-in-i}(T_{MRT-in-i} - T_{in-i}) \tag{A.37}$$

where

$T_{MRT_in_i}$ is the mean radiant temperature of the enclosure with respect to surface i [K]

T_in_i is the temperature of surface i [K]

ε_{in_i} is the emissivity of surface i [-]

$\varepsilon_{sphere_in_i}$ is the weighed average of the emissivities of the other surfaces [-]

$\alpha_{rad_in_i}$ is the radiative heat transfer coefficient defined in analogy to the convective heat transfer coefficient [W/m^2-K].

Consider an "enclosure" consisting of two infinitely long and wide walls facing each other. If the two walls can be represented as black bodies, the radiative heat exchange between them can be written as:

$$q_{12} = \sigma(T_1^4 - T_2^4) = \alpha_{rad-in-i}(T_1 - T_2) \tag{A.38}$$

with

$$\alpha_{rad-in-i} = \sigma(T_1^3 + T_1^2 T_2 + T_1 T_2^2 + T_2^3) \tag{A.39}$$

where σ is the Stefan-Boltzmann constant (equal to 5.67x10^{-8} W/m^2-K^4). $\alpha_{rad_in_i}$ is equal to 5 - 7 W/m^2-K over the temperature range occurring in buildings.

Raber and Hutchinson [8] mention the influence of reflectance, and state that the reflectance may be neglected if emissivities are higher than 0.9. Assuming that $\alpha_{rad_in_i}$ is the same for all pairs of walls, Raber and Hutchinson derive:

$$T_{MRT-in-i} = F_{i1}T_1 + F_{i2}T_2 + \ldots + F_{ij}T_j \tag{A.40}$$

where

$T_i, \ldots, T_j$ are the temperatures of the surfaces of the enclosure

F_{ij} is the shape factor of surface i to surface j, equal to the fraction of the long wave radiation emitted by surface i that is absorbed by surface j.

The calculation of the shape factors is relatively simple in the case of flat surfaces (see [9]), but rather complicated in the case of rounded surfaces. Section A.9.3 will present the calculation method used to determine the shape factors in the "preliminary data processing" section of RADCOOL.

The net-radiation approach

The net-radiation approach [9] provides a method to calculate the net (equilibrium) radiation incident on each surface of the enclosure. This approach does not impose any

approximations regarding the types of surfaces in an enclosure, such as a range of emissivities over which equation (A.40) holds, and it therefore suits RADCOOL better than the mean radiant temperature approach.

Consider the area A_i of the enclosure. If q^i_{out} and q^i_{in} are the radiant flux leaving from surface i, and incident on surface i, respectively, a flux balance at the surface can be written as:

$$q^i_{net} = q^i_{in} - q^i_{out} \tag{A.41}$$

where

$$q^i_{out} = \varepsilon_{in-i}\sigma T^4_{in-i} + (1 - \varepsilon_{in-i})\, q^i_{in} \tag{A.42}$$

Since the incoming radiant flux is a combination of outgoing radiant flux from the other surfaces, an additional equation can be written:

$$q^i_{in} = \sum_{j=1}^{N} F_{ij} q^j_{out} \tag{A.43}$$

By solving the system of equations (A.41) - (A.43), the net radiant gain for each surface can be determined.

A.4.4.3 Solar and internal radiation incident on the interior surface of a wall

Two other sources of radiation on the interior surface of a wall are the short wave (solar) radiation entering the window and the heat radiated by occupants and equipment.

Short wave radiation in a space

In a typical building, short wave solar radiation enters a space through windows and other transparent surfaces (transparent walls, skylights, etc.). This radiation is incident on the different surfaces in the space, according to the position of the windows with respect to the sun, and of the surfaces with respect to the windows. A thorough calculation of this effect would determine the position of the sun at each moment, and, based on the position of the windows in the space, the fraction of the solar radiation entering the space that is incident on each surface. This calculation is not only time consuming, but also needs a follow-up in which the multiple reflections between the different surfaces are determined.

To avoid lengthy calculations and complicated distribution functions for the transmitted

solar radiation, the RADCOOL user performs solar calculations in the "preliminary data processing" section. These calculations (see section A.9.2 for details) determine the solar radiation incident on each building envelope surface, as well as the fractions of the total solar radiation entering the space at each moment.

RADCOOL adopted the DOE-2 approach, in which a given combination of surfaces inside the space receives a certain fraction of the total radiation entering the space. Assuming that each surface in a given combination receives the same amount of radiation per unit area, the incident short wave radiation on each surface can be calculated as:

$$q_{short-wave-in-i} = fraction_{in-i} \frac{\sum_{windows} A_{window-j} q_{short-wave-window-j}}{A_{surfaces-in-i}} \quad (A.44)$$

q_short_wave_window_j is the amount of solar radiation entering the space through window *i* [W/m^2]

A_window_j is the area of window *i* through which *q_short_wave_window_j* solar radiation enters the space [m^2]

A_surfaces_in_i is the area of the combination of walls including wall *i*, that receives *fraction_in_i* of the total solar radiation entering the space [m^2]

fraction_in_i is the fraction of the total short wave radiation entering the room that is incident on the combination of walls having the total area *A_surfaces_in_i* [-]

q_short_wave_in_i is the amount of solar radiation entering the space that is incident on the combination of walls having the area *A_surfaces_in_i*, including wall *i* [W/m^2].

Occupants and equipment inside a space

The occupants and equipment (including lights) in a space are internal heat sources. In RADCOOL the occupants and equipment are considered to be grey bodies that participate in the long wave radiation exchange in the space (see section A.4.4.2), and sources of sensible and latent heat for the heat and moisture balances in the room air module (see section A.7).

A.4.5 The four-layer passive floor with thermal mass

A.4.5.1 Comparison between the floor and the wall with thermal mass

The main difference between a ground-level floor and an exterior vertical wall is that, while the exterior surface of the floor is in contact with the ground, the exterior surface of a vertical wall is in contact with the outside air, and is exposed to solar radiation.

The exterior surface of a floor therefore participates in conductive heat exchange with the ground, but is not subject to convective or radiative heat exchange. Based on these considerations, the case of a floor can easily be modeled starting with the model of the vertical wall:

- the heat conduction/storage for the four-layer floor with thermal mass is the same as for the four-layer wall with thermal mass (see section A.4.2),
- the interior surface radiant heat balance of a floor is the same as that for a vertical wall (see section A.4.4), and
- the heat balance for the exterior surface node of a floor contains only conduction terms.

A.4.5.2 The exterior surface radiant heat balance for a passive floor with thermal mass

The heat balance for the exterior surface of a floor describes the contact between the floor and the ground. The equivalent of equation (A.17) for this case is

$$q_{ground-out-i} = \frac{t_{out-obj-i} - t_{w-out-obj-i}}{\frac{R_1}{3}} \tag{A.45}$$

In RADCOOL a resistance is modeled between the floor and the ground temperature nodes. The heat flux incident on the exterior surface of the floor can be calculated as:

$$q_{gound-out-i} = \frac{t_{ground-out} - t_{out-obj-i}}{R_{floor-ground-obj-i}} \tag{A.46}$$

where

$R_{floor_ground_obj_i}$ is the floor-ground resistance [m^2-K/W]

t_ground_out is the ground temperature [°C]

t_out_obj_i is the temperature of the exterior surface of the floor number *i* [°C].

A.4.6 The two-pane window with thermal mass

A.4.6.1 Comparison between a two-pane window and a multi-layer wall

With the exception of solar radiation effects, a multi-pane window behaves like a multi-layer wall in which one or more of the layers are air (or a different gas). If a temperature difference is created between two window surfaces, or if thermal radiation is directed on one window pane, the glass will undergo heat conduction and storage.

A glass pane and a wall layer have different thermal behavior due to the numerical values of their thermal properties. In a wall layer, the conduction and storage heat transfer are both important, resulting in a significant temperature difference between the two boundaries (surfaces) of the wall layer. In a window pane, the temperature difference between the two surfaces of the glass is small because of the high conductivity of the glass. As glass window panes are usually thin (3 - 6 mm), their thermal storage is also small. However, in a multi-pane window, the overall temperature difference across the window can be significant, especially if the glass has low emissivity coating, and/or the "gap" spaces are filled with a low-conductivity gas.

A.4.6.2 Heat conduction/storage for a two-pane window

The SPARK model for a two-pane window was designed based on the thermal properties of glass. Because of the high conductivity and low heat capacity of a glass pane, a model of one resistance and one capacity was adopted for each pane. A resistance was added between the panes to account for the thermal resistance of the gas fill. Figure A.11 shows the RC model for a two-pane window.

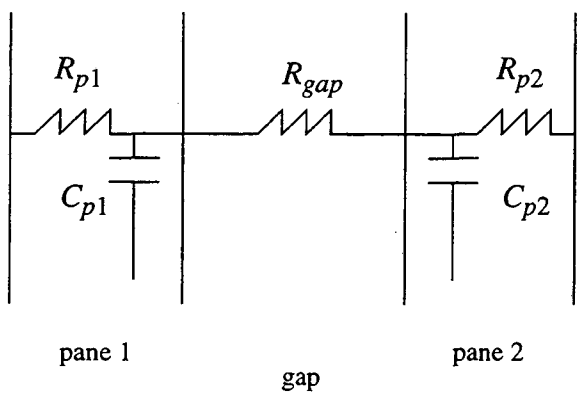

Figure A.11. The RC circuit of a two-pane window.

Two temperature nodes were modeled for each of the two panes, one on the exterior surface and one on the surface facing the "gap".

The equations that describe the heat balance for the two panes are the following:

• for the exterior (weather-exposed) temperature node, the equivalent of equation (A.17) with R_{p1} instead of $R_1/3$ gives

$$q_{rad-out} = \frac{T_{w1,out} - T_{w1,gap}}{R_{p1}} \tag{A.47}$$

where

q_{rad_out} is the overall radiative heat incident on the exterior pane [W/m^2]

$T_{w1,out}$ is the temperature at the exterior node of the exterior pane [°C]

$T_{w1,gap}$ is the temperature at the "gap"-facing node of the exterior pane [°C]

R_{p1} is the thermal resistance of the exterior pane [m^2-K/W].

• for the gap-exposed temperature node of the exterior pane:

$$\frac{T_{w1,out} - T_{w1,gap}}{R_{p1}} + C_{p1}\frac{\partial T_{w1,gap}}{\partial t} = \frac{T_{w1,gap} - T_{w2,gap}}{R_{gap}} \tag{A.48}$$

where

C_{p1} is the thermal capacity of the exterior pane [J/m^2-K]

R_{gap} is the thermal resistance of the gas filling the "gap" [m^2-K/W]; it is calculated for each type of window to include thermal diffusion and convection effects

$T_{w2,\ gap}$ is the temperature at the "gap"-facing node of the interior pane [°C].

• for the gap-exposed temperature node of the interior pane:

$$\frac{T_{w1,gap} - T_{w2,gap}}{R_{gap}} = C_{p2}\frac{\partial T_{w2}}{\partial t} + \frac{T_{w2,gap} - T_{w2,in}}{R_{p2}} \tag{A.49}$$

where

C_{p2} is the thermal capacity of the interior pane [J/m^2-K]

R_{p2} is the thermal resistance of the interior pane [m^2-K/W]

$T_{w2,in}$ is the inside temperature at the interior node of the interior pane [°C].

• for the interior (room-exposed) temperature node, the equivalent of equation (A.17), with R_{p2} instead of $R_4/3$ gives

$$\frac{T_{w2,gap} - T_{w2,in}}{R_{p2}} = q_{rad} \tag{A.50}$$

where

q_{rad} is the total incident radiation on the interior pane [W/m^2].

The notation q_{rad} was chosen for the right-hand side of equation (A.50), rather than q_rad_in, to emphasize that the heat balance for the second pane of a window also includes a fraction of the solar radiation transmitted by the first pane.

A.4.6.3 The heat balance for the exterior pane of a two-pane window

The heat balance for the exterior pane of a two-pane window is the same as that for the exterior surface of a wall. The equation that applies is:

$$q_{conv-out} + q_{lw-out} + q_{solar-1} = q_{rad-out} \tag{A.51}$$

The left-hand terms of equation (A.51) are calculated as in sections A.4.3.1 through A.4.3.3.

A.4.6.4 The heat balance for the interior pane of a two-pane window

The heat balance for the interior pane of a two-pane window is similar to that of a wall, except that the solar radiation transmitted through the first pane also contributes to the balance. The transmitted solar radiation calculated in this module will contribute to the overall short wave radiation inside the space. The heat balance equation is:

$$q_{conv-in} + q_{lw-in} + q_{rad-in} + q_{solar-2} = q_{rad} \tag{A.52}$$

The first three terms in the left-hand side of equation (A.52) are calculated as in sections A.4.4.1 through A.4.4.3.The last left-hand term is calculated as in section A.4.3.3, with the absorption coefficients corresponding to the overall coefficients for the solar radiation transmitted by the exterior pane.

The solar radiation transmitted through the two-pane window is calculated using the DOE-2 method. If the overall transmissivity coefficients are calculated for the window as a whole, the radiation transmitted through the window is:

$$q_{solar-interior} = I_{trans-dir-win-i} + I_{trans-diff-win-i} \tag{A.53}$$

and

$$I_{trans-dir-win-i} = trans_{dir-win-i} I_{dir-out-win-i} \quad (A.54)$$

$$I_{trans-diff-win-i} = trans_{diff-win-i} I_{diff-out-win-i} \quad (A.55)$$

where

$I_{dir_out_win_i}$ is the direct solar radiation incident on exterior surface of window i [W/m^2]

$I_{diff_out\ win_i}$ is the diffuse solar radiation incident on the exterior surface of window i [W/m^2].

$I_{trans_dir_win_i}$ is the portion of the direct solar radiation incident on the window i that is transmitted through the window [W/m^2]

$I_{trans_diff_win_i}$ is the portion of the diffuse solar radiation incident on the window i that is transmitted through the window [W/m^2]

$trans_{dir_win_i}$ is the overall transmission coefficient of window i in direct solar radiation

$trans_{diff_win_i}$ is the overall transmission coefficient of window i in diffuse solar radiation.

In order to perform RADCOOL calculations, hourly values for the glass transmission coefficients are obtained from a DOE-2 calculation.

After calculations are performed with equations (A.53) - (A.55) for all the windows of a space, the short wave radiation inside the space can be calculated as:

$$q_{short-wave-tot-in} = \sum_i I_{trans-win-i} \quad (A.56)$$

A.5 The Active Building Components

A.5.1 Two-dimensional heat transfer analysis

The one-dimensional heat transfer approximation presented in Section A.4.1 does not yield good results in the case of building components incorporating a heat source or sink (e.g. a core-cooling ceiling). Modeling the thermal behavior of such building components requires the use of two-dimensional heat transfer analysis. Two-dimensional heat transfer analysis describes the temperature variation of the given building component in two "main directions" of heat flow (usually the two directions of a cross-section through the building component).

A.5.1.1 The two-dimensional heat conduction/storage equations

Consider a solid ceiling with homogeneous and isotropic material properties. The two-dimensional heat transfer analysis is based on the assumption that the temperature of this ceiling is a function of only two dimensions of the ceiling, and is constant in the third dimension (e.g. the temperature varies over the cross-section of the ceiling, but all the planes parallel to the cross-section under study have the same thermal behavior).

In analogy with Section A.4.1.1, the temperature in the cross-section of a wall can be considered a function of space and time, $T = T(x, y, t)$.

Consider a volume element of this wall slab, and a heat flux incident at one surface, as in Figure A.2. The 2-D Fourier equation for heat transfer in one direction is analogous to equation (A.1) and has the form

$$Q(x, t) = -k\Delta A \frac{\partial T(x, y, t)}{\partial x} \tag{A.57}$$

where

Q is the total heat flux at the surface [W]

k is the thermal conductivity of the ceiling material [W/m-K]

ΔA is the area of the face of the volume element normal to the heat flux [m^2].

The same type of reasoning as in Section A.4.1.1 yields a two-dimensional diffusion equation of the form

$$\frac{\partial T}{\partial t} = \alpha \left(\frac{\partial^2 T}{\partial x^2} + \frac{\partial^2 T}{\partial y^2} \right) \tag{A.58}$$

where

α is the thermal diffusivity given by equation (A.9) [m^2/s].

A.5.1.2 The RC solution to the two-dimensional heat conduction/storage equations

The approach of Section A.4.1.2 can be used to express equation (A.58) as a finite difference equation. The two-dimensional ceiling can be described as a collection of parallel boxes, with the discretization (the grid) covering a plane normal to the surface of the ceiling. Since this discretization is mainly performed to describe the heat transfer due to the presence of cooling pipes inside the ceiling, the assumption was made that the analysis of a "cross-section sample" can correctly describe the temperature profile of the whole ceiling. Consequently, the parallel boxes have one dimension equal to a fraction

of the thickness of the ceiling, a second dimension equal to a fraction of the (future) distance between two cooling pipes, and the third dimension equal to the length of the ceiling divided by the distance between two cooling pipes. The remainder of this section discusses the heat transfer inside a passive two-dimensional ceiling. Section A.5.2 will describe the modeling of the actively cooled two-dimensional ceiling.

In an analogy to electrical circuits, a lumped thermal resistance can be defined in relation to the heat conduction through each box in a given direction, as:

$$Q_\xi = \frac{\Delta T_\xi}{R_\xi} \tag{A.59}$$

where ξ denotes a direction in the three-dimensional space. Similarly, a lumped thermal capacity can be defined in relation to the heat stored inside each box, as:

$$Q = C\frac{\partial T}{\partial t} \tag{A.60}$$

The resistance and capacity are calculated by the thermal properties of the ceiling material as:

$$R_\xi = \frac{\Delta \xi}{k \Delta A_\xi} \tag{A.61}$$

$$C = \rho c_t \Delta V \tag{A.62}$$

where

ΔA_ξ is the area of the box surface normal to the direction ξ [m^2]

ΔV is the box volume [m^3]

ρ is the density of the ceiling material [kg/m^3]

c_t is the specific heat of the ceiling material [J/kg-K]

k is the conductivity of the ceiling material [W/m-K].

A.5.1.3 The two-dimensional model of the ceiling in SPARK

SPARK programs were written to simulate several grids covering the sample section of the ceiling. Figures A.12 and A.13 show two alternative RC circuits, the one in Figure A.13 displaying a "finer" grid structure than the one in Figure A.12.

In the grid model in Figure A.12, the boxes have one dimension equal to a third of the ceiling thickness, and a second dimension equal to a quarter of the distance between the

cooling pipes. In the grid model in Figure A.13, the boxes have one dimension equal to a fifth of the ceiling thickness, and a second dimension equal to a quarter of the distance between the cooling pipes.

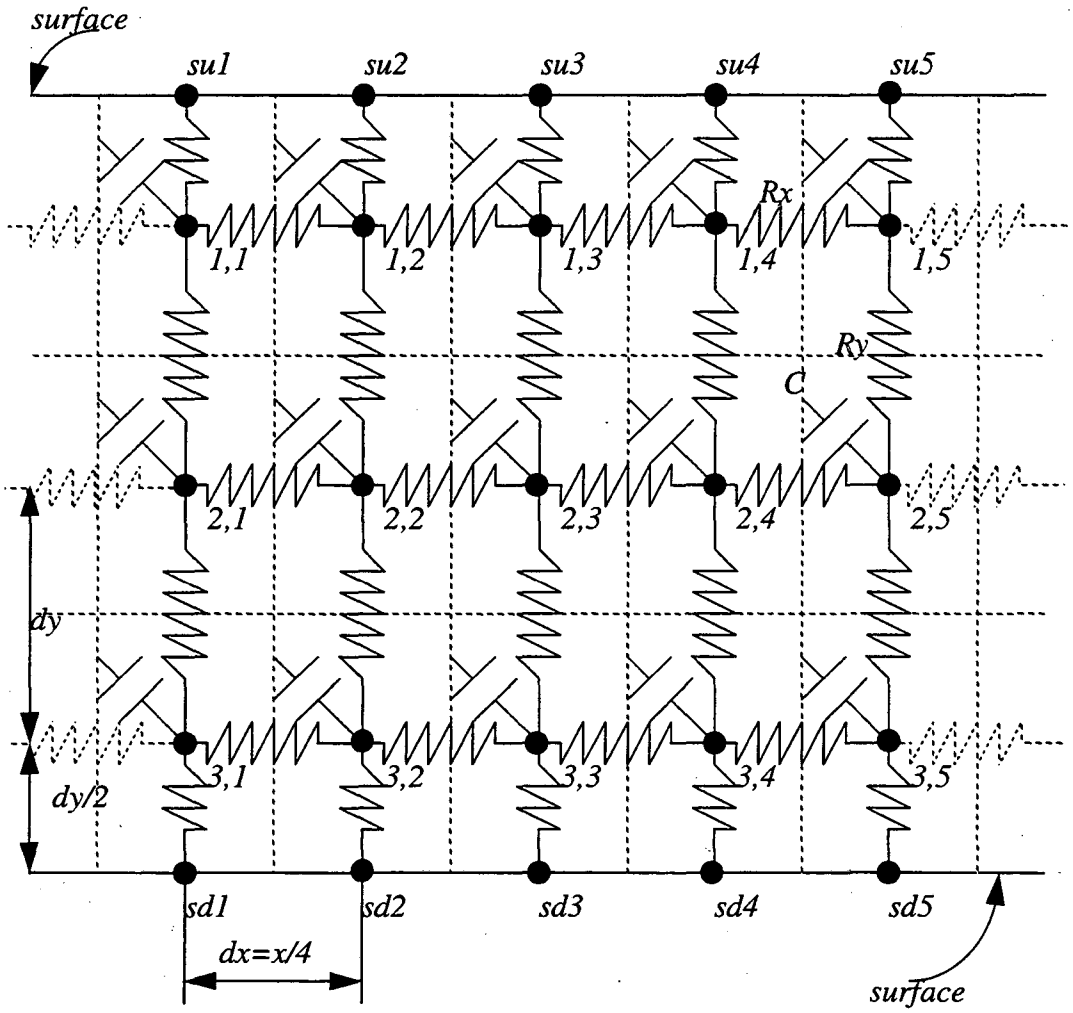

Figure A.12. A 3 x 5 grid. RC equivalent circuit for heat transfer calculations.

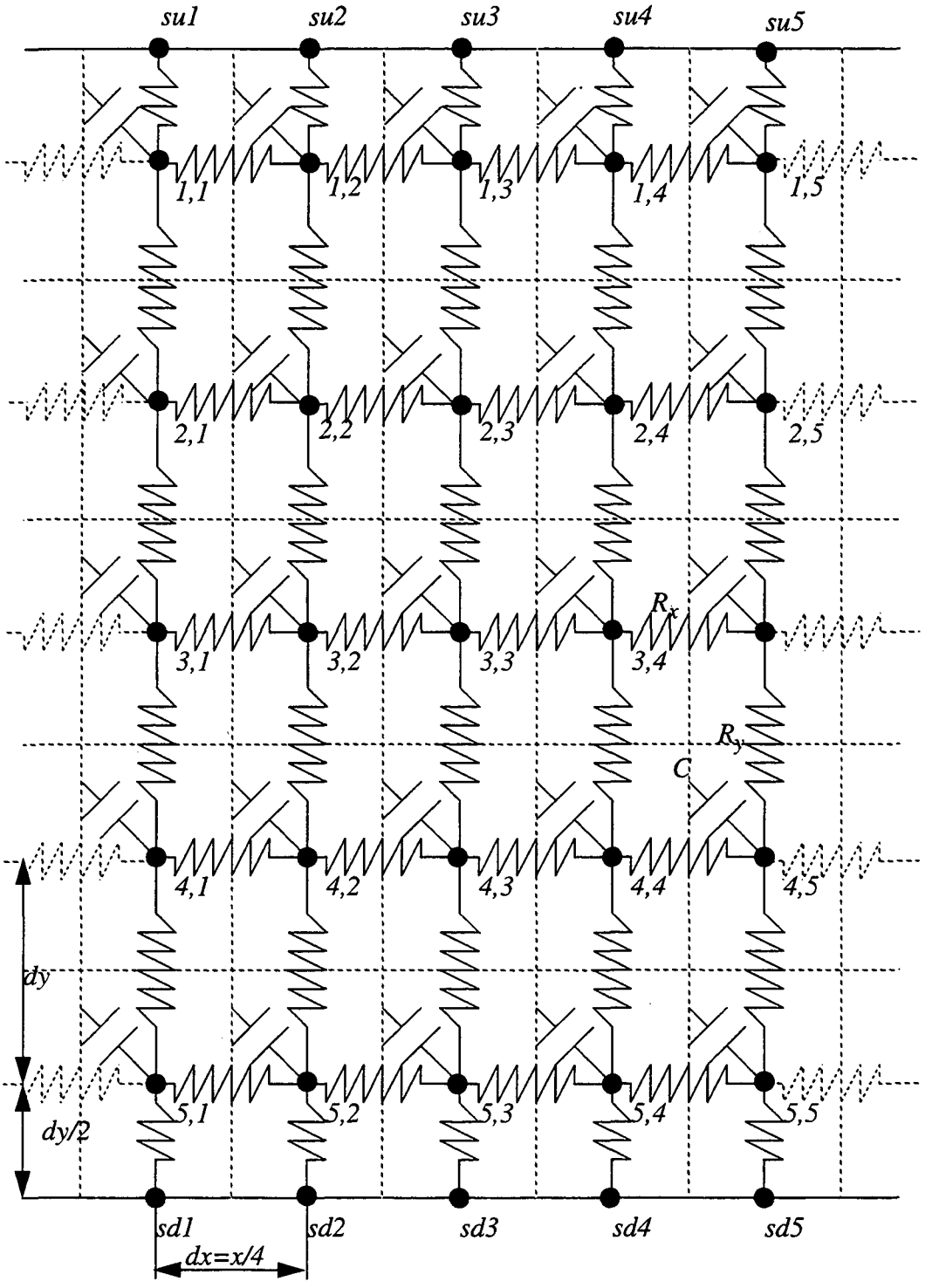

Figure A.13. A 5 x 5 grid. RC equivalent circuit for heat transfer calculations.

The resistances and capacitances in Figures A.12 and A.13 are calculated as

$$R_x = \frac{dx}{kdydz} \tag{A.63}$$

$$R_y = \frac{dy}{kdxdz} \tag{A.64}$$

$$C = \rho c_t \Delta V \tag{A.65}$$

and

$$dx = \frac{distance - between - pipes}{n_x} \tag{A.66}$$

$$dy = \frac{thickness - of - wall}{n_y} \tag{A.67}$$

$$\Delta V = dxdy \times z \tag{A.68}$$

where $dz = z$ is the length of the ceiling. For the case in Figure A.12, the number of "cells" in the x direction is $n_x = 4$, and the number of cells in the y direction is $n_y = 3$. For the case in Figure A.13, $n_x = 4$ and $n_y = 5$.

Note. The discretization over the cross-section of the ceiling is not set rigidly in the SPARK model. While the "box thicknesses", *dx*, are always calculated with (A.66), the "box heights", *dy*, can be input by the user to reflect the structure of the ceiling. *dy* can be different for each box layer, and can represent the thicknesses of the different material layers in the ceiling.

The heat balance at the temperature nodes can be derived by analogy with the one-dimensional situation (equations (A.15)-(A.17)). The heat balance for the interior node (*i,j*) is

$$\frac{T_{i-1,j} - T_{i,j}}{R_{x,i-1}} + \frac{T_{i,j-1} - T_{i,j}}{R_{y,j-1}} = C_i \frac{dT_{i,j}}{dt} + \frac{T_{i,j} - T_{i+1,j}}{R_{x,i+1}} + \frac{T_{i,j} - T_{i,j+1}}{R_{y,j+1}} \tag{A.69}$$

where

$T_{i,j}$ is the temperature at node (*i,j*)

$R_{x,k}$ and $R_{y,k}$ are thermal resistances connecting the node (*i,j*) with the rest of the network, in the *x* and *y* directions, respectively [W/K]

C_i is the capacitance of a cell in row *i* [J/K].

The heat balance for a surface node (i,j) is:

$$Q_{i,j} = \frac{T_{i,j-1} - T_{i,j}}{R_{y,j-1}} \tag{A.70}$$

where

$Q_{i,j}$ is the total heat flux at the surface [W].

A.5.1.4 Test to determine the accuracy of the RC model for two-dimensional heat transfer

The same problem as in Section A.4.2.2 was simulated for the two grid models. The results from the two-dimensional model with the dimensions $dx = 2.5$ cm, $dy = 4$ cm and $z = 10$ m agree with the analytical solution (see Figures A.14 for the results of the 3x5 grid model and A.15 for the results of the 5x5 grid model).

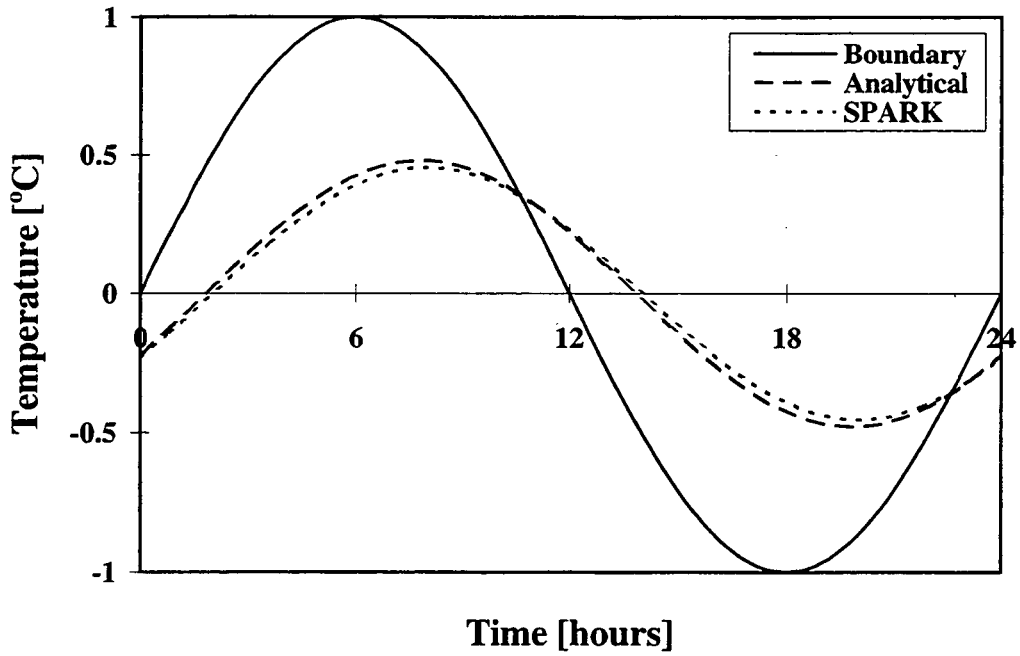

Figure A.14. Temperature at the midpoint of a homogeneous ceiling: comparison between the 3x5 grid SPARK model and the analytical solution.

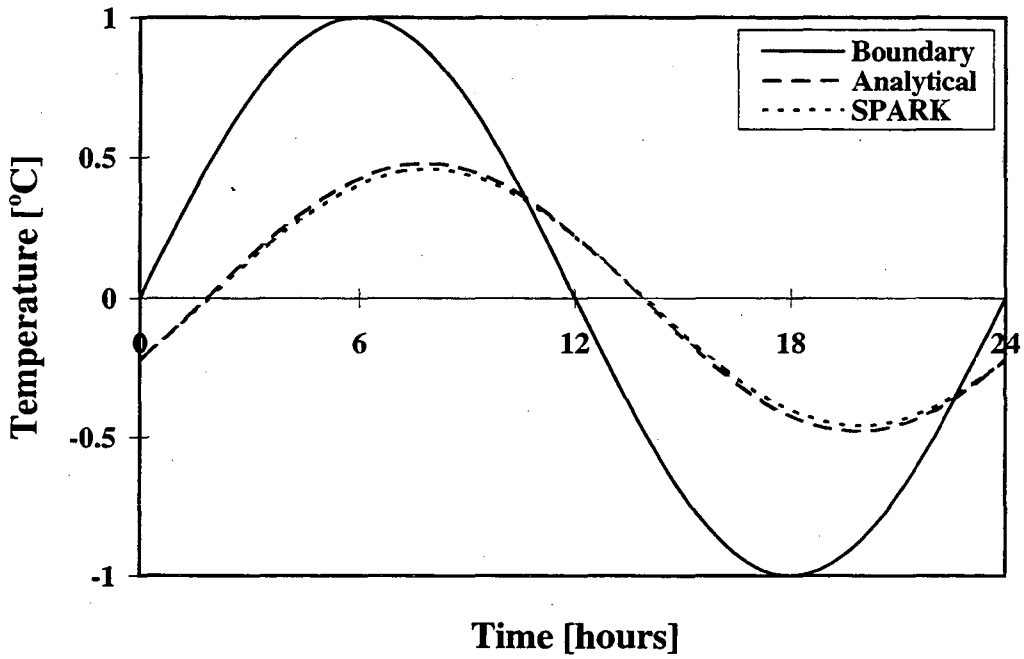

Figure A.15. Temperature at the midpoint of a homogeneous ceiling: comparison between the 5x5 grid SPARK model and the analytical solution.

A.5.2 The two-dimensional SPARK model of the core cooling ceiling

A core cooling ceiling consists of a layer of parallel pipes imbedded in concrete or plaster. Figure A.16 shows the structure of a core cooling ceiling with imbedded pipes.

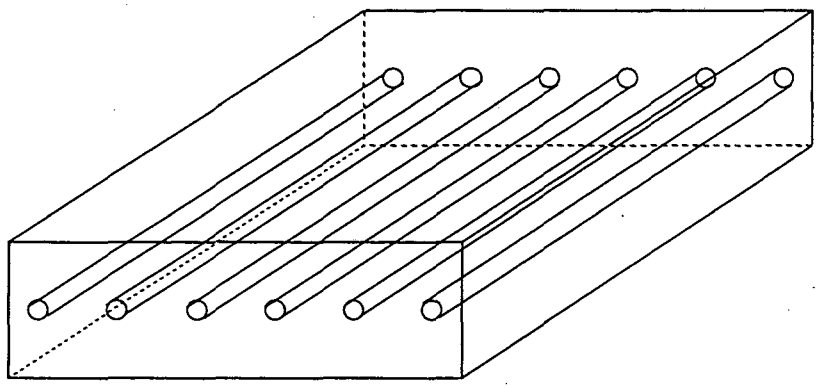

Figure A.16. Structure of a cooled ceiling with imbedded pipes.

The model of a passive two-dimensional ceiling can be easily adapted to reflect the heat transfer through the active core cooling ceiling by declaring the heat transfer between a given pipe and its adjacent grid box as a boundary condition on the grid box.

A.5.2.1 Heat transfer between the pipe and the water when the water is flowing

Consider a water pipe at a given temperature. If water is circulated through the pipe, and if the water temperature is different from the temperature of the pipe, heat is transferred between the pipe and the water. The heat transfer can be expressed as:

$$Q_{convected-water} = hA\,(T_{pipe} - T_{water-average}) \tag{A.71}$$

where

h is the convection heat transfer coefficient [W/m^2-K]

A is the total surface area for the heat transfer [m^2]

T_{pipe} is the pipe temperature [°C]

$T_{water_average}$ is the bulk temperature of the water, defined as the well mixed temperature of the water in the pipe [°C]

$Q_{convected_water}$ is the heat transferred from the pipe into the water [W].

The convection heat transfer coefficient can be expressed in terms of the fluid and flow characteristics as follows [10]:

$$h = \frac{k}{d}Nu \tag{A.72}$$

where

k is the conductivity of the fluid [W/m-K]

d is the pipe diameter [m]

Nu is the Nusselt number for the flow [-].

In the case of fully developed turbulent flow in a smooth pipe, the Nusselt number has the following empirical expression [10]-[11]:

$$Nu = 0.023Re^{0.8}Pr^{n} \tag{A.73}$$

where

Re is the Reynolds number for the flow [-], calculated as

$$Re = \frac{4}{\pi}\frac{\dot{m}}{\mu d} \tag{A.74}$$

and

$\dot{m}$ is the mass flow of the water inside the pipe[kg/s]

μ is the dynamic viscosity of the water [kg/m-s]

d is the pipe diameter [m]

Pr is the Prandtl number of the water [-]

$n = 0.4$ if the water is heated by forced convection, and $n = 0.3$ if the water is cooled by forced convection [12].

The heat convected from the pipe is stored in the water, therefore

$$Q_{stored-water} = \dot{m}_{water} c_{water} (T_{return} - T_{inlet}) \tag{A.75}$$

where

c_{water} is the specific heat of water [J/kg-K]

T_{inlet} is the inlet water temperature

T_{return} is the return water temperature

Q_{stored_water} is the heat stored in the water as a result of the heat transfer [W].

The bulk temperature of the water in equation (A.71) can be calculated as

$$T_{water-average} = \frac{T_{return} - T_{inlet}}{2} \tag{A.76}$$

A.5.2.2 Heat transfer between the pipe and the water when the water is recirculated

In order to provide comfort inside a room cooled by radiant cooling, the cooling system must have some control system. Depending on the inlet water temperature, the thermal mass of the ceiling, and the room loads, circulating the water without interruption might cool the room too much, making it uncomfortable. However, if the water flow is discontinued, or if the temperature of the inlet water is raised, the room will not be cooled as fast, and the chances of creating discomfort are reduced.

When the heat transfer between the room and the water accounts for only a small fraction of the cooling power, water recirculation represents a convenient way in which the

cooling system can adjust its output to meet the room cooling loads. The cold water from the chiller is mixed with warmer return water, with the obvious result that the inlet ceiling water temperature becomes higher than that of the cold water supplied by the chiller. The recirculation of water also provides a way to save chiller power.

Consider that two quantities of water m_{cold} and m_{warm}, at different temperatures T_{low} and T_{high}, are mixed together. This process will result in a quantity of water $m_{total} = m_{cold} + m_{warm}$, with a temperature T_{mix} given by

$$m_{warm} c_{water} (T_{high} - T_{mix}) = m_{cold} c_{water} (T_{mix} - T_{low}) \tag{A.77}$$

where c_{water} is the specific heat of water. The temperature of the water after the mixing process is

$$t_{mix} = \frac{m_{cold} t_{low} + m_{warm} t_{high}}{m_{total}} \tag{A.78}$$

or,

$$t_{mix} = x t_{low} + (1 - x)\, t_{high} \tag{A.79}$$

with the "mixing ratio" expressed as $x = \dfrac{m_{cold}}{m_{total}}$

In the case where water is mixed from two water streams, $\dot{m}_{total} = \dot{m}_{cold} + \dot{m}_{warm}$ and

$$x = \frac{\dot{m}_{cold}}{\dot{m}_{total}}.$$

In the case of a cooled ceiling, the two water streams represent cold water from the chiller and warmer return water. The quantity that is constant is the water flow through the ceiling. In this situation, the mass flows corresponding to the cold and warm water streams must be adjusted to the room conditions at each moment.

The most efficient to make the adjustment is based on knowing the response of the room to a change in inlet water temperature. This type of calibration curve provides a relationship between a given room air temperature and the inlet water temperature which must be supplied in order to remove the room loads. However, extensive measurements are necessary in order to determine the calibration curve. An alternative is to substitute the calibration curve with the "opening characteristic" method, which is not as efficient as the calibration curve method, but is more intuitive and requires less financial investment.

Consider a given room air temperature range that provides occupant comfort. The low end, T_{low_end}, of this range can be then made to correspond to the temperature at which the cooling ceiling starts to function, and the high end, T_{high_end} to a temperature at and above which only unmixed cold water is circulating through the ceiling. The mixing ratio is determined in this case as follows:

- when the room air temperature falls below T_{low_end} a "water switch" stops the water flow; the mixing ratio is zero.

- for room air temperatures above T_{high_end} only cold water is circulated; the mixing ratio is 1.

- for room temperatures between T_{low_end} and T_{high_end} a mixture of cold water and warm return water is circulated; the mixing ratio is between 0 and 1.

In general, if the room air temperature is known and the opening characteristic is linear between T_{low_end} and T_{high_end}, the formula expressing the mixing ratio is:

$$x = \frac{T - T_{low-end}}{T_{high-end} - T_{low-end}} \tag{A.80}$$

where T is equal to

- T_{low_end} if $T_{room_air} < T_{low_end}$
- T_{room_air} if $T_{low_end} < T_{room_air} < T_{high_end}$
- T_{high_end} if $T_{room_air} > T_{high_end}$.

A.5.2.3 Heat transfer between the pipe and the water when the water is stagnant

In the case when the water flow is discontinued, heat from the ceiling is conducted through the pipe and stored in the stagnant water. The heat conducted from the pipe to the stagnant water can be written as

$$Q_{conducted-water} = U_{pipe-water}(T_{pipe} - T_{water-average}) \tag{A.81}$$

where

$U_{pipe\text{-}water}$ is the heat transfer coefficient between the pipe and the water [W/K]

T_{pipe} is the pipe temperature [°C]

$T_{water_average}$ is the average temperature of the water [°C].

The heat conducted from the pipe into the water warms the water:

$$Q_{stored-water} = m_{water} c_{water} \frac{\partial T_{water-average}}{\partial t} \tag{A.82}$$

where

$m_{water} = \rho_{water} V_{pipe}$ is the mass of the water inside the pipe.

A.5.2.4 The two-dimensional model of a cooled ceiling

The theoretical model from section A.5.1.3 can be applied to determine the heat transfer between a cooled ceiling and its surroundings. Figure A.13 shows the 5x5 grid of a RC circuit in which each horizontal layer can have a different material structure. The nodes *vj_i,i+1* are interface nodes between two layers. Only vertical heat flow is modeled at the interfaces, so the heat balance for node *vj_i,i+1* is

$$\frac{T_{i-1,j} - T_{vj-i-1,i}}{\frac{R_{y,i-1,j}}{2}} = \frac{T_{vj-i-1,i} - T_{i,j}}{\frac{R_{y,i,j}}{2}} \tag{A.83}$$

where

$R_{y,i,j}$ is the vertical thermal resistance on column j and in row i.

To model the thermal contact between the ceiling nodes and the water, the exterior of the pipe is considered as having the same temperature as the adjacent ceiling node, while the interior of the pipe is considered as having a temperature equal to the average temperature of the water. Between these two nodes an additional horizontal resistance is introduced, to model the thermal resistance of the pipe itself (see Figure A.17). The additional resistance is a function of the conductivity of the pipe material and reflects the cylindrical symmetry of the pipes:

$$R_{x-pipe-water} = \frac{ln\left(\frac{d_{outside-pipe}}{d_{inside-pipe}}\right)}{2\pi z k_{pipe}} \tag{A.84}$$

where

$d_{outside_pipe}$ is the outside diameter of the cooling pipe [m]

d_{inside_pipe} is the inside diameter of the cooling pipe [m]

z is the total length of the pipe [m]

k_{pipe} is the conductivity of the pipe material [W/m-K].

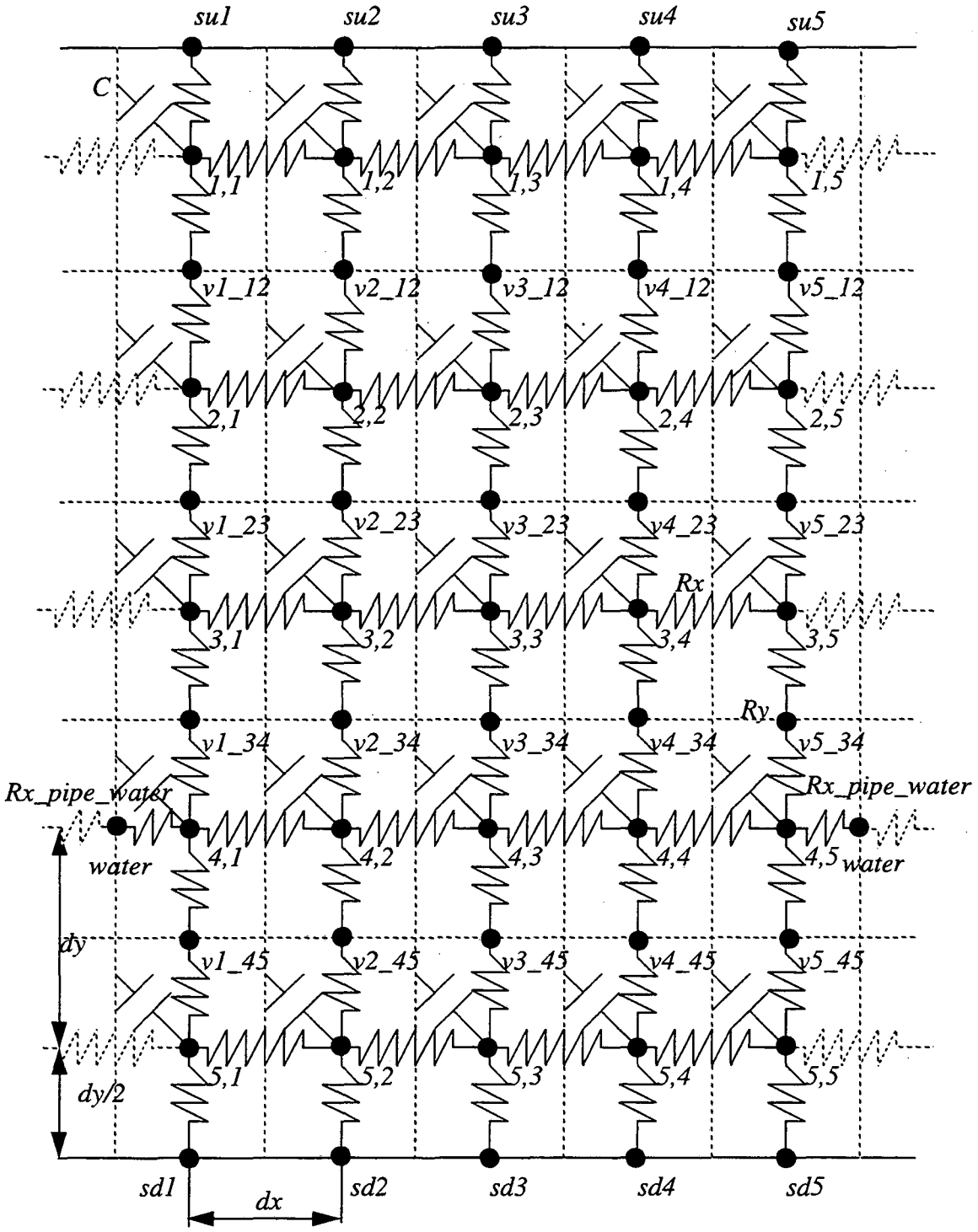

Figure A.17. Equivalent RC circuit for heat transfer calculation in the case of a cooled ceiling.

When the water is flowing, the heat balance at the pipe surface is

$$Q_{conducted-pipe} = Q_{convected-water} = Q_{stored-water} \tag{A.85}$$

where

$$Q_{conducted-pipe} = \frac{T_{wall-node} - T_{pipe}}{R_{x-pipe-water}} \tag{A.86}$$

$Q_{convected_water}$ is given by equation (A.71)

Q_{stored_water} is given by equation (A.75).

In the case where the water flow is zero, the heat balance at the pipe surface is:

$$Q_{conducted-pipe} = Q_{convected-water} = Q_{stored-water} \tag{A.87}$$

where

$Q_{conducted_water}$ is given by equation (A.81)

Q_{stored_water} is given by equation (A.82).

A.5.3 The cooling panel

A different type of radiant cooling system is the cooling panel system. This system is consists of aluminum panels with metal pipes connected to the rear of the panel. When cold water is circulated through the pipes a good thermal contact between the pipes and the panel provides very low resistance to heat conduction. As a result, the surface temperature of the panel is virtually equal to the water temperature. For a given room air temperature, the panel surface can be maintained cold by circulating water through the pipes at a given rate. This system is more efficient than the core cooling system because it can respond virtually instantly to a change in room loads.

A.5.3.1 The model of the cooling panel

Cooling panel heat transfer

Consider a room with a cooling panel system. Figure A.18 shows the placement of the different components.

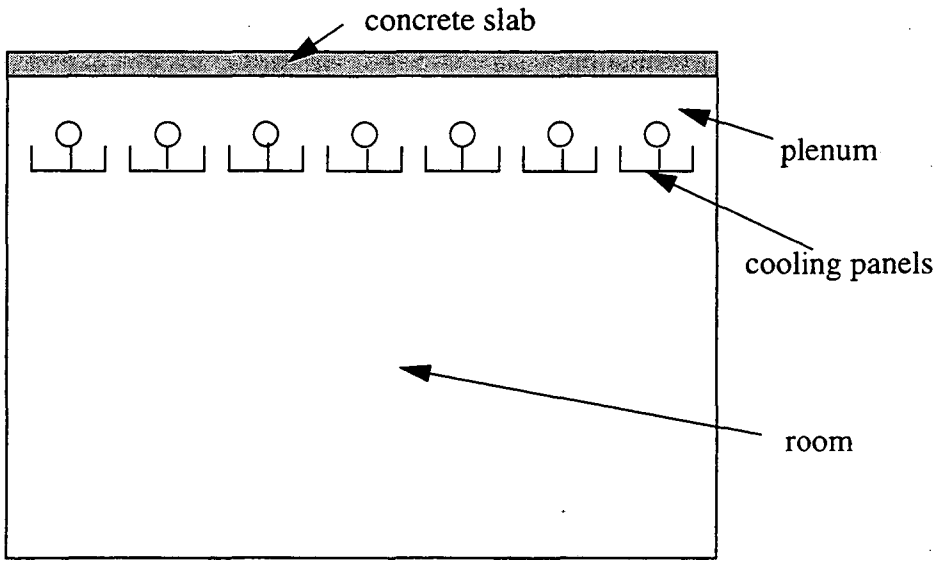

Figure A.18. Layout of a cooling panel system.

The cooling panel exchanges radiation with the other surfaces in the room and with the concrete slab above the plenum. As a result, the room walls, floor, and the plenum slab are cooled. These surfaces will therefore absorb long wave radiation from sources inside the room and will cool the room air by convection. An additional cooling effect is achieved when there is heat exchange between the room air and the plenum air by means of air flow through the interstices between two adjacent panels. In this case, warm room air will rise, will penetrate in the plenum, and will mix with the cooler plenum air.

Heat balance for the cooling panel

Figure A.19 shows the overall heat balance for the cooling panel.

The balance equations are

$$sum-fluxes-room = conv-flux-room + q-lw-room + q-sw-room \quad \text{(A.88)}$$

$$sum-fluxes-plenum = conv-flux-plenum + q\text{–}lw-surf-plenum \quad \text{(A.89)}$$

$$cond-flux-panel-pipe = sum-fluxes-room + sum-fluxes-plenum \quad \text{(A.90)}$$

where

conv_flux_room is the convective flux on the room side of the panel [W/m^2]

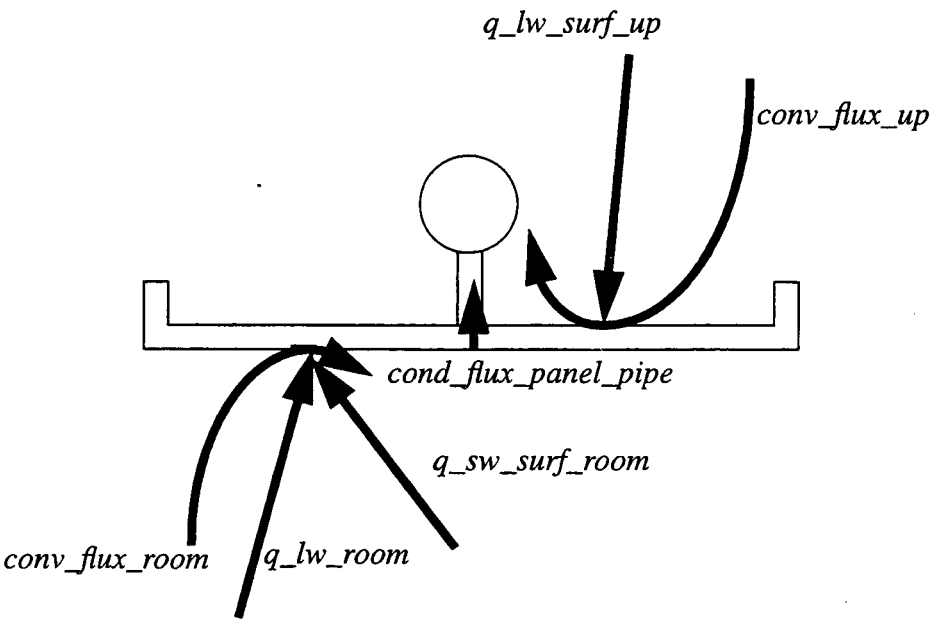

Figure A.19. The heat balance in the case of the cooling panel.

q_lw_room is the long wave flux on the room side of the panel [W/m^2]

q_sw_room is the short wave flux on the room side of the panel [W/m^2]

sum_fluxes_room is the overall flux on the room side of the panel [W/m^2]

conv_flux_plenum is the convective flux on the plenum side of the panel [W/m^2]

q_lw_flux_plenum is the long wave flux on the plenum side of the panel [W/m^2]

sum_fluxes_plenum is the overall flux on the plenum side of the panel [W/m^2]

cond_heat_panel_pipe is the conductive heat flux from the panel to the pipe [W/m^2].

The heat transfer from the pipe to the water is given by

$$Q-cond-pipe-water = A\text{–}panel \times cond-heat-pane-pipe \qquad (A.91)$$

where

Q_cond_pipe_water is the heat conducted into the water [W]

A_panel is the area of the panel [m^2].

The mechanisms by which the heat conducted into the water is removed are the same as those for the concrete core cooling (see sections A.5.2.1 - A.5.2.3).

A.6 Types of Radiant Cooling System Controls

As stated in section A.5.2.2, it is possible to maintain comfort conditions inside a room conditioned by radiant cooling by controlling the water flow in the cooled ceiling. However, core cooling systems have a long heat transfer time constant, and the response of the radiant surface temperature to a change in water temperature and/or water flow is relatively slow. In such a case, a control mechanism is needed that allows the occupant to modify the response of the radiant system to specific building loads. This section presents three mechanisms that are used to control the output of existing radiant cooling systems.

A.6.1 The thermostat-based control

The most common type of control for any air-conditioning system is the thermostat-based control. The air temperature inside the room or inside the return plenum is measured. When the loads cause the temperature to rise above a pre-determined setpoint, cooling is started. When the room temperature drops below the setpoint, cooling is stopped.

In the case of radiant cooling systems, the thermostat-based control is used to start or to stop the flow of cold water (see Figure A.20). The thermostat-based control can be represented by the following algorithm:

$$\dot{m}_{water} = \dot{m}_{design} \text{ if } t_{room-air} \geq t_{setpoint}$$

$$\dot{m}_{water} = 0 \text{ if } t_{room-air} < t_{setpoint} \tag{A.92}$$

The advantage of the thermostat-based control consists of its easy implementation. Its main disadvantage is that it cannot address the problem of the delay of the radiant surface response to a change in the system. The thermostat-based control is therefore more suitable for cooling panel systems. Because a cooling panel system has low thermal mass, it can respond quickly to a change dictated by a thermostat-based control system.

A.6.2 The timer-based control

Another type of control is the timer-based control that causes the cooling system to function according to a pre-determined schedule. Figure A.21 shows a schematic of timer-based control.

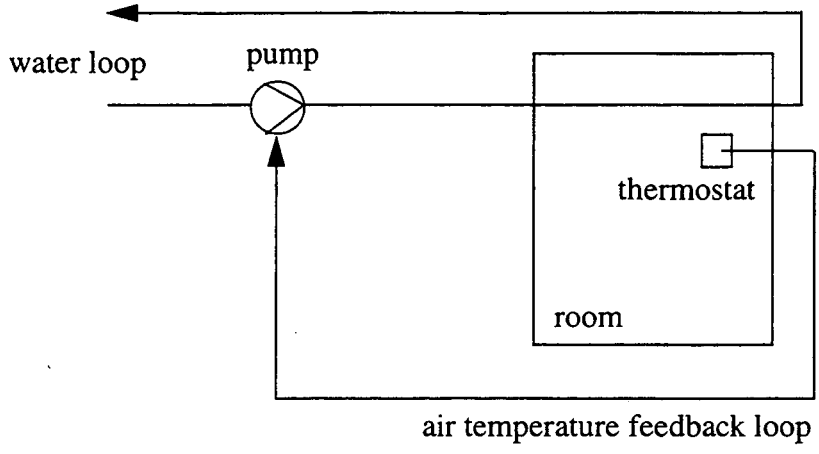

Figure A.20. Thermostat-based control strategy.

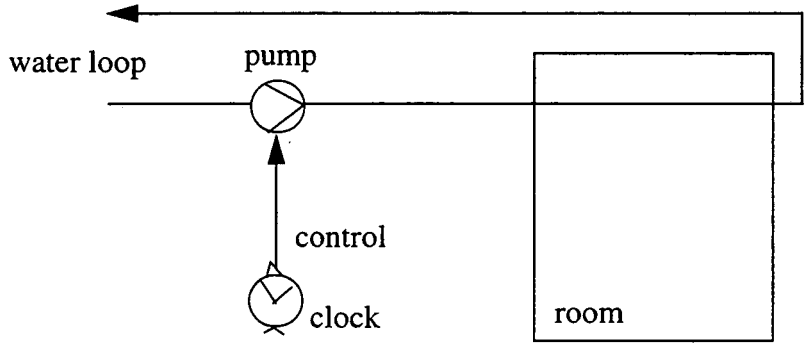

Figure A.21. Timer-based control strategy.

When the response of the building to weather-induced loads and internal loads is known, and the timer-control is done according to this response, the building peak load can be shifted away from its "natural" time of occurrence. For example, if the cooling is done overnight, the time of occurrence of the peak load can be shifted to the evening hours, or even night-time hours.

The timer-based strategy will not, however, respond to rapidly-occurring loads. This observation leads to the conclusion that the timer-based strategy is appropriate only for

certain building types (those with large thermal mass) and certain climates (those with daily temperature amplitudes that are stable over a long period of time).

A.6.3 The hybrid control

The hybrid control is based on the idea of varying the water flow and/or inlet water temperature according to some predetermined information about the cooling system. If the room response to a given change in the operation of the cooling system is known, the system can be operated to "adapt" to the cooling load. If the response of the room is not known, an "opening characteristic" can be used instead (see section A.5.2.2).

One type of a hybrid control strategy for a radiant cooling system is based on adjusting the water inlet temperature to the room load. This control strategy can be achieved by using water recirculation. The ratio of recirculated to total flow is controlled by the room conditions. The schematic of this control strategy is shown in Figure A.22.

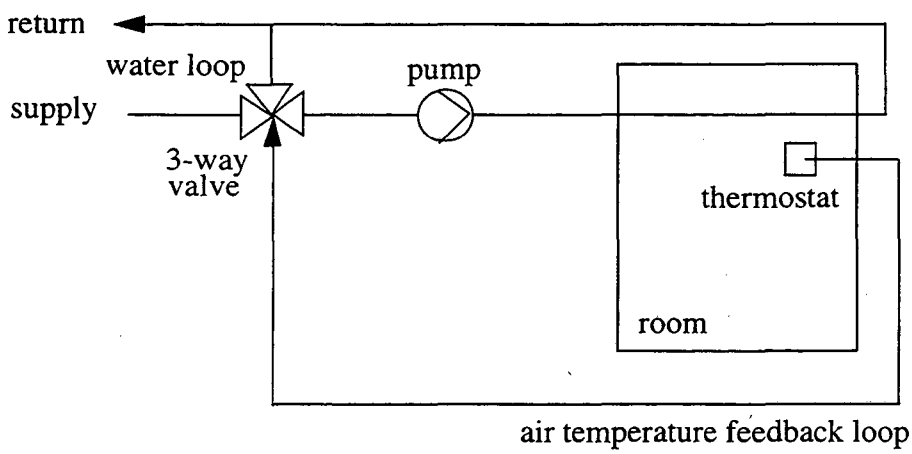

Figure A.22. Hybrid control.

The hybrid control system used in the RADCOOL simulations in Chapter 3 is based on the following formulas:

$$\dot{m}_{inlet} = \dot{m}_{cold} + \dot{m}_{return} \text{ and } T_{inlet} = \frac{\dot{m}_{cold}T_{cold} + \dot{m}_{return}T_{return}}{\dot{m}_{inlet}}$$

where

if $T_{room-air} < T_{setpoint-low}$ then the water flow is stopped, and $\dot{m}_{inlet} = 0$,

If $T_{room-air} \geq T_{setpoint-low}$ then the water flows in the pipes,

$\dot{m}_{cold} = x\dot{m}_{inlet}$, $\dot{m}_{return} = (1-x)\,\dot{m}_{inlet}$, and

$$x = max\left[\frac{T_{room-air} - T_{setpoint-low}}{T_{setpoint-high} - T_{setpoint-low}}, 1\right].$$

In RADCOOL, the temperature interval [$T_{setpoint-low}$, $T_{setpoint-high}$] is required as input.

A.7 The Indoor Air

A.7.1 The air temperature

The indoor air temperature is a function that depends on a large number of parameters. Time, the location inside a space, the thermal properties of air, the nature of the contact between the air and the room envelope surfaces, the presence of an active cooling system, the presence of a ventilation system, space occupancy, and equipment schedules are a few of these parameters. Assuming that the thermal properties of air and the air pressure are constant at any given moment, the room air temperature can be expressed as a function of time and position:

$$T_{air} = T_{air}(x, y, z, t) \tag{A.93}$$

Determining the space-time function for the air temperature is a complicated task. Because of the dependence of the room air temperature on a large number parameters, it is difficult to find a closed form for T_{air}. However, approximate solutions for the air temperature at discrete points can be found.

One way to obtain approximate solutions for the air temperature is to discretize the air domain inside a space and to calculate the mass and heat flows between the subdomains. This procedure constitutes the object of computational fluid dynamics, and is extremely time consuming. Considering the purpose of RADCOOL, it is clear that the interest is not so much in knowing the air temperature at a large number of nodes inside a space, as it is in determining the air temperature at a few points of interest. The "interesting" air temperature points inside a room ar shown in Figure A.23.

The air temperatures shown in Figure A.23 are the following:

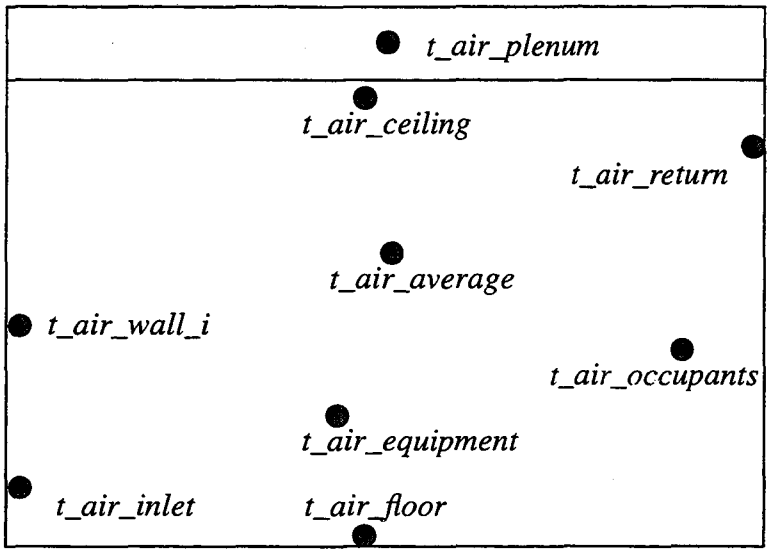

Figure A.23. Air temperatures nodes in a room modeled by RADCOOL.

t_air_inlet is the temperature of the supply air

t_air_average is the air temperature in a room with fully mixed air

t_air_return is the temperature of the air exhausted from the room

t_air_wall_i is the air temperature near wall *i*

t_air_floor is the air temperature near the floor

t_air_ceiling is the air temperature near the ceiling

t_air_occupants is the air temperature near any occupants

t_air_equipment is the air temperature near the equipment

t_air_plenum is the air temperature inside the plenum.

A.7.2 Discretization of the room air domain in RADCOOL

In order to discretize the room air domain some assumptions pertaining to the different air temperatures are necessary. In RADCOOL, each air temperature is expressed as a sum of the temperature of the well-mixed air temperature and a temperature increment:

$$t_{air-wall-i} = t_{air-average} + t_{increment-wall-i} \quad (A.94)$$

$$t_{air-floor} = t_{air-average} + t_{increment-floor} \quad (A.95)$$

$$t_{air-ceiling} = t_{air-average} + t_{increment-ceiling} \quad (A.96)$$

$$t_{air-occupants} = t_{air-average} + t_{increment-occupants} \quad (A.97)$$

$$t_{air-equipment} = t_{air-average} + t_{increment-equipment} \quad (A.98)$$

where *t_increment_...* may be constant, or proportional to the cooling load (see [13]).

In the current version of RADCOOL all the increments are input by the user.

The SPARK calculation of the well-mixed air temperature inside a room is based on heat and moisture balances.

A.7.3 Room air heat balance

The air inside a room exchanges heat with the surfaces in the room envelope (walls and windows), and with people and equipment. The air inside a room can also be heated or cooled by the air that infiltrates, and by the air supplied to the room by the ventilation system. If the room is connected to a plenum, the air inside the room can also be cooled through interaction with the plenum air, if the plenum is cooler than the room.

The heat balance for the room air is described in Figure A.24.

The heat balance corresponding to Figure A.24 is:

$$Q_{cap-air} + Q_{conv-in-tot} = Q_{vent-air-room} + Q_{infil-air-room} - Q_{from-room} + Q_{people} + Q_{equipment} \quad (A.99)$$

where

Q_cap_air is the heat stored in the room air as a result of the heat transfer [W]

Q_conv_in_tot is the total convective heat generated by lights and equipment and lost to the room envelope [W]

Q_vent_air_room is the heat brought into the room by the ventilation system [W]

Q_infil_air_room is the heat brought into the room by air infiltration [W]

Q_conv_from_room is the heat lost by the room to the colder plenum [W]

Q_people is the sensible and latent (convective) heat generated by room occupants [W].

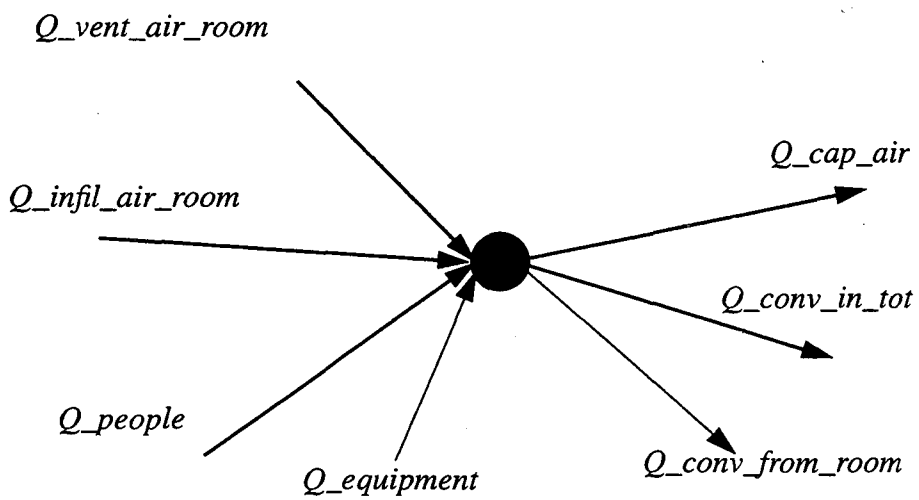

Figure A.24. Heat balance for the room air.

The heat balance is applied to a control volume with a boundary identical with the room envelope boundary. The SPARK algorithms used to calculate the heat terms in equation (A.99) are the following.

Q_cap_air_room

This term represents the heat stored in the room air:

$$Q_{cap-air-room} = \rho_{air} V_{room} c_{p-air} \frac{\partial T_{air-average}}{\partial t} \tag{A.100}$$

where

$T_{air_average}$ is the absolute temperature of the room air [K]

w_{room_air} is the room air humidity ratio [kg of vapor/ kg of dry air]

V_{room} is the room volume [m^3]

ρ_{room_air} is the room air density [kg/m^3], calculated as

$$\rho_{room-air} = \frac{0.62\,(1 + w_{room-air})\,p_{air}}{287.5\,(0.62 + w_{room-air})\,T_{air-average}} \tag{A.101}$$

and

p_{air} is the air pressure inside the room [N/m^2]

c_{p_air} is the specific heat of the room air, [J/kg-K], calculated as (see [14]):

$$c_{p-air} = (1 - w_{room-air})\, c_{p-dry-air} + w_{room-air} c_{p-vapor} \tag{A.102}$$

where

$c_{p_dry_air}$ is the specific heat of dry air, considered constant and equal to 1006 J/kg-K

c_{p_vapor} is the specific heat of water vapor, considered constant and equal to 1805 J/kg-K.

Q_conv_in_tot

This term represents the heat lost by the room air to the room envelope, through convective heat transfer. The convective heat flux at each of the room surfaces is described in section A.4.3.1.

To conveniently use the fluxes (A.23), the convective heat in equation (A.99) is calculated as the sum of all the heat fluxes lost to all the wall surfaces (see section A.4.3.1), multiplied by the respective surface areas, plus the heat losses to the occupants and the equipment (including lights) in the room:

$$Q_{conv-in-tot} = \sum_i A_{in-i} q_{conv-in-i} + Q_{conv-occupants} + Q_{conv-equipment} \tag{A.103}$$

Q_vent_air_room

This term corresponds to the heat added to the room air by ventilation air (or air-conditioning, in the case of an all-air system). Considering that the density and pressure of the air is constant at a given moment, and neglecting the influences of differences in velocities and potential energy of the air flow domain, the ventilation heat term in the room air heat balance is expressed as [15]:

$$Q_{vent-air-room} = \dot{m}_{vent-air-flow} c_{p-air} (t_{inlet} - t_{air-average}) \tag{A.104}$$

where

$\dot{m}_{vent-air-flow}$ is the mass flow of the ventilation air [kg/s].

Q_infil_air_room

This term corresponds to the heat added to the room air by air infiltration. Based on the same assumptions as in the section about ventilation heat, the infiltration term in the

room heat balance is:

$$Q_{infil-air-room} = \dot{m}_{infil-air-flow} c_{p-air} (t_{air-out} - t_{air-average}) \qquad (A.105)$$

where

$\dot{m}_{infil-air-flow}$ is the mass flow of the infiltration air [kg/s].

It is generally difficult to obtain realistic infiltration data. Special computer programs, such as COMIS [16] address this problem in detail. Although several straightforward approaches have been found to estimate the air flow due to infiltration (see below), it is questionable whether the results obtained by using these approaches are accurate.

Infiltration air flow is proportional to the air change rate: this method assumes that the mass flow due to infiltration is proportional to the ventilation air flow. This is approach is very convenient because the air supplied by the ventilation system is generally known. However, this method fails for residential buildings.

DOE-2 Methodology: DOE-2 [6] users can select one of three different approaches to be used in the building simulation: no infiltration, the air change method, and the residential building method.

The "no infiltration" method ignores the influence of infiltration on the thermal balance of the building.

The "air change" method requires user input for the infiltration air flow. The infiltration air flow in this case is either constant, or corrected for the influence of wind speed near the building.

The "residential building" method considers that the infiltration air flow has a linear dependence of the wind speed near the building, and of the temperature difference between the interior and the exterior of the building. This method requires the user to provide the coefficients in the linear function.

From A Database: this method requires the program to access a database at each time step, provide data regarding the indoor and outdoor conditions, and extract the infiltration flow rates corresponding to those conditions. If the database has been obtained from calculations with programs designed especially for the modeling of infiltration (for example COMIS), this method can provide the most accurate results.

Due to the limitations of SPARK, the RADCOOL user must provide information regarding the infiltration air flow at each time step. Consequently, the user must specify the infiltration air flow as an input.

Q_conv_from_room

This term represents the heat transferred from the room to the plenum.

Consider the case where the room and plenum air have different temperatures. If the two spaces communicate, and if the room air is warmer than the plenum air, convection will cause mass and heat exchange between the room and the plenum. If the room air is colder than the plenum air, thermal stratification stops the mass and heat exchange.

This situation is analogous to Epstein's work on "air flow through horizontal openings" [17]. Epstein identifies four different regimes that depend on $\frac{L}{D}$, where L is the depth of the opening and D is the diameter of the opening.

In the case of a cooled panel, the opening area through which this air exchange takes place is the total "interstitial area" in the panel-covered ceiling. The existence of the interstitial area may be either due to the imperfect coverage of the ceiling with panels, or intentionally created by the system designer.

Consider a room with a 4 m x 5 m ceiling. The ceiling of the room could be covered with panels that are 20 cm thick and 5 m long. In this case the total crack length can be calculated as:

$$length_{crack} = \left(1 + \frac{width_{ceiling}}{width_{panel}}\right) length_{ceiling} = 105m \tag{A.106}$$

Assuming that the interstices are 3 mm wide, the total interstitial area is

$$area_{crack} = length_{crack} width_{crack} = 0.32m^2 \tag{A.107}$$

which gives a "lumped diameter"

$$D = \sqrt{\frac{4}{\pi} area_{crack}} = 0.63m \tag{A.108}$$

If the vertical depth of the crack is L = 1 cm (equal to the thickness of the panels), the ratio $\frac{L}{D}$ = 0.015. This corresponds to Epstein's Regime I, in which $\frac{L}{D} < 0.1$. According to

Epstein, this regime is governed by a Taylor instability in which the room air and panel air intrude into each other in the interstitial zone, leading to an oscillatory exchange. The regime is characterized by a constant dimensionless Froude number, and the air flow rate between the room and plenum depends only on the densities (or the temperatures) of the air in the room and plenum. According to Epstein, the fluid volume ratio in Regime I is:

$$\dot{V} = 0.04 D^{\frac{5}{2}} \left(g \frac{\Delta\rho}{\bar{\rho}}\right)^{\frac{1}{2}} \tag{A.109}$$

where

g is the acceleration due to gravity, 9.81 m/s^2

$\Delta\rho$ is the difference in density between the two fluids

$\bar{\rho}$ is the average density of the two fluids [kg/m^3].

Assuming that the fluid exchange takes place at constant pressure (a good approximation for the case of room-plenum air exchange), equation (A.109) is equivalent to

$$\dot{V} = 0.04D^{\frac{5}{2}}\,(g\frac{-\Delta T}{\bar{T}}) \tag{A.110}$$

where

ΔT is the temperature difference between the room air and plenum air; the minus sign indicates that the flow occurs from the colder to the warmer zone.

$\bar{T}$ is the average between the room and plenum air temperatures.

Equation (A.110) can be used to determine the heat flow between the room and the plenum due to the air exchange, given by

$$Q_{conv-heat-from-room} = \rho_{air}\dot{V}c_{air}\,(T_{room} - T_{plenum}) \text{ if } T_{room} \geq T_{plenum} \text{ and}$$

$$Q_{conv-heat-from-room} = 0 \text{ if } T_{room} < T_{plenum}. \tag{A.111}$$

Q_people

This term represents the heat generated by the occupants in the room:

$$Q_{people} = Q_{sensible} + Q_{latent} + \{Respiration, Conduction, Transpiration\} \tag{A.112}$$

In equation (A.112), $Q_{sensible}$ and Q_{latent} are calculated as in DOE-2 [6]. The expression for $Q_{sensible}$ is:

$$Q_{sensible} = 0.293\,\{A_s + \left[B_s\,(\frac{9}{5}t_{dry-air} + 32)\right]\} \tag{A.113}$$

where

$t_{dry\text{-}air}$ is the dry-bulb temperature of the room air (denoted so far by $t_{air_average}$)

A_s and B_s are given by

$$A_s = 28 + 909.6Q_m - 119.5Q_m^2 \tag{A.114}$$

$$B_s = 1.2 - 100.48Q_m + 1.49Q_m^2 \tag{A.115}$$

and

Q_m is the heat gain due to the metabolic rate of the room occupants [W]:

$$Q_m = number_{occupants}\bar{A}_{occupant}(metabolic - rate) \tag{A.116}$$

In equation (A.116)

$A_{occupant}$ is the average body area given by the Dubois empirical equation:

$$\bar{A}_{occupant} = 0.203W^{0.425}H^{0.725} \tag{A.117}$$

where

W is the weight of the person [kg]

H is the height of the person [m].

The metabolic rate is usually expressed in *met* units (1 met = 58.15 W/m^2). The metabolic rate depends on the air temperature around a person, on the person's clothing and on the type of activity that the person performs [7].

The expression for Q_{latent} is:

$$Q_{latent} = 0.293\,\{A_l + \left[B_l(\frac{9}{5}t_{dry-air} + 32)\right]\} \tag{A.118}$$

with

$$A_l = 206 - 733.8Q_m + 160.9Q_m^2 \tag{A.119}$$

$$B_l = -6.7 + 15.16Q_m - 2.558Q_m^2 \tag{A.120}$$

Equations (A.113) and (A.118) give $Q_{sensible}$ and Q_{latent} in units of [W]. The respiration, conduction and transpiration terms in equation (A.112) are neglected in RADCOOL.

A.7.4 Plenum air heat balance

The plenum air interacts by convection with the back surface of the panel and with the ceiling surface. The plenum air can also be heated or cooled by the room air that enters the plenum. The heat balance for the plenum air is analogous to that for the room air (see Figure A.24):

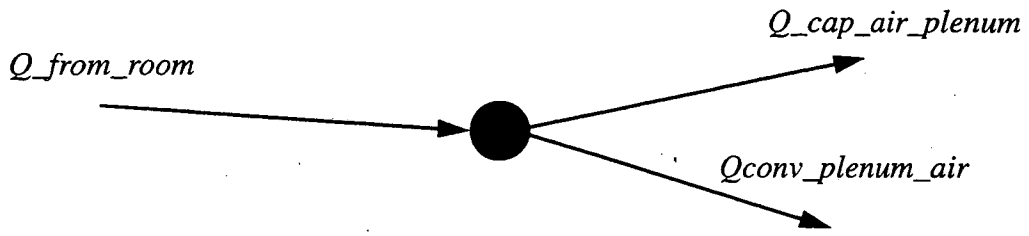

Figure A.25. Heat balance for the plenum air.

The heat balance equation for the plenum air is:

$$Q_{from-room} = Q_{cap-air-plenum} + Q_{conv-plenum-air} \tag{A.121}$$

where

Qcap_air_plenum is the heat stored in the plenum air as a result of the heat transfer [W]

Qconv_plenum_air is the total convective heat lost to the plenum surfaces [W]

Q_conv_from_room is the heat lost by the room to the colder plenum [W].

The heat balance is applied to a control volume whose boundary corresponds to the interior surfaces of the plenum. The algorithms to calculate the terms in equation (A.121) are similar to the ones described in section A.7.3.

The term representing the heat infiltrated from the room is the same (equations (A.106) - (A.111)).

In the case of the heat storage term, the only difference is that instead of room air quantities, equations (A.100) - (A.102) should be based on the specific heat, density, etc. corresponding to the plenum air.

The convection term in the plenum air balance can be calculated with the equation

$$Q_{conv-plenum-air} = \sum_i A_{in-i} q_{conv-in-i} \tag{A.122}$$

where the products in the right-hand side are calculated for all the surfaces inside the plenum.

A.7.5 Room air moisture balance

Moisture can be added to the room air by the supply air, the infiltration air, internal sources such as people, cooking, etc., and desorption from the internal surfaces of the room. Moisture leaves the room air in the exhaust air and through adsorption in the internal surfaces of the room. The balance equation for the room air humidity ratio, w_{room}, can be written as:

$$V_{room}\frac{dw_{room}}{dt} = \dot{v}_{vent}(w_{vent} - w_{room}) + \dot{v}_{infil}(w_{out} - w_{room}) + \frac{Q_{latent}}{\rho_{room}\lambda} + \frac{1}{\rho_{room}}W \tag{A.123}$$

where

V_{room} is the room volume [m^3]

w_{room} is the room air humidity ratio [kg vapor/kg dry air]

$\dot{v}_{vent}$ is the ventilation air volume flow [m^3/s]

$\dot{v}_{infil}$ is the infiltration air volume flow [m^3/s]

w_{vent} is the ventilation air humidity ratio [kg vapor/kg dry air]

w_{out} is the outside air humidity ratio [kg vapor/kg dry air]

Q_{latent} is the latent heat production by people in the room [W], and can be calculated with equation (A.118)

ρ_{room} is the density of the room air [kg/m^3]

λ is the latent heat of vaporization for water [J/kg]

W is the rate of vapor adsorption/desorption on the walls [kg/s].

In RADCOOL, the rate of vapor adsorption/desorption is calculated based on the Cunningham theory of water sorption on building materials.

The main assumption in the Cunningham theory ([18] - [20]) is that the flux of water vapor through the surface of a wall is due to the difference in partial pressures between the wall material and the room air:

$$W = A_w h (p_w - p_{0w}) \tag{A.124}$$

where

A_w is the wall area involved in moisture exchange [m^2]

h is the moisture transfer coefficient under partial pressure forces [s/m]

p_w is the partial pressure of vapor inside the wall material [N/m^2]

p_{0w} is the partial pressure of vapor in the room air [N/m^2].

The moisture balance inside the wall material can be written as:

$$V_w \frac{dm_w}{dt} = -W \tag{A.125}$$

where

V_w is the wall volume involved in moisture exchange [m^3]

m is the mass of water found in the unit volume of wall material [kg/m^3].

It is obvious that equations (A.123) and (A.125) are coupled. Since there are no moisture sources inside a typical wall construction, the vapor sorption process is driven by the time variation of the moisture in the room air.

In practice, the humidity ratio of the room air can be roughly represented as having a cyclic variation with a given period (typically 24 h). The sorption process is therefore also periodic. Based on this observation, and on the slow character of moisture diffusion through a wall material, Cunningham [21] assumes that the wall volume involved in moisture exchange, V_w, represents only a small fraction of the wall volume. V_w can most conveniently be estimated using the "effective penetration depth theory" [22]. The effective penetration depth is defined as the wall depth reached by the moisture diffusion process under transient and cyclic conditions. V_w thus becomes:

$$V_w = d_{eff} A_w \tag{A.126}$$

where

d_{eff} is the effective penetration depth of the wall material [m].

Cunningham [21] shows that the effective penetration depth of a wall exposed to moisture variations on only one side can be calculated as:

$$d_{eff} = 2\sqrt{\frac{D_w}{2\omega}} = \sqrt{\frac{D_w T}{\pi}} \tag{A.127}$$

where

D_w is the water-vapor-in-wall-material diffusion coefficient [m^2/s]

ω is the frequency of variation of the room air humidity ratio [s^{-1}]

T is the period of variation of the room air humidity ratio (usually equal to 24 h) [s].

If the wall is exposed to moisture variation on both sides, the effective penetration depth is

$$d_{eff} = \frac{l}{3} \tag{A.128}$$

where

l is the thickness of the wall [m].

Generally, the sorption properties of building materials are communicated in the form of sorption curves. According to Cunningham [19] the sorption curves can be used in the calculation of W as follows. The partial pressure of vapor inside the wall material (see equation (A.124)) can be calculated as:

$$p_w = km \tag{A.129}$$

where

$$k = \frac{d(RH)}{d(MC)} \frac{p_{0w,sat}}{\rho_{wall}} \tag{A.130}$$

RH is the relative humidity of the room air [-]

MC is the moisture content of the wall material [kg water/kg dry wall material]

$d(RH)/d(MC)$ is the slope of the sorption curve [-]

$p_{0w,sat}$ is the saturation partial pressure of water vapor in the room air [N/m^2]

ρ_{wall} is the density of the wall material [kg/m^3]

and

$$m = (MC)\,\rho_{wall} \tag{A.131}$$

The partial pressure of water vapor in the room air (see equation (A.124)) can be calculated based on the relative humidity as:

$$p_{0w} = (RH)\, p_{0w,\,sat} \tag{A.132}$$

The substitution of equations (A.129) - (A.132) in (A.124) leads to the following expression for W:

$$W = A_w h \left[\frac{d(RH)}{d(MC)} (MC) - (RH) \right] p_{0w,\,sat} \tag{A.133}$$

By substituting equation (A.131) in the left-hand side of equation (A.125), the balance equation for the vapor content of the wall becomes:

$$V_w \frac{dMC}{dt} = -\frac{1}{\rho_{wall}} W \tag{A.134}$$

The sorption curves for a number of building materials are provided in [23]. These curves have the analytical form

$$ln\,(MC - MC_0) = A + B ln\,[\,(0.01RH)^{-c} - 1] \tag{A.135}$$

where

MC, MC_0 and RH are expressed as percentages

A, B and c are material-specific coefficients [-].

Equation (A.135) allows the calculation of the slope $d(RH)/d(MC)$ as:

$$\frac{d(RH)}{d(MC)} = -\frac{100}{Bc} \times \frac{(0.01RH)^{-c-1}}{(0.01RH)^{-c} - 1} \times \frac{1}{exp\,\{A + B ln\,[\,(0.01RH)^{-c} - 1]\,\}} \tag{A.136}$$

Table A.1 contains the material-specific coefficients for some building materials.

Equation (A.130), expressing k as a function of the sorption curve slope, is correct in the approximation that the sorption curve is a line passing through the origin. For higher values of the RH, this approximation is obviously false. However, for high values of the RH, equation (A.130) can be replaced with:

$$k = \left(\frac{RH}{MC}\right) \frac{p_{0w,\,sat}}{\rho_{wall}} \tag{A.137}$$

TABLE A.1 Material-specific coefficients occurring in equation (A.136)[23].

Material	ρ [kg/m^3]	A	B	c	MC_0 [%]
Pine wood	530	2.97	-0.170	4.48	0
Hardboard	950	2.57	-0.160	4.50	0
Particle board	630	2.83	-0.195	3.50	0
Urea foam	10	3.31	-0.194	3.75	0
Fiberglass	17	1.59	-0.156	3.33	0
Asbestos cement	1310	2.03	-0.174	5.37	0
Concrete block	1580	0.841	-0.195	3.24	0
Brick	2020	1.02	-0.256	2.28	0
Limestone	1590	-1.21	-0.305	1.37	0
Gypsum plaster	740	1.784	-0.0492	7.134	8.65
Fibrous plaster	850	2.140	-0.0437	7.529	16.47

where the fraction *RH/MC* can be calculated using equation (A.135):

$$\frac{RH}{MC} = \frac{RH}{exp\,\{A + Bln\,[\,(0.01RH)^{-c} - 1]\,\}} \tag{A.138}$$

Where *RH* is expressed in %.

RH/MC as expressed in (A.138) is only a function of *RH*, and is therefore straightforward to calculate for a given *RH* if the coefficients *A*, *B* and *c* of the sorption curve are known.

The coefficient of moisture transfer under partial pressure forces in equations (A.124) and (A.133) is defined as:

$$h = \frac{h_m}{\dfrac{RT_{air,\,room}}{M_{vapor}}} \tag{A.139}$$

where

R is the universal gas constant [J/kmol-K]

$T_{air,room}$ is the absolute room air temperature [K]

M_w is the molecular weight of water vapor [kg/kmol]

h_m is the mass transport coefficient under concentration gradient forces [m/s].

According to the Lewis theory of convection, h_m can be calculated as:

$$h_m = \frac{h_{conv}}{\rho_{air} c_{p,air} (Le)^{\frac{2}{3}}} \tag{A.140}$$

where

h_{conv} is the convection film coefficient [W/m^2-K]

$c_{p,air}$ is the specific heat of air under constant pressure [J/kg-K]

Le is the Lewis number of air

$$Le = \frac{\alpha}{D} \tag{A.141}$$

α is the air heat diffusion coefficient [m^2/s]

D is the water-vapor-in-air diffusion coefficient [m^2/s].

As an example, for air at 25 °C and a convection coefficient of 3.25 W/m^2-K, h_m is 3.03x10^{-3} m/s, and h is 2.2x10^{-8} s/m.

The diffusion coefficient can be calculated based on the vapor permeability of the wall material. The permeability is defined as:

$$\mu = -\frac{g}{\frac{dP}{dx}} \tag{A.142}$$

where

μ is the permeability of the material [kg/m-s-Pa] = [s]

g is the mass flux of water into the material [kg/m^2-s]

P is the partial vapor pressure inside the material [N/m^2]

x is the distance inside the material where P is measured [m].

Based on the permeability of the material, the material water-vapor-diffusion coefficient can be calculated [24] as:

$$D_w = \mu \frac{p_{0w,sat}}{\rho_{wall} \frac{d(MC)}{d(RH)}} \tag{A.143}$$

Introducing (A.130) in (A.143) leads to

$$D_w = \mu k \tag{A.144}$$

Tviet [25] measured the variation in permeability due to changes in the relative humidity of the room air. The permeability variation with relative humidity can be expressed as:

$$\mu = exp\,(f_0 + f_1 RH + f_2 RH^2) \tag{A.145}$$

where f_0, f_1 and f_2 are material-specific coefficients (see Table A.2).

TABLE A.2 Material-specific coefficients occurring in equation (A.145) [25].

Material	f_0	f_1	f_2
Pine wood	-28.71886	-0.1194911	4.158788
Hardboard	-26.62005	-0.3730495	1.386730
Particle board	-25.32247	0.0357264	0.781466
Urea foam	-23.72120	0.9761170	-0.2620779
Fiberglass	-22.67872	0.	0.
Asbestos cement	-25.35854	-0.2456131	1.526852
Concrete block	-27.78411	-0.1738898	1.451546
Brick	-24.98131	0.	0.
Limestone	-26.12126	0.0790142	0.9812424
Gypsum plaster	-26.08942	-0.3126156	2.503194
Fibrous plaster	-26.72177	0.7450913	0.5223077

Table A.3 contains the permeability, diffusion coefficient and effective penetration depth for different materials. The data corresponds to a *RH* of 50% and an air temperature of 25 °C. Data referring to the permeability curves of materials can also be found in [26].

Thomas and Burch [27] present experimental data regarding the moisture content of two building materials, and computer simulation efforts to model the results of their asymptotic-type experiments.

In order to evaluate the model presented in this section, an effort was made to simulate the results obtained by Thomas and Burch in their experiments. During the process of modeling, however, it became clear that the effective penetration depth theory is appropriate for asymptotic-type experiments only if the calculated effective depth is equal to, or larger than the material thickness. In the cases where this condition does not apply, a multiple-node model is necessary.

TABLE A.3 Permeability, diffusion coefficient, and effective penetration depth of different materials [25].

Material	μ [10^{12} kg/m-s-Pa]	k [m^2/s^2]	D_w [10^{10} m^2/s]	d_{eff} [10^3 m]
Pine wood	0.898	32.3	0.29	0.89
Hardboard	3.22	27.7	0.89	1.56
Particle board	12.5	31.2	3.90	3.27
Urea foam	76.1	1204.3	916.4	50.2
Fiberglass	141.0	4642.9	6546.5	134.1
Asbestos cement	12.5	31.7	3.96	3.30
Concrete block	1.13	92.9	1.05	1.70
Brick	14.1	54.4	7.67	4.59
Limestone	6.01	564.3	33.91	9.66
Gypsum plaster	7.47	129.7	9.69	5.16
Fibrous plaster	4.11	83.1	3.41	3.06

The multiple-node model can be formulated similarly to the Thomas and Burch model [27]. For a two-node model, the balance equations are:

$$V_{eff}\frac{dMC_{eff}}{dt} + \frac{1}{\rho_{wall}}W_{eff} = \frac{1}{\rho_{wall}}W_{deep} \tag{A.146}$$

and

$$V_{deep}\frac{dMC_{deep}}{dt} = -\frac{1}{\rho_{wall}}W_{deep} \tag{A.147}$$

where

V_{eff} is the volume of the effective layer, given by (A.126) [m^3]

V_{deep} is the volume of the material less the volume of the effective layer [m^3]

W_{eff} is the flux of water vapor leaving the material, described by (A.133) [kg/s]

W_{deep} is a similar flux of water vapor, occurring inside the material [kg/s].

$$W_{deep} = \rho_w A_w D_w \frac{MC_{deep} - MC_{eff}}{d_{deep}} \tag{A.148}$$

and

d_{deep} is the thickness of the material less the thickness of the effective layer [m].

It is obvious that for $d_{deep} \rightarrow \infty$, $d_{eff} \rightarrow d_{material}$, $W_{deep} \rightarrow 0$, and (A.146) becomes (A.134).

In the present version, RADCOOL performs air moisture calculations based on the two-node model for the wall (equations (A.146)-(A.147)), and on the moisture balance described in equation (A.123).

A.8 Linking Objects

The class of components entitled "linking objects" is composed of the objects that connect the other classes of components together. In the present version of RADCOOL there are four types of linking objects:

- the total convective heat for the air heat balance (equation (A.103))
- the air temperatures in the vicinity of the room surfaces (equations (A.94) - (A.98))
- the total short wave radiation entering the room through transparent surfaces (equation (A.44)), and
- the long wave radiation between the interior room surfaces (equations (A.41) - (A.43)).

It is obvious that the specific content and size of each of the linking objects depend on the number of surfaces defined in a particular room. The SPARK programs corresponding to these linking objects must be "customized" to fit each particular situation. For this reason, the SPARK programs corresponding to linking must be created in the preliminary data processing phase of RADCOOL. However, once created, these linking programs can be saved in the SPARK library, and can be reused whenever a new situation occurs that involves a room layout similar to a situation already examined in the past.

A.9 Tasks Performed in the "Preliminary Data Processing" Section

A.9.1 Data collection

The first task performed in the "preliminary data processing" section is the acquisition of information about the building to be modeled. At the end of this task, the collected data should provide a unique description of the building to be modeled.

Relevant data include:

- the characteristics of the building: number, type (passive, radiant), and position of walls, number and position of windows, types and positions of floors, etc.
- the characteristics of the building site: location and orientation of the building, and weather information (solar radiation, outside air temperature, ground temperature, wind, etc.)
- occupancy and equipment schedules: number of occupants, types of activities performed, equipment installed in the building, etc.
- the air flow characteristics (ventilation flow rate and supply temperature, infiltration flow rate)
- the HVAC system characteristics (thermostat setpoints, etc.)
- the quantities that the user desires as a result of the calculation.

After this information has been collected, the user must convert it into input for the SPARK program. Some data, such as the thermal properties of building materials, the hourly weather data, etc. may be available in databases. Other data, such as shape factors and weather-dependent thermal properties, must be calculated. The remainder of this section will describe the procedures presently used in RADCOOL to calculate shape factors and weather-related inputs.

A.9.2 Weather-related data

Weather-related quantities that are required as input include primary weather data (such as ambient drybulb and dew-point temperatures), soil temperature, and cloud cover. These quantities can usually be found in the weather file corresponding to a particular site. Other weather-related data must be calculated. These data include:

- the outside surface convective film coefficient h_{conv_out} of each exterior wall; h_{conv_out} depends on the outside temperature, the exterior surface temperature, the wind speed and direction, etc.; in RADCOOL this value is currently obtained by performing a DOE-2 calculation at the same location and printing the DOE-2 hourly output for the convection film coefficient.
- the sky emissivity ε_{sky}, which depends on the outside air dew-point temperature and on the sky cover (equation (A.25)).
- the direct and diffuse solar radiation incident on each exterior surface, which depend on the position of the Sun, on cloud cover, and on the orientation of the surface; in RADCOOL these values are currently obtained from DOE-2 hourly output.

• the solar absorptivity of each glazing layer, and the overall solar transmittance of each window, which depend on the glazing type, the window orientation, and the position of the Sun; in RADCOOL these values are currently obtained from DOE-2 hourly output.

In order to offer an idea about the complexity of the weather-related calculations, the next section describes the algorithm used in DOE-2 for the calculation of the direct and solar radiation incident on an exterior surface.

A.9.2.1 Algorithms to calculate the direct and diffuse solar radiation on a surface

Among other quantities, a typical weather file includes the following hourly measured data: direct normal solar radiation, diffuse horizontal solar radiation, and global horizontal solar radiation. As stated in section A.4.3.3, in order to perform a heat balance calculation for an exterior surface, the user must supply information about the direct and diffuse solar radiation incident on the surface. The following algorithms describe the calculations performed to obtain the direct and diffuse solar radiation incident on a surface with an arbitrary orientation from the data supplied by a typical weather file. These algorithms are used in DOE-2, and are based on [28].

Weather file quantities

The values used in the calculation are the direct normal solar radiation, I_{DN}, and the total horizontal solar radiation, I_{tH}, as reported in the typical weather file.

Solar position-related quantities

The calculation of direct and diffuse irradiance on a surface with an arbitrary orientation requires inputs related to the following sun-related quantities: the apparent solar time and the solar angles with respect to the given surface.

a. Apparent solar time

The apparent solar time depends on the local civil time, the geographical position of the building site, and the fluctuations in the velocity of the Earth [28], according to

$$AST = LST + ET + 4\,(LSM - LON) \tag{A.149}$$

where

AST is the apparent solar time [hours]

LST is the local standard time [hours]

ET is the value of the equation of time for the day of the year when the calculation is made [hours]

LSM is the local standard time meridian [degrees of an arc]

LON is the local longitude [degrees of an arc]

4 is the number of minutes it takes the Earth to rotate 1° of an arc.

According to [6], ET can be developed in a Fourier series as a function of the day of the year, *n*:

$$ET = A_0 + A_1 \cos W + A_2 \cos 2W + A_3 \cos 3W + B_1 \sin W + B_2 \sin 2W + B_3 \sin 3W \tag{A.150}$$

with

$$W = \left(\frac{2\pi}{365}\right) n \tag{A.151}$$

The coefficients in (A.151) are given in Table A.4.

TABLE A.4 Coefficients for equation (A.150) [6].

A_0	A_1	A_2	A_3	B_1	B_2	B_3
0.000696	0.00706	-0.0533	-0.00157	-0.122	-0.156	-0.00556

b. Solar angles

The position of the sun with respect to the site is usually described by the solar altitude β, and solar azimuth ϕ, measured from the south. The solar azimuth is positive for afternoon hours and negative for morning hours. Both these angles depend on the solar declination δ, the hour angle *H*, and the latitude *L*, according to:

$$\sin\beta = \cos L \cos\delta \cos H + \sin H \sin\delta \tag{A.152}$$

$$\cos\phi = \frac{\sin\beta \sin L - \sin\delta}{\cos\beta \cos L} \tag{A.153}$$

Consider a surface with azimuth Ψ measured from south and a tilt angle Σ. The surface solar azimuth γ, is defined as:

$$\gamma = \phi - \Psi \tag{A.154}$$

If $90° < \gamma < 270°$, the surface is in shadow.

The angle of incidence ϑ, of direct radiation on the surface is defined as the angle between the normal to the surface and the ray from the surface to the sun. The angle ϑ is given by

$$\cos\vartheta = \cos\beta\cos\gamma\sin\Sigma + \sin\beta\cos\Sigma \tag{A.155}$$

Direct solar radiation incident on a surface with an arbitrary orientation

The direct solar radiation I_D, incident on a surface depends on the direct normal solar radiation, I_{DN}, and on the angle of incidence, ϑ:

$$I_D = I_{DN}\cos\vartheta, \text{ if } \cos\vartheta > 0$$

$$I_D = 0, \text{ if } \cos\vartheta \leq 0 \tag{A.156}$$

Diffuse solar radiation incident on a surface with an arbitrary orientation

The diffuse solar radiation, I_d, is the sum of diffuse ground-reflected radiation, I_{dg}, and diffuse sky radiation, I_{ds}.

$$I_d = I_{dg} + I_{ds} \tag{A.157}$$

A simple expression for I_{ds} is

$$I_{ds} = CI_{DN}F_{sky} \tag{A.158}$$

where

F_{sky} is the sky form factor (A.26), with $\Phi_{wall} = \Sigma$.

Similarly, I_{dg} is given by

$$I_{dg} = I_{th}\rho_g F_{ground} \tag{A.159}$$

where

ρ_g is the ground reflectance

F_{ground} is the ground form factor (A.29), with $\Phi_{wall} = \Sigma$.

In equations (A.158) and (A.159) C is the sky diffusion factor:

$$C = A_0 + A_1\cos W + A_2\cos 2W + A_3\cos 3W + B_1\sin W + B_2\sin 2W + B_3\sin 3W \tag{A.160}$$

with W calculated as in equation (A.151).

The coefficients in (A.160) are given in Table A.5.

TABLE A.5 Coefficients for equation (A.160) [6].

A_0	A_1	A_2	A_3	B_1	B_2	B_3
0.0905	-0.041	0.0073	0.0015	-0.0034	0.0004	-0.0006

For vertical surfaces, it is possible to express the diffuse radiation in terms of the total horizontal solar radiation, I_{tH}:

$$I_d = YI_{tH} \tag{A.161}$$

where the factor Y can be written as:

$$Y = 0.55 + 0.437\cos\vartheta + 0.313\,(\cos\vartheta)^2 \qquad \text{if } \cos(\vartheta) > -0.2$$

$$Y = 0.45 \qquad \text{if } \cos\vartheta \leq -0.2 \tag{A.162}$$

A.9.3 Surface-to-surface shape factors

As stated in section A.4.4.2, every surface in an enclosure exchanges long wave (IR) radiation with the other surfaces in the enclosure. The net long wave radiation absorbed by surface i in an N-surface enclosure is given by equations (A.41) - (A.43). This section describes the calculation of the shape factors F_{ij}.

The shape factor F_{ij} between surface i and surface j represents the fraction of the total long wave radiation emitted by surface i that is incident on surface j. In an N-surface enclosure, the shape factors depend only on the geometry of the surfaces. The general equation for F_{ij} for surfaces i and j having the areas A_i and A_j respectively, is [9]:

$$F_{ij} = \frac{1}{A_i}\int_{A_i}\int_{A_j}\frac{\cos\theta_i\cos\theta_j}{\pi S^2}dA_i dA_j \tag{A.163}$$

where

S is the distance between a point on i and a point on j

θ_i is the angle between the normal on surface i and the line connecting surfaces i and j

θ_j is the angle between the normal on surface j and the line connecting surfaces i and j.

The integral in the right hand side of (A.163) is not always easy to calculate. In the case of rectangular surfaces, the shape factors can be calculated through shape factor algebra. Shape factor algebra provides relationships between analytically calculated shape factors corresponding to a given relative position of two surfaces, and shape factors corresponding to another given relative position of two surfaces [9].

The simplest relative positions in which two rectangular surfaces can be found in a building are (see Figure A.26)

- parallel to each other, and
- making a 90° angle with each other.

Solving equation (A.163) for these two relative positions yields exact solutions for the shape factors F_{12} and F_{21}. For example, in the case of two walls making a 90° angle, F_{12} can be calculated as [9]:

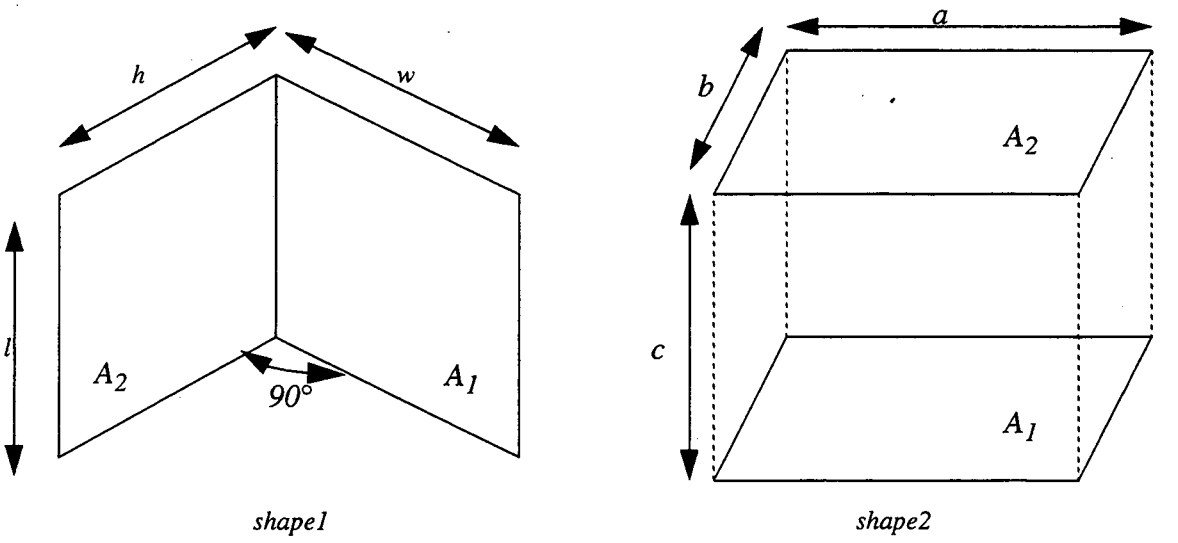

Figure A.26. Relative positions of two rectangular surfaces that give exact solutions for the shape factors.

$$F_{12} = \frac{1}{\pi W}(term_1 - term_2) \tag{A.164}$$

where

$$term_1 = W\text{atan}\frac{1}{W} + H\text{atan}\frac{1}{H} - \sqrt{H^2 + W^2}\,\text{atan}\frac{1}{\sqrt{H^2 + W^2}} \tag{A.165}$$

$$term_2 = \frac{1}{4} ln\,\{\frac{(1 + W^2)\,(1 + H^2)}{1 + W^2 + H^2} term_3\} \tag{A.166}$$

$$term_3 = \left[\frac{W^2\,(1 + W^2 + H^2)}{(1 + W^2)\,(W^2 + H^2)}\right]^{W^2} \left[\frac{H^2\,(1 + H^2 + W^2)}{(1 + H^2)\,(H^2 + W^2)}\right]^{H^2} \tag{A.167}$$

$$H = \frac{h}{l} \tag{A.168}$$

$$W = \frac{w}{l} \tag{A.169}$$

In the case of two parallel walls, F_{12} can be calculated as:

$$F_{12} = \frac{2}{\pi XY}(term_4 + term_5) \tag{A.170}$$

where

$$term_4 = ln\left[\frac{(1 + X^2)\,(1 + Y^2)}{1 + X^2 + Y^2}\right]^{\frac{1}{2}} - X\text{atan}X - Y\text{atan}Y \tag{A.171}$$

$$term_5 = X\sqrt{1 + Y^2}\,\text{atan}\frac{X}{\sqrt{1 + Y^2}} + Y\sqrt{1 + X^2}\,\text{atan}\frac{Y}{\sqrt{1 + X^2}} \tag{A.172}$$

$$X = \frac{a}{b} \tag{A.173}$$

$$Y = \frac{c}{b} \tag{A.174}$$

Once the shape factor F_{12} has been calculated, F_{21} can be calculated by using the basic relationship of shape factor algebra:

$$F_{ji} = \frac{A_i}{A_j} F_{ij} \tag{A.175}$$

Another useful relationship of shape factor algebra describes the long wave radiation exchange between two surfaces when one of the surfaces is subdivided in two or more sub-surfaces (see Figure A.27).

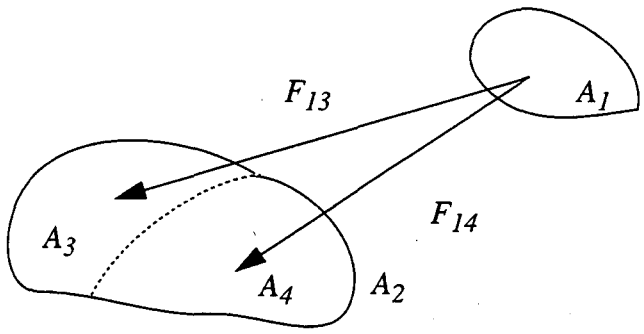

Figure A.27. Radiation exchange between finite areas with one area subdivided.

Consider an arbitrary area A_1 exchanging radiation with a second area A_2. The shape factor F_{12} is the fraction of the total radiation emitted by A_1 that is incident on A_2. If A_2 is divided into two parts, A_3 and A_4, the fraction of the total energy leaving A_1 that is incident on A_3 and the fraction of the total energy leaving A_1 that is incident on A_4 must add up to F_{12}. Therefore

$$F_{12} = F_{13} + F_{14} \tag{A.176}$$

To calculate the shape factors between arbitrarily located rectangles, both integration and shape factor algebra are necessary.

In RADCOOL, the shape factor calculations are performed by using a TRNSYS subroutine [29]. The TRNSYS subroutine calculates shape factors for all the surfaces that form an enclosure. The input information required by this subroutine refers to the relative positioning of the surfaces inside the enclosure.

A.10 References

1. Edward F. Sowell, W. F. Buhl, A. E. Erdem, and F. C. Winkelmann, *A prototype object-based system for HVAC simulation*. Proc. Second Int. Conf. System Simulation in Buildings, Liège, Belgium, 1986. Rep. LBNL-22106.

2. Fred Buhl, E. Erdem, J.-M. Nataf, F. C. Winkelmann, M. Moshier and E. Sowell, *Advances in SPARK*. Proc. Third Int. Conf. System Simulation in Buildings, Liège, Belgium, 1994. Rep. LBNL-29419.

3. H. S. Carslaw and J. C. Jaeger, *Conduction of heat in solids*. Clarendon Press, Second edition, Oxford, 1978.

4. Joseph H. Klems, *U-Values, solar heat gain and thermal performance: recent studies using the MoWiTT*. Rep. LBL-25487, 1989. Revised, Mo-254.

5. *TARP Reference manual*. NBSIR 83-2655, 1981.

6. Simulation Research Group (LBL) and Group Q-11 (LANL), *DOE-2 Engineering manual*. Rep. LBNL-11353, 1982.

7. P. O. Fanger, *Thermal comfort*. McGraw-Hill, New York, 1970.

8. B. F. Raber and F. W. Hutchinson, *Panel heating and cooling analysis*. John Wiley, New York, 1947.

9. R. Siegel and J. R. Howell, *Thermal radiation heat transfer*. Second Edition, Hemisphere Publishing Corporation, 1981.

10. Jack P. Holman, *Heat transfer*. Seventh Edition, McGraw-Hill, New York, 1990.

11. Frank P. Incropera and D. P. Dewitt, *Fundamentals of heat and mass transfer - third edition*. New York: Wiley, 1990.

12. R. W. Shoemaker, *Radiant heating*. McGraw-Hill, Second Edition, New York, 1954.

13. C. Q. Chen and J. Van der Kooi, *Accuracy - a program for combined problems of energy analysis, indoor air flow and air quality*. ASHRAE Trans. (94) 1988.

14. R. Brandemuehl, S. Gabel, and I. Andresen, *A toolkit for secondary HVAC system energy calculations*. Prepared for ASHRAE, University of Colorado at Boulder, 1993.

15. H. D. Baehr, *Thermodynamik*. 7th Edition, Springer Verlag, 1989.

16. Helmut E. Feustel and A. Rayner-Hooson, Ed., *COMIS Fundamentals*. Rep. LBNL-28560, 1990.

17. M. Epstein, *Buoyancy-driven exchange flow through small openings in horizontal partitions*. Trans. of the ASME, Journal of Heat Transfer, (110) 1988.

18. M. J. Cunningham, *A new analytical approach to the long term behavior of moisture concentrations in building cavities - I. Non-condensing cavity*. Building and Environment, (18) (3) 1983.

19. M. J. Cunningham, *Further analytical studies of building cavity moisture concentrations*. Building and Environment, (19) (1) 1984.

20. M. J. Cunningham, *The moisture performance of framed structures - a mathematical model*. Building and Environment, (23) (2) 1988.

21. M. J. Cunningham, *Effective penetration depth and effective resistance in moisture transfer*. Building and Environment, (27) (3) 1992.

22. A. Kerestecioglu, M. Swami and A. Kamel, *Theoretical and computational investigation of simultaneous heat and moisture transfer in buildings: "effective penetration depth" theory.* ASHRAE Trans., (96) (1) 1990.

23. M. J. Cunningham and T.J. Sprott, *Sorption properties of New Zealand building materials.* Research Report R43, Building Research Association of New Zealand, Judgeford, 1984.

24. D. M. Burch, W.C. Thomas and A.H. Fanney, *Water vapor permeability measurements of common building materials.* ASHRAE Transactions, (98) (2) 1992.

25. A. Tviet, *1966 Measurements of moisture sorption and moisture permeability of porous materials.* Rep. Norwegian Building Research Institute - 45, Oslo, 1966.

26. R. R. Zarr, D.M. Burch and A.H. Fanney, *Heat and moisture transfer in wood-based wall construction: measured versus predicted.* NIST Building Science Series 173, 1995.

27. W. C. Thomas and D.M. Burch, *Experimental validation of a mathematical model for predicting water vapor sorption at interior building surfaces.* ASHRAE Transactions, (96) (1) 1990.

28. ASHRAE Handbook, *Fundamentals.* American Society for Heating, Refrigeration and Air-Conditioning Engineers, Inc., Atlanta, 1993.

29. Solar Energy Laboratory, *TRNSYS, a transient simulation program. Reference manual.* University of Wisconsin, Madison, 1994.

Appendix B

ENERGY CONSUMPTION AND PEAK POWER DEMAND OF THE RADIANT COOLING AND ALL-AIR SYSTEMS: RESULTS OF THE PARAMETRIC STUDY

TABLE B.1. Energy Consumption and Peak Power Demand in New Orleans. SW orientation, new building construction.

	RC system continuous ventilation	All-air system continuous ventilation	RC system no ventilation at night	All-air system no ventilation at night
Results for the typical week:				
Air sensible energy [kWh_{th}]	14.8	64.7	11.8	63.6
Air latent energy [kWh_{th}]	34.6	35.5	21.7	24.3
Water sensible energy [kWh_{th}]	34.1	-	34.7	-
Chiller energy [kWh_e]	27.8	33.4	22.7	29.3
Fan energy [kWh_e]	1.3	5.7	1.0	7.3
Pump energy [kWh_e]	0.2	-	0.2	-
Weekly energy consumption [kWh_e]	29.3	39.1	23.9	36.6
Results for the week of system peak:				
Peak load components				
Air sensible [kW_{th}]	0.30	1.44	0.33	1.38
Air latent [kW_{th}]	0.69	0.51	0.54	0.63
Water sensible [kW_{th}]	0.78	-	0.93	-
Fan and pump [kW_e]	0.03	0.19	0.03	0.19
Peak load [kW_e]	0.62	0.84	0.63	0.86

TABLE B.2. Energy Consumption and Peak Power Demand in Cape Hatteras. SW orientation, new building construction.

	RC system continuous ventilation	All-air system continuous ventilation	RC system no ventilation at night	All-air system no ventilation at night
Results for the typical week:				
Air sensible energy [kWh_{th}]	8.0	55.0	6.3	55.4
Air latent energy [kWh_{th}]	29.0	30.5	17.5	18.5
Water sensible energy [kWh_{th}]	33.2	-	33.7	-
Chiller energy [kWh_e]	23.4	28.5	19.2	24.6
Fan energy [kWh_e]	1.3	5.2	1.0	6.7
Pump energy [kWh_e]	0.2	-	0.2	-
Weekly energy consumption [kWh_e]	24.9	33.7	20.4	31.3
Results for the week of system peak:				
Peak load components				
Air sensible [kW_{th}]	0.30	1.41	0.27	1.47
Air latent [kW_{th}]	0.75	0.69	0.75	0.69
Water sensible [kW_{th}]	0.90	-	0.93	-
Fan and pump [kW_e]	0.03	0.19	0.03	0.20
Peak load [kW_e]	0.68	0.89	0.68	0.92

TABLE B.3. Energy Consumption and Peak Power Demand in New York City. SW orientation, new building construction.

	RC system continuous ventilation	All-air system continuous ventilation	RC system no ventilation at night	All-air system no ventilation at night
Results for the typical week:				
Air sensible energy [kWh_{th}]	4.6	36.9	4.5	40.6
Air latent energy [kWh_{th}]	6.2	6.5	5.1	5.7
Water sensible energy [kWh_{th}]	32.4	-	33.7	-
Chiller energy [kWh_e]	14.4	14.5	14.4	15.4
Fan energy [kWh_e]	1.3	4.7	1.0	6.1
Pump energy [kWh_e]	0.2	-	0.2	-
Weekly energy consumption [kWh_e]	15.9	19.2	15.6	21.5
Results for the week of system peak:				
Peak load components				
Air sensible [kW_{th}]	0.30	1.23	0.30	1.17
Air latent [kW_{th}]	0.45	0.45	0.45	0.54
Water sensible [kW_{th}]	0.81	-	0.84	-
Fan and pump [kW_e]	0.03	0.15	0.03	0.16
Peak load [kW_e]	0.55	0.71	0.56	0.73

TABLE B.4. Energy Consumption and Peak Power Demand in Fort Worth. SW orientation, new building construction.

	RC system continuous ventilation	All-air system continuous ventilation	RC system no ventilation at night	All-air system no ventilation at night
Results for the typical week:				
Air sensible energy [kWh_{th}]	12.2	65.1	8.8	64.5
Air latent energy [kWh_{th}]	29.3	33.1	17.8	20.7
Water sensible energy [kWh_{th}]	33.8	-	34.5	-
Chiller energy [kWh_e]	25.1	32.7	20.4	28.4
Fan energy [kWh_e]	1.3	5.4	1.0	7.4
Pump energy [kWh_e]	0.2	-	0.2	-
Weekly energy consumption [kWh_e]	26.6	38.1	21.6	35.8
Results for the week of system peak:				
Peak load components				
Air sensible [kW_{th}]	0.39	1.62	0.39	1.68
Air latent [kW_{th}]	0.33	0.30	0.33	0.48
Water sensible [kW_{th}]	1.02	-	1.05	-
Fan and pump [kW_e]	0.03	0.18	0.03	0.18
Peak load [kW_e]	0.61	0.82	0.62	0.90

TABLE B.5. Energy Consumption and Peak Power Demand in Chicago. SW orientation, new building construction.

	RC system continuous ventilation	All-air system continuous ventilation	RC system no ventilation at night	All-air system no ventilation at night
Results for the typical week:				
Air sensible energy [kWh_{th}]	6.0	49.2	4.9	51.6
Air latent energy [kWh_{th}]	7.2	8.3	4.1	5.3
Water sensible energy [kWh_{th}]	34.4	-	34.8	-
Chiller energy [kWh_e]	15.9	19.2	14.6	18.6
Fan energy [kWh_e]	1.3	6.8	1.0	8.2
Pump energy [kWh_e]	0.2	-	0.2	-
Weekly energy consumption [kWh_e]	17.4	26.0	15.8	26.8
Results for the week of system peak:				
Peak load components				
Air sensible [kW_{th}]	0.33	1.32	0.33	1.32
Air latent [kW_{th}]	0.36	0.51	0.42	0.48
Water sensible [kW_{th}]	0.96	-	0.93	-
Fan and pump [kW_e]	0.03	0.14	0.03	0.16
Peak load [kW_e]	0.58	0.75	0.59	0.76

TABLE B.6. Energy Consumption and Peak Power Demand in Boston. SW orientation, new building construction.

	RC system continuous ventilation	All-air system continuous ventilation	RC system no ventilation at night	All-air system no ventilation at night
Results for the typical week:				
Air sensible energy [kWh_{th}]	4.0	34.4	3.5	37.6
Air latent energy [kWh_{th}]	2.9	3.0	1.9	2.3
Water sensible energy [kWh_{th}]	32.8	-	32.9	-
Chiller energy [kWh_e]	13.3	12.5	12.8	13.1
Fan energy [kWh_e]	1.3	4.9	1.0	6.1
Pump energy [kWh_e]	0.2	-	0.2	-
Weekly energy consumption [kWh_e]	14.8	17.4	14.0	19.2
Results for the week of system peak:				
Peak load components				
Air sensible [kW_{th}]	0.33	1.50	0.33	1.53
Air latent [kW_{th}]	0.36	0.36	0.36	0.36
Water sensible [kW_{th}]	0.96	-	0.99	-
Fan and pump [kW_e]	0.03	0.19	0.03	0.19
Peak load [kW_e]	0.58	0.81	0.59	0.82

TABLE B.7. Energy Consumption and Peak Power Demand in San Jose, CA. SW orientation, new building construction.

	RC system continuous ventilation	All-air system continuous ventilation	RC system no ventilation at night	All-air system no ventilation at night
Results for the typical week:				
Air sensible energy [kWh_{th}]	7.7	45.2	6.9	47.9
Air latent energy [kWh_{th}]	5.8	5.7	4.9	5.4
Water sensible energy [kWh_{th}]	33.9	-	34.0	-
Chiller energy [kWh_e]	15.8	17.0	15.3	17.8
Fan energy [kWh_e]	1.3	5.2	1.0	6.2
Pump energy [kWh_e]	0.2	-	0.2	-
Weekly energy consumption [kWh_e]	17.3	22.2	16.5	24.0
Results for the week of system peak:				
Peak load components				
Air sensible [kW_{th}]	0.36	1.44	0.36	1.50
Air latent [kW_{th}]	0.60	0.60	0.63	0.60
Water sensible [kW_{th}]	0.87	-	0.87	-
Fan and pump [kW_e]	0.03	0.17	0.03	0.18
Peak load [kW_e]	0.64	0.85	0.65	0.88

TABLE B.8. Energy Consumption and Peak Power Demand in Phoenix. SW orientation, new building construction.

	RC system continuous ventilation	All-air system continuous ventilation	RC system no ventilation at night	All-air system no ventilation at night
Results for the typical week:				
Air sensible energy [kWh_{th}]	22.4	101.3	15.8	98.7
Air latent energy [kWh_{th}]	3.4	3.5	2.8	2.9
Water sensible energy [kWh_{th}]	52.9	-	53.9	-
Chiller energy [kWh_e]	26.2	34.9	24.2	33.9
Fan energy [kWh_e]	1.3	8.3	1.0	10.0
Pump energy [kWh_e]	0.2	-	0.2	-
Weekly energy consumption [kWh_e]	27.7	43.2	25.4	43.9
Results for the week of system peak:				
Peak load components				
Air sensible [kW_{th}]	0.27	2.16	0.33	2.25
Air latent [kW_{th}]	0.42	0.18	0.39	0.18
Water sensible [kW_{th}]	1.23	-	1.23	-
Fan and pump [kW_e]	0.03	0.25	0.03	0.28
Peak load [kW_e]	0.67	1.03	0.68	1.09

TABLE B.9. Energy Consumption and Peak Power Demand in Scottsbluff. SW orientation, new building construction.

	RC system continuous ventilation	All-air system continuous ventilation	RC system no ventilation at night	All-air system no ventilation at night
Results for the typical week:				
Air sensible energy [kWh_{th}]	5.6	46.4	4.9	48.9
Air latent energy [kWh_{th}]	0.6	0.4	0.5	0.3
Water sensible energy [kWh_{th}]	34.1	-	34.2	-
Chiller energy [kWh_e]	13.4	15.6	13.2	16.4
Fan energy [kWh_e]	1.3	7.4	1.0	8.5
Pump energy [kWh_e]	0.2	-	0.2	-
Weekly energy consumption [kWh_e]	14.9	23.0	14.4	24.9
Results for the week of system peak:				
Peak load components				
Air sensible [kW_{th}]	0.30	1.68	0.30	1.68
Air latent [kW_{th}]	0.30	0.21	0.30	0.24
Water sensible [kW_{th}]	1.08	-	1.11	-
Fan and pump [kW_e]	0.03	0.22	0.03	0.22
Peak load [kW_e]	0.59	0.85	0.60	0.86

TABLE B.10. Energy Consumption and Peak Power Demand in Salt Lake City. SW orientation, new building construction.

	RC system continuous ventilation	All-air system continuous ventilation	RC system no ventilation at night	All-air system no ventilation at night
Results for the typical week:				
Air sensible energy [kWh_{th}]	4.5	64.5	3.9	66.1
Air latent energy [kWh_{th}]	0.0	0.0	0.0	0.0
Water sensible energy [kWh_{th}]	51.6	-	51.7	-
Chiller energy [kWh_e]	18.7	21.5	18.5	22.0
Fan energy [kWh_e]	1.3	8.9	1.0	9.7
Pump energy [kWh_e]	0.2	-	0.2	-
Weekly energy consumption [kWh_e]	20.2	30.4	19.7	31.7
Results for the week of system peak:				
Peak load components				
Air sensible [kW_{th}]	0.36	1.86	0.36	1.92
Air latent [kW_{th}]	0.00	0.00	0.00	0.00
Water sensible [kW_{th}]	1.38	-	1.41	-
Fan and pump [kW_e]	0.03	0.23	0.03	0.23
Peak load [kW_e]	0.61	0.85	0.62	0.87

TABLE B.11. Energy Consumption and Peak Power Demand in Seattle. SW orientation, new building construction.

	RC system continuous ventilation	All-air system continuous ventilation	RC system no ventilation at night	All-air system no ventilation at night
Results for the typical week:				
Air sensible energy [kWh_{th}]	0.6	23.9	0.6	27.6
Air latent energy [kWh_{th}]	0.5	0.4	0.4	0.4
Water sensible energy [kWh_{th}]	31.7	-	31.6	-
Chiller energy [kWh_e]	10.9	8.1	10.9	9.3
Fan energy [kWh_e]	1.3	5.1	1.0	6.3
Pump energy [kWh_e]	0.2	-	0.2	-
Weekly energy consumption [kWh_e]	12.4	13.2	12.1	15.6
Results for the week of system peak:				
Peak load components				
Air sensible [kW_{th}]	0.21	1.35	0.21	1.38
Air latent [kW_{th}]	0.06	0.06	0.06	0.06
Water sensible [kW_{th}]	1.02	-	1.05	-
Fan and pump [kW_e]	0.03	0.20	0.03	0.20
Peak load [kW_e]	0.46	0.67	0.47	0.68

TABLE B.12. Energy Consumption and Peak Power Demand in New Orleans. NE orientation, new building construction.

	RC system continuous ventilation	All-air system continuous ventilation
Results for the typical week:		
Air sensible energy [kWh_{th}]	10.6	46.7
Air latent energy [kWh_{th}]	45.2	48.3
Water sensible energy [kWh_{th}]	30.5	-
Chiller energy [kWh_e]	28.7	31.7
Fan energy [kWh_e]	1.3	3.9
Pump energy [kWh_e]	0.2	-
Weekly energy consumption [kWh_e]	30.2	35.6
Results for the week of system peak:		
Peak load components		
Air sensible [kW_{th}]	0.27	1.23
Air latent [kW_{th}]	0.69	0.66
Water sensible [kW_{th}]	0.87	-
Fan and pump [kW_e]	0.03	0.16
Peak load [kW_e]	0.64	0.79

TABLE B.13. Energy Consumption and Peak Power Demand in Phoenix. NE orientation, new building construction.

	RC system no ventilation at night	All-air system no ventilation at night
Results for the typical week:		
Air sensible energy [kWh_{th}]	13.5	83.7
Air latent energy [kWh_{th}]	0.0	0.0
Water sensible energy [kWh_{th}]	52.6	-
Chiller energy [kWh_e]	22.0	27.9
Fan energy [kWh_e]	1.0	9.5
Pump energy [kWh_e]	0.2	-
Weekly energy consumption [kWh_e]	23.2	37.4
Results for the week of system peak:		
Peak load components		
Air sensible [kW_{th}]	0.27	1.83
Air latent [kW_{th}]	0.42	0.39
Water sensible [kW_{th}]	1.41	-
Fan and pump [kW_e]	0.03	0.21
Peak load [kW_e]	0.73	0.95

TABLE B.14. Energy Consumption and Peak Power Demand in New Orleans. SW orientation, old building construction.

	RC system continuous ventilation	All-air system continuous ventilation
Results for the typical week:		
Air sensible energy [kWh_{th}]	14.4	104.0
Air latent energy [kWh_{th}]	35.3	35.5
Water sensible energy [kWh_{th}]	69.3	-
Chiller energy [kWh_e]	39.7	46.5
Fan energy [kWh_e]	1.3	9.8
Pump energy [kWh_e]	0.4	-
Weekly energy consumption [kWh_e]	41.4	56.3
Results for the week of system peak:		
Peak load components		
Air sensible [kW_{th}]	0.30	2.67
Air latent [kW_{th}]	0.54	0.54
Water sensible [kW_{th}]	1.92	-
Fan and pump [kW_e]	0.04	0.36
Peak load [kW_e]	0.96	1.43

TABLE B.15. Energy Consumption and Peak Power Demand in Phoenix. SW orientation, old building construction.

	RC system no ventilation at night	All-air system no ventilation at night
Results for the typical week:		
Air sensible energy [kWh_{th}]	20.8	160.9
Air latent energy [kWh_{th}]	0.1	0.1
Water sensible energy [kWh_{th}]	86.1	-
Chiller energy [kWh_e]	35.7	53.7
Fan energy [kWh_e]	1.0	13.7
Pump energy [kWh_e]	0.4	-
Weekly energy consumption [kWh_e]	37.1	67.4
Results for the week of system peak:		
Peak load components		
Air sensible [kW_{th}]	0.42	4.32
Air latent [kW_{th}]	0.21	0.24
Water sensible [kW_{th}]	2.52	-
Fan and pump [kW_e]	0.04	0.58
Peak load [kW_e]	1.09	2.10

Ernest Orlando Lawrence Berkeley National Laboratory
One Cyclotron Road | Berkeley, California 94720

Prepared for the U.S. Department of Energy under Contract No. DE-AC03-76SF00098